Oil Shale

As an Alternative energy Source

in selected

Sites of Sumatra

OIL SHALE POTENTIAL

AS AN ALTERNATIVE ENERGY SOURCE
IN SELECTED SITES OF SUMATRA ISLAND

NANA SUWARNA
M. HERI HERMIYANTO JAZULI
M. IQBAL
RIAN KOSWARA

OIL SHALE POTENTIAL

AS AN ALTERNATIVE ENERGY SOURCE
IN SELECTED SITES OF SUMATRA ISLAND

GEOLOGICAL AGENCY

2024

OIL SHALE POTENTIAL
As an Alternative Energy Source in Selected Sites of Sumatra Island

AUTHOR

Nana Suwarna
M. Heri Hermiyanto Jazuli
M. Iqbal
Rian Koswara

EDITORS

Hermes Panggabean
Yunus Kusumahbrata

DESIGN COVER

Agus Soma

ARTISTIC & LAYOUT

Rian Koswara

PUBLISHED BY

FOREWORDS

Geological Agency, Indonesian Ministry of Energy and Mineral Resources, proudly presents this special publication entitled " OIL SHALE POTENTIAL AS AN ALTERNATIVE ENERGY SOURCE IN SELECTED SITES OF SUMATRA ISLAND". The main purpose of this publication is to document significant geological aspects related to the oil shale deposits especially in elected sites of Sumatra, so that the geoscientist community can learn from the oil shale publication for a better advancement of geological science as well as successful oil shale exploration in the future. This book is published as one of the geoscience publication of Geological Agency.

Geological Agency, particularly concerns about making this documentation available because of the rarity of such geological references on oil shale in Sumatra. In contrast to petroleum references, we hardly ever found any publications on Indonesian oil shale geology, particularly in Sumatra. This rarity might be explained by the absence of such geological events on coal geology and mineral in Indonesia.

On behalf of Gological Agency, I would like to thank all the authors of the published book, reviewers, and to the editorial team as well. Their effort eventually leads to the Geological Agency publication which hopefully can be used as one contribution to the geoscience community in Indonesia.

Bandung, November 2024

A.M. Wafid
Head of Geological Agency

PREFACE

The continuing decline of petroleum supplies all over the world is a challenge for geologist to find other alternative energy resources. Recently, in the view point of resource energy interest, the generation potential of oil shales, particularly as a source for oil, has been considered significantly as new energy resources. Oil shales have long been of interest as a direct resource for hydrocarbon and as a possible source rock for hydrocarbon during maturation. Thereby, the oil-shale deposits in Indonesia, particularly in Sumatra, which have not been explored intensely, may be expected to be the new fossil energy resources in the year ahead.

To gain a better understanding on the potential on unconventional fossil fuel, research on oil shales has been conducted in selected sites of intra-mountain basins in Sumatra Island, indicated to contain Eo-Oligocene oil shale deposits, such as Kabanjahe, Kapur IX, Kebuntinggi, Kuansing, Ombilin, Kiliranjao, Bukit Susah, East-30 Mountains, Bukit Bakar, Sinamar, and Asai-Rawas regions. To evaluate the characteristics of oil shales, related to their potential, petrographic and geochemical conditions, as well as geological condition is the focus of the research.

Several field geologic investigations and detailed organic petrographical and geochemical analyses, using fresh and subcropped of selected number of representative oil shale/mudrock, were carried out.

Furthermore, this publication, entitled "Oil Shale Potential As An Alternative Energy Source In Selected Sites Of Sumatra Island", is aimed to present information regarding the potential of oil shale as the unconventional energy resources, in the response to the fuel needs. The materials were obtained both from field and laboratory analyses and augmented with data from other sources. Moreover, the publication is also aimed to provide basic knowledge, introduction, and information for geologists majoring unconventional energy sector.

This work would not appear as presented here without the supports and participations of many parties. First of all, the authors wish to express their gratitude to the Head of Geological Agency, Dr. M. Wafid, for the permission to publish, and to Joko Parwoto, M.T. who always encourage to finish the publication. The same gratitude and appreciation were forwarded to Dr. Hermes Panggabean and Dr. Yunus Kusumahbrata who have reviewed in detail the manuscript. Moreover, the authors would like to thank all colleagues who have helped and assisted authors during field and laboratory work took place.

Bandung, December 2024

Authors

OIL SHALE POTENTIAL
AS AN ALTERNATIVE ENERGY SOURCE
IN SELECTED SITES OF SUMATRA ISLAND

CONTENTS

1. INTRODUCTION

1.1. Background

Besides the conventional fossil fuels to provide energy, other sources such as oil shale which is classed as unconventional fossil fuel resources have a high potential to be developed. Moreover, oil shales occurring as a sedimentary rock, with an ash content of more than 33 % and contain organic matter yield oil when destructively distilled (Gavin, 1924).

Since 1950's oil shale has become the special interest of geologists and economists, because of their potential to generate oil through heating at sufficiently high temperature. Among sedimentologists, oil shales are also interesting because of the information they convey about ancient depositional environment.

Recently, in the viewpoint of energy resource interest, the generation potential of shale oil generated from oil shales, particularly as source for an alternative energy, has been considered significantly as new energy resources. The oil shale has long been of interest as an indirect resource for fuel (energy) generated by a retorting process.

For many countries, oil shale represents a valuable potential source of liquid hydrocarbons and energy. Production of shale oil from oil shale is not one of the available energy generation alternatives. However, the continuing decline of petroleum supplies, accompanied by increasing costs of petroleum-based products may present opportunities for oil shale to supply some of energy needs.

For decades, there has been talk about finding and developing alternative energy sources to solve the problems of a significant and worldwide energy crisis. Today, more than ever, momentum is building as key factors align to make it economically feasible to pursue domestic solutions to the energy problem. Oil shale is one of the most abundant and accessible energy resources in the country.

The continuing decline of petroleum supplies from many basins in Indonesia requires a serious effort for geologists to find other alternative energy resources of fossil fuel origin. Recently, in the viewpoint of energy resource interest, the generation potential of oil shales, particularly as a source for oil, has been considered significantly as new energy resources. The oil shales have long been of interest as an indirect resource for hydrocarbon and as a possible source rock for hydrocarbon during maturation. Current studies on oil shale strata have revealed many of the factors controlling its formation and diagenesis. Most such studies have considered the main source for oil and condensate. Thereby, the oil-shale deposits in Indonesia, which have not been explored intensely, may be expected to be the new fossil energy resources in the future.

Fossil fuel resources currently still have an important role to supply energy to national energy demand and have significantly contributed to the national foreign exchange. With the remaining of national petroleum reserve at 8.6 billion barrels (Thaib, 2006), consisting of 4.2 billion barrels of proven reserves and 4.4 billion barrels of potential reserves, it is predictable that in the by 2010, Indonesia will be a net importer petroleum country. Some measures are needed to be taken in sustaining the production and reducing the depletion of reserves, supplemented by intensifying exploration in the marginal area to gain more oil reserve and upgrading exploitation technology to increase efficiency of production. In addition, diversifying to different types of energy could be considered.

As reported in several reports and publications (Suwarna *et al*., 2000, 2001, 2002, 2005; Kusumahbrata *et al*.,2002, 2003, 2004; Heryanto *et al*., 2002; Susanto *et al*., 2004; Hermiyanto *et al*., 2008, 20.., 20.., 20..; Wiryadi Rahmola, 20..) oil shales occur in some parts of Sumatra (Figure 1.1.a,b), including northern Sumatra (Kabanjahe Sub-Basin), Riau (Kebuntinggi, Kuansing, Bukit Susah, and East Tigapuluh areas), western Sumatra (Kiliranjao, Sitiung, Ombilin Basin, and Koto IX), and southern Sumatra (Sinamar,
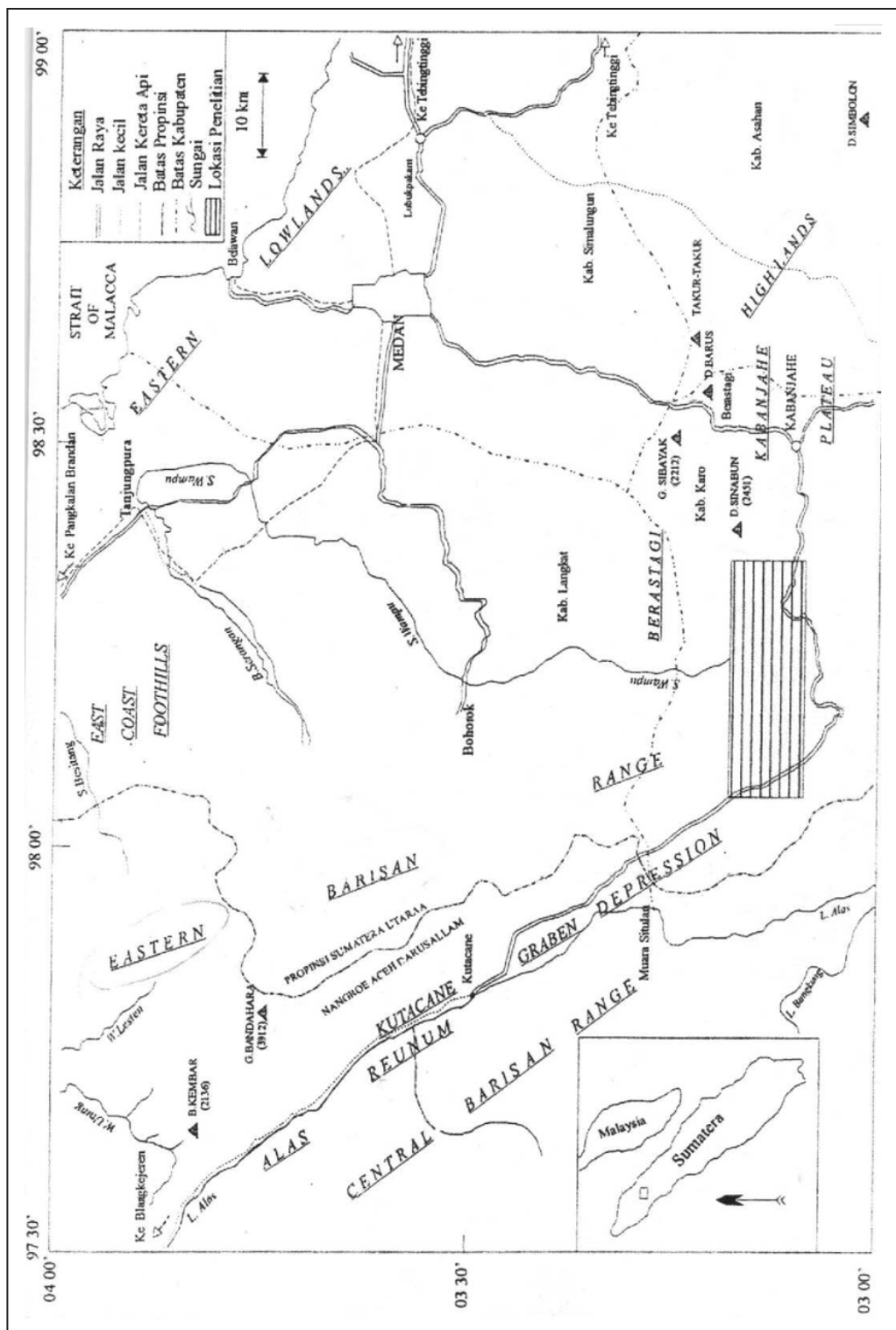
Figure 1.1. Locality map of the studied sites. a). Kabanjahe Area, northern Sumatra.
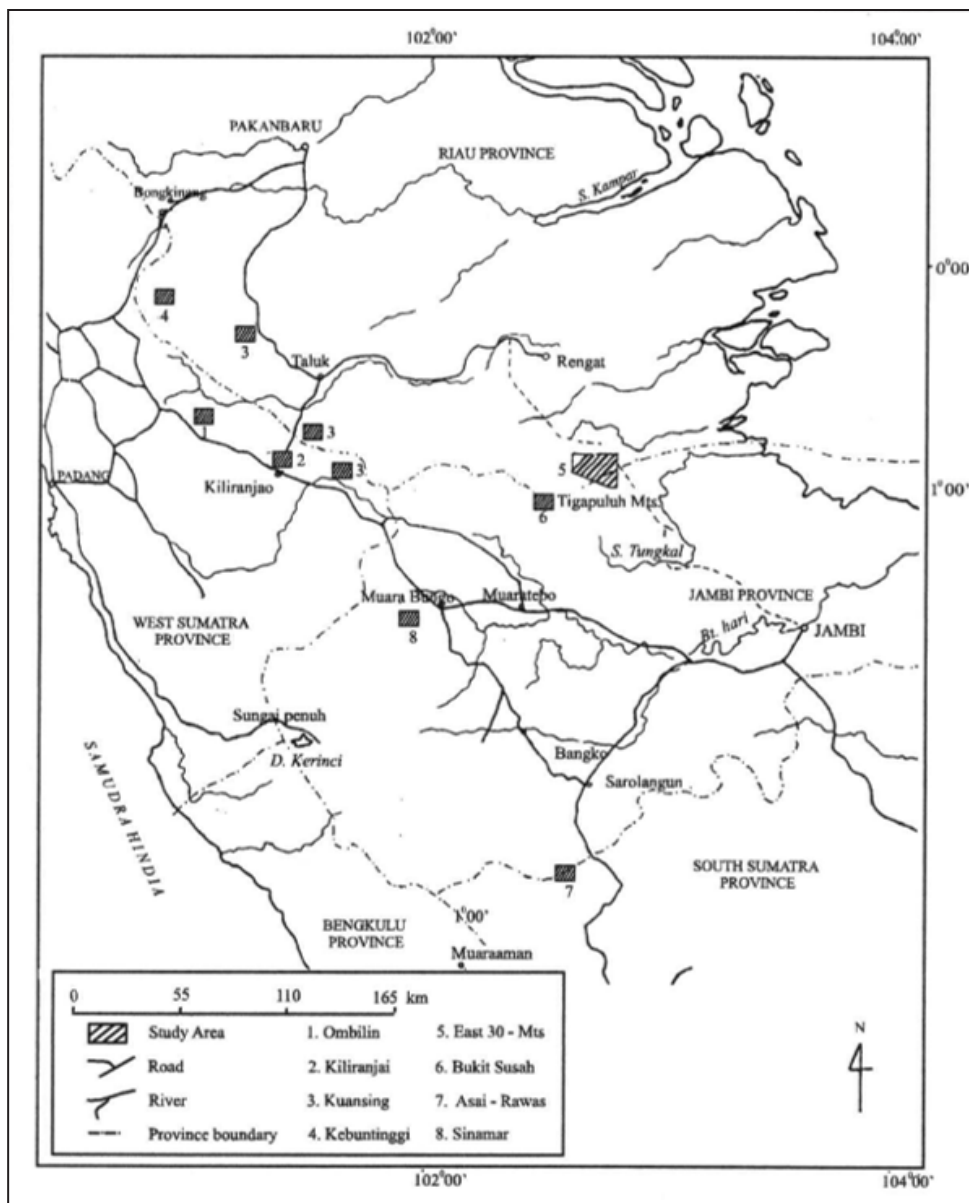
Figure 1.1. Locality map of the studied sites. a). Kabanjahe Area, northern Sumatra. b). Central- and southern Sumatra areas.

Bukit Bakar, and Asai-Rawas areas). Those oil shales have preliminary been studied, however their potential and quality have been known. These oil shale basins seem to superimpose the oil, gas, and coal basins, and thereby their basin setting is similar to the tectonic configuration of the clastic depositional system (Panggabean and Heryanto, 2003).

To gain a better understanding on the potential of unconventional fossil fuel, researches on oil shale have been conducted by Geological Research and Development Centre (GRDC), Ministry of Energy and Mineral Resources, at selected sites of Sumatera (Figure 1.1), which then continued by Center of Geological Survey, under Geological Agency. The researchs were focused to be conducted in some selected areas within small intra-montane basins of

Sumatra, such as Kabanjahe, Ombilin Basin, Kiliranjao Sub-basin, Koto IX, Kuansing, Kebuntinggi, East Tigapuluh Mountains, Bukit Susah, Bukit Bakar, and Asai-Rawas areas (Figure 1.1), which are indicated to contain oil shale deposits of Eo-Oligocene age.

In 2000, the first oil shale research was perfomed by GRDC team in East Tigapuluh Mountains and Kiliranjao areas (Figure 1.1.a), in order to gain a better understanding on the potential and resources of the oil shale in part of Sumatra Island. This activity carried out under the Thematic Geological Information and Research Project (PKIGT), a Program of the GRDC, has taken place until 2005. After that, in 2008, the oil shale research has been continued in the Sinamar regions by a team of Geological Survey Institute, Geological Agency. Furthermore, in 20.., oil shale investigation in Bukit Susah had been revisited by Geological Survey Center. In 20.., Geological Survey Centre had carried out a research on oil shale in Bukit Bakar, Jambi area.

The current data have also been supported by the previous research data gained from both published and unpublished types. That previous research reveals more actual data focused on pre-Tertiary rocks, which then was continued by several minor researches on Tertiary sediments of the southern part of Sumatra Island. Those activities reveal more actual data leading to a better understanding on Tertiary sediments, especially its stratigraphy and sedimentology to decipher oil and coal resource possibilities (Suwarna *et al.,* 2000). On the other hand, a general basic information on the presence of oil shale in Sumatra was also gained from the geological maps scale 1:250.000, published by Geological Research and Development Centre (now Geological Survey Center), Bandung. Additional data having been extracted from the oil and coal company geological reports, including additional stratigraphic relationships, sedimentology, and paleontology of the Old Tertiary sediments in Sumatera basins. Thesis of students are also used as additional data.

Deposits range from small occurrences of little or no economic value to those of enormous size that occupy thousands of square miles and contain many billions of barrels of potentially extractable shale oil. Total world resources of oil shale in 2016 are conservatively estimated at 6.05 trillion barrels (962 billion cubic metres) of shale oil, where the United States oil shale resources are more than 80% of the world ones (World energy resources. Oil, 2016). However, petroleum-based crude oil is cheaper to produce today than shale oil because of the additional costs of mining and extracting the energy from oil shale. Because of these higher costs, only a few deposits of oil shale are currently being exploited in China, Brazil, Estonia, and Australia. However, with the continuing decline of petroleum supplies, accompanied by increasing costs of petroleum-based products, oil shale presents opportunities for supplying some of the fossil energy needs of the world in the years ahead.

The availability and price of petroleum ultimately affect the viability of a large-scale oil-shale industry. Today, few, if any deposits can be economically mined and processed for shale oil in competition with petroleum. Nevertheless, some countries with oil-shale resources, but lack petroleum reserves, find it expedient to operate an oil-shale industry. As supplies of petroleum diminish in future years and costs for petroleum increase, greater use of oil shale for the production of electric power, transportation fuels, petrochemicals, and other industrial products seems likely.

1.2. Distribution and Potential of Oil Shale in Indonesia

Several preliminary field researches and inventarisations on oil shale deposits, started since pre-2000 until the present, have been carried out by Geological Research and Development Centre and Directorate of Mineral Inventory (previous name). Those activities indicate that the age of oil shale-bearing unit varies from Eocene to Miocene, but the pre-Tertiary unit is also recognized in eastern Indonesia. In the sedimentary basins located in Sumatra, in general, oil shale was deposited in lacustrine environments, associated with coal depositions. The narrow rock distribution, almost parallel to the direction of Great Sumatra Fault, and bounded by faults, indicates that the oil shale deposits were accumulated within the "syn-rift" basins. The Indonesian basins known as accumulation sites of the oil shale seams are: Kabanjahe Sub-basin (North Sumatra), Central Sumatra Basin, Ombilin Basin with some small intra-montanes, Jambi Sub-basin, South Sumatra Basin, Kutai Basin, Barito and Asem-Asem Basins, intra-montane basins in Sulawesi and Jawa, and Salawati Basin in Papua.

Several researchers show that some prospect areas are occupied by high oil content levels and have good prospects to be developed, such as Kebuntinggi – Riau, Sangkarewang – West Sumatera, Kiliranjao – Riau, Sitiung – West Sumatera, Kuansing – Riau, Bukit Susah – Riau, Ayah region – Central Java, and Lok Pikat area – South Kalimantan. Shale oil content (oil yield) from these areas is more than 40 l/ton-rock. Hypothetical oil shale potency in Indonesia until 2003 is presented in Table 1.1.

Regarding conventional fossil fuels diminish in amount, oil shales may eventually have to provide a substantial part of world energy. Although the cost of mining and processing oil shales are too high to compete with conventional petroleum production, oil shales may have a brighter future.

1.3. Terminology

Oil shale does not have definite geological definition nor a specific chemical formula. Different type of oil shales varies by the chemical composition, type of kerogen, age, and depositional history, including the organisms from which they were derived. Based upon environment of deposition, different oil shales could be divided into three groups, those are terrestrial, lacustrine, and marine origin.

Oil shale is a fine-grained sedimentary rock containing high proportion of organic matter in the form of exinite maceral (preserved algae, sapropel, and other carbonaceous material) which is capable to yield substantial amounts of oil and combustible gaseous hydrocarbon upon destructive distillation or retorting (............, 19..). The amount of oil that can be retorted from oil shale deposits ranges from 4% to more than 50% of the weight of the rock, or approximately 10 – 150 gallons of oil per ton of rock (Duncan, 1976).

Most of oil shales are actually bituminous, non-marine marlstones containing kerogen. The colour is brownish black or yellowish brown, very well laminated; in some cases of papery texture, tough, resinous, giving a "woody" sound when struck. In commercially deposits, the organic matter content, that may be either sapropelic or humic, or any mixture of the two, is at least 30% largely derived from algae, spores, or pollen (.........., 19..); therefore much higher than it is in most oil-source sediments, but it has to be in a low maturity that liquid oil has never been expelled from the kerogen.

Moreover, Yen and Chilingarian (1976) classified oil shale as "composites" of tightly bound organic and inorganic components as displayed in Table 1.2. The ratio of organics to inorganics rarely exceeds ¼.

Most of the organic matter is insoluble in ordinary organic solvents; therefore, it must be decomposed by heating to release such materials. It is potential for the economic recovery of energy, including shale oil and combustible gas, as well as a number of by-products. A deposit of oil shale having economic potential is generally

Table 1.1. Hypothetic Resources of Oil Shale in Indonesia (modified from Fatimah and Hadiyanto, 2003)

No	Location	Formation	Oil Yield (l/ton)	Hypothetic Resources	
				Rocks (million ton)	Oil (million Barrel)
A. West Sumatra					
1	PangkalanKotabaru	Sangkarewang	7 - 99	4,50	1,13
2	Sijunjung	?	?	390,00	61,70
3	Sawahlunto	?	?	708,50	115,00
4	Kotabuluh	Butar	2 - 4	108,00	2,05
5	Galugur	Sihapas	15 - 60	0,87	0,27
6	Kiliranjau	Pematang	6 - 44	?	?
B. Riau					
7	Tangko	Lower Telisa	5 - 212	52,80	16,70
8	Kebon Tinggi	Sangkarewang	5 - 140	15,22	71,00
9	Bukit Susah	?	?	?	?
10	Kuantan Sengingi	?	?	?	?
C. Jambi					
11	Mengkua Limun	Mengkarang	20 - 30	0,64	0,14
12	Jambi	Muara Enim	35	?	?
D. Central Java					
13	Gombong	?	?	7,80	3,70
14	Bentarsari	?	?	24,38	2,05
15	Ayah	Kalipucang	8 - 140	?	7,80
E. East Kalimantan					
16	Sepaso	Balikpapan Manumbar Pulubalang	1 - 28	1,33	0,12
17	Loa Janan	Balikpapan Pulubalang	5 - 15	1,17	0,11
18	Lok Paikat	Warukin Tanjung	1 - 102	?	5,38
F. Central Kalimantan					
19	Kandui	Montalat	2 - 5	66,50	1,47
20	Ampah	Montalat	5 - 10	9,80	0,37
G. South Kalimantan					
21	Tapin	Warukin Tanjung	?	6,40	2,02
H. South Sulawesi					
22	Tonasa	Malawa	4	?	0,83
23	Camba	Malawa	12	0,83	0,04
I. Southeast Sulawesi					
24	Buton/Pasarwajo	Winto Sampolakosa	14 - 248	40,50	35,57
25	Sampolawa	Winto Sampolakosa	60 - 127	7,69	6,52
26	Kapontori	Sampolakosa	60 - 127	38,00	22,21
Total Resources				**1484,93**	**356,18**

Table 1.2. General Scheme of the Oil Shale Components
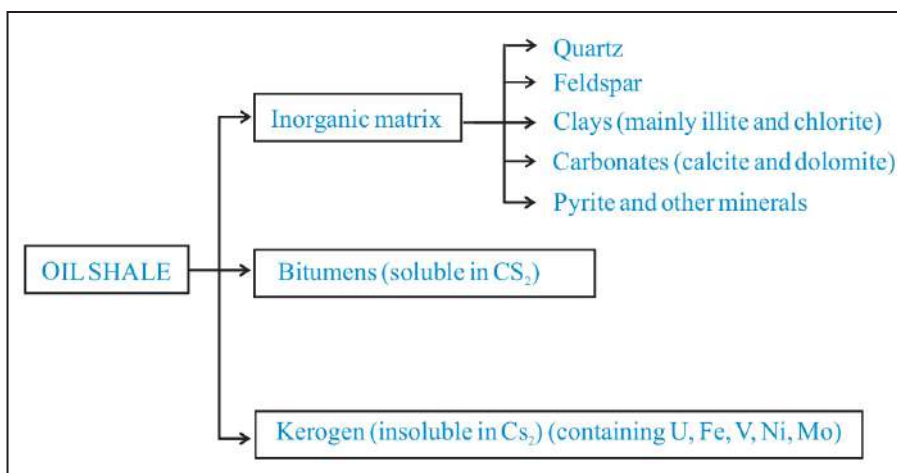
one that is at or near enough to the surface to be developed by open-pit or conventional underground mining or by in-situ methods.

On the basis of organic matter types contained in the sediments, Hutton *et al*. (1980), classified oil shale into two categories, those are sapropelic coal and and sapropelite, as shown in Figure 1.2.

Furthermore, Hutton (1987) proposed another classification of the sediments rich in organic matter into four categories, those are oil shale, bitumen-impregnated rock, humic coal, and tar sands (Figure 1.3).

Lithologically, oil shales possess a distinctive variety of colour depending on their chemical composition and are found in a wide variety of depositional setting (from lakes to marine) and age (Cambrian to Tertiary) (Duncan, 1976). Geologically, oil shales are the deposits of shallow marine on continental platforms and continental shelves, in areas where circulation of water near the sea floor was restricted; large lake basins (lacustrine), and small freshwater lakes, bogs, and lagoons, where they may also be associated with coal seam sequences (Duncan, 1976). Those features suggest that oil shales may be present in both Tertiary and older sediments in Indonesia. In central Sumatera, the occurrence of Tertiary oil shales is associated with lacustrine

sedimentation in the intra-montane basin as well as in the foreland basin (back-arc).

Oil shales range widely in organic content and oil yield. Commercial grades of oil shale, as determined by their yield of shale oil, ranges from about 100 to 200 liters per metric ton (l/t) of rock. When economic consideration comes into play, a cut of grade value 5% by weight of exinite maceral can be used. The U.S. Geological Survey has used a lower limit of about 40 l/t for classification of Federal oil-shale lands. Others have suggested a limit as low as 25 l/t.

In terms of mineral and elemental content, oil shale differs from coal in several distinct ways:

1). Oil shales typically contain much larger amounts of inert mineral matter (60–90 %) than coals, which have been defined as containing less than 40 % mineral matter.

2). The organic matter of oil shale, which is the source of liquid and gaseous hydrocarbons, typically has a higher hydrogen and lower oxygen content than that of lignite and bituminous coal.

Although shale oil in today's world market is not competitive with petroleum, natural gas, or coal, it is used in several countries that possess easily exploitable deposits of oil shale but lack other fossil fuel resources. Some oil-shale deposits contain minerals and metals that add by-prod-
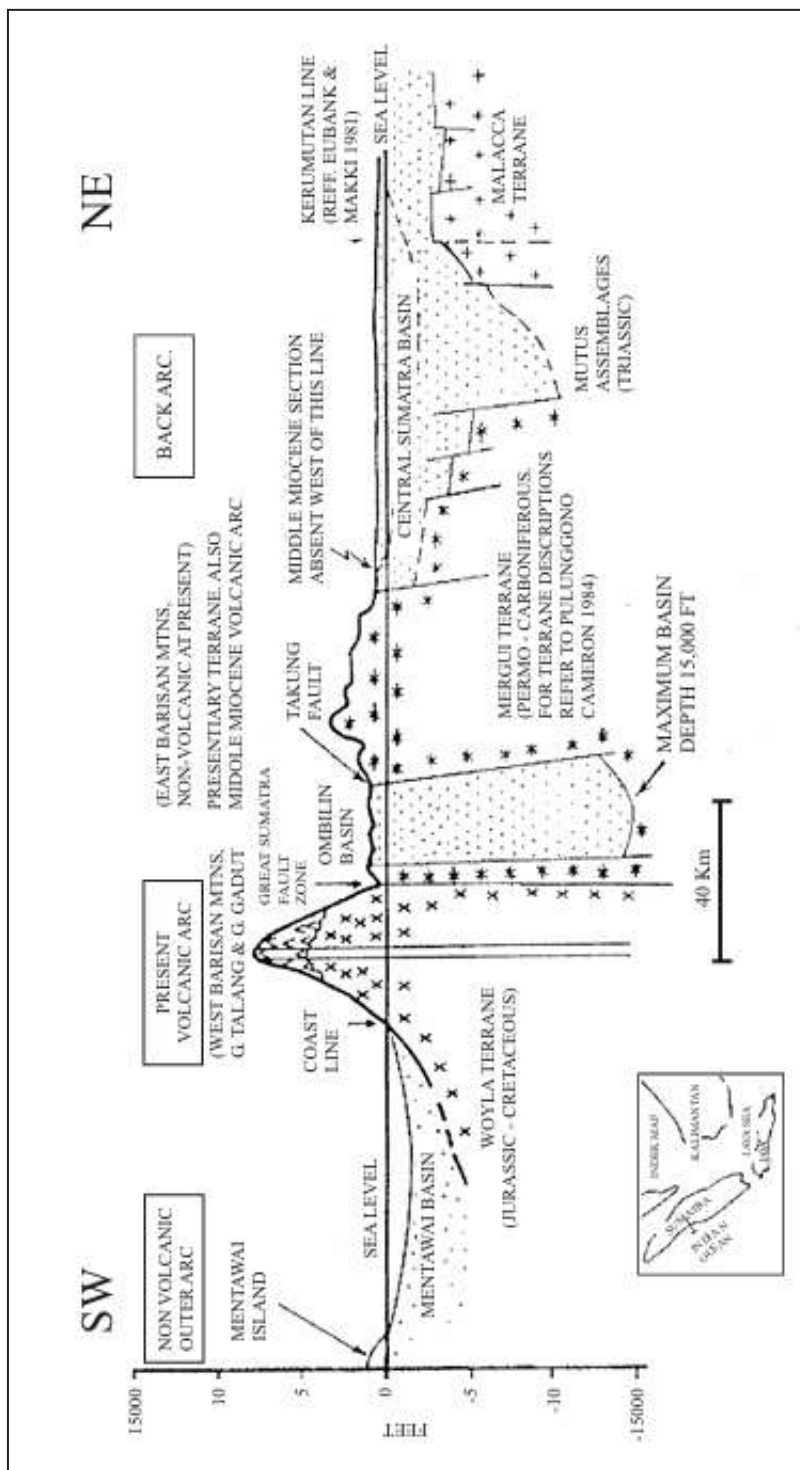
Figure 1.2. Classification of sapropelites and sapropelic coals (Hutton et al., 1980).
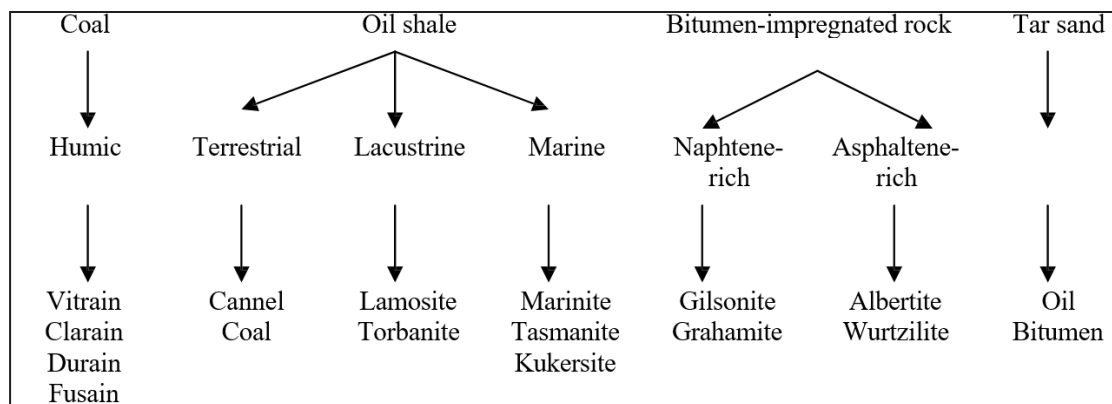
Coal	Oil shale			Bitumen-impregnated rock		Tar sand
↓	↙	↓	↘	↙	↘	↓
Humic	Terrestrial	Lacustrine	Marine	Naphtene-rich	Asphaltene-rich	
↓	↓	↓	↓	↓	↓	↓
Vitrain Clarain Durain Fusain	Cannel Coal	Lamosite Torbanite	Marinite Tasmanite Kukersite	Gilsonite Grahamite	Albertite Wurtzilite	Oil Bitumen

Figure. 1.3. Classification of organic-rich rocks (Hutton, 1987).

uct value such as alum [$KAl(SO_4)_2 12H_2O$], nahcolite ($NaHCO_3$), dawsonite [$NaAl(OH)_2CO_3$], sulphur, ammonium sulphate, vanadium, zinc, copper, and uranium.

The grade of oil shale has been determined by many different methods with the results expressed in a variety of units. The heating value of the oil shale may be determined by using a calorimeter. Values obtained by this method are reported in English or metric units, such as Btu/pound of oil shale, cal/g rock, kcal/kg rock, MJ/kg rock, and other units. The heating value is useful for determining the quality of an oil shale that is burned directly in a power plant to produce electricity. Although the heating value of a given oil shale is a useful and fundamental property of the rock, it does not provide information on the amounts of shale oil or combustible gas that would be yielded by retorting (destructive distillation).

The grade or quality of oil shale can be determined by measuring the yield of oil of a shale sample in a laboratory retort. This is perhaps the most common type of analysis that is currently used to evaluate an oil-shale resource. Khummongkol and Suwannathong (2007), based on the oil content generated, divided the quality of oil shales into four grades, those are low, middle, good, and high levels.

The commercial development of an oil-shale deposit depends upon many factors. The geologic setting and the physical and chemical characteristics of the resource are of primary importance. Roads, railroads, power lines, water, and available labor are among the factors to be considered in determining the viability of an oil-shale operation. Oil-shale lands that could be mined may be preempted by present land usage such as population centers, parks, and wildlife refuges. Development of new in-situ mining and processing technologies may allow an oil-shale operation in previously restricted areas without causing damage to the surface or posing problems of air and water pollution.

I.4. Objectives

The Indonesian Region is known to have large and various energy resources potential. The oil shale deposits, one type of fossil fuel energy resources, are distributed in a lacustrine lake of intra-montane and back-arc basins. Most of them, however, have not been studied in detail due to many constraints, where one of them is the lack of model for small oil shale pilot project in Indonesia to be used as a reference. Therefore, inventarisation, exploration, and pilot project to discover new insight regarding to oil shale utilization should be intensively done.

The information obtained from oil shale analyses is important for having a better understanding on the sediments and organic matter

content relating to shale oil (hydrocarbon) potential, predominantly, especially within the Eocene-Oligocene sediments in Sumatra Island. The report also informs "potential source rocks" those with sufficient organic content to produce hydrocarbons, whether it is oil-prone or gas-prone category, at generative temperatures, and "effective source rocks" - those potential source rocks which can be shown to have reached generative temperatures.

The information within this book attempts to evaluate and discuss the potential of shale sequences exposed in some selected basins in Sumatra on the basis of lithofacies, organic petrography, Rock-Eval pyrolysis, GC (gas chromatography) and GC-MS (gas chromatography and mass spectrometry, molecular geochemistry (Pr/Ph), and mineralogical analyses (SEM and XRD). The understanding of studied oil shale characteristics will be useful in selecting efficient and effective techniques for their resource potential assessments.

2. GEOLOGY

2.1. Geological Setting

Sumatra Island is situated along the south-western edge of the Sunda Shelf, part of the Eurasia Continental Plate, directly adjoining the Indian-Australian Oceanic Plate (Figure 2.1.1). Due to the collision between those two plates, an oblique subduction zone was produced, situated along the Sunda Trench, outside the western coast of Sumatra Island (Hamilton, 1979; Curray *et al*., 1979).

The subduction taking place since Late Permian (Katili, 1972; Cameron *et al*., 1980; Pulunggono and Cameron, 1984); Pulunggono *et al.,* 1992) led to the presence of magmatic arc such as Barisan Mountains and dextral strike-slip fault parallel to the plate edge, that is called the Sumatra Great Fault System (Fitch, 1972). Moreover, the intermontane basins were formed almost parallel in direction to the fault system, that is northwest – southeast direction.

Tectonically, the study areas are located the Back-Arc Zone and Inter-Arc Zone (Figure 2.1.1), underlain by pre-Tertiary rocks, which then is overlain by Cenozoic sediments and volcanics.

The South Sumatra basin was formed by three major tectonic phases (Figure 2.1.2):

- Extension during Late Paleocene to Early Miocene forming north-trending grabens that were filled with Eocene to Early Miocene deposits;
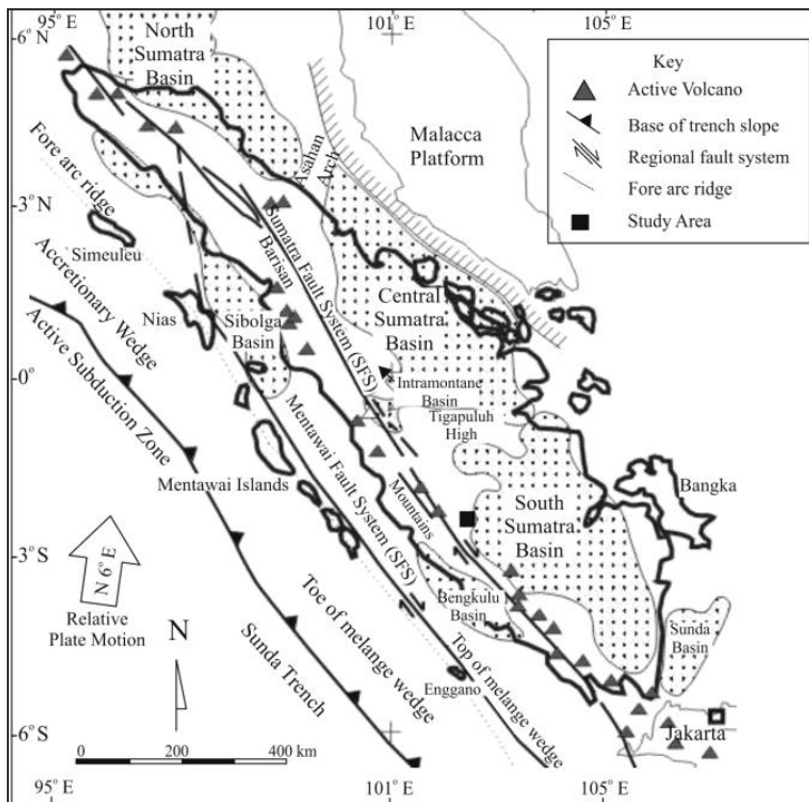

Figure 2.1.1. Locality, basin, and regional tectonic map of Sumatra Island, including study areas (modified from de Coster, 1978; Yarmanto *et al*., 1997).

UMUR		FORMASI	LITOLOGI	MARKER	PALEON		SEJARAH GEOLOGI/ TEKTONIKA
					FORAM	NANNO	
KUARTER		ALLUVIAL		SEAL			
PLIOSEN		KASAI			N 12	NN9	Compression and uplift
MIOSEN	AKHIR	MUARAENIM		SEAL	N 11	NN8	
					N 10	NN7	
	TENGAH	AIRBENAKAT		RESERVOIR ROCK	N 9	NN6	Sag Basin
					N 8	NN5	
	AWAL	GUMAI		SEAL + RESERVOIR ROCK	N 7	NN4	
					N 6	NN2-3	
		BATURAJA			N 5	NN2	
					N 12	NN1	
OLIGOSEN		TALANG AKAR		SOURCES + RESERVOIR ROCK	N 4 (?)		
		LAHAT / KIKIM			INDETERMINATE	INDETERMINATE	Graben fill
EOSEN							
PALEOSEN							
PRA- TERSIER		BATUAN DASAR					

Figure 2.1.2. General tecteonics and stratigraphic column of South Sumatra Basin (modification after Tarazona *et al.*, 1999).

- Relative quiescence with late normal faulting from Early Miocene to Early Pliocene (Sag Basin);
- Basement-involved compression.

Many of the normal faults forming the depositional basins in south Sumatra have been reactivated and some have been reversed during Miocene to Plio-Pleistocene compression and basin inversion (Zeliff *et al.*, 1985; Moulds, 1989; Sudarmono *et al.*, 1997). Uplift of the Barisan Mountains, resulting from the subduction, began in Late Miocene, but primarily occurred in the Plio-Pleistocene (Hamilton, 1979; Sudarmono *et al.*, 1997). In the Eocene to Oligocene, tectonic stress and extension, resulting from northward movement of both the Indian-Australian Plate to the east and the Indian Plate to the west, and rotation of Kalimantan, formed rifts or half-graben

complexes along much of the Sumatra Island (Hall, 1997a, b; Longley, 1997; Sudarmono *et al*., 1997). These rift basins overlie unconformably on a variety of pre-Tertiary rocks. The grabens and major faults of the South Sumatra Basin are oriented north-northwest to south-southeast. This is a similar alignment to the grabens of Central Sumatra Basin, but they are deeper and larger basins (Figure 2.1.3). The Palembang Basin in South Sumatra is greater than 4,500 m deep (Hutchinson, 1996). The fault-bounded Benakat
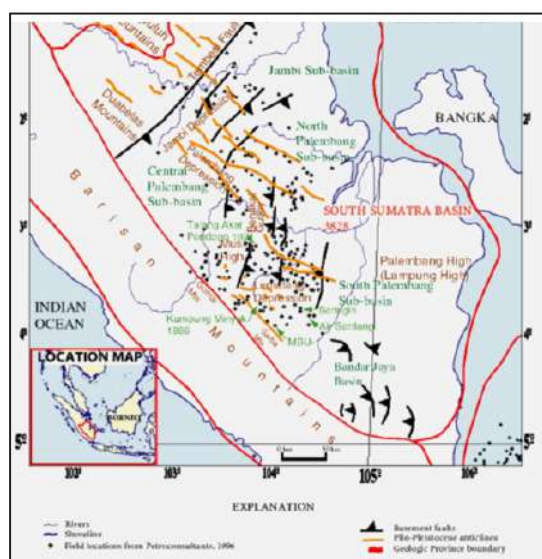

Figure 2.1.3. Structural features of the South Sumatra Basin: Jambi Sub-basin, North Palembang Sub-basin, Central Palembang Sub-basin, South Palembang Sub-basin, and Tembesi Fault (after Hutchison, 1996).

Gulley connects the major basin complexes of the Lematang Depression and the Palembang Depression. The NS Benakat Gulley is similar in trend to the Bengkalis depression in Central Sumatra, the fault zone that forms the eastern coast of Sumatra and the grabens of North Sumatra Basin (Moulds, 1989; Pulunggono *et al*., 1992; Hutchinson, 1996). A fault zone that trends southwest to northeast, the Tembesi Fault, forms the northwestern edge of the Jambi Sub-basin.

The overall Tertiary depositional filling in the South Sumatra Basin began in the Eocene with continental sediments derived from local erosion (Courteney *et al*., 1990; Cole and Crittenden, 1997). Sediments began to fill these basins in response to the half-graben architectural style and subsidence of the basins (Bishop, 1988; Wicaksono *et al*., 1992). Additional synrift deposits of tuffaceous sands, conglomerates, breccias and clays were deposited in faulted and topographic lows by alluvial, fluvial, and lacustrine processes.

2.2. Tectonic Setting

South Sumatra Basin configuration and development (Figure 2.1.2) are closely related and controlled by tectonic activities (De Coster, 1974; Eubank and Makki, 1981; Robinson and Kamal, 1988; Heruyono and Villaroel, 1989). It is assumed that the basin is a pull apart type bounded by big strike-slip faults due to Late Cretaceous oblique movements towards NE direction, between Eurasian Continent Plate and Indian-Australian Oceanic Plate. The basin was formed at early Late Eocene (Ryacudu, 2005) which then developed until Early Oligocene to Miocene.

Folding and faulting structures within Tertiary rocks in the basin, in general, are in NW – SE directions. However, some structures occur in SW – NE even relatively N – S directions.

The formation of folds in the whole basin led to the presence of anticlinorium which is in accordance with the basement rock configurations in the form of Early Tertiary Highs. Different from fold structures, fault directions vary, especially subsurface fault (Wahab *et al*., 1982). NW-SE and NE-SW faults cutting each other are Early Tertiary pair of faults reactivated in Plio-Pleistocene (Suwarna *et al*., 1984; Gafoer *et al*., 1992, 1993, 1995; and Kusumah *et al*., 2000). Those faults led to the formation of highs and grabens. The NW-SE structures produced Duabelas Mountains, Telisa, Bukit Susah, and Bukit Bakar Highs, and North Palembang Depression.

De Coster (1974) and McCourt (1993) stated, that the tectonic evolution happened highly affected depositional history of South Sumatra Basin.

Late Cretaceous – Early Oligocene is the early rifting phase leading to the presence of graben and half-graben forming basement configuration of South Sumatra Basin. On the same time, in the graben, a fluvial and lacustrine depositional phase took place.

2.2.1. Kabanjahe Sub-basin

Geographically, the Butar Formation occupies the Tigabinanga, Kutabangun, Kutabangunpunti, Juhar, Juhar Perinte, Sarinembah, Kutabuluh/ Laubuluh. Payung, and Penampen regions (Figure 2.2.1.1) within the Kabanjahe Sub-basin, Karo Regency. This sub-basin has been filled with approximately 235 m-thick clastic sediments of Eocene age (Polhaupessy, 2003, written com.).

The sub-basin, occupying the Eastern Barisan Range and Kabanjahe Highland, is presumably an intermontane basin or southwestern part of the North Sumatera Basin, and it has been filled with approximately 235 m of the Eocene Butar Formation comprising clastic sediments.

On the basis of lithofacies assemblage, Kusumahbrata *et al.* (2002) subdivided the formation into three members: the Lower, Middle, and Upper Members. The important member, in the viewpoint of organic-rich content, is the Upper Member. The member is a 60-m thick sedimentary sequence dominated by shale, claystone, and mudstone beds, with intercalations of fine-grained sandstone. The shale sequence is part of an extensive, organic-rich shale depositional system covering large areas of the Kabanjahe Basin. The shale showing variety of colour and density is fissile - papery to flaggy, containing carbonaceous/humic matter, and some are calcareous. In some places, thin coal beds (30 cm thick) occur in limited lateral distributions. The member crops out around the rim of the sub-basin. The presence
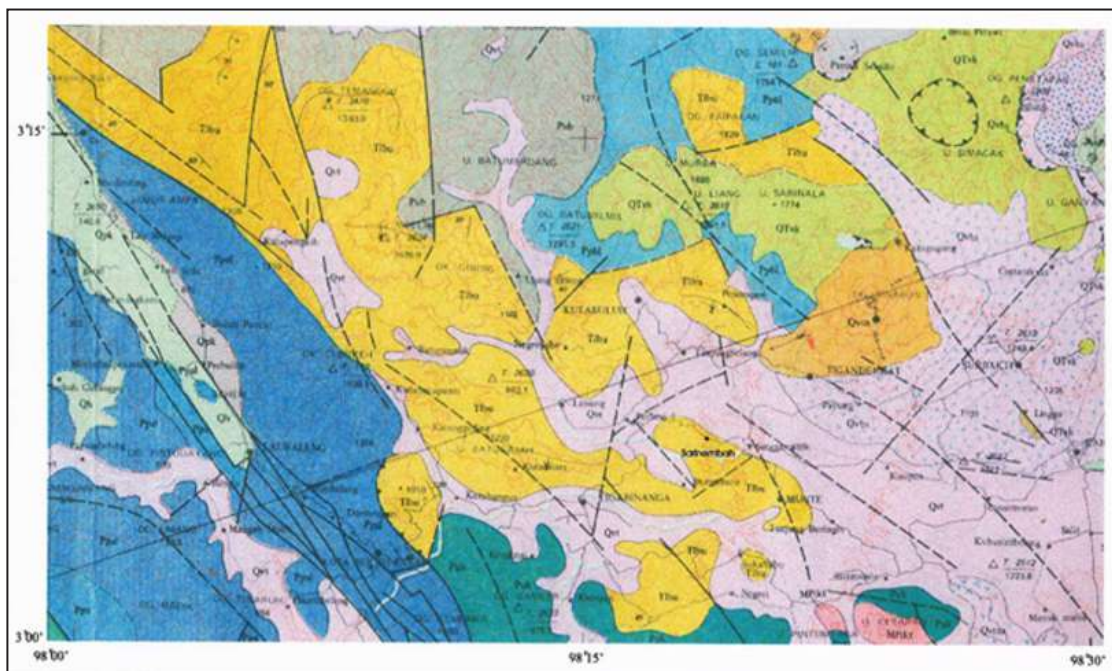

Figure 2.2.1.1. Geological Map of the Karo Region showing rock distribution and location of studied area (after Cameron *et al.*, 1982), as well as geographical sites of the research.

of plenty framboidal pyrite content, foraminifera fossils, and a palynomorph assemblage tends to indicate a meandering river depositional environment influenced by a marine incursion.

2.2.2. Kapur IX

Stratigraphic setting of the Kapur IX region is referred to Kusdji *et al*. (2001). Geologic investigation was carried out in Kototuo, Kotobangun, and Galugur, Kapur IX Sub-regency, West Sumatra Province (Rahmola, 2019) (Figure 2.2.2.1).

In Kototuo, the sedimentary sequence is variated comprising fine- to coarse-grained sandstone, shale, and claystone. However, shale dominates, dark grey, well bedded – massive, flaggy, hard (Figure 2.2.2.2). Kusdji *et al*. (2001) noted that the sedimentary sequence was equivalent to Pematang Formation in Central Sumatra Basin. Furthermore, it can be correlated to the sedimentary sequences of Eocene Sangkarewang Formation occurring in the Ombilin and Kebuntinggi Intramontane Basins.

Geologic observation carried out in Kotobangun area revealed that the sediments outcrop as conglomeratic sandstone, carbonaceous claystone, and coal seams (Figure 2.2.2.3). This sedimentary sequence underlies calcareous claystone presumed to be Telisa Formation (Kusdji *et al*. 2001 or Lower Member of Telisa Formation (Silitonga and Kastowo, 1975).
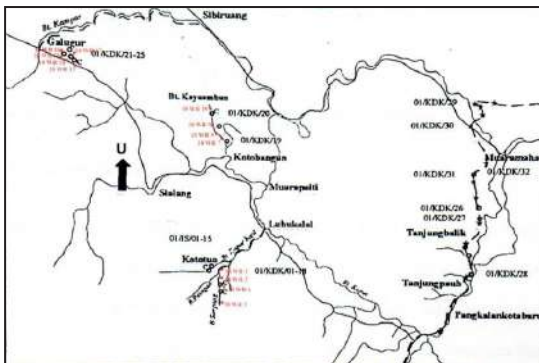
Figure 2.2.2.1. Locality map of study areas in Kapur IX, west Sumatra.

Figure 2.2.2.2. Photographs of shale, dark grey, well bedded – massive, flaggy, and hard, outcropping in Kototuo (Rahmola, 2019).

In Galugur site (Figure 2.2.2.4), the sediments consist of coal seam and black claystone having oil-smell character.

Figure 2.2.2.3. Photographs of shale/mudstone outcrops in Kotobangun (Rahmola, 2019).

Figure 2.2.2.4. Photographs of coal seam and black clay-stone, having oil-smell in Galugur area (Rahmola, 2019).

2.2.3. Kebuntinggi Sub-basin

Physiographically, the Kebuntinggi region occurring in the form of a small sub-basin (Figure 2.2.3.1) is situated in the west flank of Barisan Mountains and Anticlinorium Barisan Mountains.

The area occurs as horst and graben showing drainage patterns flowing to the west.
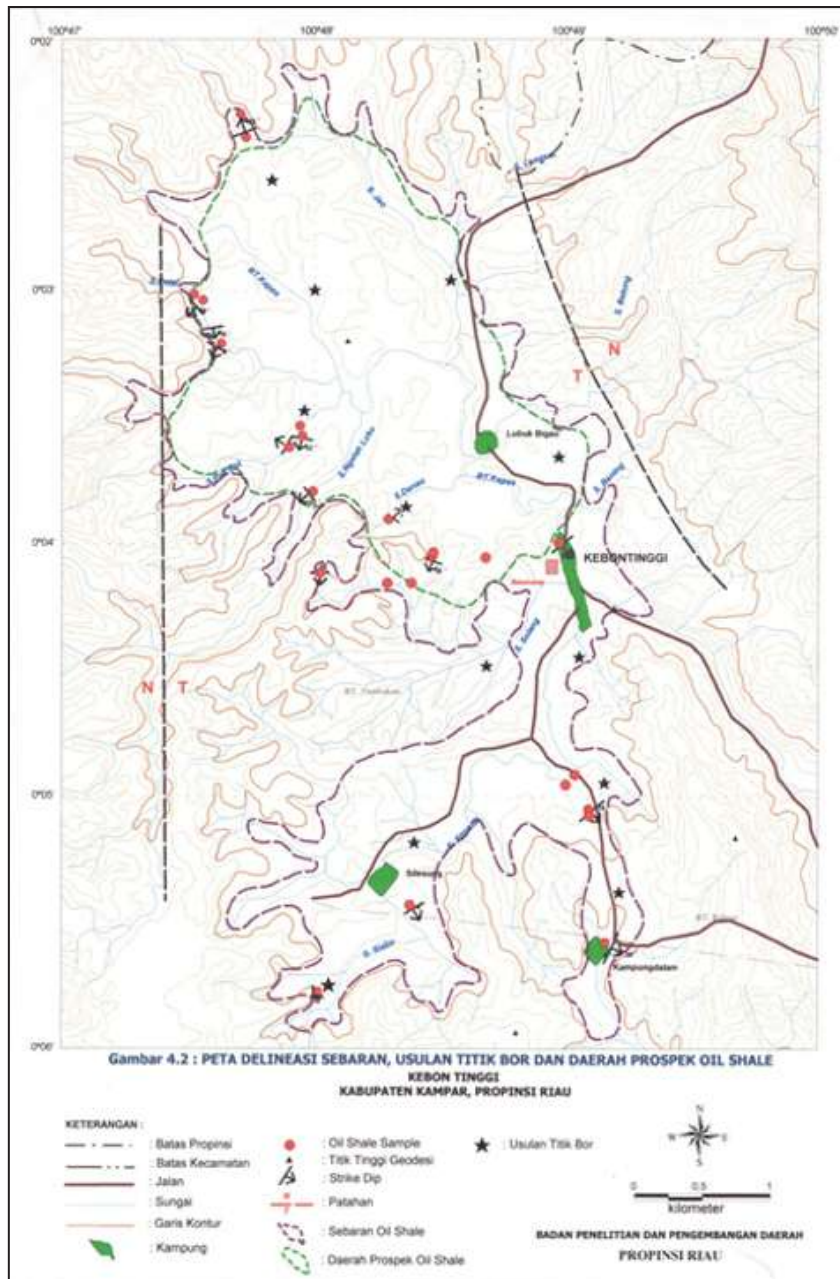
Figure 2.2.3.1. Locality map of the studied area, Kebuntinggi Sub-basin, west Sumatra.

On the basis of study done by Clarke *et al*. (1982), Silitonga and Kastowo (1975), and Koesoemadinata and Matasak (1981), geologically the Kebuntinggi Sub-basin is an intermountain type formed since Early Tertiary, shown by the deposition of the Eocene Brani and Sangkare-

wang Formations, underlain by metasediments of the pre-Tertiary Kuantan Formation.

The Kebuntinggi Sub-basin is located to the north of the Ombilin Basin, occupied by the sedimentary succession comprises the Brani and Sangkarewang Formations of Late Paleocene in age (Koesoemadinata and Matasak, 1981), whilst Moss and Howells (1996) indicated that the age is Eocene-Oligocene. However, GRDC's analysis tends to indicate Eocene age (Suwarna *et al.*, 2001).

2.2.4. Kuansing Area

The Keruh Formation crops out in the western part of the Kuantan-Singingi Regency, Riau Province (Figure 1.1-b). The study area is situated in the southwest margin of the Central Sumatera Basin, one of the Indonesian oil producing back-arc basins. The basin is underlain by the pre-Tertiary basement rocks, and it has been filled by the Eocene to Plio-Pleistocene siliciclastic-dominated sediments. The Keruh Formation is a new proposed formation (Kusumahbrata and Suwarna, 2003) with its type locality situated in the Keruh River, about 10 km northwest of the Petai Village, northwestern part of the regency.

The geology of the Kuansing area is shown in Figure 2.2.4.1-1. The oldest rock in the study area is the Permo-Carboniferous Kuantan Formation. It comprises Lower Member (quartzite and quartz sandstone with interbedded slate, phyllite, shale, volcanic rock, chloritic tuff, conglomerate and chert), Limestone Member (limestone, slate, phyllite, silicified shale and quartzite), and Phyllite and Shale Member (phyllite and shale with intercalated slate, quartzite, siltstone, chert and lava flow).

The Triassic Tuhur Formation formed by Limestone Member (sandy and conglomeratic limestones), and Slate and Shale Member (slate, shale, marly shale with interbedded radiolarian chert, black silicified shale and thinly bed metamorphosed greywacke) underlies unconformably the Kuantan Formation. These Pre-Tertiary rocks are intruded by Triassic-Jurassic granitic rocks

consisting of granite, granodiorite, and quartz porphyry. All of the Pre-Tertiary rocks act as a basement of the Tertiary Central Sumatera Basin.

Based on the Geological Map of the Solok Quadrangle (Silitonga and Kastowo, 1995), the Tertiary succession consists of Telisa Formation which comprises Lower and Upper Members (Figure 2.2.4.1-1). According to this map, the rock unit studied is included into the Lower Member of Telisa Formation comprising marly claystone, sandstone, lignite, tuff andesitic, breccia and glauconitic sandstone.

Palynological analyses indicate a Late Eocene age for the unit. Therefore, Kusumahbrata and Suwarna (2003) introduced this Lower Member of Telisa Formation as the Keruh Formation which can be correlated to the Pematang Group of the Central Sumatra Basin and Kelesa Formation in the Tigapuluh Mountains. Moreover, the Lower Member of Telisa Formation is correlated to the Sihapas Formation in Central Sumatra Basin and the Lakat Formation in the Tigapuluh Mountains.

The Upper Member of the Telisa Formation consists of shale and marly limestone with thinly intercalation of andesitic tuff of an Early to Middle Miocene age. This member is known as the Telisa Formation in the Central Sumatera Basin and correlated to the Gumai Formation in the Tigapuluh Mountains (Suwarna e*t al.,* 1994).

2.2.5. Ombilin Basin

The geologic setting and history of the Ombilin Basin has been described in several previous publications (Silitonga and Kastowo, 1975; Cameron *et al.*, 1981; Koning, 1985). An area of approximately 25 km by 60 km, trending parallel to the Sumatera axis, is present as the exposed portion of the Ombilin Basin (Figure 2.2.5.1). The basin developed in an intermontane setting as a result of the subduction of the Indian-Australian Plate beneath the Southeast Asian Plate, during the late Cretaceous - Early Tertiary. It is a graben-like, pull-apart basin formed as a series of fault-bounded troughs (Figure 2.2.5.2; Koning, 1985). Predominantly, these troughs were
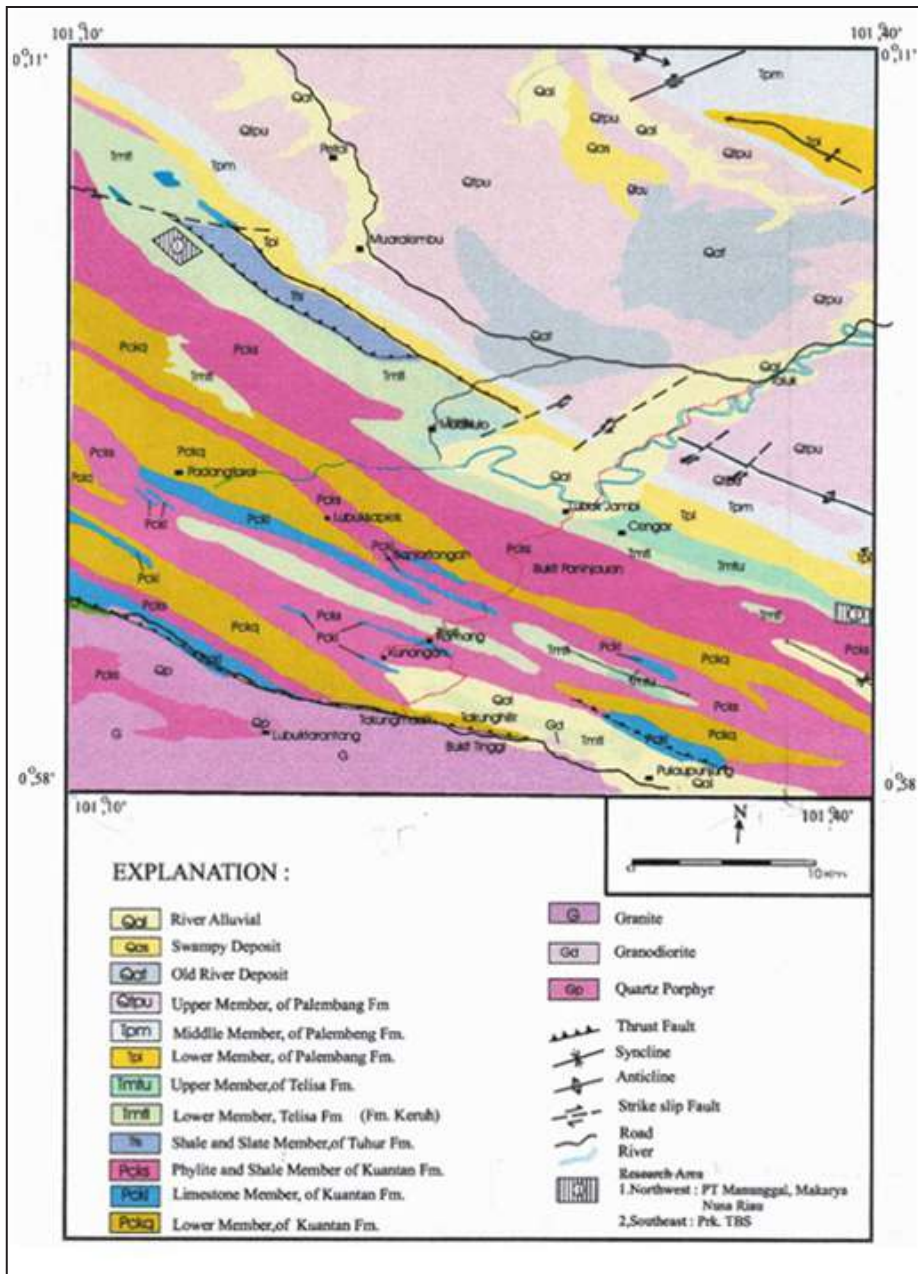
Figure 2.2.4.1. Geological map of the Kuansing Area (1) and Kiliranjao Sub-basin (2) (modified after Silitonga and Kastowo, 1995).

filled with Tertiary terrestrial clastics; those are lacustrine and fluvial sediments, which overlie a complex pre-Tertiary basement (Figure 2.2.5.3).

Sedimentation of the Tertiary sedimentary units were tectonically controlled, and each rock unit is separated along their lower and upper contacts

19
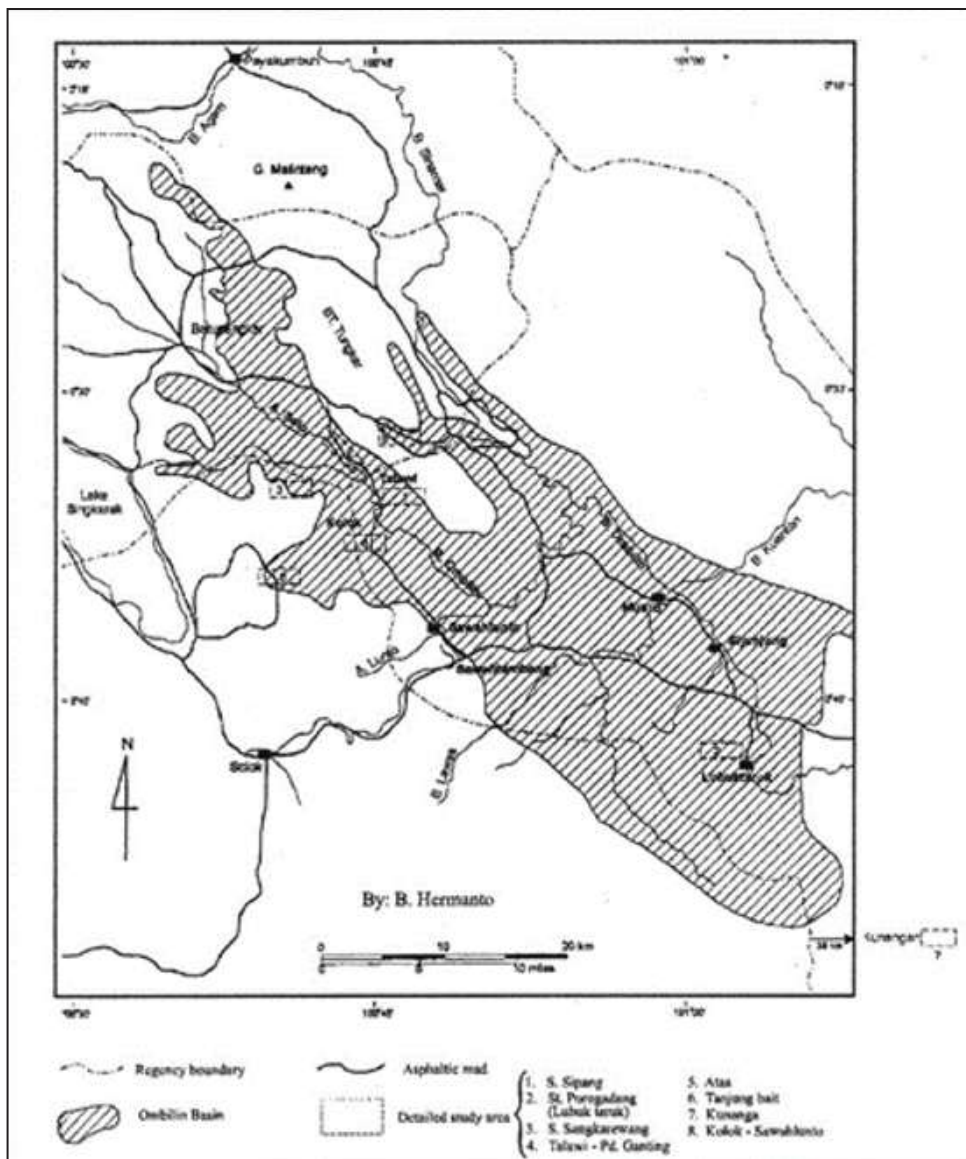
Figure 2.2.5.1. An area of approximately 25 km by 60 km, trending parallel to the Sumatra axis, is present as the Ombilin Basin and site location of study areas (modified after Koning, 1985).

by a well-defined conformity with local depositional hiatus.

Four major Tertiary stratigraphic sequences observed are the (1) Eocene - Early Oligocene Sangkarewang Formation, (2) Early - Late Oligocene Sawahlunto Formation, (3) Late Oligocene Sawahtambang Formation, and (4) Early Miocene Ombilin Formation The Eocene Sangkarewang and Early - Late Oligocene Sawahlunto Formations, filling in the Ombilin Basin, are the sedimentary sequences containing oil shale seams (Suwarna *et al.*, 2001).

The principal source of the shale oil is the Eocene - Early Oligocene Sangkarewang Forma-
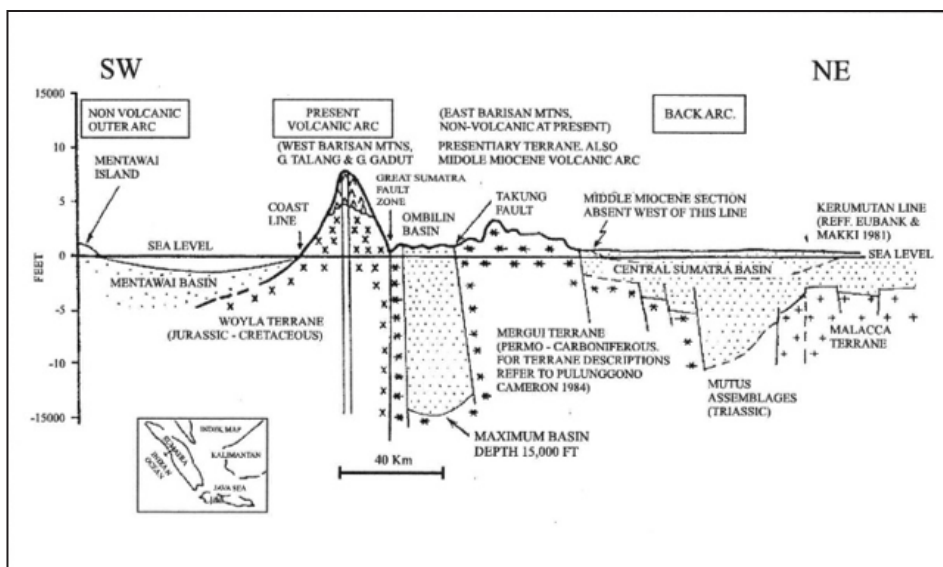
Figure 2.2.5.2. A graben-like, pull-apart Ombilin Basin formed as a series of fault-bounded troughs (after Koning, 1985).

tion, which is lacustrine sedimentary rock, was deposited in a subsiding basin under tropical conditions. In the deeper part of the basin, the rock unit comprises mainly calcareous shale and marl, brown to black, parallel laminated to very fissile; containing plant, fish, bird track fossils, pyrite, and locally showing; slump structure. Intercalations of calcareous quartz and feldspathic sandstone, fine- to very coarse-grained, blackish to yellowish grey, graded-bedding, fining upwards, with slump structure locally. Thickness of the sandstone unit varies from 1.5 - 30 cm,

however, layers of 3 m-thick frequently occur. Total thickness of the formation up to 900 m. Calcareous characteristics of the rock are due to the abundance of limestone debris and bicarbonate-rich river water during the deposition of the sediments.

Stratigraphically, the Sangkarewang Formation rests unconformably on the Pre-Tertiary rocks, and is conformably overlain by the Sawahlunto Formation. The Sawahlunto Formation, which is classified as coal measures, was deposited during a regressive period in Early Oligocene to Late Oligocene. The formation characterised

by coal layers, mainly comprises brownish grey shales, siltstones and silty shales, and claystones, with minor intercalations of compact brown quartz sandstone. These rock sequences were deposited mainly in fluvial environments.

Shales outcrop as underclays, are carbonaceous, or contain coal fragments and flakes. Coals are commonly interbedded with grey siltstone and coaly siltstone. Splitting and wedging of the coal strata also occur. Fining upwards, cross-bedding, ripple-marks, and sharply eroded bottom, are recognised within the quartz sandstone unit. These structural characteristics tend to show that the rock unit was deposited in a point bar of the fluvial environment. Thereby, the depositional environment of the formation is flood plains of meandering rivers. Terrestrial organic input from meandering systems may have restricted the potential of the Sawahlunto Formation to generate significant amounts of hydrocarbons.

Being concomitant with the fine clastic sediment deposition in the deeper part of the basin, thick layers of breccia, conglomerate, and conglomeratic coarse sandstone were deposited as alluvial deposits in the basin margin. De Haan
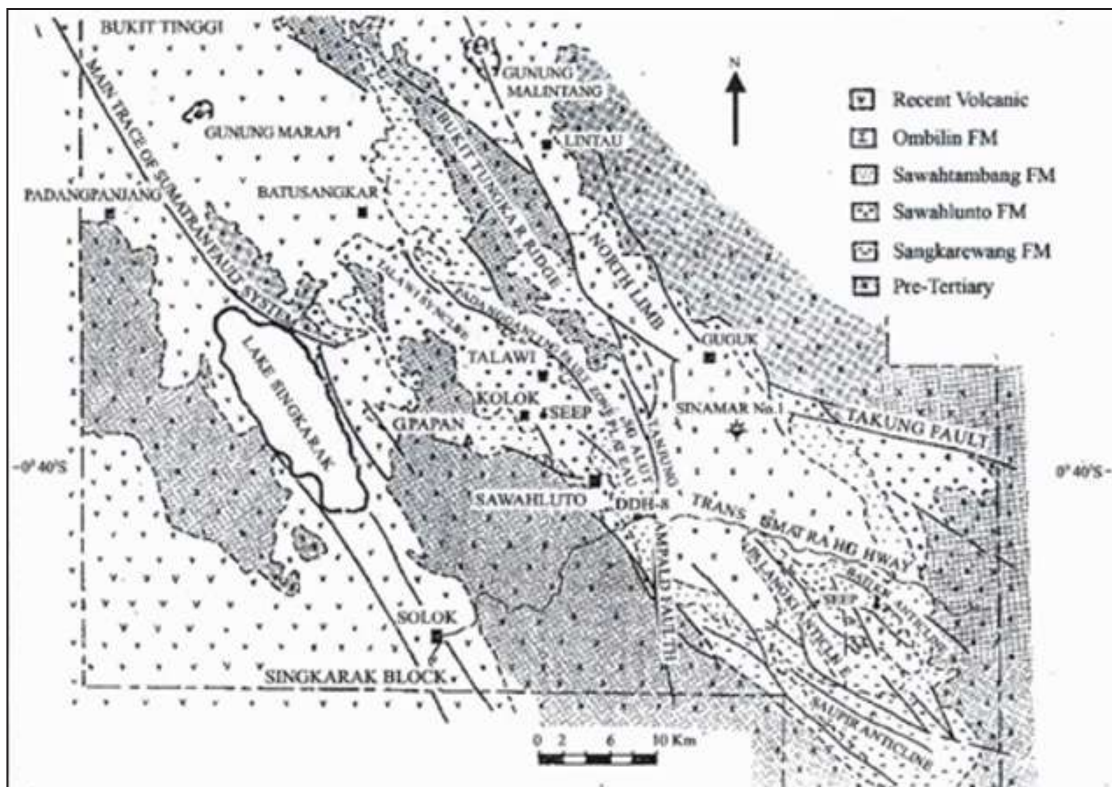
Figure 2.2.5.3. Simplified geological map of the Ombilin Basin (after Koning, 1985).

(1942), and Koesoemadinata and Matasak (1981) called this coarse sedimentary unit as Brani Formation. Along all margins of the Ombilin Basin, the Sangkarewang Formation outcrops intermittently. Stratigraphically, the Sangkare-wang Formation rests unconformably on the Pre-Tertiary rocks, and is conformably overlain by the Sawahlunto Formation.

The Sawahlunto Formation, which is classified as coal measures, was deposited during a regressive period in Early Oligocene to Late Oligocene. The formation characterised by coal layers, mainly comprises brownish grey shales, siltstones and silty shales, and claystones, with minor intercalations of compact brown quartz sandstone, that were deposited mainly in fluvial environments. Shales outcrop as underclays, are carbonaceous, or contain coal fragments and flakes. Coals are commonly interbedded with grey siltstone and coaly siltstone. Splitting and wedging of the coal strata also occur. Fining up-wards, cross-bedding, ripple-marks, and sharply eroded bottom, are recognised within the quartz sandstone unit.

These lithological characteristics tend to show that the rock unit was deposited in a point bar of the fluvial environment. Thereby, the depositional environment of the formation is interpreted as flood plains of meandering rivers. Terrestrial organic input from meandering systems may have restricted the potential of the Sawahlunto Formation to generate significant amounts of hy-drocarbons. The formation conformably underlies and likely interfingers with the Sawahtambang Formation. However, a field observation shows that the Sawahlunto Formation is overlain by

the Sawahtambang Formation with an angular unconformity (Cameron *et al*., 1981).

The Sawahtambang Formation, which was deposited during a braided-river system phase in the Late Oligocene, consists of thick layers of quartz- and feldspathic sandstones, showing cross-bedding structure. In places, intercalations of shales and siltstones, and also conglomerates occur. Thin coal layers and mudstones, which occur at the upper part of the formation, were developed in a meandering system containing peat swamps, probably close to the end of the terrestrial cycle. Fining upward structure characterises the formation. However, in places, a distinct marine incursion evidenced by the presence of a calcareous nannofossil assemblage, occurs near the base of the Sawahtambang Formation. A significant unconformity between the Sawahtambang and the Ombilin Formations is recognised.

During Early Miocene, a transgression phase occurred into the basin. This activity led to the deposition of the Early Miocene Ombilin Formation, comprising light to medium grey, well-bedded, parallel-laminated shales, which are mainly calcareous, and commonly contain nodules of limestone, plant remains, and shells of molluscs; poorly bedded coral limestones; and thin intercalations of glauconitic sandstone also occur. *Globigerinoides primordius* and *Globigerinoides trilobus* contents tend to show the age of N4 - N5 (Early Miocene). The rock unit was deposited in a marine environment, varying from outer neritic to upper bathyal.

2.2.6. Kiliranjao Sub-basin

The Kiliranjao Sub-basin, situated in West Sumatera Province of approximately 30 km to the east of the Ombilin Basin, is filled with siliciclastic-dominated sediments of the Kiliran Formation (Figures 2.2.4.1 and 2.2.6.1). Sedimentation of the rock unit was tectonically controlled (Figures 2.2.6.2 and 2.2.6.3), and it
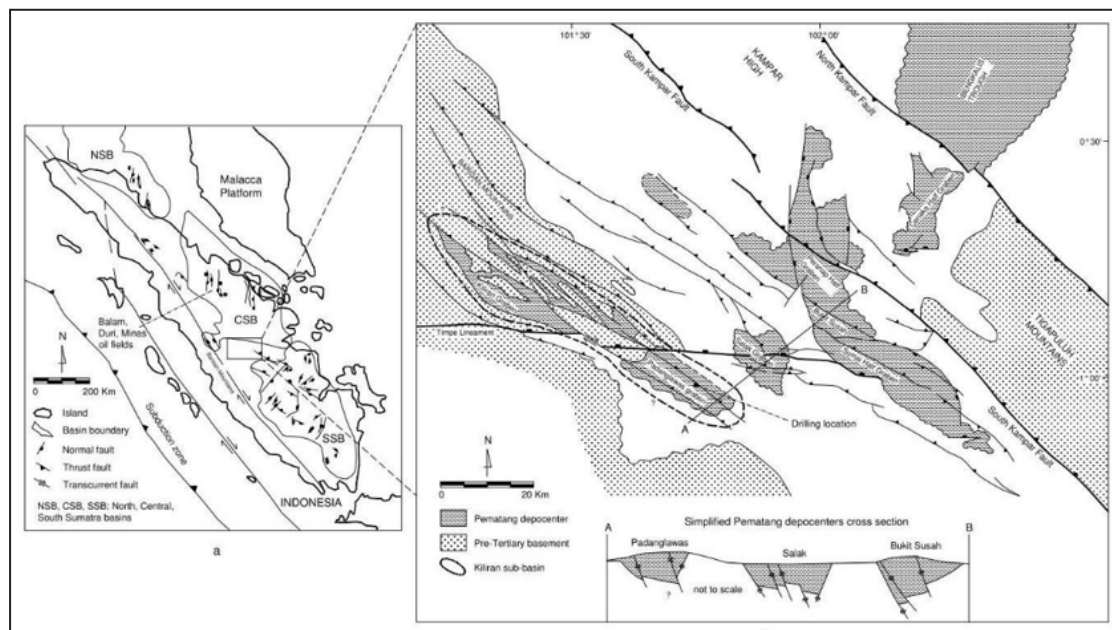
Figure 2.2.6.1. a). Locality map of Kiliranjao and Bukit Susah Sub-basins; b). Geological map with main graben structures, showing arbitrary boundary between Central and South Sumatra Basins containing Pematang depocenters (Widayat, ….; modified after Wain and Jackson, 1995; Darman and Sidi, 2000; PSDG, 2006).

Figure 2.2.6.2. Folded well-bedded oil shale layers of Kiliran Formation, in the Kiliranjao Sub-basin.

Figure 2.2.6.3. Highly faulted Kiliran Formation, recognized at the westernmost part of the sub-basin.

developed in a periodically growing pre-Tertiary half-graben sub-basin. The sedimentary sequence containing oil shale seams was deposited in a la-

custrine to marginal facies. Impressions of woody organic detritus (leaves, twigs, and barks) up to several centimetres in size are common to occur on bedding-plane surfaces within the siltstones (Figure 2.2.6.4).

Figure 2.2.6.4. Impressions of woody organic detritus to several centimetres commonly occur within the siltstone in Kunangan area, Kiliranjao Sub-basin.

The study area is part of the westernmost of the Central Sumatera Basin, one of the Indonesian important oil producing back-arc basins. Even-though, it is probably an isolated small intra-montane basin, present as a southeast-northwestward elongate form (Figures 2.2.4.1 and 2.2.6.1).

Carnell *et al*., 1998) stated that the Kiliran Sub-basin has been assumed as a small rift basin of the Early synrift stage. On the basis of Wain and Jackson (1995), the Kiliran Sub-basin terminates abruptly against the Pre-Tertiary Timpe lineament.

The geology of the study area and its surroundings are shown in Figures 2.2.4.1 and 2.2.6.1. The oldest rock in the study area is the Permo - Carboniferous Kuantan Group, comprising Quartzite (PCkq), Sandstone (PCks), and Limestone (PCkl) Members. All of the Pre-Tertiary rocks outcropping in the study area occur as a basement of the sub-basin filled by Early Tertiary siliciclastic-dominated sediments and

Quaternary Alluvium deposits. Sedimentation of the Tertiary sedimentary unit was tectonically controlled.

The rock formation in the sub-basin so-called Kiliran Formation, generally, comprises a sequence of graben fill sediments, containing variegated shales and mudstones, sandstones, conglomerates, and coals. Predominantly, microlaminated to massive slightly calcareous organic-rich, brown to light grey mudstone forms the unit. The microlaminae occur as dark organic-rich and lighter claystone doublets, reasonable sized fauna have ever lived in the lake are found. Evidence of bioturbation occurs, and bottom conditions are presumed to have been anoxic. The association of frequent freshwater mollusc fossil (Figure 2.2.6.5) and *Botryococcus* algae contents indicates a lacustrine setting. Furthermore, the presence of preserved assemblages of spores and pollen, suggest the occurrence of a freshwater with minor marine incursion environment.

Figure 2.2.6.5. Association of frequent freshwater mollusc fossils in the Kiliran Formation, recognized as a thick horizon.

2.2.7. Bukit Susah Area

Situated in the eastern slope of Barisan Mountains and Bukit Barisan Anticline, physiographically, the study area is interpreted to be an intermontane basin within northwest – southeast direction (Figure 2.2.6.1) (Clarke, 1982). Most likely, the eastern slope of Barisan Mountains extends in northwest – southeast direction, and shows elevation of 150-500 m asl., is part of horst and graben. The Barisan Anticline situated in the southwestern tip of the study area occupies elevation between 500 - 1.000 m asl.

An inverted half-graben, some 20 km south of the Cenako half-graben, was fill with a complex sequence of lacustrine evolution with organic rich, lacustrine mudstones being periodically exposed during tectonically control "low stands" (19). The Bukit Susah feature exhibits several terrain types. Most diagnostic is a riled topography, suggestive of steeply dipping, sedimentary facies – prograding from NW to SE, and were interpreted to represent fan-deltas. A gentler dipping escarpment, visible on the northern flank of Bukit Susah, was interpreted to represent thick, post-rift fluvial clastics, whilst a undulated hilly terrain on the southern flank was interpreted as pre-Tertiary basement (19).

The basin evolved from an initial alluvial-fluvial episode with frequent and prolonged exposure, through a shallow to lake margin-swamps phase, followed by a rapid inundation and drowning. A well established, semi-permanent (?deep) lacustrine phase ensued and, finally, the basin was infilled by coarse-grained alluvial facies which appear to have prograded axially along the basin (19.). The facies are dated palynologically as Early-Mid Oligocene.

At Bukit Susah, the sequence of Kelesa Formation starts with a basal breccia comprising angular to sub-round pebbles of quartzite and phyllite, which overlies Pre-Tertiary basement (Figure 2.2.7.1). Subsequent facies associations include stacked pebbly sands and pebble to cobble grade conglomerates that are laterally discontinuous. Strong burial compaction and the muddy matrix impart little reservoir potential to these facies which are interpreted as alluvial braid-plain sediments. Separating the coarser clastic units is mottled, red to pale grey-green mudstones, silts and poorly sorted sandstones.

Figure 2.2.7.1. Photograph of Kelesa oil shale succession resting directly unconformable upon the pre-Tertiary Gangsal Formation as a basement. Location: Headwater of Putikayu River, Bukit Susah, Riau

Figure 2.2.7.2. Laminated brown shales intercalate with fine-grained sandstone, conglomerates, and red mudstones, in the Puti Kayu River, Bukit Susah.

Figure 2.2.7.3. Photograph of strongly laminate grey shale horizon, probably exceeding 80 m thick. Location: Putikayu River.

In the western part of Bukit Susah, where the Kelesa Formation is thick, thin beds (10 cm) of laminated brown shales intercalate with fine-grained sandstone, conglomerates, and red mudstones (Figure 2.2.7.2). In eastern Bukit Susah, similar relationships are also observed, except that here the brown shales are much better developed and probably exceed 80 m in thickness (Figure 2.2.7.3). Both above and below the brown shales, thick variegated, reddish, pebbly sandstone crops out.

The oldest rock exposed is the Gangsal Formation of Permocarboniferous in age (Figure 2.2.7.1) and is present as the basement of Eo-Oligocene Kelesa Formation. The formation is overlain by the Late Oligocene-Early Miocene Lakat Formation.

2.2.8. East Tigapuluh Mountains

The geology of the area has been described in the Geological Map of Rengat Quadrangle of 1:250.000 in scale (Suwarna *et al*., 1987 and 1991). In general, the study area is located in the Central Sumatra Basin, one of the Indonesian important oil producing back-arc basins. The oldest sedimentary rock in the area is the Eo-Oligocene Kelesa Formation, resting on top of granite wash layer. In turn, the Kelesa Formation is overlain conformably by the Oligocene Lakat Formation (Suwarna *et al*., 1991). Sedimentation process of the units was tectonically controlled. The units developed in a periodically growing pre-Tertiary half-graben.

The Oligocene Lakat Formation, occupying the East Tigapuluh Mountains, lithologically, is subdivided into the lower and upper parts. The lower part comprises thick, fine- to coarse-grained sandstones and occasional interbedded light grey shales with subordinate amounts of conglomerate and mudstone beds, as well as coal and carbonaceous mudstone (Figure.2.2.8.1). This part was deposited as a fluvial deposit with stacking fining-upward cycles. The well-developed sandstone, achieving a thickness of 350 m, generally ill-sorted, conglomeratic, kaolinitic, massive to cross-bedded, and glauconitic. The sandstone is considered to be transported from north to southwards, in the central part of the basin. The Upper Lakat Formation is composed of fluvial channel sandstones, shale, and flood plain/swampy deposits. The shale is grey to green, occasionally calcareous and burrowed. These rocks may represent a sedimentation under submergent conditions of

Figure 2.2.8.1. Photograph of Lakat Formation outcropping in the East Tigapuluh Mountains region.

tidal flat to shallow marine shelf environment. The sequence gradationally overlying the lower part of the formation. The rock distribution in the East Tigapuluh Mountains area is displayed in Figure 2.2.8.2
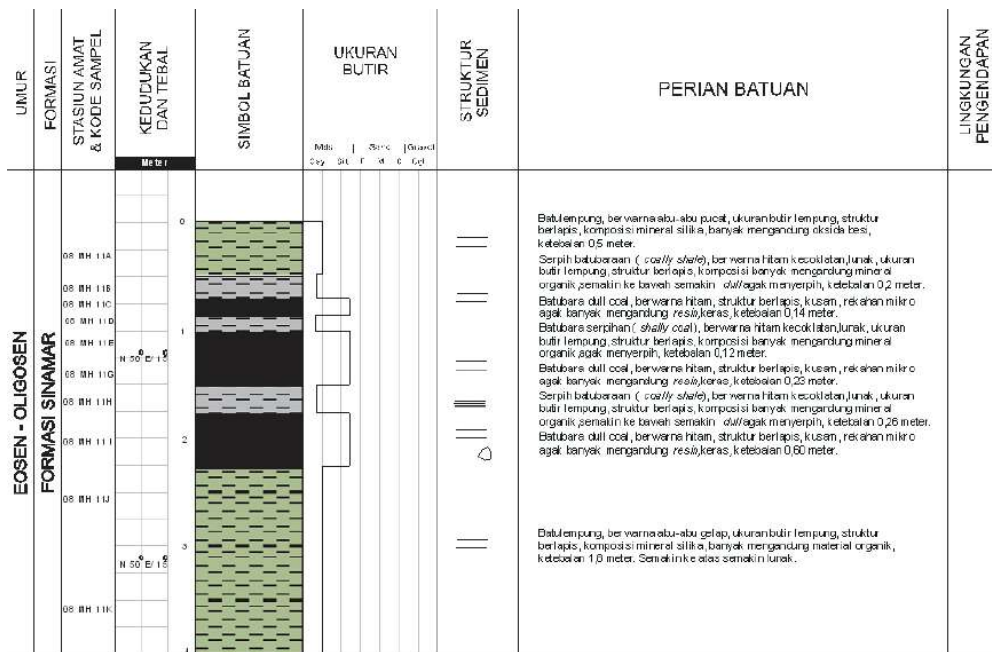
Figure 2.2.8.2. Rock distribution in the East Tigapuluh Mountains region, occupying a small part of the Geological Map of Rengat Quadrangle (modified after Suwarna *et al*., 1991.).

2.2.9. Bukit Bakar Area
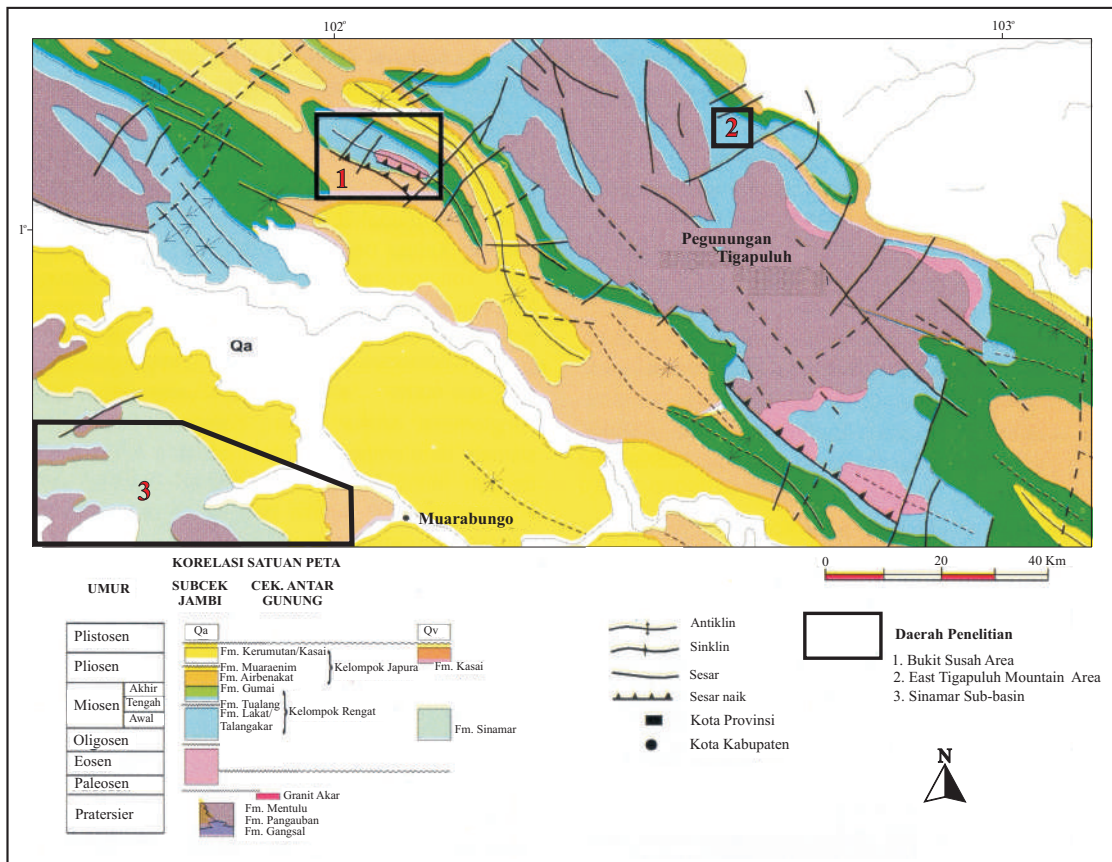
Figure 2.2.9.1. Geological map of Bukit Bakar area, southeastern part of Geological Map of Muarabungo Quadrangle (Simanjuntak et al., 19..).
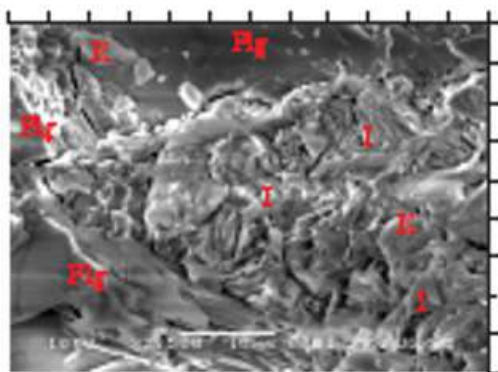
Figure 2.2.9.2. Photograph of Eo-Oligocene oil shale outcrop of the Lahat Formation in Bukit Bakar area.

2.2.10. Sinamar Sub-basin

The Sinamar area is seemingly to be a small isolated or probably an intra-mountain sub-basin, located to the western tip of Jambi Sub-basin (Figure 2.2.10.1). The area occupies the eastern flank of Barisan Mountains and Bukit Barisan Anticline (de Coster, 1974) stretching along northwest-southeast direction, almost parallel to the long axis of Sumatra Island, with elevation of $150 - \geq 1,000$ m asl.

Rosidi *et al*. (1996) described lithology and stratigraphy of the sediments filling-in the sub-basin (1996) and presented in the Geological Map of the Painan and northeastern part of Muarasi-
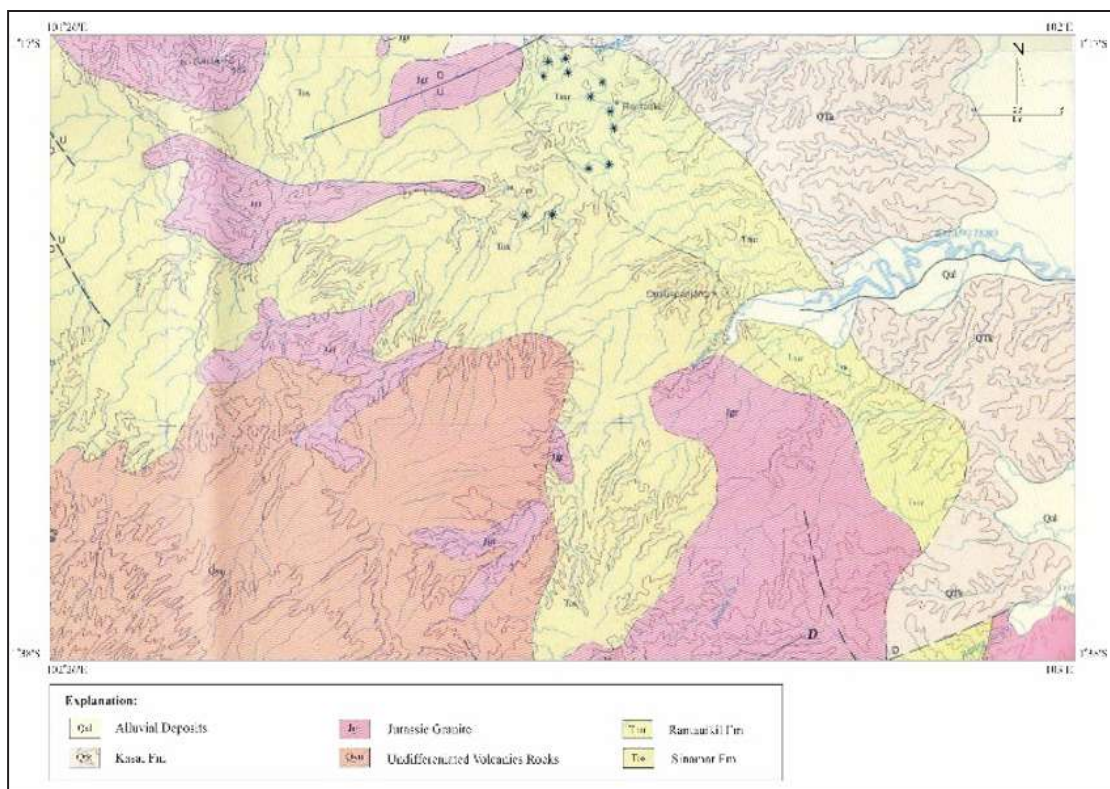
Figure 2.2.10.1. Geological map and the geologically position of isolated or probably an intra-mountain Sinamar Sub-basin, located to the western tip of Jambi Sub-basin, Sumatra (modified after Rosidi et al., 1996).

berut Quadrangle, scale of 1:250.000. The basement of those sediments is Jurassic Granite unit, whilst the sediments filling in the basin comprise Oligocene Sinamar Formation overlain conformably by Oligo-Miocene Rantauikil Formation.

Stratigraphically, the Oligocene Sinamar Formation (Tos) is underlain unconformably by the Jurassic Granite (Jgr). In turns, the Sinamar Formation is conformably overlain by the Oligo-Miocene Rantauikil Formation (Tomr). The youngest unit cropping out is the Plio-Pleistocene Kasai Formation (QTk) overlying unconformably the Rantauikil Formation. The Sinamar Formation comprises conglomeratic sandstone occupying the bottom part of the sequence, then blackish grey claystone, intercalated by coal seam of around 20 cm thick. Upwards, the rock unit is characterized by the presence of massive pebbly

sandstone, shale, shaly claystone, and mudstone. Coal intercalations of 0.30 – 7.0 m in thickness are recognized. The rock unit was deposited in a fluvial – deltaic (Rosidi *et al.*, 1996) or lacustrine paleodepositional environment (Zajuli and Panggabean, 2013). Furthermore, the Rantauikil Formation, predominantly consists of claystone, tuffaceous sandstone, clayey sandstone, and marl, with microforam fossils. Moreover, the Kasai Formation comprises pumiceous tuff and tuffaceous sandstone. Alluvial deposits as the youngest rock unit observed, are made up of riverine pebbles, gravels, sands, and muds.

Configuration and development of the South Sumatra Basin, including Jambi Sub-basin, were close related and controlled by tectonic activity (De Coster, 1974; Eubank and Makki, 1981; Robinson and Kamal, 1988; Heruyono and Vil-

laroel, 1989). It is presumed that the basin is a pull-apart basin bounded by major normal faults due to an eastward oblique movement in Late Cretaceous, between Eurasia Continental Plate and Indian-Australian Plate. Ryacudu (2005) considered that the basin formed in Late Eocene, then developing within Early Oligocene, due to the continuing normal fault movements which then changed in Early Miocene.

Folds and faults, occupying the Tertiary rocks, in general, are in a northwest – southeast direction. However, some are in northeast – southwest directions, even north – south. Folds form anticlinorium groups in accordance with basin configuration present as Early Tertiary paleohighs and grabens. Whilst, directions of faults are varied, especially the subsurface ones (Wahab *et al*., 1982). NW-SE and NE-SW faults cross-cuting each others are in pairs formed in Early Tertiary reactivated in Plio-Pleistocene (Suwarna *et al*., 1984; Gafoer *et al*., 1992, 1993, 1995; and Kusumah *et al*., 2000). Pulunggono *et al*. (1992) also stated that the faults, cutting through anticline-syncline of Sinamar and Rantauikil Formations, show east-west and northeast-southwest directions.

Tectonic evolution present, highly influenced depositional history of South Sumatra Basin (De Coster, 1974; McCourt, 1993). The Late Cretaceous – Early Oligocene period, was the beginning of rifting leading to the formation of grabens and half-grabens, which then formed basement configuration of the South Sumatra Basin. In the same time, fluvial and lacustrine sedimentation took place in the grabens.

Geological structures recognized in the study area are northwest-southeast anticline-syncline structures and normal faults. The faults, cutting through anticline-syncline of Sinamar and Rantauikil Formations, show east-west and northeast-southwest directions (Pulunggono *et al*., 1992).

2.2.11. Asai-Rawas (Kasiro) Sub-basin

Geology of the study area shown on Figure 2.2.11.1 (Suwarna and Suharsono, 1984; Suwarna

et al., 1992) indicates distribution and structure of Jurassic to Quaternary rocks. The study area, focussed on Kasiro Formation (Teok), occurs as an intermontane basin having a narrow size that stretches along the west northwest – south southeast direction, almost parallel to the long axis of Sumatra Island. The region situated in the northeastern flank of Barisan Mountains, is occupied by slightly sloping to steep slope of undulated hilly morphology. The area, in general, comprises pre-Tertiary and Tertiary rocks. Western part of the area is occupied by steep hilly unit which also comprises pre-Tertiary and Tertiary rocks.

The Jurassic Asai Formation (Ja) is the oldest rock exposed in the study area, composed of alternating meta-sandstone, phyllite, slate, silicified siltstone, and greywacke, with intercalations of meta-limestone (Suwarna and Suharsono, 1984; Suwarna *et al*., 1992,1996, 1998, and 2007). This formation is overlain by the Jurassic Mersip limestone (Jm) and Jurassic-Cretaceous Peneta Formation (KJp) comprising slate, shale, siltstone, and sandstone, with limestone intercalations. The pre-Tertiary Asai and Peneta Formations occur as basements of the Tertiary oil shale-bearing sedimentary unit (Kasiro Formation/Teok).

The Eo-Oligocene fine clastic sediments named Kasiro Formation (Teok), situated in a small intra-mountain basin, at the eastern flank of Barisan Mountain, southern Sumatra region, Indonesia (Figure 2.1.1). Geographically, the study areas are bounded by coordinates of 2°25'-2°40' S and 102°10'-102°22' E (Figure 2.2.11.1. The narrow sediment distribution occurring in northwest-southeast direction is almost parallel to the Great Sumatra Fault direction (Figure 2.1.1). The Kasiro shale area bounded by faults, tends to indicate the oil shale deposits were accumulated within a "syn-rift" basin.

2.3. Geological Zone

Based on the sedimentation process and tectonic influence, geological characteristics of oil shale-bearing unit, deposited within the nine studied areas mentioned above, can be divided

Figure 2.2.11.1 Geological map of the study area and its surroundings (after Suwarna and Suharsono, 1984; Suwarna *et al*., 1992; Suwarna *et al*., 2007).

into three groups, those are: simple geology zone, moderate geology zone, and complex geology zone.

2.3.1. Simple Geology Zone

Oil shale deposits within this zone, in general, are not influenced by tectonic activity, such as fault, fold, and or intrusion. Position of the sediments is nearly flat, and laterally continuous till hundreds to thousands of meters. Laterally, the thickness and quality of oil shale layer is quite similar. This group can be recognized in the central part of Central Sumatra Basin and Sinamar area

2.3.2. Moderate Geology Zone

This zone is occupied by the oil shale deposited within varieted sedimentation condition, and has altered to special level, post-sedimentation and tectonic influence. Some faults and fold of moderately level. Moderate dip of bed and lateral thickness variation, and splitting develops. Oil shale quality is directly related to the changes level, both on the sedimentation process and post-sedimentation. In places, igneous intrusion influences bed structure and oil shale quality. This group can be recognized in the South Sumatra Basin.

2.3.3. Complex Geology Zone

Oil shale exposed was commonly deposited within a complex sedimentation system or has been deformed intensely, which led to the formation of oil shale beds in varieted thickness. Quality of the oil shale was highly affected by the changes taking place during sedimentation process or post-sedimentation, such as fracturing. Tight faulting and folding occurred, therefore, the oil shale layer is difficult to be correlated, and tend to be present in steep dipping. Laterally, oil shale distribution is limited. Group of oil shale of this zone occupies the western part of Sumatra including Ombilin Basin, Sinamar, Asai-Rawas, Bukit Susah, and East Tigapuluh Mountains Areas.

3. ANALYTICAL PROCEDURE AND METHODS

In order to achieve the aims of this study, various geologic field investigations and laboratory techniques were used. Primary fieldwork activity includes accurate determination, observations, and measurement on sedimentology, paleontology, organic matter characteristics, and detailed stratigraphy of the strata containing oil shales. Afterwards, collection of field data and samples for geochemical including pyrolysis, sedimentological, organic petrographic, and paleontological analysis purposes were carried out.

The laboratory techniques predominantly deal with hydrocarbon potential, organic matter content, mineralogy, palynology, and fossil content of the shales and mudstones forming the formation. The techniques are based on detailed analyses of petrographic and geochemical characteristics of the organic matter (DOM) and fine-grained clastics (shales and mudstones).

By measuring the quantity, quality, and state of thermal maturity of the contained organic matter, it is possible to understand the origin of hydrocarbon accumulations and potential, and to predict areas of most favourable for future exploration. Furthermore, to gain effective source rock information, determination on its organic content, organic type, and thermal maturity have to be conducted.

The grade of oil shale has been determined by many different methods with the results expressed in a variety of units. The heating value of the oil shale may be determined using a calorimeter. Values obtained by this method are reported in English or metric units, such as Btu/pound of oil shale, cal/gm rock, kcal/kg rock, MJ/kg rock, and other units. The heating value is useful for determining the quality of an oil shale that is burned directly in a power plant to produce electricity. Although the heating value of a given oil shale is a useful and fundamental property of the rock, it does not provide information on the amounts of shale oil or combustible gas that would be yielded by retorting (destructive distillation).

3.1 Organic Petrology

The pinpoint characterization tools used in organic petrology to assess the thermal evolution of the organic constituents are based on the visual assessment or direct measurement of optical properties, either in transmitted light on palynologic residues, or in incident light on polished sections. As diagenetic evolution proceeds, the actual physical and chemical properties of the macerals alter and tend to converge. The whole organic content evolves progressively towards a carbon residue. When possible, the direct measurement of these properties (transmittance in transmitted light, reflectance in natural incident light and fluorescence under UV incident excitation) thus allows one to record the thermal evolution of the different organic constituents.

3.1.1. Maceral Analysis

The laboratory technique, performed in organic petrology mode, is important to have a better understanding of the macerals and mineral matter contents and characteristics. Interpretations of organic facies are based on semi-quantitative organic petrological examinations of selected organic matter assemblages. Petrographic analysis required for the study was focused on macerals determination, especially exinite macerals and vitrinite reflectance.

The samples were prepared as polished briquettes or blocks by using Australian Standard procedures (Australian Standards 2061 and 2856, 1986). The polished briquettes were prepared from crushed 1 mm-size samples reprinting each sample, which then mounted in epoxy resin. Maceral composition and characteristics of the samples are gained from semi-quantitative examinations of polished samples.

The analysis determines quantitatively the volume of organically derived, microscopically recognizable substances of organic matter, which are defined by their morphology and colour. The methods used for estimating organic carbon abundance, maceral type and composition, and vitrinite reflectance are outlined in Cook and Kantsler (1982), Sappal (1986), and Struckmeyer and Felton (1990).

Optical method used in organic petrology analysis is reflected light method with and without fluorescence mode. The main advantage is to discriminate and locate organic matter of different types and macerals, and to measure their respective rank of evolution path. The analysis provides different types of information on the thermal evolution of organic matter, particularly based on vitrinite reflectance measurements. The vitrinite reflectance now considered as one of the best parameters to define coalification stages, its measurements are extended to particles of disseminated organic matter (DOM) occurring in shales and mudstones. Thermal evolution of the source rocks, during diagenesis, catagenesis, and metagenesis, will change many physical or chemical properties of the organic matter. These properties are considered to be indicators for maturation.

The analysis based on 500 counts on each sample under reflected white light, was performed microscopically on polished sample sections. Ordinary white reflected light from a tungsten lamp and violet-blue light from a high-pressure mercury lamp to initiate fluorescence were used for illumination. Maceral observation was conducted on a Leitz MPV-2 photomicroscope in GRDC (Figure 3.1) and Tekmira (Figure 3.2) Laboratories.

Most macerals determined are defined by the International Committee for Coal Geology (ICCP, 1963 and 1971). Hutton (1980) introduced alginite A and B terms, based on their significant morphological differences between constituents of the alginite. Alginite A or telalginite is defined as discrete colonial or unicellular algal bodies related to either *Botryococcus* or *Pachysphaera (*Figure 3.3a*)*, whilst alginite B or lamalginite comprises a small unicellular or thin-walled colonial alginite, derived from benthonic algae, planktonic algae or related organism (Figure 3.3b).

Depending upon the sample, different optical characteristics of the amorphous organic matter (color, grain size, texture) are observed. Combat proposed, a classification of the amorphous organic matter into "grumeleuse" (curdled), "granuleuse" (granular), "sub-colloidal", "pelliculaire" (as pellicles) and "gelifide" (gelified).

Figure 3.1. A Leitz MPV-2 photomicroscope in GRDC (Geological Research and Development Centre; now Centre of Geological Survey) Laboratory used to analyze maceral observation, including type of macerals, vitrinite reflectance, and thermal alteration index, all operated in reflected white light and on fluorescence modes.

Figure 3.2. A Leitz MPV-2 photomicroscope in Tekmira Laboratory used to analyze maceral observation, including type of macerals, vitrinite reflectance, and thermal alteration index, all in reflected white light and on fluorescence modes.

Recent work using transmitted electron microscopy has shown that structures can be revealed in amorphous organic matter on a scale finer than that of optical microscopy (Raynaud *et al*., 1990). Indeed, it is possible to observe fibrous structures, the nature of which has not yet been established, sometimes associated with ovoid particles resembling bacterial bodies.
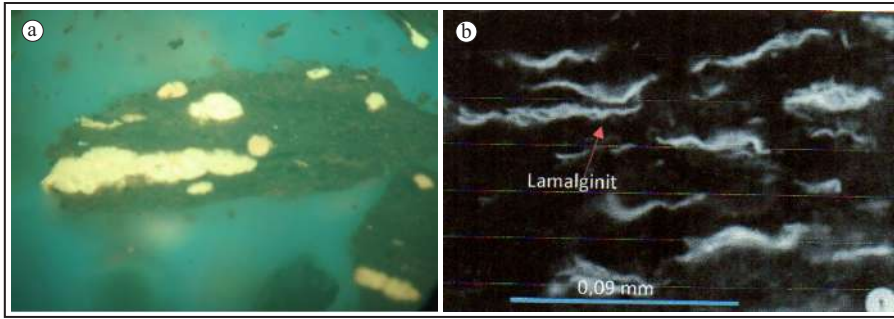
Figure 3.3. Photomicrographs of: a). Alginite A or telalginite forming discrete colonial or unicellular algal bodies (*Botryococcus* or *Pachysphaera*); b). Alginite B or lamalginite Rundle Type; a small unicellular or thin-walled colonial alginite, forming a parallel layer. a and b in fluorescence mode.

3.1.2. Vitrinite Reflectance (Rv)

Thermal maturity of organic matter in oil shale is also determined by the reflectance of vitrinite (a common constituent of coal derived from vascular land plants), if present in the rock. Vitrinite reflectance is commonly used by petroleum explorationists to determine the degree of thermal alteration of petroleum source rocks in a sedimentary basin. A scale of vitrinite reflectances has been developed that indicates when the organic matter in a sedimentary rock has reached temperatures high enough to generate oil and gas. However, this method can pose a problem with respect to oil shale, because the reflectance of vitrinite may be suppressed by the presence of lipid-rich organic matter. Equipments used are shown on Figures 3.1 and 3.2, presented above.

Vitrinite may be difficult to recognize in oil shale because it resembles other organic material of algal origin and may not have the same reflectance response as vitrinite, thereby leading to erroneous conclusions. For this reason, it may be necessary to measure vitrinite reflectance from laterally equivalent vitrinite-bearing rocks that lack the algal material.

In areas where the rocks have been subjected to complex folding and faulting or have been intruded by igneous rocks, the geothermal maturity of the oil shale should be evaluated for proper determination of the economic potential of the deposit.

Vitrinite reflectance remains the best indicator for day-to-day source rock maturity evaluation, although it should be identified carefully and used as a succession versus depth of histograms. Results should be cross-checked with other thermal indicators.

3.1.3. Thermal Alteration Index (TAI)/Spore Colour Index (SCI)

Organic petrographers are able to assess rapidly the rank of a sample by employing a set of criteria related to the colour, transparency or morphology of components of isolated organic matter in slides (Gutjahr, 1966), and reflectance of vitrinite in polished blocks. The need to express this evaluation on a scale common to all users, led them to evaluate the progressive darkening of spores and pollen by the use of a visual chart (Figures 3.4, 3.5, and 3.6). The Thermal Alteration Index or TAI (Correia, 1967; Staplin, 1969) ranges from a value of 1 for the strictly immature spores and pollen (pale-yellow in color) to a value of 5 for those having undergone a strong thermal evolution corresponding to the dry-gas zone or above (dark-brown color). The weakness of this method is related to the subjectivity of the observation in assessing the TAI as well as the sedimentary and botanic diversity of the microfossils.

3.2. SEM and XRD

SEM and X-ray diffraction (XRD) techniques were used to study the mineralogy of oil shale and its associated sedimentary rocks. The XRD analysis is focused on the identification of clay

35
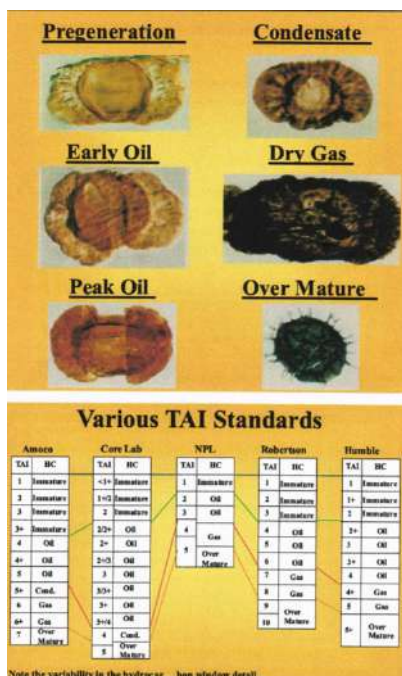
Figure 3.4. Various TAI (Thermal Alteration Index) Standards used in measuring thermal maturity level.

bulk composition and mineralogy, whilst the SEM analysis has been applied particularly to identify the mineral constituents such as clay minerals, as well as to study concerning rock diagenesis (Pittman, 1979, Wilson and Pittman, 1977). Organic matter can also be identified by Scanning Electron Microscope (SEM). The most significance feature of SEM is that it enables to provide excellent information for revealing the type of rocks, organic and bitumen constituents, diagenesis feature and regime, and also the property of rocks.

In fact, this analysis reveals the oil shale characters in the study area. The texture and mineral identification are generally based on Scholle (1979), Wilson (1984), Wilson and Pittman (1977), and Schmidt and McDonald (1979).

Diagenesis characters are identified by the presence of authigenic clays, such as kaolinite and smectite-illite, but compaction and crystal orientations are also significantly indicators. All observations regarding SEM and XRD-modes were carried out in GRDC's Laboratory.

3.3. Organic Geochemical Analysis

In order to analyze organic geochemistry, screening tests comprising total organic content (TOC), Rock-Eval pyrolysis, and also Retort Oven analysis are conducted in Lemigas

Laboratory, Jakarta. Pyrolytic assay provides information on generation potential (ultimate

Figure 3.5. Munsell spore/pollen colour standard showing thermal maturity level of organic matter (Humble Geochemical; Division of Humble Instruments and Services, Inc.).

Figure 3.6. Spore/pollen colour index showing level of Thermal Alteration Index (TAI) and Spore Colour Index (SCI) (modified from Traverse *et al*., 2007 and Almash-ramah, 2011; in Saeed, 2013).

hydrocarbon yield) and expected hydrocarbon product (gas and/or oil). Furthermore, the 'Rock-Eval' pyrolysis, with its limitations, can be used to characterize the type of organic matter and the general nature of the hydrocarbon product (*e.g.* oil vs. gas) which will be generated upon thermal maturation (Espitalie *et al*., 1977; Katz, 1983). This characterization is accomplished using a modified Van Krevelen diagram, where the hydrogen index (HI = S2/TOC) is substituted for atomic O/C ratio obtained from isolated kerogen.

3.3.1. Rock-Eval Pyrolysis

The quantities of organic matter in oil shale samples were determined on the basis of the total content of organic carbon (TOC) measured by LECO analyzer and on genetic potential (GP/Py; the sum of S1 and S2 values) established by Rock-Eval pyrolysis. Hydrogen index HI (S_2/TOC) and oxygen index OI ($_{S3}$/TOC) were used to characterize the kerogen type. A plot of these indices on a van Krevelen diagram shows the type of organic matter present in oil shale samples. Production index $S_1/(S_1+S_2)$ and T_{max} were used to characterize the maturity of kerogen.

The Rock-Eval pyrolysis provides information on generation potential (ultimate hydrocarbon

yield) and expected hydrocarbon product (gas and/or oil). The total generation potential (S_1+S_2) is free distillable hydrocarbons + generatable hydrocarbons. The analysis can with limitations, be used to characterize type of organic matter and general nature of the hydrocarbon products (*i.e.* oil *vs*. gas) which would be generated upon thermal maturation (Espitalie *et al*., 1977; Katz, 1983).

This characterization is accomplished using a modified van Krevelen diagram, where the Hydrogen Index (HI= S_2/TOC: S_3 represents organically derived CO_2) is substituted for the atomic O/C ratio obtained from isolated kerogen.

3.3.2. Retort Oven Analysis

The grade of oil shale can be determined by measuring the yield of oil of a shale sample in a laboratory retort. This is perhaps the most common type of analysis that is currently used to evaluate an oil-shale resource. The process was carried out in Lemigas Laboratory, Jakarta. The method commonly used in the United States is called the "modified Fischer assay," first developed in Germany, then adapted by the U.S. Bureau of Mines for analyzing oil shale of the Green River Formation in the western United States (Stanfield and Frost, 1949). The technique was subsequently standardized as the American Society for Testing and Materials Method D-3904-80 (1984). Some laboratories have further modified the Fischer assay method to better evaluate different types of oil shale and different methods of oil-shale processing.

The standardized Fischer assay method consists of heating a 100-g sample crushed to –8 mesh (2.38-mm mesh) screen in a small aluminium retort to 500ºC at a rate of 12ºC per minute and held at that temperature for 40 minutes. The distilled vapors of oil, gas, and water are passed through a condenser cooled with ice water into a graduated centrifuge tube. The oil and water are then separated by centrifuging. The quantities reported are the weight percentages of shale oil (and its specific gravity), water, shale residue, and "gas plus loss" by difference.

The Fischer assay method does not determine the total available energy in an oil shale. When oil

shale is retorted, the organic matter decomposes into oil, gas, and a residue of carbon char remaining in the retorted shale. The amounts of individual gases—chiefly hydrocarbons, hydrogen, and carbon dioxide—are not normally determined but are reported collectively as "gas plus loss," which is the difference of 100 weight percent minus the sum of the weights of oil, water, and spent shale. Some oil shales may have a greater energy potential than that reported by the Fischer assay method depending on the components of the "gas plus loss"

The Fischer assay method also does not necessarily indicate the maximum amount of oil that can be produced by a given oil shale. Other retorting methods, such as the Tosco II process, are known to yield in excess of 100 percent of the yield reported by Fischer assay. In fact, special methods of retorting, such as the Hytort process, can increase oil yields of some oil shales by as much as three to four times the yield obtained by the Fischer assay method (Schora *et al*., 1983; Dyni *et al*., 1990). At best, the Fischer assay method only approximates the energy potential of an oil-shale deposit.

Newer techniques for evaluating oil-shale resources include the Rock-Eval and the "material-balance" Fischer assay methods. Both give more complete information about the grade of oil shale, but are not widely used. The modified Fischer assay, or close variations thereof, is still the major source of information for most of the deposits.

Shale oil is produced from the organic matter in oil shale when the rock is heated in the absence of oxygen (destructive distillation). This heating process is called retorting, and the equipment that is used to do the heating is known as a retort. The rate at which the oil is produced depends upon the temperature at which the shale is retorted. Most references report retorting temperatures as being about 500°C (930°F).

It would be useful to develop a simple and reliable assay method for determining the energy potential of an oil shale that would include the total heat energy and the amounts of oil, water, combustible gases including hydrogen, and char in sample residue.

To explain a geochemical framework against the nature of any hydrocarbons produced from the oil-shale samples for forthcoming exploration is the main purpose of geochemical analysis.

Collecting freshest possible oil shale samples were carried out, and their weathering rinds were removed both in the field and as well as in the laboratory. The relatively freshest exposures used in the study, but the surfaces of the oil shales had already been weathered to a buff color, varies from pale grey to brown.

3.4. Palynological Analysis

Palynology is the only biostratigraphic technique which permits crossfacies correlation, and the only micropaleontological method for correlation of non-marine sediments (Morley, 1991). The analysis can also be used to determine a relative age and depositional environment of the rock occupied by the pollen analyzed. Under standard palynological preparation method, commonly used in palynology analysis, selected samples were prepared by using HCl, HF, $ZnCl_2$, KOH, and acetolysis.

3.5. GC-MS

Oil generated from source rocks containing land plant material are generally light, highly paraffinic, with a high wax content (Hedberg, 1968). They characteristically have a high pristane/phytane (> 3.0) and pristane/nC_{17} (> 1.0) ratios due to deposition of the source rocks under relatively low reducing conditions and a relatively low pH e.g. in peat swamp environments (Sofer *et al*., 1989). It is possible to distinguish oils derived from terrigenous source material on the basis of their biomarker distributions. The depositional environment and maturity level of the source rocks having generated the crude oils may also be estimated. In certain cases, it is also possible to distinguish oils from different geologic periods. The presence of 18α(H)-oleanane, for example, appears to be indicative of Tertiary oils containing a significant proportion of terrigenous source material (Philp and Gilbert, 1986).

3.5.1. Gas Chromatography

The saturated hydrocarbon fractions were analyzed using a HP 5890A Chromatograph equipped

with a flame ionization detector (FID) and a 50 m x 0.31 mm fused silica capillary column coated with crosslinked methyl silicone (OV-1).

Gas chromatography (GC) is a widely applied technique in many branches of science and technology. Over half a century, GC has played a fundamental role in determining how many components and in what proportion they exist in a mixture (Stashenko and Martinez, 2014). Due to the ability to establish the nature and chemical structure of these separated and quantified compounds is ambiguous and reduced, it requires a spectroscopic detection system. The most used is the mass spectrometric detector (MSD), which allows obtaining the "fingerprint" of the molecule, i.e., its mass spectrum. Mass spectra provide information on the molecular weight, elemental composition, if a high-resolution mass spectrometer is used, functional groups present, and, in some cases, the geometry and spatial isomerism of the molecule.

In a gas chromatographic system, the sample to be analyzed may be a liquid solution or a collection of molecules adsorbed on a surface, e.g., the solid-phase microextraction (SPME) system. During the transfer into the GC, the sample is volatilized by rapid exposure to a zone kept at relatively high temperature (200-300°C) and mixed with a stream of carrier gas (Ar, He, N_2, or H_2). The resulting gaseous mixture enters the separation section, a chromatographic column, which in its current version is a fused-silica tubular capillary coated internally with a thin polymer film. For correct GC operation, among other conditions, this gateway to the column should remain unpolluted, clean, inert, and leak-free. The main requirement for an analyte in GC is that it should be volatile enough to be present in detectable amounts in the mobile phase.

3.5.2. Gas Chromatography-Mass Spectrometry

GC-MS (Gas Chromatography-Mass Spectrometry) is highly effective and versatile analytical techniques with numerous scientific applications to cater the field of applied Sciences and Technology. This review elaborates the significant uses of this technique. It is a very useful for analytical research

and quality control, as well as impurity profiling and maintenance for human welfare and development (Chauhan *et al*., 2014). These techniques (GC-MS) is a hyphenated analytical technique that combines the separation properties of gas-liquid chromatography with the detection feature of mass spectrometry to identify different substances within a test sample (Figure 3.8.??).
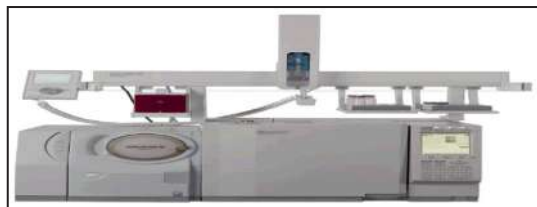
Figure 3.8. An example of typical GC-MS with head space of Shimazu Company (Chauhan *et al*., 2014).

Stashenko and Martinez (2014) stated that gas chromatography (GC) is a widely applied technique in many branches of science and technology. For over half a century, GC has played a fundamental role in determining how many components and in what proportion they exist in a mixture. However, the ability to establish the nature and chemical structure of these separated and quantified compounds is ambiguous and reduced, which requires a spectroscopic detection system.

Liquids, gases, or solids can be analyzed. For liquids and gases the sample is commonly directly injected into the GC. For solids, the analysis is carried out by solvent extraction, outgassing (desorption) or pyrolysis. Desorption experiments are performed under helium flow at a controlled temperature between 40-300 ºC, with analytes being collected on a cryogenic trap during desorption. The sample chamber is a 1.25"x4" cylinder.

GC-MS is used for analyzing aromatic solvents, sulphur, impurities in polypropylene, sulphur in methane, natural gases, 1,3 butadiene, ethylene, gas oil, unleaded gasoline, polyethene, diesel.oil, unleaded gasoline, polyethylene, diesel, modified biomass, grafted polymers etc. GC-MS has triggered a new arena of research and taken to new heights

of impactful presentation and characterization of compounds by its wide range of applications.

GC-MS analysis of the saturated hydrocarbon fractions was made using a KRATOS MS25RFA mass spectrometer coupled to a Carlo Erba gas chromatograph fitted with a 25 m x 0.31 mm i.d., CP-Sil 5-CB fused silica with a rate flow rate of 2 ml/min. each sample was injected in the split mode (25:1) at 50° C and programmed to 160°Cat 5°C/min and then to 280°C at 3°/min with a final hold at 100 µA, electron ionization energy of 70 eV and ion source temperature of 240°C. data were acquired and processed using an SS90 Data System.

Apart from the full scan mode, the samples were also analyzed using using the Selected Metastable Monitoring (SMIM) technique by monitoring metastable transition; M^+ --217^+ for steranes and M^+ -- 191^+ for triterpanes, where M^+ is the molecular ion.

GC requires the analyte to have significant vapor pressure between 30 and 300°C. GC presents a insufficient proof of the nature of the detected compounds. The identification is based on retention time matching that may be inaccurate or misleading. GC-MS represents the mass of a given particle (Da) to the number (z) of electrostatic charges (e) that the particle carries. The term m/z is measured in DA/e. GCMS commonly uses electron impact (EI) and chemical ionization (CI) techniques.

The volatile and thermally stable substitutes in a sample can be separated by GC, whereas GC-MS fragments the analyte to be identified on the basis of its mass. The further addition of mass spectrometer in it leads to GC-MS/MS. Superior performance is achieved by single and triple quadrupole modes.

Significantly enhanced molecular ions that are always observed, isomer and structurally significant mass spectral peaks and extended range of low volatilite hydrocarbons that are amenable for analysis including waxes up to $C_{74}H_{150}$ makes the GC-MS a most valuable technique. Broad range of petrochemicals, fuels and hydrocarbon mixtures, including gasoline, kerosene, naphthenic acids, diesel fuel, various oil types, transformer oil, disesl and biodiesel, natural gases, wax and broad range of geochemical samples, aromatic solvents, impurities in polypropylene, sulphur in methane, ethylene, polyethene, unleaded gasoline, polyethylene, can be analyzed by GC-MS.

GC-MS has triggered a new arena of research and taken to new heights of impactful presentation and characterization of compounds by its wide range of applications. GC-MS is an advanced technique that cannot be compared with other modern analytical equipment but can be complemented by mass spectrophotometer to achieve GC-MS/MS. It has broad range of applications that caters to academic research, quality control as well as industrial applications. This versatile analytical technique could be explored for better prospects in future.

The need to unequivocally identify the components of complex mixtures was the motivation for the development of different instrumental coupling techniques (tandem), including the widely and successfully used (with volatilizable substances), gas chromatography coupled with mass spectrometry (MS). GC-MS is an extremely favorable, synergistic union, as the compounds susceptible to be analyzed by GC (low-molecular weight, medium or low polarity, in ppb-ppm concentration) are also compatible with the MS requirements.

3.5.3. API gravity

API gravity is normally used as a first checkpoint on crude oils. The values can be used to classify crude oils into biodegraded/water washed oils, normal oils, and condensates, and also gives a crude measure of thermal maturity. Oils with low API gravities (10 to 25°) are classified as immature, while oils with high API gravities (35 to 60°) are classified as mature. Additional factors affecting API gravity include biodegradation and water washing (both increase the API gravity.

The API gravity values for the oils analyzed in this study are given in Table 1. The API gravities for normal, non-waxy oils range from 30 to 38°, and for waxy oils, the API gravities range from 34 – 46°. Biodegraded oils are usually associated with low API gravities, generally below 25°.

4. SEDIMENTOLOGY

Since 2000 to 2005, Geological Research and Development Centre had conducted oil shale researches in the selected sites of Sumatra Island (Figure 4.1.). Furthermore, in 2008, the activity continued to take place in the Sinamar area, Jambi Province. Moreover, in 204 and 2005, Centre of Geological Survey, Geological Agency carried out oil shale investigation in Bukit Bakar and respectively.

4.1. Kabanjahe

On the basis of lithofacies assemblage, the formation can be subdivised into three members (Kusumahbrata *et al.*, 2002), starting with the lower portion at the base and progressing upward through the middle and upper portions, those are termed as the Lower, Middle, and Upper Members.

The Lower Member unconformably overlies dolomitic crystalline limestone of the Kluet Formation acting as a basement of the basin (Figure 4.1.1). The member showing thickness of approximately 55 m comprises alternating mudstone, shale, and fine- to medium-grained sandstone (Figure 4.1.2). Horizontal and wavy laminations are common. Depositional environment of the sediment is interpreted as a floodplain area of a meandering river system.

The Middle Member of the Butar Formation is characterized by a sedimentary sequence of 60 m thick and fining-upward type (Figure 4.1.1). The sediments comprise sandstone commonly conglomeratic, mudstones, siltstone, and shale (Figure 4.1.2). The sequence is a massive sandstone unit (Figure 4.1.3). Sedimentary structures recognized are parallel and wavy laminations, ripple marks, and cross-lamination (Figure 4.1.4). Trace fossils are common (Figure 4.1.5). Environment of deposition might be flood plains and abandoned channels of a meandering system or tidal environment.

The Upper Member of Butar Formation forming a 60-m thick sequence (Figures 4.1.6 - 4.1.8) is dominated by shale, claystone, and mudstone beds, with intercalations of fine-grained sandstone. The shale sequence is part of an extensive, organic-rich shale depositional system covering large areas of the Kabanjahe Basin.

The shale showing variated colour and density, is fissile - papery to flaggy, containing carbonaceous/humic matter (Figure 4.1.9) and some are calcareous with foraminifera fossil (Figures 4.1.10 and 4.1.11). In some places, thin coal beds (30 cm thick) occur in limited lateral distributions. Well-developed sedimentary structures are parallel and wavy laminations.

The member crops out around the rim of the sub-basin. Depositional environment of the unit is presumed to be a meandering river influenced by a marine incursion, evidenced by the presence of plenty framboidal pyrite content (Figure 4.1.12), micro-foraminifera fossil, and a palynomorph assemblage.

Silica components (quartz) dominate the black shales, showing values of 46.0 to 72.0 %, except in Sarinembah, where the quartz contents are 32 %. The shales also contain abundant calcite, smectite-montmorillonite, and smectite-illite, with common kaolinite and illite (Figure 4.1.13). Calcite (Figure 4.1.14) and iron oxide cements (Figure 4.1.15) also observed. The minerals recognized by SEM and XRD are presented in Table 4.1.

Palynological study reveals the occurrence of *Pometia*, *Florschuetzia trilobata*, *Dicolpopollis malesianus*, *Crasoretitriletes vanraadshooveni*, and *Verrucatosporites usmensis* within shales. This assemblage tends to indicate a littoral depositional environment. Additionally, the presence of *Crasoretitriletes vanraadshooveni* and *Verrucatosporites usmensis* indicates Late Eocene age.

4.2. Kapur IX

Stratigraphic setting of the Kapur IX region is referred to Kusdji *et al*. (2001). Geologic investigation was carried out in Kototuo, Kotobangun,
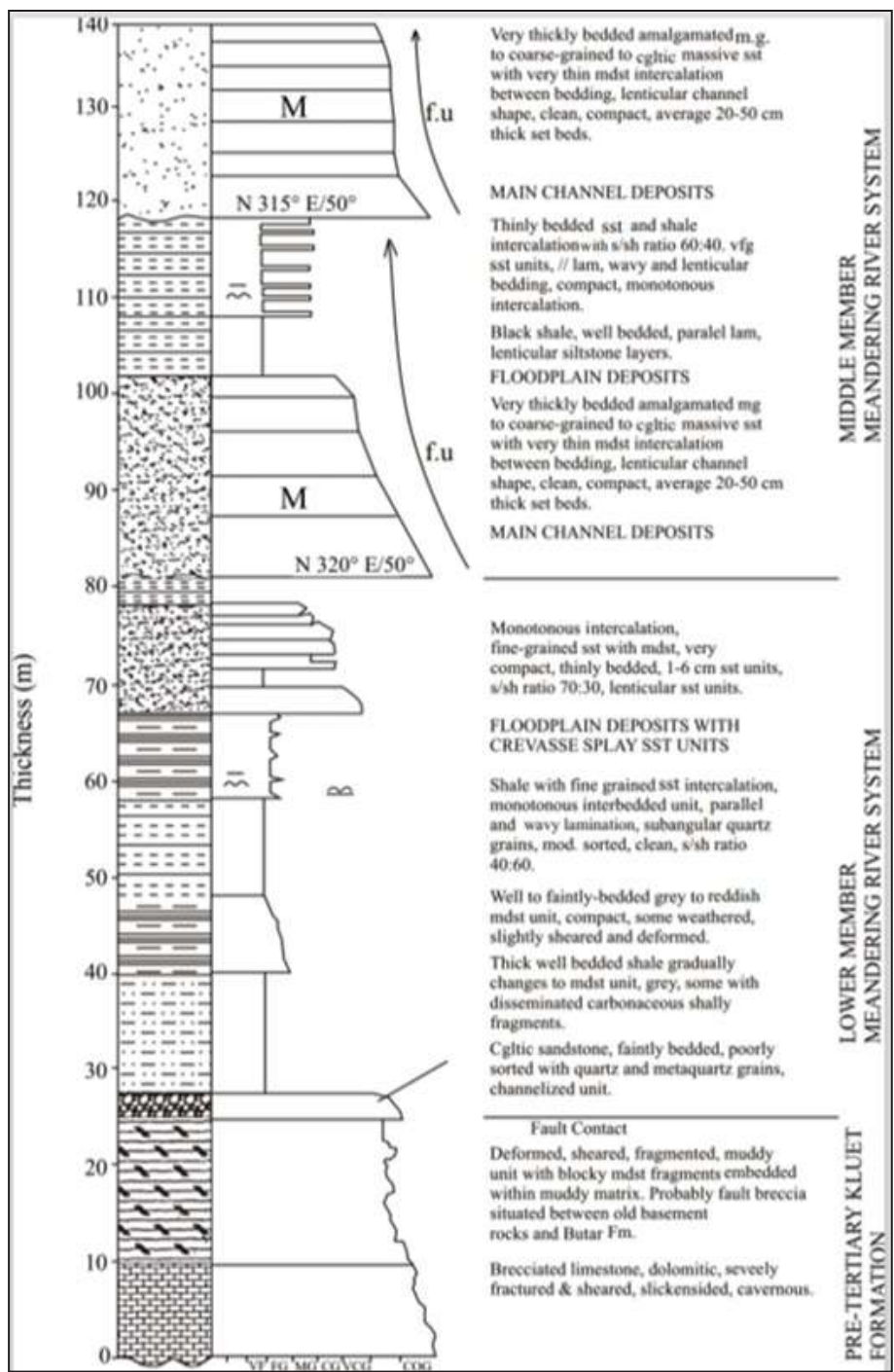
Figure 4.1.1. Columnar measured section of Lower and Middle Members of Butar Formation, showing the Lower Member unconformably overlies the dolomitic crystalline limestone of the Kluet Formation nearby Butar Village (Kusumahbrata, 2002).
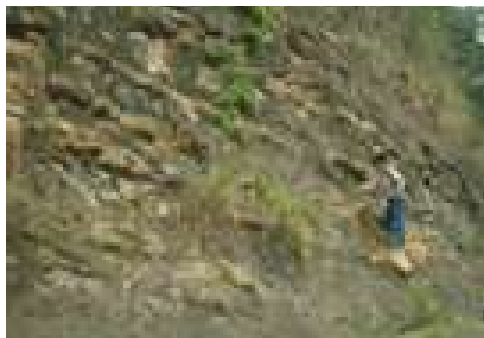
Figure 4.1.2. Alternating light to dark grey mudstone and fine-grained sandstone of the Middle Member of Butar Formation. Location: Around 3 km to the north of Perbesi Village. (Kusumahbrata, 2002).

Figure 4.1.3. Outcrop of thick-bedded to massive sandstone, containing intercalations of claystone of Middle Member of Butar Formation, present as a channel deposit of wide and deep main river (Kusumahbrata, 2002).
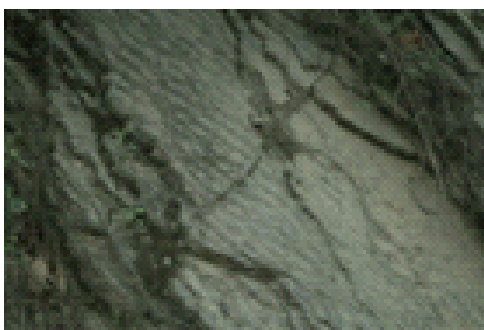
Figure 4.1.4. Ripple mark structure recognized within well-bedded fini- to medium-grained sandstone of the Middle Member of Butar Formation. Location: Road cliff nearby Kemkem Village. (Kusumahbrata, 2002).

Figure 4.1.5. Mudstone bed of the upper part of the Middle Member – lower part of Upper Member of Butar Formation, cut vertically by ichnofossil of *Scolithos* type. This biogenic structure is indicative of foreshore-shoreface intertidal zones of marine environment. Location: Nearby Juhar Village. (Kusumahbrata, 2002).

and Galugur, Kapur IX Sub-regency, West Sumatra Province (Rahmola, 2019) **(Figure 2.1.2.1). belum ada Figure 4.2.1.**

In Kototuo, the sedimentary sequence is variated comprising fine- to coarse-grained sandstone, shale, and claystone. However, shale dominates, dark grey, well bedded – massive, flaggy, hard (Figure 4.2.2).

Kusdji *et al.* (2001) noted that the sedimentary sequence was equivalent to Pematang Formation in Central Sumatra Basin. Furthermore, it can be correlated to the sedimentary sequences of Eocene Sangkarewang Formation occurring in the Ombilin and Kebuntinggi Intramontane Basins.
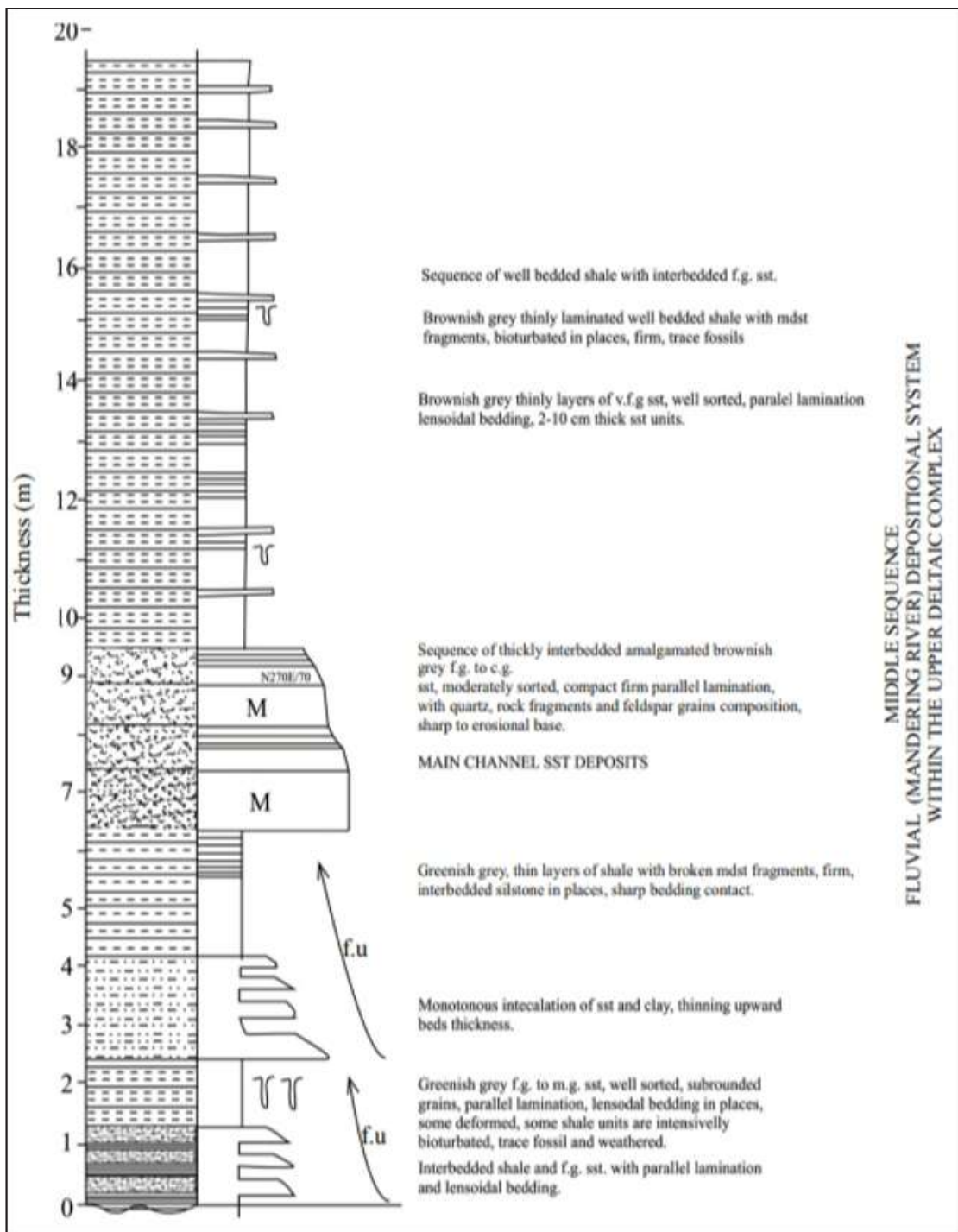
Figure 4.1.6. Columnar measured section in Juhar-3 (03°01'41.8" N and 98°18'45.2" E) Showing characteristics of the Middle to ?Upper Member of Butar Formation (Kusumahbrata, 2020).
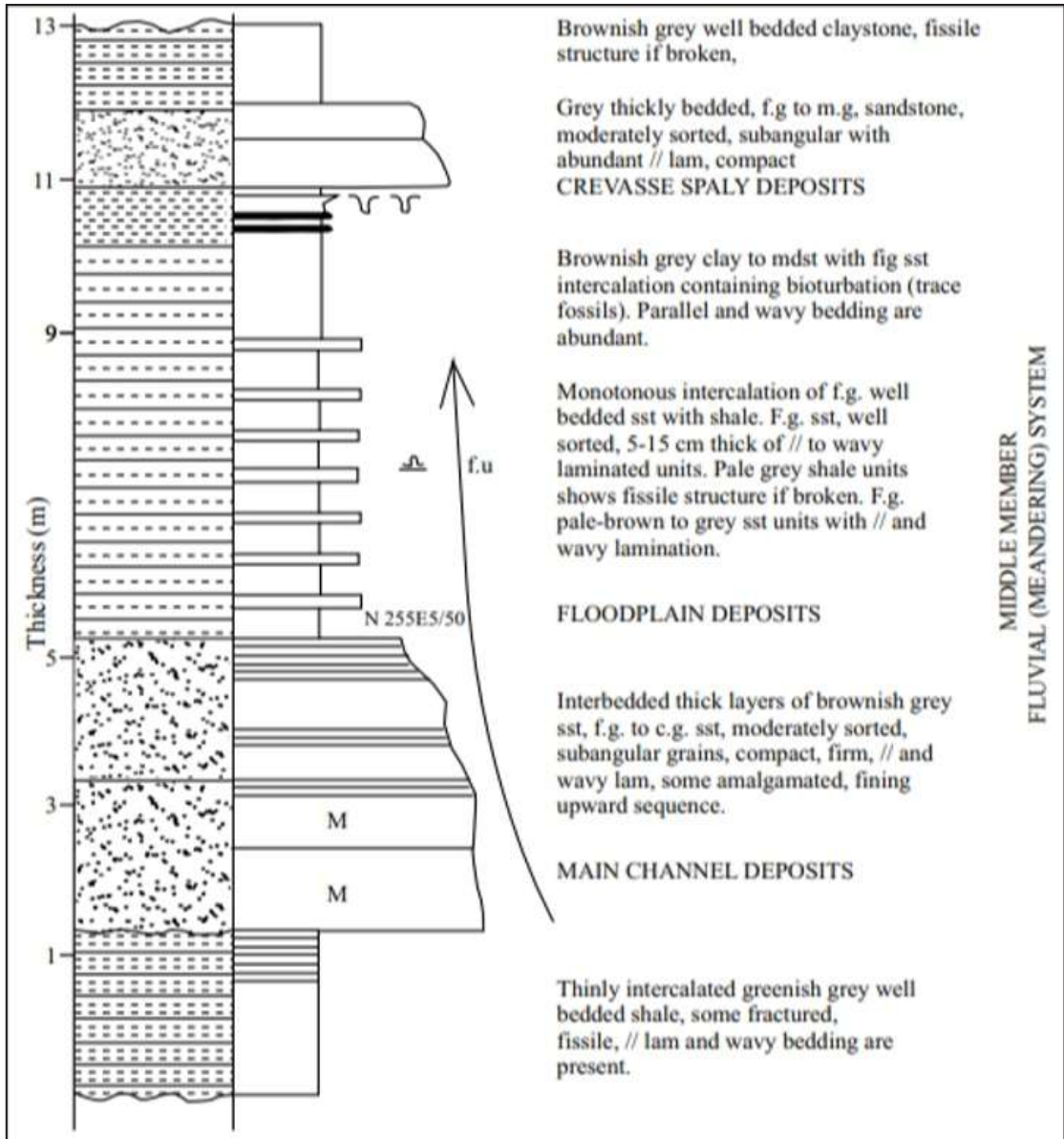
Figure 4.1.7. Columnar measured section of the Upper Member of Butar Formation, showing a fining-upward sequence and bioturbation within mudstone. Location: Juhar Village. (Kusumahbrata, 2020).

Geologic observation carried out in Kotobangun area revealed that the sediments outcrop as conglomeratic sandstone, carbonaceous claystone, and coal seams (Figure 4.2.3). The sedimentary sequence underlies calcareous clay-stone presumed to be Telisa Formation (Kusdji *et al*. 2001.

In Galugur site (Figure 4.2.4), the sediments consist of coal seam and black claystone having oil-smell.
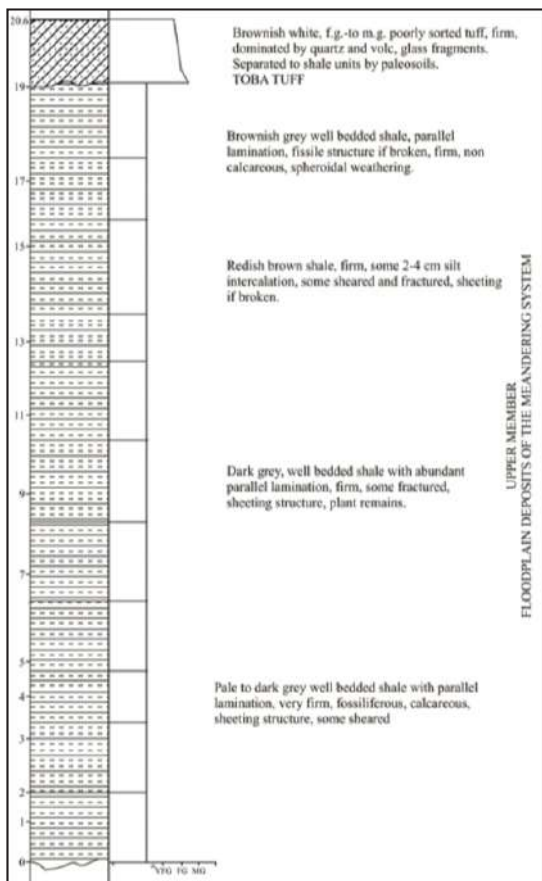
Figure 4.1.8. Columnar measured section the Upper Member of Butar Formation, displaying a thick bedded sequence shale overlain by Toba Tuff. Location: Kutabuluh-1 (Kusumahbrata, 2020).

Figure 4.1.10. SEM photomicrograph of planktonic foraminifera surrounded by clay and calcite minerals, embedded within claystone of the Butar Formation. Sample 02HR13A. Location: Laubuluh Village.
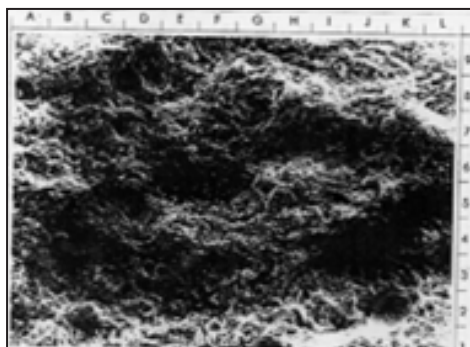
Figure 4.1.11. SEM photomicrograph of abundant micro-foraminifera fossil, surrounded by clays and calcite, within calcareous mudstone of Butar Formation. X400. Sample 02RH03A. Location: Penampen.

Figure 4.1.9. The uppermost part of Butar Formation, near Kutabuluh Village, comprising thinly bedded-fissile, parallel laminated calcareous grey shale, containing microforam fossil.

Figure 4.1.12. Photomicrographs of framboidal pyrite embedded within clay mineral matrix of the Butar Formation. X200. Reflected light. Sample 02HR14C. Reflected light. Location: Laubuluh.
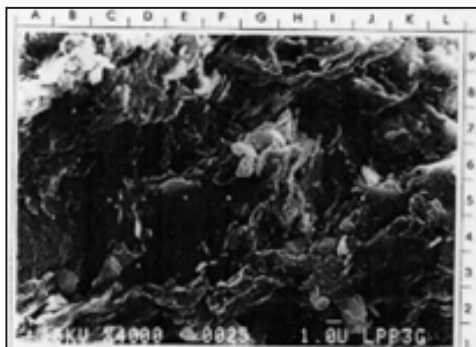
Figure 4.1.13. SEM photomicrograph of semi-oriented smectite-illite, mixed with calcite and a little kaolinite, Butar claystone. X4000. Sample 02RH06A. Location: Laubuluh.
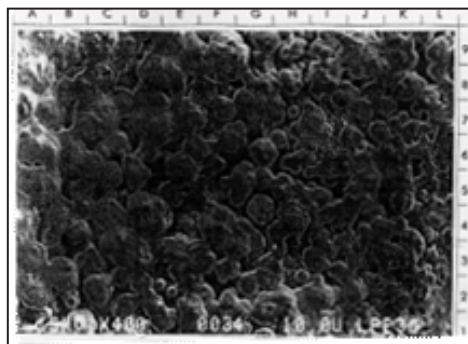
Figure 4.1.15. SEM photomicrograph of iron oxide (hematite) within Butar claystone. X400. Sample 02NS16A. Location: Butar.

4.3. Kebuntinggi Sub-Basin

The formation equivalent to the Brani Formation deposited in the edge of basin comprises conglomerate, polymict breccias, and sandstone; whilst the sediments equivalent to the Sangkarewang Formation are composed of shale, carbonaceous shale, claystone, siltstone, and sandstone, showing parallel lamination which tend to indicate a lacustrine environment characteristic (Moss and Howells, 1996). Physically, in the Kebuntinggi area, the sedimentary succession comprising oil shale can be determined as the Sangkarewng Formation. However, Silitonga and Kastowo (1975) stated that this sedimentary unit belongs to Lower Member of Ombilin Formation.

Figure 4.1.14. SEM photomicrograph of sparry calcite (D-I, 5-8) surrounded by clays, Butar claystone. X600. Sample 02HR14C. Location: Laubuluh.

Table 4.1.1. Result of SEM and XRD analyses of Butar sediments

No.	Sample No.	Q (%)	K (%)	I (%)	Sm (%)	Sm-I (%)	Ca (%)	Fe (%)	Sd (%)
1	03SM-05	96.0	2.3	0.8	0.7	0.2	0.0	0.0	0.0
2.	03SM-08	96.0	2.8	0.6	0.6	0.0	0.0	0.0	0.0
3	03SM-11	94.2	2.8	1.7	0.9	0.4	0.0	0.0	0.0
4	03SM-14A	93.5	3.6	1.4	0.7	0.8	0.0	0.0	0.0
5	03SM-17A	96.0	2.4	0.6	0.6	0.4	0.0	0.0	0.0
6	03SM-20	95.8	3.6	0.0	0.6	0.0	0.0	0.0	0.0
7	03SG-06A	67.2	7.7	9.4	0.0	0.0	0.0	0.0	15.7
8	03SG-07A	97.3	1.4	0.7	0.3	0.3	0.0	0.0	0.0
9	03SG-08B	72.7	4.7	2.5	0.7	1.5	15.1	2.8	0.0
10	ES-13A	40.2	5.6	1.2	0.0	0.0	53.0	0.0	0.0
11	NS-13A	72.6	23.0	0.0	4.4	0.0	0.0	0.0	0.0
12	NS-16A	69.7	6.4	13.3	0.6	7.0	3.0	0.0	0.0

Remarks: Q : quartz   I : illite   Sm-I :smctite-illite   Fe : hematites
K : kaolinite   Sm: smectite   Ca : calcite   Sd : siderite

Oil Shale Potential as an Alternative Energy Source, in Selected Sites of Sumatra Island

Figure 4.2.1. Stratigraphic columnar section and photographs of shale, dark grey, well bedded – massive, flaggy, and hard, outcropping in Kototuo (Rahmola, 2019).

Figure 4.2.2. Stratigraphic columnar section and photographs of shale, dark grey, well bedded – massive, flaggy, and hard, outcropping in Kototuo (Rahmola, 2019).

Figure 4.2.3. Stratigraphic columnar section and photographs of shale/mudstone outcrops in Kotobangun (Rahmola, 2019).

Figure 4.2.4. Stratigraphic columnar section of coal seam and black claystone, having oil-smell in Galugur area (Rahmola, 2019).

Conformably, both formations mentioned above are overlain by the Lower Member of Ombilin Formation (Silitonga dan Kastowo, 1975) composed of micaceous quartz sandstone, with intercalations of arkose, shale, and coal seams. The lower part of the Lower Member of Ombilin Formation shows thickness up to 300 m (Kosoemadinata and Matasak, 1981; Moss and Howells, 1996).

Then, Sawahlunto Formation made up of red to green to purple river and flood plain deposits is composed of siltstone, and shale associated with channel deposit (sandstone) and coal seams. Thickness of this commercial coal seams reaches 15 m (Moss and Howells, 1996).

The formation was deposited in a meandering river environment with some lakes around the river areas (Koesoemadinata and Matasak, 1981). The Sawahlunto Formation underlies the Sawahtambang Formation (600 m thick) comprising braided river deposits, mainly coarse-grained sandstone and conglomerate, locally intercalated by marine sediments (Moss and Howells, 1996).

Rocks outcropping in the Kebuntinggi and adjacent areas, in general, can be divided into three groups, those are :
• Shale Unit
• Mudstone and Siltstone Unit
• Sandstone Unit

Oil shale deposit in the Kebuntinggi Sub-basin exists as a narrow strip stretching in a northwest – southeast direction. The sediments mainly occupy the flank of low relief hill bounded by faults. The thickness of unit around 16 m in the centre of the basin, then thinning to the western area (3 – 5 m thick).

In the Kebuntinggi Sub-basin, oil shale outcrops mainly well recognized within river gullies, such as Jao River (Figure 4.3.1), Petai River (Figure 4.3.2), Pakboi, Ngalau Luko, Putui, Batang Kapas (Figure 4.3.3), and Siabu River (Figure 4.3.4).

Physical features of the oil shale can be divided into two types; those are the blackish dark grey papery – flaky – flaggy, and the light grey

Figure 4.3.1. Outcrop of well bedded shale, brownish grey, flaky to flaggy, rather soft, oxidated, slightly weathered, outcropping in Jao River.

Figure 4.3.2. Outcrop of well bedded shale, grey, fissile, flaky-flaggy, firm, alternations of mudstone are common. Location: Petai River.

Figure 4.3.3. Outcrop of shale, well-bedded, grey, *flaky - flaggy*, *firm*, underlain by polymict breccia. Location: Kapas River.

Figure 4.3.4. Shale outcrop, well thinly bedded, light grey, *papery,* brittle, rather soft, rich in carbon matter, contains freshwater mollusc. Outcrops in a tributary of Siabu River.

papery – flaky ones. The dark type occupies the northern area, whereas the light colour one is situated in the southern area. The sediments were derived from suspension material within laminations. In general, the thickness of oil shale varies from 2 – 24 m. The thickest beds can be found in Diano River and its tributary, and in Pakboi River, whilst in Petai, Jao, and Siabu Rivers, and also in Dalam Village, the oil shale beds are thinning to 2 - 5 m.

In the research area, interseam sediments comprise blocky – massive grey mudstone and light grey siltstone. The upper part of unit is composed of sandstone, yellow to white colour, medium- to coarse-grained, subangular – angular, compact, massive, and is presumed to be alluvial fan deposits.

Depositional environment of the sediments is interpreted to be lacustrine of a varieted depth, based on sedimentary structure and lithofacies association. (*lacustrine environment*) dengan kedalaman yang bervariasi.

Rock-Eval Pyrolysis and organic petrographic analysis data tend to indicate that the dark grey oil shale occurring in the northern part area is presumed to be deposited in a deep lake of anaerobic condition where algae and resinite was well preserved. On the contrary, the light grey oil shale recognized in the southern area was deposited in a shallow lake where oxygen content was high, led to rare algae development.

4.4. Kuansing Area

Based on the lithological appearance, generally the Keruh Formation in Kuansing region, is presumed to be an oil shale-bearing formation comprising conglomerate which upward turned to be bedded sandstone with intercalation of parallel laminated mudstone in the lower part. Then this sequence is overlain by coal seams with some interbedded carbonaceous shale and mudstone in the middle part (Figure 4.4.1). Interbedded laminated shale and mudstone occupy the upper part of the formation is also observed (Figure 4.4.2). These upper and middle parts of the Keruh Formation appear as an oil source rock sequence. Those parts are underlain by coal seams with some interbedded carbonaceous shale and mudstone (Figures 4.4.3 and 4.4.4). Locally, in the PT. Manunggal Coalfield, an elongated leaf fossil is recognized embedded within a mudstone layer (Figure 4.4.5).

Shale and mudstone, light to blackish grey, flaky to thickly laminated, show a parallel lamination in places, abundant organic material and contain iron oxide intercalations (Figure 4.4.6). Physically, these rocks are hard when fresh and soft when altered. Those rocks are

Figure 4.4.1. Photograph of well-bedded, flaggy oil shale with mudstone intercalations, underlie 12.3 m thick coal seams, in Mia Coalfield, Muaralembu area, Kuansing.

Figure 4.4.2. Outcrop of monotonous interbedded grey to blackish grey shale and mudstone, flaky to thinly lamination, as upper part of the Keruh Formation, in PT Manunggal Coalfield, Muaralembu.

also recognized to be interbedded by a light grey mudstone layer with a poor organic material content. These shale and mudstone beds are

well developed in the PT Nusariau Coalfield, northwestern part of the studied area, with the bedding thickness ranging from 0.5 to 5 m. In the northwestern and southeastern parts of research area, some interseam sediments within coal seams, consisting of dark grey to black shale are recognized.

On the basis of lithological characteristics, the lower part of the Keruh Formation was deposited in a fluvial system, whilst the middle part was accumulated in a swampy area, interconnected

Moreover, lithofacies development of the Keruh Formation is displayed in Table 4.4.1 as follows.

The presence of *Palmaepollenites kutchensis, Florschuetzia, Durio, Discoidites borneensis, fungal spore* and small diatomea tends to show a littoral or fresh water conditions (Figure
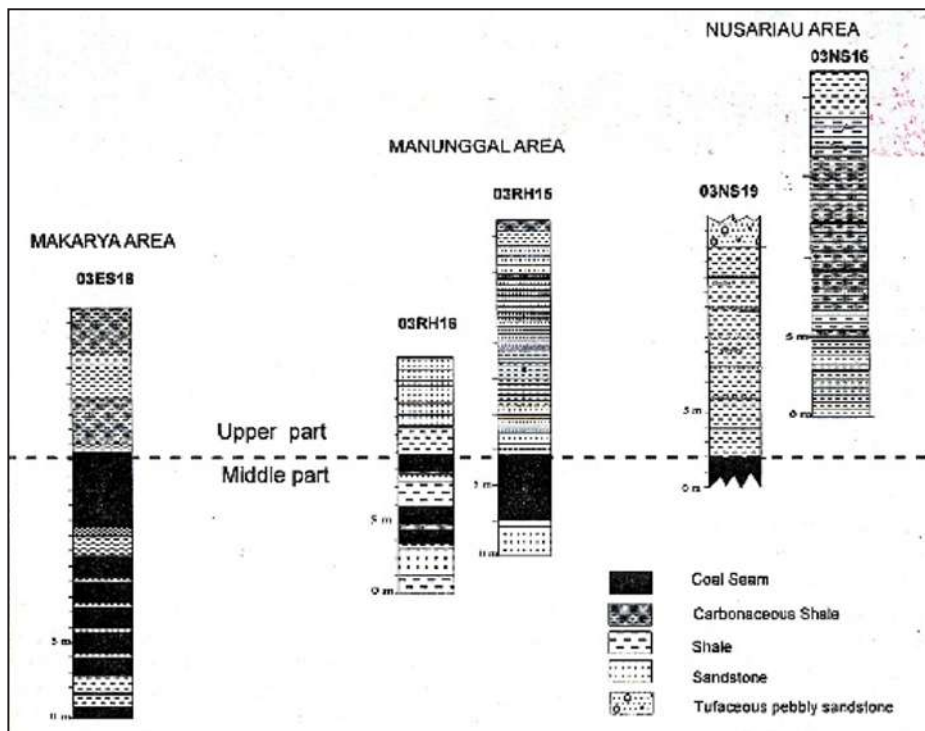
Figure 4.4.3. Columnar measured sections of the upper and middle parts of Keruh Formation, in the northwestern part of studied area, appear as a potential oil source rock sequence.
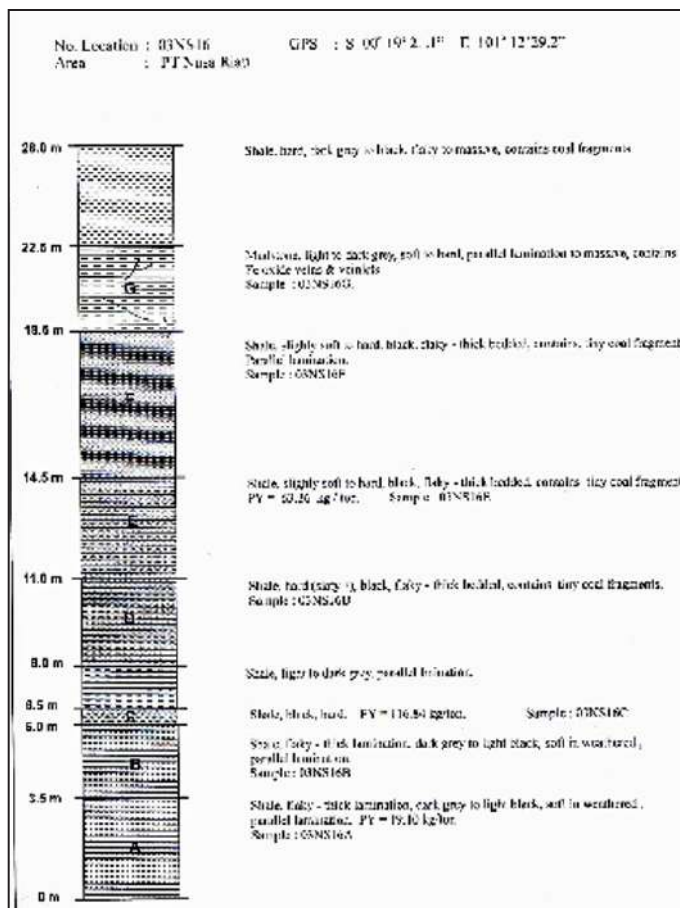
Figure 4.4.4. Columnar measured section of the upper part of Keruh Formation at sample location 03NS16, Nusa Riau coalfield, representing lacustrine environment.

Figure 4.4.5. Close-up of an elongated leaf fossil embedded within a shale layer overlying coal seam of Keruh Formation, located in PT Manunggal Coalfield.

4.4.7). It is also supported by the appearance of lamalginite (Figure 4.4.8) and Eel fossil (Figure 4.4.9). However, the presence of framboidal pyrites (Figure 4.4.10) as well as telalginite-*Botryococcus* tend to indicate that a brackish to marine condition occurred. Thereby, the suitable depositional environment for the hydrocarbon source rocks sequence of the Keruh Formation is a lacustrine with some influence of marine conditions.

Based on the SEM analysis of fifteen samples from the Keruh Formation, the hydrocarbon source rocks are composed of shale, claystone/mudstone, sandy claystone/mudstone and

Figure 4.4.6. Outcrop of semi-fresh shale and mudstone intercalations, within road-cut cliff, nearby PT. Nusa Riau coalfield. The upper part of shale layer shows thick-bedded, flaggy character, grey, containing thin intercalations of Fe-oxides, presumably occur as weathered tuffaceous material.
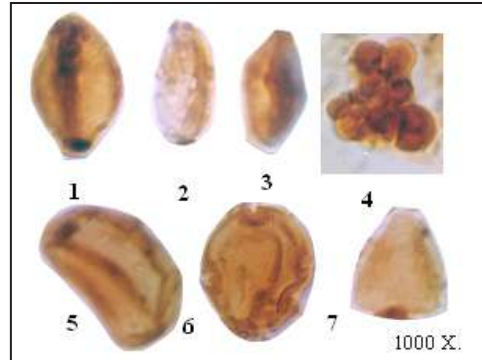
Figure 4.4.7. Photomicrograph of polen *Florscheutzia trilobata* (1, 2, 3), *Meyeripollis naharkotensis* (4), *Palmaepollenites kutchensis* (5), *Durio sp.* (6), and *Dicolpollis malesianus* (7), indicating Eocene age and depositional environment of littoral / fresh water. Samples: 03RH15G, 03ES13A, 03NS13A, and 03NS19A

Table 4.4.1. Lithofacies Development of the Keruh Formation in the Kuansing Sub-basin

DOMINANT LITHOFACIES	DEPOSITIONAL ENVIRONMENT	REMARK	AGE
Cg-vcg-cgltic Sst to subordinate cgl, amalgamated, stacked thickly bedded massive sst.	Alluvial Fan Deposits	Initial basin fill afer major tectonic event. Unconformity above the pre-Tertiary Kuantan Formation	Mid – Late Eocene
Intercalation between mg-cg massive sst with thin laminated mdst.	Fluvial channel with overbank deposits	Variable thickness of beds, laterally discontinuous, probably deposited as High Sinuousity rive flowing southeastward.	Mid – Late Eocene
Bright to bright-banded coal seam with abundant pyrite (framboidal spots and flakes), and resin.	Upper Deltaic Facies Swamp – Marsh interconnected system	Strong marine influence, brackish water condition, low and high plant source of organic matter.	Late Eocene
Dark grey to subordinate brown shales intercalated with blocky mdst and laminated carbonaceous siltstone.	Upper Deltaic Facies to Upper Estuarine, Floodplain	Frequent levee breaching resulting in the progradation of blanket crevasse splay sands into floodplain setting	Late Eocene
Thickly bedded cg, vcg, to cgltic massive to faint low angle x-bed sst with subordinate carbonaceous mdst	Fluvial dominated distributary channel facies.	Tectonic reactivation of basement rocka resulting in high coarse-grained quartz-rich sedimentary influx.	Late Eocene
Grey to dark grey, dark brown, black laminated shales with subordinate interbeded mdst and siltstone.	Lacustrine facies Probably paralic lake	Rapid subsidence of the basin and abundant particulate organic matter supply dumped into deep anoxic lake.	Late Eocene to ?Early Oligoc.

Figure 4.4.8. Photomicrograph of lamalginite (Al). (Fluorescence mode). X350. Sample 03NS16C.

Figure 4.4.9. Eel fossil embedded within mudstone of Keruh Formation.
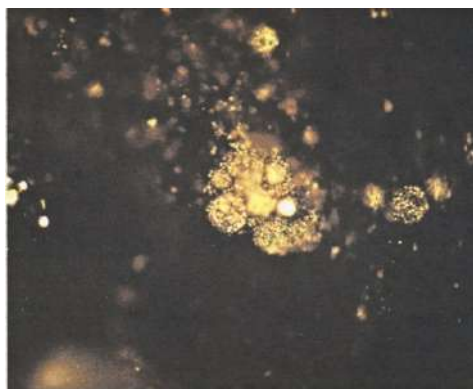
Figure 4.4.10. Photomicrograph of framboidal pyrite in oil shale, Keruh Formation. Sample 03ES16L.

very fine-middle grained sandstone (Table 4.4.2). The diagenetic features indicate that the depth of burial was more than 1000 m or at the end of Eodiagenesis to Early Mesodiagenesis (Burley *et. al.*, 1998). Moreover, XRD analysis results depicted in Table 4.4.3 indicate that quartz mineral is predominated. Clay minerals recognized comprise quartz, followed by some illite with smectite, kaolinite, quartz, and calcite (Figures 4.4.11 and 4.4.12).

Table 4.4.2. Result of SEM Analysis on Keruh Sediments

No Sample	Lithology	Composition	Clay Minerals	Texture/Structure Of Clay minerals	Element of "fosil fuel"	Diagenetic Features	Diagenetic Stage	Remark
03ES13A	Shale	Calcite, kaolinite a few illite	Kaolinite & illite	Laminated & oriented	-	Compaction &auth. Clay mins	Early Mesodiagenesis	More than 1000 m buried
03NS13A	Mudstone	Kaolinite, smectite & some illite	Kaolinite, smectite & some illite	Disoriented	Sporinite & drop oil	Compaction &auth. Clay mins	Early Mesodiagenesis	More than 1000 m buried
03NS16A	Shale	Illite, kaolinite & some calcite	Illite & kaolinite	Well oriented	-	Compaction &auth. Clay mins	Early Mesodiagenesis	More than 1000 m buried
03SG02A	Shale	Kaolinie, illite, smectite, org. pyrite	Kaolinite , illite smectite	Laminated and oriented	Vitrinite	Auth. Clay mins	Late Eodiagenesis	Less than 1000 m buried
03SG04A	Shale	Illite with some smectite	Illite , smectite	Lamnated, well oriented & curly	-	Compaction &auth. Clay mins	Early Mesodiagenesis	More than 1000 m buried
03SG06A	Mudstone	Kaolinite and illite	Kaolinite and illite	Disoriented	-	Compaction &auth. Clay mins	Early Mesodiagenesis	More than 1000 m buried
03SG07A	Fine-grained sandstone	Qrtz, flpr, kaolinite & smecctite	Kaolinite and smectite	Book texture	-	Compaction &auth. Clay mins	Early Mesodiagenesis	More than 1000 m buried
03SG08B	Fn to med-grained sandstone	Qrtz, flpr, kaolinite smectite, illite	Kaolinite, smectite & illite	Disoriented	-	Compaction &auth. Clay mins	Early Mesodiagenesis	More than 1000 m buried
03SM01A	Mudstone	Smectite and illite	Smectite and illite	Disoriented	-	Compaction &auth. Clay mins	Early Mesodiagenesis	More than 1000 m buried
03SM05	Mudstone	Kaolinite, illite & smectite	Kaolinite, illite & smectite	Disoriented	-	Compaction &auth. Clay mins	Early Mesodiagenesis	More than 1000 m buried
03SM08	Shale, flaky	Calcite, kaolinite & illite	Kaolinite & illite	Mostly oriented and laminated	-	Compaction &auth. Clay mins	Early Mesodiagenesis	More than 1000 m buried
03SM11	Mudstone	Kaolinite & a few smectite	Kaolinite and smectite	Book and vermicular textures	-	Compaction &auth. Clay mins	Early Mesodiagenesis	More than 1000 m buried
03SM16	Sandy mudstone	Qrtz, flpr, kaolinite & smectite	Kaolinite and snectite	Disoriented	-	Compaction &auth. Clay mins	Early Mesodiagenesis	More than 1000 m buried
03SM17A	V. fn. sandstone	Qrtz, flpr, kaolinite smecttie, illite	Kaolinite, smectite & illite	Disoriented	-	Compaction &auth. Clay mins	Early Mesodiagenesis	More than 1000 m buried
03SM20	Fn. Sandstone	Qrtz, flpr, kaolinite & smectite	Kaolinite and smectite	Disoriented	-	Compaction &auth. Clay mins	Early Mesodiagenesis	More than 1000 m buried

Table 4.4.3. XRD Analysis Results of Keruh Sediments, Kuansing, Riau

No.	Sample No.	Q (%)	K (%)	I (%)	Sm (%)	Sm-I (%)	Ca (%)	Fe (%)	Sd (%)
1	03SM-05	96.0	2.3	0.8	0.7	0.2	0.0	0.0	0.0
2.	03SM-08	96.0	2.8	0.6	0.6	0.0	0.0	0.0	0.0
3	03SM-11	94.2	2.8	1.7	0.9	0.4	0.0	0.0	0.0
4	03SM-14A	93.5	3.6	1.4	0.7	0.8	0.0	0.0	0.0
5	03SM-17A	96.0	2.4	0.6	0.6	0.4	0.0	0.0	0.0
6	03SM-20	95.8	3.6	0.0	0.6	0.0	0.0	0.0	0.0
7	03SG-06A	67.2	7.7	9.4	0.0	0.0	0.0	0.0	15.7
8	03SG-07A	97.3	1.4	0.7	0.3	0.3	0.0	0.0	0.0
9	03SG-08B	72.7	4.7	2.5	0.7	1.5	15.1	2.8	0.0
10	ES-13A	40.2	5.6	1.2	0.0	0.0	53.0	0.0	0.0
11	NS-13A	72.6	23.0	0.0	4.4	0.0	0.0	0.0	0.0
12	NS-16A	69.7	6.4	13.3	0.6	7.0	3.0	0.0	0.0

Remarks: Q : quartz   I : illite   Sm-I :smectite-illite   Fe : hematites
K : kaolinite   Sm: smectite   Ca   : calcite   Sd : siderite
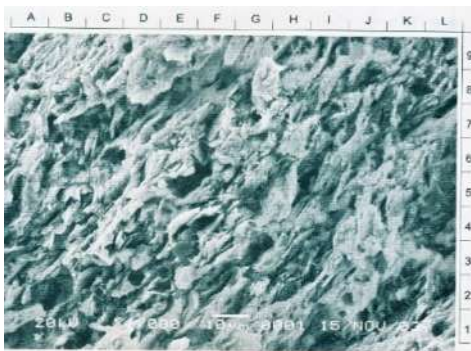
Figure 4.4.11. SEM photomicrograph of shale comprising oriented illite with some smectite, kaolinite, and calcite. Location: PT Nusa Riau Coalfield, Logas.
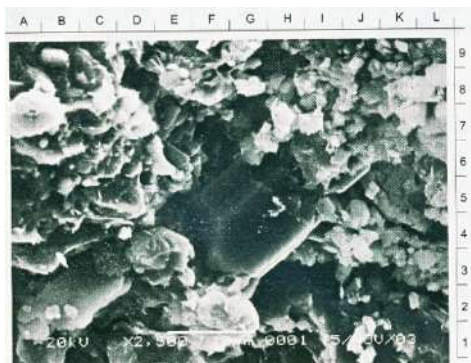
Figure 4.4.12. SEM photomicrograph of sandy mudstone showing an authigenic quartz (E-1, 3-6), kaolinite, smectite, and illite. Sample 03SM08. Location: PT Manunggal Coalfield, Logas.

4.5. Ombilin

4.5.1. Sedimentary Facies

The study, focused on some man-made exposures, in order to minimize the effects of outcrop weathering, was performed on the fresh cliff section of the Sangkarewang (Lubuktaruk) and Kiliran Formations (Kunangan) cut by coal exploitation activity, and along the river and road (Sipang River/ Tigatumpuk and Sangkarewang River). Furthermore, in the Setangkai (Atar), Padangganting, and Tanjungbalit areas, the observations were focused on the road-cut showing a nearly fresh Sangkarewang Formation outcrops. However, a study within the Sawahlunto Formation was carried out in the area between Kolok and Sawahlunto, on the cliff of an abandoned coal exploitation activity.

General sedimentary facies analysis of each formation is described as follows:

Sangkarewang Formation

The rock outcropping in the studied areas predominantly comprises well-bedded and laminated grey siltstones and shales (Figure 4.5.1), thin- to thick-bedded grey and reddish brown mudstones (Figure 4.5.2) that in places are spongy, and fine- to coarse-grained sandstone (Figure 4.5.3) with intercalations of conglomeratic coarse sandstone locally (Figure 4.5.4).

Thin to thick coal seams are also recognised (Figure 4.5.5). Sedimentary structure recognised are parallel plane laminae and graded bedding. Impressions of mollusk fossils are common to occur within the mudstones (Figures 4.5.6 and 4.5.7).

Figure 4.5.1. Well-bedded and laminated grey siltstones and shales.

Figure 4.5.2. Thin- to thick-bedded grey and reddish brown mudstones.

Figure 4.5.3. Fine- to coarse-grained sandstone

Figure 4.5.4. Intercalations of conglomeratic coarse sandstone locally.

Figure 4.5.5. Thin to thick coal seams are also recognized

Figure 4.5.6. Impressions of mollusk fossils are common to occur within the mudstones

The columnar sections of Sangkarewang sediments of the 2-selected localities situated in the Ombilin Basin are shown in Figures 4.5.7 – 4.5.8, whilst Figure 4.5.9 shows a columnar
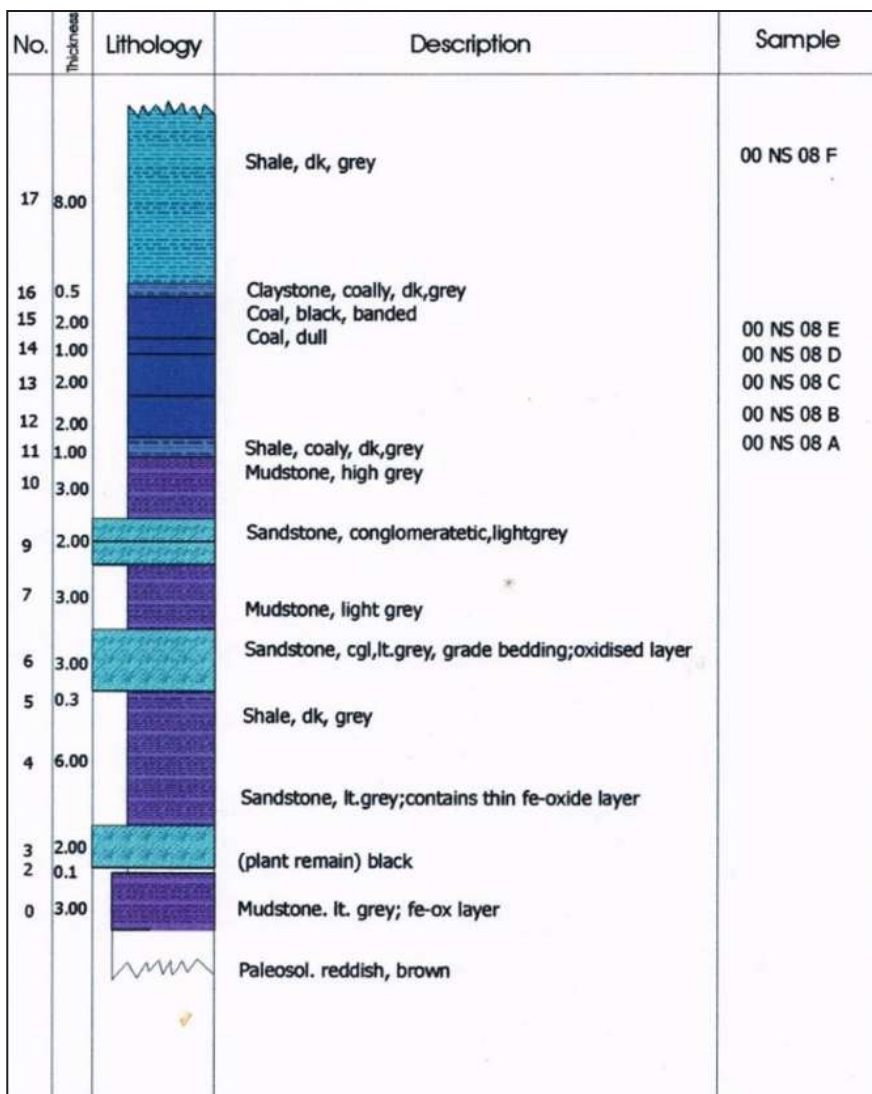
Figure 4.5.7. Columnar measured section of some rock sequence of the Sangkarewang Formation, showing interbedded shales, mudstone, and claystone, with sandstone intercalations, Ombilin Basin.

sedimentary section of the Sawahlunto Formation. The rock sequence can be interpreted as a lacustrine lake facies, with an interruption of a fluvial and alluvial-fan facies indicated by the occurrence of fining-upward (graded bedding) sandstone deposits.

SEM and X-ray diffraction (XRD) techniques were used to study the mineralogy of oil shale and its associated sedimentary rocks. The SEM analysis has been applied particularly to identify the mineral constituents such as clay minerals, as well as to study concerning rock diagenesis (Pittman, 1979; Wilson and Pittman, 1979). The most significance feature of SEM is that it enables examination of very small scale (micron size) constituents or minerals, textural relationship of
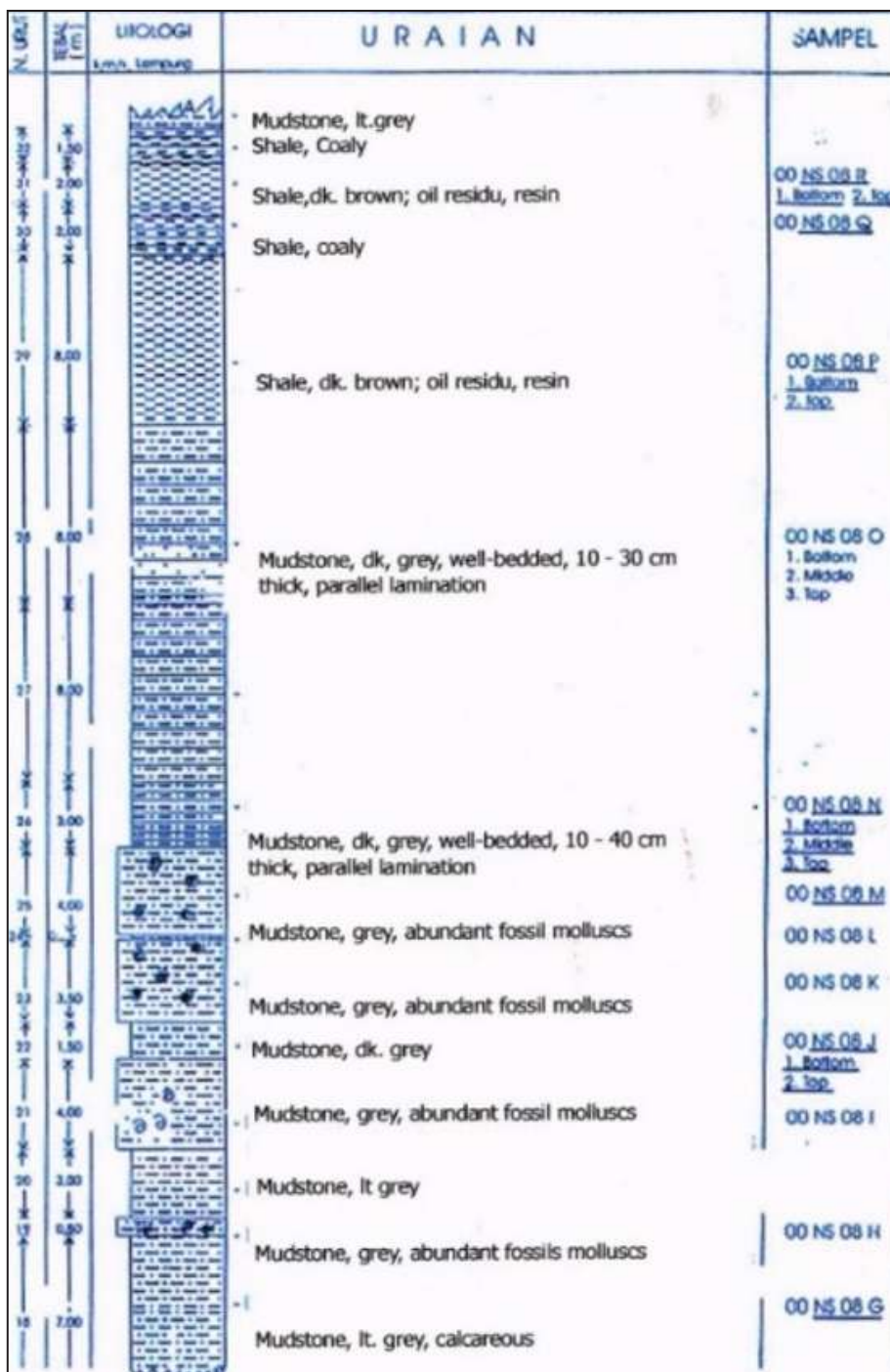
Figure 4.5.8. Columnar measured section of rock sequence of the Sangkarewang Formation. The lower and middle parts of the section is composed of mudstone in parts calcareous, containing abundant fossil molluscs. In the upper part, shale containing resin and mudstone occur. Location: Ombilin Basin.

No.	Thickness	Lithology	Description	Sample
17	8.00		Shale, dk, grey	00 NS 08 F
16	0.5		Claystone, coally, dk,grey	
15	2.00		Coal, black, banded	00 NS 08 E
14	1.00		Coal, dull	00 NS 08 D
13	2.00			00 NS 08 C
12	2.00			00 NS 08 B
11	1.00		Shale, coaly, dk,grey	00 NS 08 A
10	3.00		Mudstone, high grey	
9	2.00		Sandstone, conglomeratetic,lightgrey	
7	3.00		Mudstone, light grey	
6	3.00		Sandstone, cgl,lt.grey, grade bedding;oxidised layer	
5	0.3		Shale, dk, grey	
4	6.00		Sandstone, lt.grey;contains thin fe-oxide layer	
3	2.00		(plant remain) black	
2	0.1			
0	3.00		Mudstone. lt. grey; fe-ox layer	
			Paleosol. reddish, brown	

Figure 4.5.9. Columnar measured section of the Sawahlunto Formation, showing interbedded shales, mudstone, and claystone, with sandstone intercalations, Ombilin Basin.

cement, matrix and grain framework of rocks, pore-throat configuration, shape, size and orientation of pores, and other factors which affect the quality of rocks for hydrocarbon study. The texture and mineral identification are generally based on Scholle (1979), Welton (1984), Wilson and Pittman (1979), and Schmidt and McDonald (1979). This analysis also provides an excellent information for revealing the type of rocks, organic, bitumen constituents, diagenesis feature and regime, and also the property of rocks. Moreover, the XRD-analysis is focused on the identification of clay bulk composition and mineralogy.

Description of SEM analysis of some selected samples is shown in Table 4.5.1, whilst Table 4.5.2 is to displays the XRD-analysis. Nine se-

Table 4.5.1. Summary of SEM Analysis Results of the Sangkarewang Oil Shale Samples, Ombilin Basin

Sample No.	Type of Rock/ Sample	Composition	Type of Clay	Texture/ structure of Clay	Fossil Fuel	Diagenesis Character/ Feature	Diagenesis Regime	Remark
00/NS-08F3	Fine silty shale, brownish gray.	Predominantly clay minerals, quartz and organic matter.	Smectite-illite and kaolinite.	"Webby morphology", crenulated flakes, irregular; many micropores.	"Algae" (typical lamalginite).	The present of clay minerals of typical mixed-layer clays such as smectite-illite; dense.	Early meso-diagenesis	Probably have been buried > 1000 m depth.
00/NS-08G	Shale, gray.	Clay minerals and organic matter.	Kaolinite	Irregular flakes, dense, micropores in between clay crystals.	Abundant alginite of typical lamalginite and subordinate ?Botryococcus; "oil drop" or bitumen is also present.	The presence of kaolinite, dense and oriented clay minerals.	Meso-diagenesis.	Probably have been buried up to > 1000 m depth.
00/NS-13	Shale, brownish grey	Predominantly clay minerals, some organic matter and "framboidal pyrite"	Kaolinite	Regular flakes of kaolinite crystals showing "booklet" structure; micro-pores are abundant within clay crystals.	Exinite of typical sporinite; "drop oil" or bitumen.	The presence of clay minerals of typical kaolinite.	Meso-diagenesis	Probably have been buried up to > 1000 m depth.

Table 4.5.2. XRD Analysis Data of Sangkarewang Oil Shale Samples, Ombilin Basin

Sample No.	Form.	Lithology	Q.	Plag.	Kaol.	Illite	Smec.	Pyrite	Gyps.	Calc.	Hematite	Chlorite	Dolo.
00/NS 08F3	P E	Shale	Abd	Ab	Com	Ab	Ab	Ab	Ab	Ab	Ab	Ab	Ab
00/NS 08J2	M A	Mdst.	Abd	Ab	Com	Ab	Ab	Ab	Ab	Ab	Ab	Ab	Ab
00/NS 08P1	T A	Shale	Abd	Ab	Com	Ab	Ab	Sp	Ab	Ab	Ab	Ab	Ab
00/NS 08R1	N G	Shale	Abd	Ab	Com	Ab	Ab	Sp	Ab	Ab	Ab	Ab	Ab

Remarks :

Mdst.	= Mudstone	Kaol.	= Kaolinite	Calc. = Calcite	Com.	= Common	(25 - 75 %)	Ab = Absent (0 %)
Q	= Quartz	Smec.	= Smectite	Dolo. = Dolomite	Sp.	= Sparse	(5 - 25 %)	
Plag.	= Plagioclase	Gyps.	= Gypsum	Abd. = Abundant (> 75 %)	R	= Rare	(< 5 %)	

lected representative samples were investigated by SEM analysis. Four samples (01NS.06A1, -08L, -10G and 01HR.01E) are typically mudstones, three samples (01NS.08A, -12A, and 01RH.02A) are shales, while two samples (01NS.12E4 and -18A) are fine-medium grained sandstones.

Kaolinite (Figures 4.5.10) and smectite (Figures 4.5.11 and 4.5.12) clays are the most prominent matrix within the shale, although

Figure 4.5.10. SEM photomicrograph showing kaolinite (F-L, 5-9 and E-G, 3-4) surrounded by smectite-illite (A-L, 1-9), calcite (H-I, 7-8) in oil shale of the Sangkarewang Formation. Sample 01NS08₁. Location: Sipang River.

mixed smectite-illite substances (Figures 4.5.13) are also significant. Moreover, organic constituents comprising abundant lamalginite of typically *Pediastrum* (01NS.06A and 08A; Figures 4.5.14), quartz and vitrinite (Figure 4.5.15), calcite and pyrite (Figure 4.5.16), and minor exinite as sporinite (01NS.10G and -12E4). Bitumen or oil drop (Figure 4.5.17) is also clearly recorded in sample 01RH.02A.

The clay minerals are mostly regular or well-oriented, where the kaolinite clays show well-ordered flakes forming booklet structure (01HR.01E; Figure 4.5.16). Some clay mineral flakes are present as irregular or disordered to

Figure 4.5.11. SEM photomicrograph showing kaolinite (F-L, 5-9 and E-G, 3-4) surrounded by smectite-illite (A-L, 1-9), calcite (H-I, 7-8) in oil shale of the Sangkarewang Formation. Sample 01NS08₁. Location: Sipang River.

Figure 4.5.13. SEM photomicrograph of "smectite-illite" (A-E, 1-9 and F-L, 13) with alga of typically *Pediastrum*-lamalginite (F-L, 4-4) in oil shale of the Sangkarewang Formation. Sample 01NS08A. Location: Sipang River.

Figure 4.5.12. SEM photomicrograph showing kaolinite (F-L, 5-9 and E-G, 3-4) surrounded by smectite-illite (A-L, 1-9), calcite (H-I, 7-8) in oil shale of the Sangkarewang Formation. Sample 01NS08₁. Location: Sipang River.

Figure 4.5.14. SEM photomicrograph of mixed "smectite-illite" containing *Pediastrum* lamalginite (B-D, 2-4) and calcite (H, 2) in oil shale of the Sangkarewang Formation. Sample 01NS06A. Location: Tanjungbalit-Paninjauan.
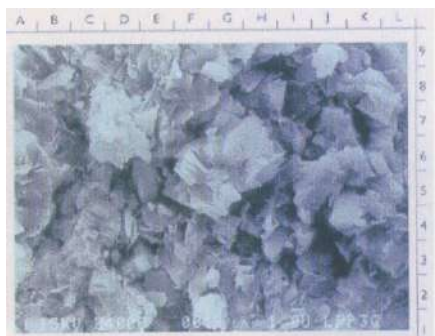
Figure 4.5.15. SEM photomicrograph of quartz fragment (E-I, 5-8) surrounded by smectite-illite matrix, organic matter/vitrinite (A-I, 1-4) in oil shale of the Sangkarewang Formation. Sample 01NS12E4. Location: Bukit Porogadang.
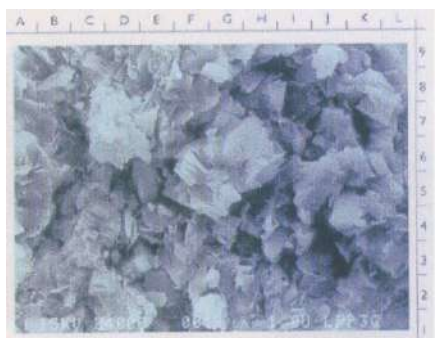
Figure 4.5.16. SEM photomicrograph of kaolinite presenting as matrix and micritic calcite (E, 2; J-K, 4; and I, 7-8) and pyrite (E,3) in oil shale of the Sangkarewang Formation. Sample 01HR01E. Location: Setangkai (Atar).
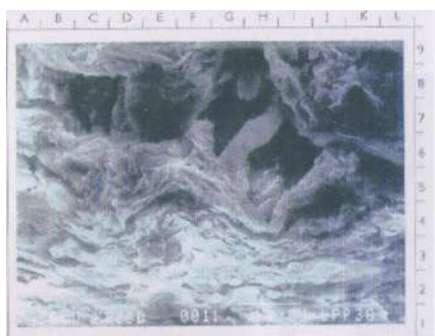
Figure 4.5.17. SEM photomicrograph showing lamalginite mixed with smectite-illite (A, 2, 1-5) and bitumen (D-F, 7-8) in oil shale of Sangkarewang Formation. X1000. Sample 01RH02A.

poorly oriented crystal shapes. The disordered clays are usually mixed crystals between smectite-illite, smectite and kaolinite, with some of them are slightly oriented shapes. The contact crystal is usually disordered latticed crystal with some floating contacts. Cement of the sediments is commonly micritic calcite.

Furthermore, the presence of inorganic matter contents is common to recognise in all shale samples, those are calcite (Figures 4.5.16), quartz (Figure 4.5.15), pyrite (Figure 4.5.16) and feldspar.

Micropores have been well developed within the clay lattices ranging from 0.05 microns up to 15 microns in diameter (01NS.06A1, -12A, -12E4, 01RH.02A, and 01HR.01E). The pore spaces have probably developed during diagenetic process due to dissolution and crystal rearrangements. However, within samples 01NS.08A, -08L, and -10G, the micropores are not well developed, due to impermeable intracrystal condition.

Diagenesis characters are identified by the presence of authigenic clays such as, kaolinite and smectite-illite, but compaction and crystal orientations are also significantly indicators. Thus, the rocks examined have mostly been realm by diagenetic processes of Eodiagenesis to Early Mesodiagenesis regimes. Most of sediments has been buried at less than 1000 m deep, which now they have been exposed on the surface; except, samples 01NS.12A and -12E4 which presumably had been buried at more than 1000 m deep.

The limited XRD-data (Table 4.5.2) suggest that the rocks comprise of abundant quartz, ranging from 28.0 - 100.0 %, with predominantly 45.0 - 80.0 %; common kaolinite (4.0 - 17.0 %), smectite - illite (3.0 - 17.0 %), and plagioclase (10.0 - 30.0 %); with sparse pyrite (up to 25 % in 01NS.12E$_4$).

Sixteen samples of shales and mudstone from the Ombilin Basin were analysed for palynological study. The presence of *Florschuetzia trilobata* (Figure 4.5.18), *Verrucatosporites*

Figure 4.5.18. Photomicrograph of *Florschuetzia trilo-bata*, contained in oil shale of the Sangkarewang Formation, Ombilin Basin

Figure 4.5.20. Photomicrograph of *Cicatricosisporites dorogensis*, contained in oil shale of the Sangkarewang Formation, Ombilin Basin

Figure 4.5.19. Photomicrograph of pollen/spore (*Verrucatosporites usmensis*) contained in oil shale of Sangkarewang Formation, Ombilin Basin.

Figure 4. 5. 21. Photomicrograph of *Palmaepollenites kutchensis* contained in oil shale of Sangkarewang Formation, Ombilin Basin.

usmensis (Figure 4.5.19)*, Cicatricosisporites dorogensis* (Figure 4.5.20), *Palmaepollenites kutchensis* (Figure 4.5.21), Polyad pollen, *Laevigatosporites, Dicolpopolis malesianus*, and *Crassoretitriletes vanraadshooveni* within the Sangkarewang Formation, represents a Middle Eocene to Oligocene age.

A terrestrial vegetation, freshwater with high plant diversity is represented by the following pollen and spore assemblage. The pollen and spore fossils are dominated by freshwater affinities, comprising *Florschuetzia trilobata, Marginipollis* type (Figure 4.5.22), *Palmaepollenites kutchensis*, Palmae, *Dicolpopollis malesianus,* and Polyad pollen; and Pteridophyte spore com-

Figure 4.5.22. Photomicrograph of *Marginipollis* type *Barringtonia*, contained in oil shale of the Sangkarewang Formation, Ombilin Basin.

63

posed of *Magnastriatites howardii, Crassoretitriletes vanraadshooveni, Cicatricosisporites dorogensis, Laevigatosporites, Triletesporites, Verrucatosisporites usmensis*, and *Verrucosisporites*. On the other hand, the presence of *Zonocostites ramonae, Acrosthicum aureum* (Figure 4.5.23) and *Discoidites borneensis* tends to show a tidal (back-mangrove/mangrove) environment. Therefore, the depositional environment of the pollen-bearing oil shale is presumed to be an alluvial or freshwater swamp, influenced by a marine incursion. Those evidence are also supported by the presence of freshwater fossil in Sipang River (Figure 4.5.24).
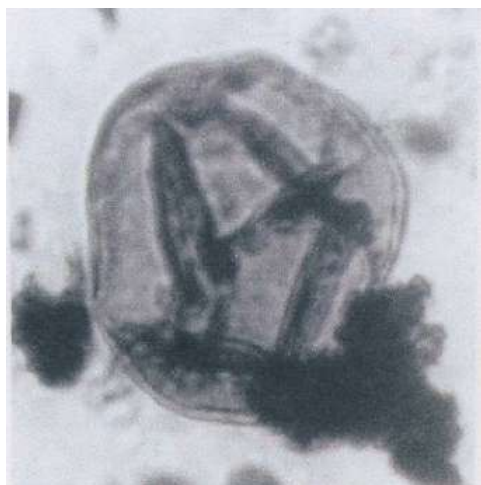
4.5.23. Photomicrograph of *Acrosthicum aureum*, contained in oil shale of the Sangkarewang Formation, Ombilin Basin.

Figure 4.5.24. Fossil of freshwater fish (*Notopterus notopterus*) contained in Sangkarewang Formation. Location: Sipang River, Ombilin Basin.

4.5.1.2. Sawahlunto Formation

One sample (01NS.16A) determined by XRD-analysis is typically sandstone, comprising 54.0 % quartz, 16.0 % calcite, 11.0 % plagioclase, 11.0 % kaolinite, and 8 % smectite Table 4.5.5).

4.6. Kiliranjao Sub-basin
4.6.1. Sedimentary Facies

General sedimentary facies analyses and facies sequences of the formation are established by describing the columnar section as shown in Figures 4.6.1-4.6.3, respectively.

The rock outcropping in the Kiliranjao (PT. Karbindo Absyapradhi Coal Mines) and Kunangan (Figure 2.1.4.1) areas, predominantly comprise well-bedded shales, laminated siltstones, and (Figures 4.6.4 - 4.6.8), and non-laminated mudstones containing freshwater fossil mollusc (Figure 4.6.9). However, minor fine-grained sandstone with conglomerate pockets (Figure 4.6.10) and resins that are very common within the reddish brown non-laminated mudstone

(Figure 4.6.10) were recognized in the Kiliranjao area. In places, the presence of resin is common to find within the reddish spongy brown non-laminated mudstone (Figure 4.6.11). Moreover, thick quartz sandstone intercalations commonly occur (Figure 4.6.12). Sedimentary structures recognised, include ripple-marks (Figure 4.6.13), parallel plane laminae (Figures 4.6.6 and 4.6.14), and bedding trace fossil/burrows (Figure 4.6.15). Moreover, pyrites are also recognized microscopically (Figure 4.6.16).

Impressions of woody organic detritus (leaves, twigs, and barks) up to several centimetres in size are common to occur on bedding-plane surfaces within the siltstones (Figures 4.6.17 and 4.6.18). The rock sequence can be interpreted as a lake marginal facies, with an interruption of a fluvial facies indicated by the occurrence of fining-upward sandstone and small (pocket) conglomerate channel deposits (Figure 4.6.19).

The limited XRD-data of four samples (00/NS-08F3, 00/NS-08J2, 00/NS-08P1, and 00/NS-
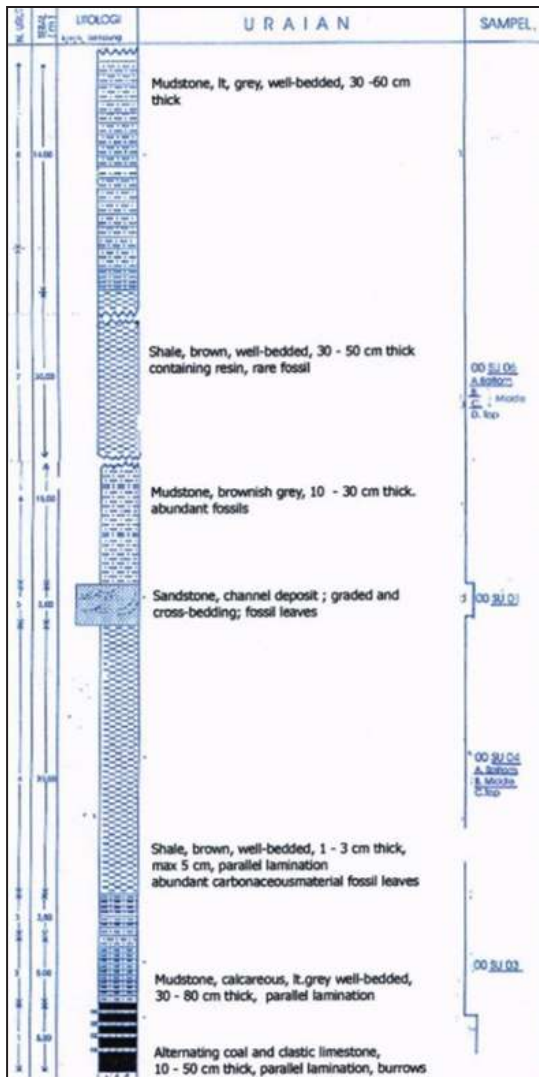
Figure 4.6.1. Columnar measured section of some rock sequence portions of the Kiliran Formation, showing interbedded shale and mudstone, with sandstone intercalation; the lower part of sequence comprises alternating coal and clastic limestone, Kiliranjao Sub-basin.

Figure 4.6.2. Columnar measured section of part of Kiliran Formation.

08R1) suggest that the rocks comprise of abundant quartz (> 75 %), common kaolinite (25 - 75 %), and sparse pyrite (5 - 25 %) (Table 4.6.1).

Three selected representative samples were investigated by means of SEM. Two samples (00/NS-08G and 00/NS-13) are typically shale, while one sample (00/NS-08F3) is fine silty shale.

Kaolinite clays are the most prominent matrix within the shale, although mixed-layer clays of smectite-illite are also present. Moreover, organic constituents, those are abundant typical lamalginites (Figures 4.6.20.and 4.6.21), some sporinites (Figures 4.6.22 and 4.6.23), and subordinate typical alginite (*?Botryococcus*) (Figure 4.6.24), oil drop (Figure 4.6.25) and bitumen (Figure 4.6.26), are significantly recognised. Framboidal pyrite is
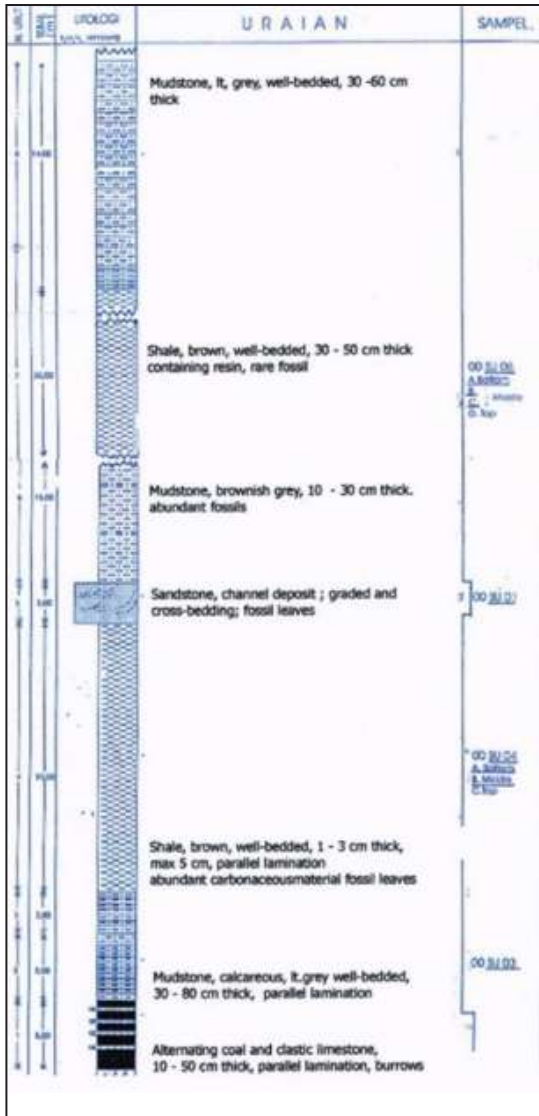
Figure 4.6.3. Columnar measured section of part of Kiliran Formation.

Figure 4.6.4. Thick cutt-off sequence of shale and inter-bedded mudstone of Kiliran Formation, outcropping in the PT. Karbindo Absyapradhi Coal Mines.

Figure 4.6.5. Folded thick well-laminated siltstones and shales of Kiliran Formation, in Kunangan coalfield.

Figure 4.6.6. Highly dipping northwards, well-bedded thick shale-mudstone of Kiliran Formation, in the PT. Karbindo Absyapradhi Coal Mines.

also present (Figure 4.6.27). The clay minerals are mostly irregular or disordered crystal shapes, except one sample (00/NS-13), where the kaolinite clays shows well crystallized forming booklet structures (Figure 4.6.28). The disordered clays are usually mixed crystals between smectite-illite and kaolinite (Figure 4.6.29), with some of them are slightly oriented shapes. The contact crystal

Figure 4.6.7. Shale outcrop showing parallel laminae structure of Kiliran Formation.

Figure 4.6.10. Fine-grained sandstone with conglomerate pockets.
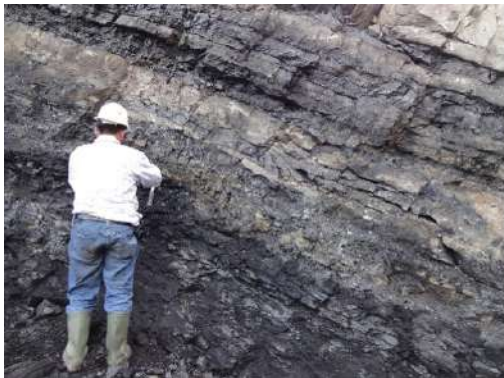
Figure 4.6.8. Well-bedded sequence of oil shale overlay conformably coam seam, exposed in Kiliran Formation.

Figure 4.6.11. Outcrop of mudstone, greyish brown, spongy, massive to thick bedded, with very common resin; exposed in Karbindo Coalfield, Kiliranjao.

Figure 4.6.9. A thick layer mudstone containing freshwater fossil mollusc horizon of Kiliran Formation.

Figure 4.6.12. Thick bedded medium-grained quartz sandstone, interbedded between mudstone; outcropping in Karbindo Coalfield, Kiliranjao.

Figure 4.6.13. Sedimentary structures recognised, ripple-marks occurring within mudstone of Kiliran Formation.

Figure 4.6.16. Framboidal and non-framboidal pyrite recognized within the mudstone of Kiliran Formation.

Figure 4.6.14. High cliff of Kiliran Formation, showing well parallen lamination structure.

Figure 4.6.17. Leaf fossil is common to found embedded in siltstone of Kiliran Formation.

(Figure 4.6.15. Bedding trace fossil/burrows)

Figure 4.6.18. Fossil of wood/tree bark embedded in very fine-grained sandstone of Kiliran Formation.

(Figure 4.6.19. Small (pocket) conglomerate channel deposits.)

is usually disordered latticed crystal with some floating contacts.

Micropores have been well developed within the clay lattices ranging from 0.05 microns up to 15 microns in diameter. The pore spaces have probably developed during diagenetic process due to dissolution and crystal rearrangements. Therefore, those micropores are believed to facilitate the liquid hydrocarbons or bitumen to migrate somewhere.

Diagenesis characters are identified by the presence of authigenic clays, such as kaolinite and smectite-illite, but compaction and crystal orientations are also significantly indicators. Thus, the rocks examined have mostly been realm by diagenetic processes of Early Mesodiagenesis to Mesodiagenesis regimes. Most of shale has been buried at more than 1000 m depth which now they have been exposed on the surface.

The clay minerals are regular or well-oriented, except sample 01NS.15B having disordered or disoriented clay mineral flakes and crystal lattices. The disordered clay mineral is kaolinite, with cement of micritic and sparry calcite. Furthermore, the presence of inorganic matter content (calcite) forming fossil trace and cement (Figure 4.6.30) is recognized in sample 01NS.15B.

Micropores have well developed within the clay crystals and lattices ranging from 0.05 microns up to 15 microns in diameter. The pore spaces have probably developed during diage-

netic process due to dissolution and crystal rearrangements.

The presence of authigenic clays such as, kaolinite and smectite-illite, identifies the diagenesis characters. However, compaction and crystal orientations are also significant indicators. Thus, the rocks examined have mostly been realm by diagenetic processes of Late Eodiagenesis to Early Mesodiagenesis regimes. The sediments had been buried at depth of less than 1000 m, which now they have been exposed on the surface.

Eighteen samples of shales and mudstone from the Kunangan area, were analysed for palynological study. From these samples, one of the most valuable age marker is *Meyeripollis naharkotensis* (Figure 4.6.31). Its age is Middle to Late Oligocene. Moreover, another guide pollen is determined, such as *Florschuetzia trilobata* and *Stenochlaenidiites usmensis / Verrucatosporites* indicating an age ranging from Eocene to Middle Miocene. Some of pollen are also clearly observed, those are *Ancrostichum aureum, Magnastriatites howardii* and *Lycodium*. On the basis of *Meyeripollis naharkotensis, Florschuetzia trilobata*, and *Stenochlaenidiites usmensis / Verrucatosporites* occurrence, generally, the Lakat Formation was deposited in Middle to Late Oligocene.

Samples occupied by high spore content and abundant freshwater and alluvial swamp flora content such as *Chepalomappa malloticarpa, Dryabalanops, Elaeocarpus, Euphorbiaceae, Iugopollis / Aglola sp.* and *Macarango* (00NS02C, 02E, 02K, UM02A, 02B and UM03A) are also determined. Some samples containing of *spore Acrosthicum aureum, Avicennia* and *Florschuetzia trilobata* (00NS04A, 04B, 04C and 04E), indicate that mangrove environment influenced during the deposition of these samples. These palynological data indicate that the depositional environment is presumed to be a transitional area.

Some selected samples of shales and mudstones from the Kiliran Formation analyzed palynologically tend to indicate that the formation is considered to be Late Eocene to Oligocene in

age. The age obtained is based on the association of *Florschuetzia trilobata, Verrucatosporites usmensis, Cicatricosisporites dorogenesis* (Figure 4.6.32), *Magnastriatites howardii, Crassoretitrileles vanraadschooveni, Palmaepolenites kutchensis, Gemmatricolporites pilatus* (Figure 4.6.33), *Discoidites pilosus*, and *Lagerstroemia.*

Furthermore, an assemblage of *Florschuetzia trilobata,* Casuarina types*, Palmaepollenites kutchensis,* Palmae*, Dicolpopollis malesianus, Gemmatricolporites Pilatus, Lagerstroemia, Retistephanocolpites williamsii,* Durio*, Magnastriatites howardii, Crassoretitrileles vanraadschooveni, Cicatricosisporites dorogenesis, Laevigatosporites, Pteris, Verrucatosporites usmensis,* and *Verucosisporites* dominates the pollen and spore types. This fossil assemblage represents a terrestrial vegetation, freshwater with a high plant diversity. However, the existence of *Zonocostites ramonae, Acrosthicum aureum* (Figure 4.6.34) and *Discoidites pilosus* shows a tidal (back mangrove/mangrove) environment. Therefore, the deposional environment of oil shale contained those pollen-spore assemblage is presumed to be an alluvial or freshwater swamp, influenced by a marine incursion.

4.7. Bukit Susah

The shale sequence predominantly comprises microlaminated organic-rich, brown mudstone (Figure 4.7.1) which is weakly calcareous and contains frequent phosphatic nodules. Other than the microlamination, depositional structures are rare. Microlaminae appear as dark organic-rich and lighter clay doublets. Skeletal debris (ostracods) is rare, however, a reasonable sized fish fauna lived in the lake. There is no evidence of bioturbation and bottom conditions are thought to have been anoxic. Thin (1-2 mm), fine-grained sandstones and siltstones occur as occasionally clustered. Tbcd turbidite interbeds. Similar clusters of thin crystal to lithic rich tuff are also present. Palynological data support a lacustrine setting, based upon the association of frequent freshwater dinoflagellates and *Pediastrum* algae. The poor

and rare preservation of spores and pollen in certain samples suggest a distal to shore setting.

4.7.1. Coarse Clastics

Three distinct coarse clastic units 3-4 m thick occur within the brown shales. The bases are erosional and the units comprise a mixture of sands, pebbly sands and conglomerate, which are generally, normally graded. The units have been variably influenced by pedogenesis as evidenced by limonitic staining and mixing of fabric through rootlet penetration, however, the units are abruptly succeeded by brown shales in each case. Sedimentary structures are poorly developed due to the pedogenesis, but include planar cross-bedding and clast imbrication. Clasts are sub-angular to sub-rounded; the most common clasts are interpreted as sandy to gravelly fluvial channel fill deposits.

Several grey shale horizons are developed within the coarse clastics and also within the brown shales. The grey shales are strongly laminated (Figure 4.7.2), and are transitional between underlying lacustrine brown shale and overlying orange paleosol. The grey shales are interpreted to have originally been lacustrine muds that have been increasingly affected by pedogenesis under waterlogged conditions in an emerging lake margin setting.

4.7.2. Lake Fill – Fan Delta Facies Associations

In the Bukit Susah area, the shale formation is succeeded by disorganised, muddy, pebble and cobble grade gravels with coarse lithic arenite. A red mottled, terrigenous, mud matrix with occasional plant debris is predominant. Large phyllite clasts are common, however, there is a relative increase in quartz and quartzite lithoclasts. Individual units are up to 40 m thick, dip at 25^0 or more and comprise stacked, normal to occasionally inversely graded beds, 1 m to 3 m thick with scoured bases.

The sequence is interpreted as a series of alluvial, fan deltas that progressively filled the Sumai Basin from the NW. The vertical distance

between the tops and bottoms of the prograding foresets is estimated to be 300 m, implying that fan deltas prograded into a lake with a depth of similar magnitude.

The brown shales are physically analogous to the shallow lake "facies" of Longley *et al*. (1990). The association with grey shales and occurrence of fungal hyphae, appears to support a relatively shallow setting with periods of exposure. Nonetheless, several key samples are impoverished in terrestrial spores and pollen and are interpreted to have been deposited distal to lake shore in, perhaps, a deep setting. The overlying lake fill facies appear to have prograded into a body of water estimated to be 300 m deep.

A complete Kelesa graben fill sequence is exposed surficially in the Bukit Susah. Four genetic stratigraphic units are recognised: alluvial-fluvial; swamp-lake margin; deep lacustrine; and, alluvial fan-delta lake fill. The Kelesa Formation succession exposed can be divided into three groups, those are: coarse clastics comprising conglomerate and breccias; medium to coarse clastics composed of conglomeratic sandstone and sandstone with siltstone intercalation; and fine clastics consisting of shale with siltstone and fine sandstone intercalations.

A complete oil shale succession, directly overlies basement rock, occupies the Putikayu River (Figure 4.7.3). Total thickness of the Kelesa Formation around 86.8 m. Oil shale bed rich in organic matter and having thickness of approximately 27.90 m (Figure 4.7.4) occupies the lower part of Kelesa Formation. The oil shale layer is associated with carbonaceous siltstone, sandstone, and conglomerate.

The oil shale unit, in general, thinly to thickly bedded, papery – flaggy, soft – hard (Figure 4.7.4), alternating blackish and brownish grey colour, containing intercalation of mudstone and fine sandstone.

4.7.3. X-Ray diffraction (XRD)

XRD performed on three shale samples, those are 03ES13A, 03NS13A, and 03NS16A, shows

that shale/mudstone contains quartz mineral varying between 40,2 and 72,6%, kaolinite from 5,6 to 23,0 %, illite between 0,0 - 13.3%, smectite from 0,0 to 4,4%, smectite-illite 0,0 to 7,0%, and calcite from 0,0 to 53,0%.

The presence of calcite suggests that there was a marine incursion within a short time.

4.8. East Tigapuluh Mountains

To minimize the effect of outcrop weathering on geochemical analyses, the study was performed on some man-made exposures, *i.e.* several new timber road-cut showing nearly fresh Lakat Formation outcrop. The Oligocene Lakat Formation, occupying the East Tigapuluh Mountains, is a transgressive marine sequence (Suwarna *et al*., 1991) (Figure 4.8.1). Lithologicaly, the formation subdivided into lower and upper parts, comprises thick sandstone with interbedded shales and subordinate conglomerate and mudstone beds, and coal and carbonaceous seams.

The Oligocene Lakat Formation, occupying the East Tigapuluh Mountains, lithologically, is subdivided into the lower and upper parts. The lower part comprises thick, fine- to coarse-grained sandstones and occasional interbedded light grey shales with subordinate amounts of conglomerate and mudstone beds, as well as coal and carbonaceous mudstone (Figure 4.8.1). This part was deposited as a fluvial deposit with stacking fining-upward cycles. The well-developed sandstone, achieving a thickness of 350 m, generally ill-sorted, conglomeratic, kaolinitic, massive to cross-bedded, and glauconitic. The sandstone is considered to be transported from north to southwards, in the central part of the basin. The Upper Lakat Formation is composed of fluvial channel sandstones, shale, and flood plain/swampy deposits. The shale is grey to green, occasionally calcareous and burrowed. These rocks may represent a sedimentation under submergent conditions of tidal flat to shallow marine shelf environment. The sequence gradationally overlying the lower part of the formation. The rock distribution in the East Tigapuluh Mountains area is displayed in Figure 4.8.2

Table 4.8.1. Summary of SEM Analysis Results on Lakat Oil Shale Samples, East Tigapuluh Mountains Area

Sample No.	Type of Rock/ Sample	Composition	Type of Clay	Texture/ structure of Clay	Fossil Fuel	Diagenesis Character/ Feature	Diagenesis Regime	Remark
00/NS-01D	Sandy shale, gray.	Fine detritals of quartz, feldspar, clay minerals; rare organics.	Kaolinite and smectite-illite	Slightly well oriented and flaky, dense, micropores are common in-between the clay crystals.	Rare	Very compact and dense, and well oriented clay minerals, probably due to tectonics and structures.	Meso-diagenesis.	Probably have been buried up to more than 1500 m depth.
00/NS-04B	Shale, brownish gray	Predominantly clay minerals, pyrite, few silica, and organic bitumen matter.	Kaolinite, few smectite.	Irregular flakes dense, micropores are developed within the kaolinite crystals.	Vitrinite, "oil drop" or bitumen.	Compaction and semi-oriented clay minerals, oil expulsion from organics.	Early meso-diagenesis.	Probably have been buried more than 1000 m depth.
00/NS-04E	Shale, brownish gray.	Predominantly clay minerals and organic matter.	Kaolinite and few smectite.	Irregular clay mineral flakes; micropores are common.	"Algae" (typical ? *botryococcus*) and "oil drop" or bitumen.	The present of kaolinite and few smectite, although less dense.	Eodiagenesis up to early meso-diagenesis	Probably have been buried of more than 1000 m depth.

Palynological analysis performed shows the occurrence *Meyeripollis naharkotensis, Florschuetzia trilobata*, and *Stenochlaenidiites usmensis/Verrucatosporites usmensis*. Thereby, generally, the age of the mudstone from the Lakat Formation is Middle to Late Oligocene, with depositional environment ranges from freshwater, transition to shallow neritic condition.

The organic matter contained in shales and mudstones of the formation, comprises predominantly algae of typical lamalginite, with minor vitrinite. A very minor amount of probable telalginite-*Botryococcus* is also recognized.

The mudstones comprise common to abundant quartz (25 - >75%), sparse to common kaolinite (5 - 75%), and rare to sparse illite (<5 - 25%), with rare smectite (< 5%), and some samples containing abundant calcite (> 75%) (Figure 4.8.2). The matrix is predominantly kaolinite, although mixed-layer smectite-illite and smectite also occur. Micropores (pore spaces) have been developed within the clay lattices ranging from 0.05 μ up to 15 μ. Therefore, the migration of liquid hydrocarbons or bitumens and also gas to somewhere, are believed to be facilitated by those micropores. Framboidal pyrites are present in most samples. The diagenetic processes are most likely included into Eodiagenesis to Mesodiagenesis regimes, indicating that the Lakat Formation has been buried at more 1000 m depth.

4.9. Bukit Bakar Area

4.10. Sinamar Sub-Basin

4.11. Asai-Rawas Area

The Tertiary sedimentary sequences recognized in the study area are composed of the Papanbetupang (Tomp) and Kasiro (Tmk) Formations (Suwarna dan Suharsono, 1984; Suwarna *et al*., 1992; Suwarna, 1996; Suwarna *et al*.,1998). The Oligocene Papanbetupang Formation occurs as conglomerate, sandstone, claystone, siltstone, with intercalation of breccias and thin coal seams. This formation interfingers with the middle part of Kasiro Formation, composed of oil shale-bearing unit. The Kasiro Formation comprising oil shale-bearing succession, in general, is pre-
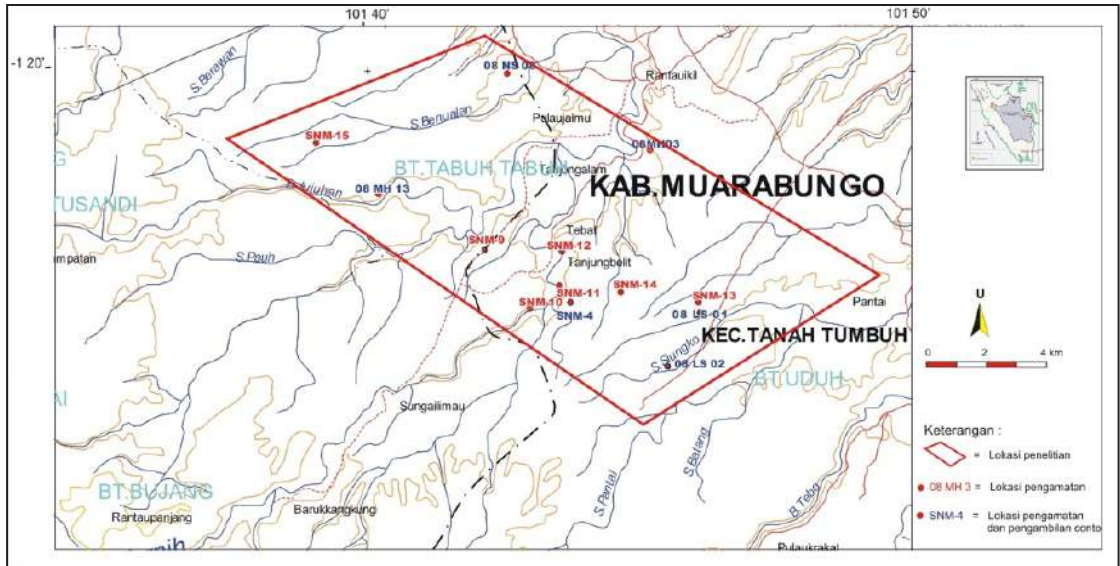
Figure 4.10.1. Locality map of studied area and sampling sites in Sinamar.
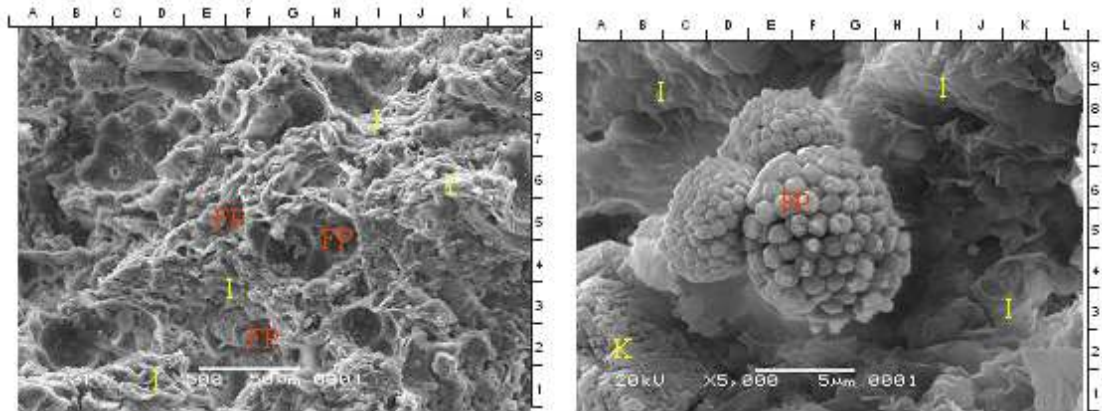
Figure 4.10.2. SEM photomicrograph of Sinamar shale showing framboidal pyrite. Sample 08NS08.

sented in columnar sections of four areas studied, those are Keruh River, Sekeladi Area, Asai River Upstream, and Lepat River (Figure 4.11.1). The sedimentary formations are composed of shale, claystone, siltstone, mudstone, with intercalations of tuffaceous sandstone, conglomeratic locally, and 1- 10 m-thick coal seams, as depicted in Figures 4.11.2. *Viviparus* (?), as a freshwater mollusc was recognized within brownish dark grey Kasiro

mudstone layer (Figure 4.11.3). This dark grey fine clastic sequence shows parallel bedding and fining upward structures. The bedding has been folded with dipping 15 – 30°. Those rocks can be correlated to *Overgangs Member* of Spruyt (1956).

Furthermore, the Kasiro Formation (Suwarna and Suharsono, 1984) can be correlated to the Keruh, Kiliran, Sangkarewang, Kelesa, Kebun-

Figure 4.10.3. Photograph of quartz sandstone Sinamar Formation outcrop
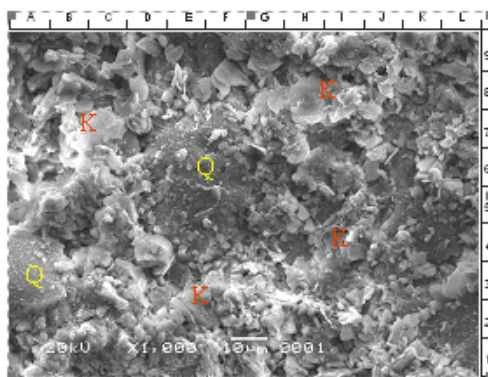
Figure 4.10.6. SEM photomicrographs of quartz (Q). Sample 08LS02.

Figure 4.10.4. Photograph of conglomeratic quartz sandstone Sinamar Formation outcrop.
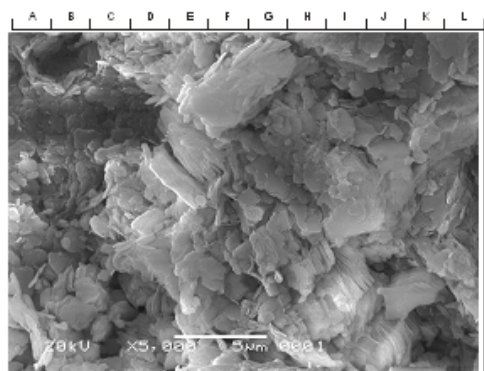
Figure 4.10.7. SEM photomicrograph of kaolinite with "booklet" structure. Sample 08LS02.

Figure 4.10.5. Photograph of conglomeratic quartz sandstone Sinamar Formation outcrop showing quartz grain layering.

tinggi, and Bukitbakar Formations, made up of shale, claystone, and mudstone, which are rich in organic matter and coal seams. The formations mentioned above are assumed to be oil shale-bearing sediments (Suwarna *et al*., 2000 and 2001; Suwarna, 2004b; Heryanto *et al*., 2003; Susanto *et al*., 2004; Kusumahbrata *et al*., 20..; Hermiyanto *et al*., 20..).

Lignitic to bright banded coal are recognized as well. The whole sediments are presumed to be deposited in fluvial-lacustrine environment under a low energy regime condition (Suwarna and Suharsono, 1984; Suwarna, 2004 a; Suwarna *et al*., 20..).

Figure 4.10.8. Trace fossil recognized in the Sinamar Formation.

Figure 4.10.9. Outcrop of well-bedded Sinamar shale.

Figure 4.10.11.

Figure 4.10.10. Freshwater fish fossil embedded in clay-stone of Sinamar Formation.

Figure 4.10.12. Photomicrograph of framboidal and non-framboidal pyrites embedded within shale of Sinamar Formation.

Figure 4.10.13. Fossil of burned log consisting of fusite, embedded within Sinamar mudstone.

Figure 4.11.5. Photograph of papery to flaggy oil shale succession of the Kasiro Formation. Location: Keruh River (Susanto, 2005).

Lacustrine Facies

The facies is represented by fine-grained sediments, light to dark grey in colour, showing parallel lamination structure, hard, no or rare bioturbation. This characteristic indicates that the sedimentary rocks were deposited within a deep and quiet water condition.

Abundant tiny coaly fragments embedded in mudstone form lamination or very thin layers and small lenses, parallel to the lamination. Those characteristics are recognized from the lowest to the upper parts of Kasiro Formation. On the basis those criteria, the Kasiro Formation can be divided into two sedimentary facies: low and high fluvial energy. However, the high energy regime only took place at the lowest part or formation.

As a whole, identified physical character of oil shale deposits shown on each measured section, can be grouped into two types, *i.e.* shale having dark grey to black in colour, papery – flaky -flaggy and brownish light grey shale, showing papery – flaky structures.

A significant physical character of oil shale located in northern area compared to southern area is recognized. In northern parts of studied area, such as Lepat River, Sekeladi, and Renahpisangsemali, oil shal beds, in general, are light to dark grey, dark grey to black, until light brown grey in colours. Flaggy structure is predominated, although papery

Figure 4.11.4. Photograph of alternating, well bedded shale and siltstone of the Kasiro Formation. Location: Keruh-Rawas River. (Susanto, 2005).

Sedimentology

Sedimentologically, Kasiro Formation is made up of two sedimentary facies, those are fluvial channel and lacustrine.

Fluvial Channel Facies

The facies is dominated by tuffaceous quartz sandstone, medium- to coarse-grained, conglomeratic locally, parallel bedding and low angle cross-bedding are rcognized. The sedimentary sequence is presumed to be deposited within low to high flow regimes, taking place during a high flooding. The facies is recorded within the lowest part of Kasiro Formation.

UMUR	FORMASI	STASIUN AMAT & KODE SAMPEL	KEDUDUKAN DAN TEBAL	SIMBOL BATUAN	UKURAN BUTIR	STRUKTUR SEDIMEN	PERIAN BATUAN	LINGKUNGAN PENGENDAPAN

The stratigraphic column descriptions (PERIAN BATUAN):

Batulempung, berwarna abu-abu pucat, ukuran butir lempung, struktur berlapis, komposisi mineral silika, banyak mengandung oksida besi, ketebalan 0,5 meter.

Serpih batubaraan (*coaly shale*), berwarna hitam kecoklatan, lunak, ukuran butir lempung, struktur berlapis, komposisi banyak mengandung mineral organik, semakin ke bawah semakin dw/agak menyerpih, ketebalan 0,2 meter.

Batubara dull coal, berwarna hitam, struktur berlapis, kusam, rekahan mikro agak banyak mengandung *resin*, keras, ketebalan 0,14 meter.

Batubara serpihan (*shally coal*), berwarna hitam kecoklatan, lunak, ukuran butir lempung, struktur berlapis, komposisi banyak mengandung mineral organik, agak menyerpih, ketebalan 0,12 meter.

Batubara dull coal, berwarna hitam, struktur berlapis, kusam, rekahan mikro agak banyak mengandung *resin*, keras, ketebalan 0,23 meter.

Serpih batubaraan (*coaly shale*), berwarna hitam kecoklatan, lunak, ukuran butir lempung, struktur berlapis, komposisi banyak mengandung mineral organik, semakin ke bawah semakin dw/agak menyerpih, ketebalan 0,26 meter.

Batubara dull coal, berwarna hitam, struktur berlapis, kusam, rekahan mikro agak banyak mengandung *resin*, keras, ketebalan 0,60 meter.

Batulempung, berwarna abu-abu gelap, ukuran butir lempung, struktur berlapis, komposisi mineral silika, banyak mengandung material organik, ketebalan 1,0 meter. Semakin ke atas semakin lunak.

Other column labels: EOSEN - OLIGOSEN; FORMASI SINAMAR; 08 MH 11A, 08 MH 11B, 08 MH 11C, 08 MH 11D, 08 MH 11E, 08 MH 11G, 08 MH 11H, 08 MH 11I, 08 MH 11J, 08 MH 11K; N 50° E/15°.

Figure 4.11.6. Photograph of Kasiro mudstone, well thick bedded to massive. Location: Rawas-Keruh River. (Susanto, 2005).

occurs in places. Whilst, in the southern parts, at Keruh River, the oil shales are light to dark grey and brownish grey in colour, showing papery and flaggy structures in an almost similar proportion.

4.11.1. Sungai Keruh

Generally, oil shale studied, in several detailed traverses, show the thickness varying from 1.0 to 4.5 m (Figures 4.11.1 and 4.11.4). Papery – flaggy structure can be reconized clearly terlihat (Figures 4.11.5); flaky structure is common. Interseam sediments, in general, comprise mudstone, brownish grey, thick well-bedded to massive (Figure 4.11.6) and well-bedded light grey siltstone.

Besides that, up to 1.5 m thick coal seam underlying oil shale occurs as well (Figure 4.11.7). Lithotypically, the coal varies from dull to dull banded; whilst locally, banded lithotype was recognized.

On the basis of sedimentary structure and lithofacies association, the oil shale-bearing sediments are presumed to be deposited in fluvial-lacustrine environments, whereas oil shale itself was deposited in a lacustrine environment of various depths, within an intramountain basin.

Organic petrographic analysis shows that lamalginite submaceral has been preserved well in Kasiro coal. This submaceral is used as one of lacustrine deposit markers, where the basin was relatively deep, with relatively low oxygen level, in an anoxic (anaerobic) condition, in which algae can flourish well.

4.11.2. Sekeladi

During the research activity in Sekeladi area, several outcrops of thick oil shale horizons, containing coal seam intercalations have been rcognized, as shown in Figure 4.11.8.

Oil Shale Potential as an Alternative Energy Source, in Selected Sites of Sumatra Island
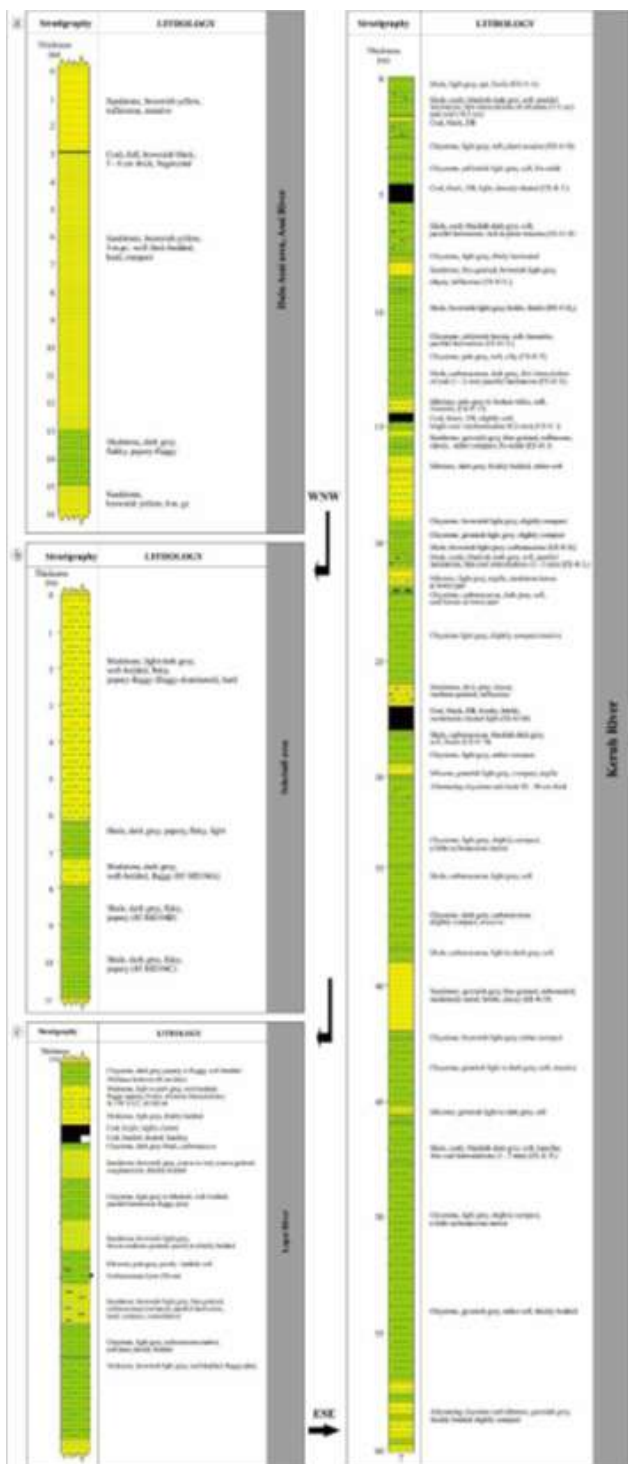
Figure 4.11.1. Columnar measured section of the Kasiro Formation in four sites of investigation.

Figure 4.11.2. Photograph of up to 1.5 m thick-coal seam outcrop of the Kasiro Formation, overlying oil shale layer. Location: Keruh River (Susanto, 2005).

Figure 4.11.5. Photograph of papery to flaggy oil shale succession of the Kasiro Formation. Location: Keruh River (Susanto, 2005).

Figure 4.11.3. Outcrop of Kasiro mudstone containing freshwater mollusc (Viviparus-*like*) fossil.

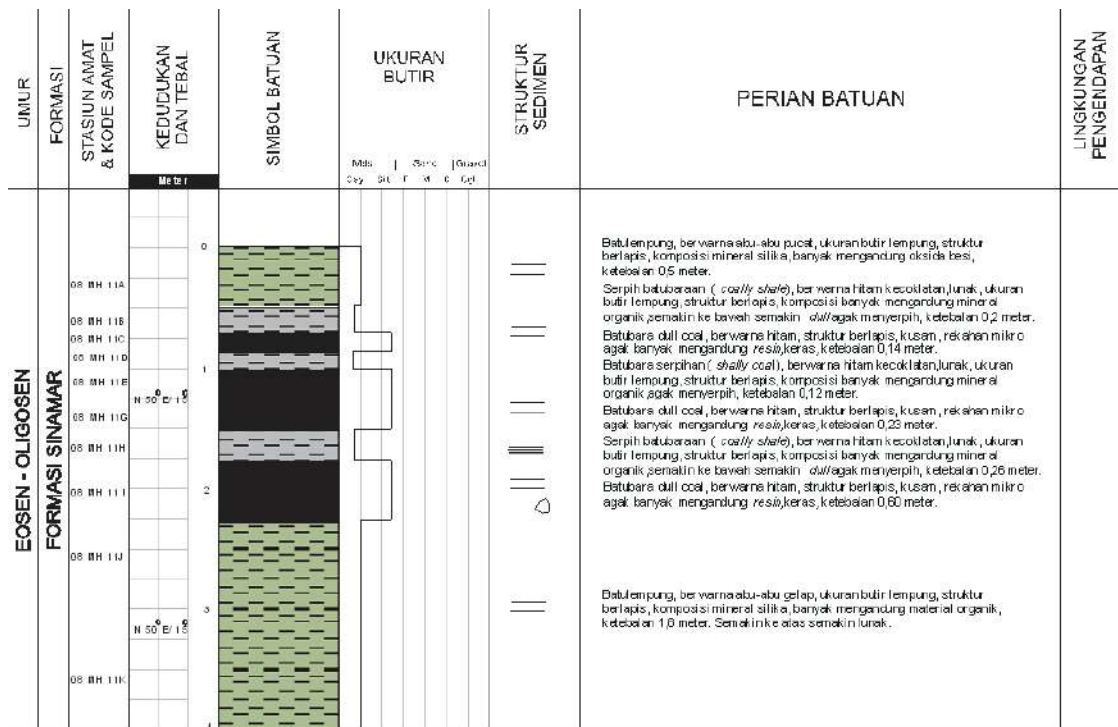Figure 4.11.6. Photograph of Kasiro mudstone, well thick bedded to massive. Location: Rawas-Keruh River. (Susanto, 2005).

Figure 4.11.4. Photograph of alternating, well bedded shale and siltstone of the Kasiro Formation. Location: Keruh-Rawas River. (Susanto, 2005).

Figure 4.11.7. Photograph of dull to dull banded coal of the Kasiro Formation. Location: Keruh-Rawas River. (Susanto, 2005).

Two oil shale seams have been detected, having thicknesses ranging from 1 – 4 m thick (Figures 4.11.9 and 4.11.10). The seams comprise shale and mudstone. Shale, light to dark grey, flaky, papery-flaggy, where the flaggy structure is dominant. Mudstone, commonly dark grey to brownish grey, hard, compact, well thin bedded, flaggy structured, flaky in fragments (Figure 4.11.10). Dipping angle around 25 – 32°.

4.11.3. Asai Upstream, Renahpisangkemali Region

Oil shale research was carried out along Asai River and its tributaries, such as Gedang and Kenaik Rivers.

Forming cliffs and base of the rivers, well bedded oil shale with its underlying and overlying well bedded sandstone and siltstone, are exposed clearly, as shown in Figures 4.11.11- 4.11.13. The oil shale together with mudstone, having thickness of 4 – 10 m, platy-papery- flaggy, flaky, predominantly light grey. Dip angle of bedding around 22^0.

Sandstone, as overlying and underlying sediments of oil shale, brownish to yellowish light grey, quartzose, sometimes tuffaceous, fine- to medium-grained, well-sorted, well-bedded, thick, hard, and compact. Locally, mafic minerals, feldspar, coal fragments, and carbonaceous matter were recognized within the sandstone. Dipping angle of the beds varies around 26-28^0.

Sungai Lepat

Oil shale study was carried out along Lepat and Tanoi Rivers. Well bedded oil shale associated with coal seams are exposed along both rivers. Four oil shale seams of 0.4 – 6.5 m thick were observed (Figure 4.11.14). Commonly they are light grey, papery – flaggy, thin to thick bedded. Intercalations of fine- to medium-grained, light grey sandstones, having thickness of 0.2 – 1.0 m, can be found. Moreover, light grey siltstone intercalations, 1.5 – 3 m thick, occur. Dipping angles recognized are 22° and 60°.

Furthermore, coal seams of 0.1 – 4.0 m thick, comprise banded to bright banded lithotype (Figure 4.11.15) with thin intercalations of bright, banded, and dull banded lithotypes occur. Dipping angles measured are 12° and 60°.

Mineralogy

SEM and X-ray diffraction (XRD) analyses were carried out to obtain mineralogical composition of oil shale and its associated fine-grained sediments. The SEM and XRD analyses performed on rock samples, mainly in order to gain the clay mineral types, as well as their diagenetic level (Pittman, 1979; Wilson and Pittman, 1979).

Based on lithological types and mineral contents obtained from SEM analysis (Table 4.11.1), oil shale unit can be grouped into lithic sandstone (Figures 4.11.16 and 4.11.17),

Figure 4.11.8. Photograph of dull- banded coal seam containing tonstein (10 – 15 cm thick) intercalations., associated with oil shale. Location: Sekeladi River. (Suwarna, 2005).

Figure 4.11.9. Photograph of outcrop of Kasiro oil shale unit, showing thickness > 4 m. Location: Sekeladi River. (Suwarna, 2005).

Figure 4.11.10. Photograph of outcrop of Kasiro mudstone unit, showing thinly to thickly bedded-flaggy structure; hard, compact. Location: Sekeladi River. (Suwarna, 2005).

Figure 4.11.13. Photograph of Kasiro oil shale bed underlain by coal seam, forming a high cliff of the Batang Asai River. Location: opposite side of Figure 4.11.12 (Suwarna, 2005).

Figure 4.11.11. Photograph of oil shale bed associated with fine clastic sediments, occurring as a cliff of riverbank. Location: Renahpisangkemali Village. (Suwarna, 2005).

Figure 4.11.14. Photograph of outcrop of Kasiro oil shale unit, showing flaky, papery – flaggy structure. Location: Sekeladi River. (Suwarna, 2005).

Figure 4.11.12. Photograph of oil shale bed of the Kasiro Formation, underlain and overlain by thick bedded fine-grained sandstone-silstone. Location: Nearby Renahpisangkemali Village. (Suwarna, 2005).
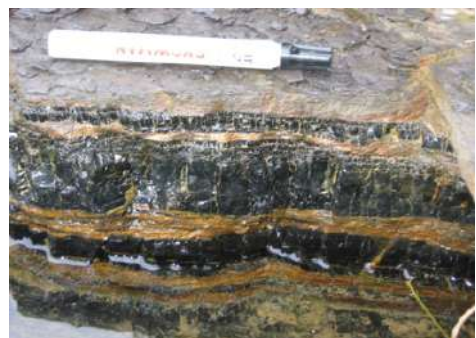
Figure 4.11.15. Photograph of bright-bright banded coal seam underlying oil shale unit. Location: Lepat River. (Suwarna, 2005).

Table 4.11.1. Result of SEM and XRD Analyses of Kasiro Mudstone Samples, Asai-Rawas Sub-basin

Sample No. (05)	Lithology	Composition	Type of clay/ cement	Matrix texture/ structure. Cement texture	Type of % porosity	Diagenetic Characters and Regime
ES26	Lithic sandstone, fine- to medium-grained	Quartz, 60-70%; feldspar (plagioclase), 10-15%, rock fragments, 3-5%; clay matrix 5-10%.	Mostly authigenic illite and kaolinite	Irregular kaolinite texture, *crenulated* illite.	Intermatrix secondary porosity <3%.	The presence of authigenic kaolinite and illite; compaction, dissolution. Meso-diagenesis, probably has been buried in > 2000 m deep.
ES29	Lithic sandstone, medium grained.	Quartz, 60-70%; feldspar, 5-10%; rock fragment, 5-8%; clay matrix, 8-12%.	Kaolinite, illite, and smectite	Book textured kaolinite, *crenulated* and *hairy* illite and smectite.	Secondary porosity, intermatrix; <3%.	The presence of authigenic kaolinite, illite, and smectite; Fe-oxides, compaction. Meso-diagenesis, probably has been buried in > 2000 m deep.
ES30	Claystone, tuffaceous.	Kaolinite (70-80%), quartz (10-15%), feldspar (2-4%), calcite <1%.	Kaolinite	Irregular texture of kaolinite.	-	Kaolinite, silica (quartz growth), compaction. Meso-diagenesis, probably has been buried in > 2000 m deep.
ES31A	Claystone, tuffaceous.	Smectite 60-70 %; silica/quartz, 20-30%.	Smectite	Crenulated smectite.	-	Smectite, silica (quartz), compaction. Meso-diagenesis probably has been buried in > 2000 m deep.
ES33E	Claystone.	Illite 60-70 %; kaolinite (10-20%), silica/quartz (5-8%), Fe-oxide (1-2%)	Illite and kaolinite	Crenulated illite, irregular kaolinite.	-	Illite and kaolinite, Fe-oxide, silica/quartz, compaction. Meso-diagenesis probably has been buried in > 2000 m deep.
ES35H	Claystone	Kaolinite (70-80%), illite (5-10%), silica/quartz (3-4%), zeolite(heulan-dite) (2-3%), calcite (2%), siderite and Fe-oxide (1%).	Kaolinite, illite.	Irregular texture of kaolinite and crenulated and hairy illite	-	Kaolinite, illite, zeolite, calcite, silica/quartz, siderite, Fe-oxides, compaction. Meso-diagenesis, probably has been buried in > 2000 m deep.
ES35i	Claystone, tuffaceous.	Smectite (60-80%), kaolinite (5-10%); silica/quartz (6-8%); siderite (1-2%).	Smectite, kaolinite	Crenulated texture of smectite, Irregular kaolinite	-	Smectite, kaolinite, siderite, compaction. Meso-diagenesis, probably has been buried in > 2000 m deep
ES36E	Claystone, sandy, tuffaceous.	Smectite (60-70%), quartz (10-15%), kaolinite (5-10%); Fe-oxide (5%).	Smectite, kaoliniet	Crenulatedand irregular kaolinite	-	Smectite, kaolinite, illite, compaction. Meso-diagenesis, probably has been buried in > 2000 m deep
ES38D	Claystone.	Smectite (70-70%), quartz (10-15%), kaolinite (1-5%); rutile (<1%).	Smectite, kaolinite	Crenulated smectite and irregular kaolinite	-	Smectite, kaolinite, silica, compaction. Meso-diagenesis, probably has been buried in > 2000 m deep

continued.....Table 4.11.1. Result of SEM and XRD Analyses of Kasiro Mudstone Samples, Asai-Rawas Sub-basin

Sample No. (05)	Lithology	Composition	Type of clay/ cement	Matrix texture/ structure. Cement texture	Type of % porosity	Diagenetic Characters and Regime
ES40D	Lithic sandstone, medium-grained.	Quartz (70-80 %), feldspar (5-10 %), rock fragments (3-5 %); clay matrix (3-5 %).	Smectite, kaolinite	Vermiculite texture, book texture of kaolinite, crenulated smectite.	Secondary porosity, inter-granular 5-10%	Smectite, kaolinite, Fe-oxides, silica, compaction. Mesodiagenesis, probably has been buried in > 2000 m deep
ES 41i	Lithic sandstone, fine- to medium-grained.	Quartz (60-70%), feldspar (10-15%); rock fragments (5-10%); clay matrix (5%);	Smectite, kaolinite, heulandite (zeolite)	Irregular texture of smectite, book texture of kaolinite.	Secondary porosity, inter-granular 5-8%	Smectite, kaolinite, heulandite (zeolite); dissolutions, compaction. Mesodiagenesis, probably has been buried in ≥ 2000 m deep
UM06	Tuffaceous claystone.	Kaolinite, (70-80%); smectite (5-10%), heulandite (3-7%), siderite and Fe-oxides (2-3%)	Kaolinite, smectite, heulandite	Irregular texture of kaolinite, crenulated smectite.	-	Kaolinite, smectite, siderite, silica, and Fe-oxides; compaction. Mesodiagenesis, probably has been buried in > 2000 m deep
UM16A	Tuffaceous claystone	Kaolinite (70-80 %), illite (5-10 %), and silica/quartz (5-10 %).	Kaolinite, illite.	Pseudo-hexagonal crystals; irregular illite.	-	Kaolinite, illite, secondary silica/quartz, compaction. Mesodiagenesis, probably has been buried in > 2000 m deep
UM18E	Tuffaceous claystone	Illite (70-80%); kaolinite 5-10%); silica/quartz (5-8%); rutile (1-2%)	Illite and kaolinite.	Hairy texture of illite and irregular kaolinite.	-	Illite and kaolinite, secondary silica/quartz, compaction. Mesodiagenesis, probably has been buried in > 2000 m deep
UM20	Tuffaceous claystone	Kaolinite (70-80%); illite (5-10%); silica/quartz (5-10%).	Kaolinite and illite	Vermiculite and book texture of kaolinite; irregular illite.	-	Kaolinite, illite, secondary silica/quartz, compaction. Mesodiagenesis, probably has been buried in > 2000 m deep
UM23	Tuffaceous claystone	Kaolinite (70-80%); silica/quartz (10-20%).	Kaolinite.	Book texture of kaolinite.	-	Kaolinite, secondary silica/quartz, compaction. Mesodiagenesis, probably has been buried in > 2000 m deep
UM24	Tuffaceous claystone	Kaolinite (60-70%); silica/quartz (10-25%), illite (2-3%), Fe-oxides (1-2 %).	Kaolinite, illite.	Hairy texture of illite and book texture of kaolinite.	-	Kaolinite, illite, secondary silica/quartz, Fe-oxides, compaction. Mesodiagenesis, probably has been buried in > 2000 m deep
UM25	Tuffaceous claystone	Kaolinite (60-70%), illite (10-20%); silica/quartz (5-10 %).	Kaolinite, illite.	Irregular and vermiculatetexture of kaolinite, and irregular illite.	-	Kaolinite, illite, secondary silica/quartz, Fe-oxides, compaction. Mesodiagenesis, probably has been buried in > 2000 m deep
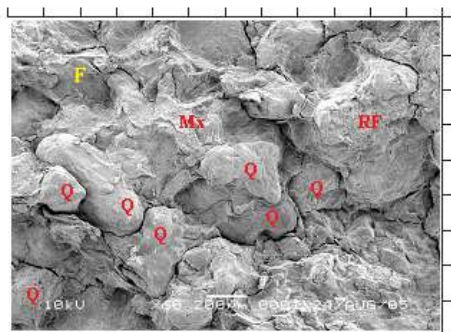
Figure 4.11.16. SEM photomicrograph of medium-grained lithic sandstone (80-300 micron), subrounded-subangular, poorly sorted; composed of quartz (Q) 70-80%, feldspar (F) 5-10%, rock fragments (RF) 3-5%, clay matrix (Mx) 3-5. Magnification X60. Sample 05ES40D.
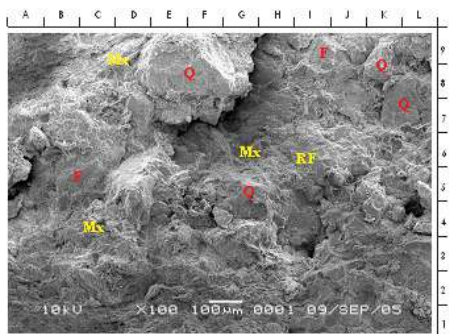
Figure 4.11.17. SEM photomicrograph of medium-grained lithic sandstone, subangular-angular, poorly sorted; grain size 20-250 microns; quartz(Q), feldspar (F) and rock fragment (RF); immature; compact; clay mineral matrix (Mx). Magnification X100. Sample 05ES47D.

sandstone (Figure 4.11.18), tuffaceous claystone (Figure 4.11.19), claystone, sandy claystone, shaly claystone (Figure 4.11.20) or mudstone, and siltstone (Table 4.11.1). The sedimentary grains are angular to subangular, embedded in lithic sandstone. Mineral composition comprises illite-smectite and smectite (50 - 80%), kaolinite (10 - 30%), quartz (2.0 - 8.0%), feldspar dominated by plagioclase (3 - 5%), rock fragments (3 - 10%), pyrite (Figure 4.11.21) and siderite (each ≤ 1.0%). Clay matrix consists of illite, smectite, illite-smectite, kaolinite

(Figures 4.11.22 - 4.11.26), as well as zeolite and heulandite in minor amounts. Whilst, XRD analysis data depict the presence of muscovite, saponite (Samples 03ES36B and 03ES39B), and montmorillonite minerals within the samples.

Furthermore, the common papery – fissile lamination of shale characteristics are recognized in SEM photomicrograph on sample 05MH03 (Figure 4.1.1.27).

Paleontologically, the presence of pollen and spores analyzed comprising *Palmae*, *Marginopollis concinus*, *Proxapertites operculatus*, *Proxapertites cursus*, *Palmaepollenites kutchensis* (terrestrial), *Discoidites borneensis*, *Zonocostites ramonae*, *Triletesporites* sp., *Discoidites*
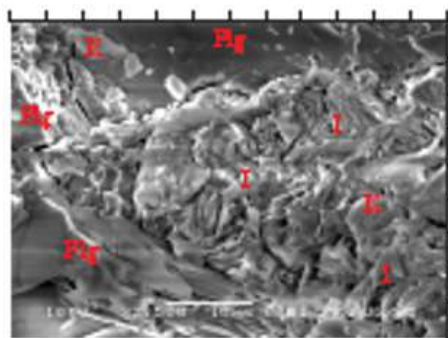
Figure 4.11.18. SEM photomicrograph of sandstone comprising illite (I), kaolinite (K), and plagioclase (Plg). Magnification X1500. Sample 05ES26.
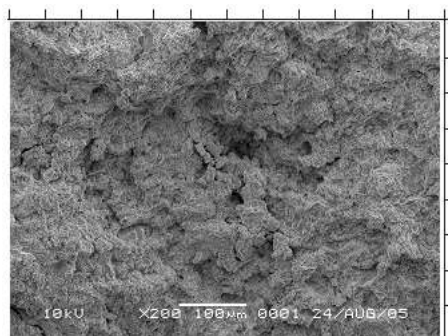
Figure 4.11.19. SEM photomicrograph of tuffaceous claystone, dense and moderately compact, composed of illite (70-80 %), kaolinite (5-10 %), quartz (5-8 %), rutile (1-2 %). Magnification X200. Sample 05UM18E.

borneensis, *Casuarina*, and *Florschuetzia* sp. (back-mangrove), depicts paleodepositional environment varying from terrestrial (freshwater) to backmangrove (brackish) zone (Suwarna *et al*., 2005), supporting the maceral and mineral analyses result mentioned above. Additionally, the occurence of fossil gastropods of *Brotia*-like and *Thiara*- like assemblages tend to indicate a freshwater condition (Aswan *et al*., 2009). Moreover, Suwarna *et al*. (2005) stated that based on the presence of *Florschuetzia trilobata*, *Verrucatosporites usmensis*, *Proxapertites opercu-*

latus, *Proxpertites cursus*, and *Palmaepollinites kutchensi*s, the age of Kasiro oil shales tends to be Late Middle Eocene to Late Eocene.

Besides it, the abundance of lamalginite content with telalginite-*Botryococcus* (Figure 4.11.21) tends to indicate that the oil shales are suggested to be deposited in a closed-restricted area or lacustrine, within predominant anaerobic (anoxic) condition.

The presence of moderate to high pyrite content, both framboidal and non-framboidal types, also tend to show a reduction zone (closed area
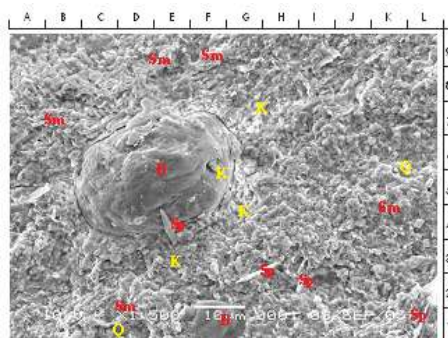
Figure 4.11.20. SEM photomicrograph of shaly claystone showing bitumen (B) surrounded clay minerals of smectite (Sm), 40-60%; kaolinite (K), 20-30%; quartz fractions (Q), 4-7%; organic matter consisting of bitumen (B), sporinite (Sp), 2-3%. Magnification X1500. Sample 05ES39B.

Figure 4.11.22. SEM photomicrograph of quartz (Q), smectite (Sm), and siderite (Sd). Magnification X5000/ Sample 05ES35i.

Figure 4.11.21. SEM photomicrograph of shale showing crenulated illite (I) (abundant), kaolinite (K) (spare), alginite of typical lamalginite (Al) (spare), framboidal pyrite (P) (rare). Magnification X3000. Sample 05MH03.
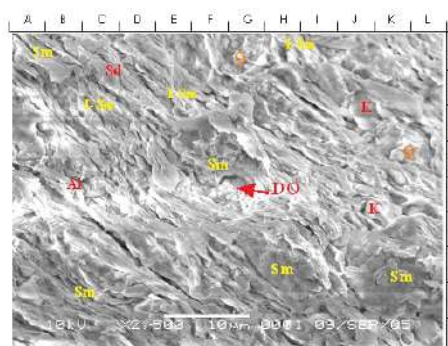
Figure 4.11.23. SEM photomicrograph of shale composed of smectite clays (Sm), 50-60%, mixed-layer of illite-smectite (I-Sm), 25-35%, quartz particles (Q), 2-3%; organic matter comprising droplet oil (DO) and alginite of typical lamalginite (Al), <2%); siderite (Sd), <1%. Magnification X2500. Sample 05ES36B.
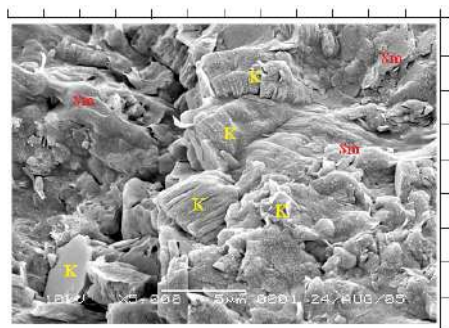
Figure 4.11.24. SEM photomicrograph of clay matrix of smectite, vermiculite and booklet texture of kaolinite (K). Magnification X5000. Sample 05ES40D.
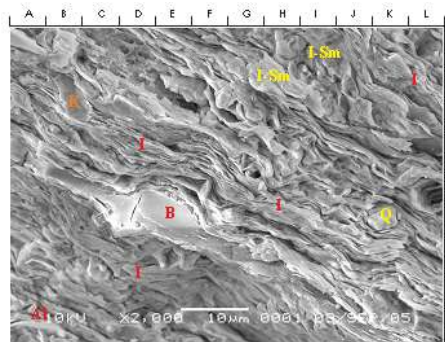
Figure 4.11.26. SEM photomicrograph of shale composed of illite (I),60-80%, illite-smectite (I-Sm), 10-15%; bitumen (B) and alginite (Al), 2%; kaolinite (K), 2%, and quartz fractions(Q), 1%; Magnification X2000. Sample 05NS21C.
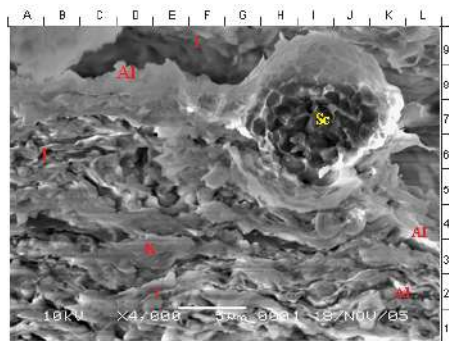
Figure 4.11.25. SEM photomicrograph of shale comprising illite (I) (abundant) interlaminated with alginite of typical lamalginite (Al) (sparse), kaolinite (K) (sparse), funginite (Sc) (rare). Magnification X4000. Sample 05MH04B.
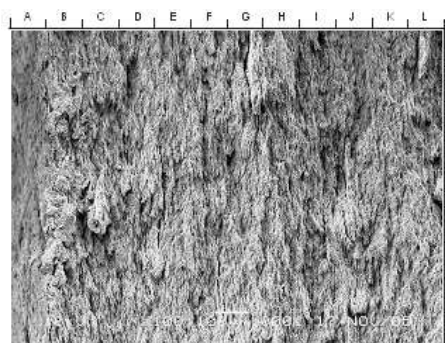
Figure 4.11.27. SEM photomicrograph of shale showing lamination, papery and fissile. Magnification X100. Sample 05MH03.

or anoxic) of depositional environment. This prediction supports the result of maceral analysis related to depositional environment. The presence of a significant amount of framboidal pyrite (0.6 - 4.0%) is indicative of a marine incursion (Table 4.11.1).

According to Jones (1987), the organic facies of Kasiro oil shales are dominated by facies BC and B, followed by C, AB, and A, with minor facies CD and D. Moreover, in accordance with Tyson's (1995), those oil shales are included into

anoxic-dysoxic division. On the basis of those Jones' facies and Tyson's division, in general, the Kasiro oil shales tend to be deposited in an anoxicdysoxic freshwater to brackish lakes, protected from oxygenated waters; with mixed biologic source; and influenced by coal-forming swampy condition. Therefore, the paleodepositional environment of oil shale sequence was a freshwater to brackish lacustrine setting within relatively anoxic or reducing condition of stagnant water, with terrestrial influence.

5. SOURCE ROCK

The quality and type of organic matter which provide the source rock potential of Eo-Oligocene oil shales of the Butar (Kabanjahe Sub-basin), Kapur X, Sangkarewang (Ombilin Basin and Kebuntinggi Sub-basin), Keruh (Kuansing Sub-basin), Kiliran (Kiliranjao Sub-basin), Lakat and Kelesa (Tigapuluh Mts.and Bukit Susah Sub-basin), Lahat (Bukit Bakar), and Kasiro (Asai – Rawas) Formations were evaluated by geochemical techniques including Rock-Eval Pyrolysis, Retort-Oven Analysis, and GC-MS, as well as by organic petrography, SEM, and XRD analyses. The result of those examinations is presented in Tables below

5.1. Kabanjahe Sub-basin

As the source rocks undergo further burial and exposure to increasing temperatures (thermal maturity), the source rocks begin to generate hydrocarbon. Thermal maturity of organic matter was estimated by T_{max} (temperature maximum of S_2) and also PI (production index) from Rock-Eval analysis, and vitrinite reflectance (Rv) from maceral analysis. Therefore, to study shale oil possibility in the Butar organic-rich shale, geochemistry and organic petrography analyses have been conducted on 7 claystone, 4 shales, 4 coaly shale, and 2 coal samples (Tables 5.1.1 – 5.1.3).

Total organic carbon (TOC) content of the samples within the three members of the formation varies from 0.07 to 1.74 %. However, within the Upper Member, distributed around the basin rim, and located in Laubuluh (Kutabuluh), Penampen, and Sarinembah areas, the total organic content of the samples ranges between 0.12 and 1.74 % (Table 5.1.1). Moreover, in these three areas, a range of 0.71 % to 1.74 % dominates the total organic carbon content. The highest total organic carbon content in the upper section of the shale occurs in Laubuluh (1.74 %; 03HR.14C) and Sarinembah (1.71 %; 03RH.06A).

T_{max} varying from 380° to 461° shows that the maturity level ranges from thermally immature to early mature. This maturity level is also supported by the values of PI dominantly ranging from 0.27 to 0.56 (Table 5.1.1).

Retort-Oven Analysis performed on 18 shale samples collected from Penampen, Juhar, Sarinembah, Kemkem, Laubuluh, Kutabangun, Kutambarupunti, and Butar tend to indicate no oil produced. However, in Kemkem and Laubuluh, oil gained from the analysis is 1 l/ton rock and trace, respectively (Table 5.1.2).

Maceral group determined is dominated by vitrinite varying from 0.4 % to 5.4 %, except two samples have values of 44.0 % (03NS.19C and 03NS.20) and one sample 51.2 % (03NS.15D2). The following rare maceral observed is inertinite ranging between 0.2 % and 0.6 %. The occurrence of vitrinite both in sediments as dispersed organic matter (DOM) and also in coals, tend to support that the shales and claystones containing organic matter might be the source and reservoir rocks of the shale-gas, due to the absence of exinite macerals (Table 5.1.3).

On the basis of vitrinite reflectance mainly varying from 0.74 % to 1.98 %, essentially, almost all the organic matter contained in the Upper Member has a high thermal maturity (Table 5.1.2). However, Penampen and Sarinembah areas are characterized by low vitrinite reflectances (0.20 % - 0.38 %) tending to show a thermally immature or low thermal maturity condition. Moreover, medium vitrinite reflectance values ranging between 0.54 % to 0.56 %, and are observed in Laubuluh area, tend to exhibit a transition from thermally immature to early mature or medium thermal maturity condition. The organic matter suggested to be derived from humic matter might be included into type III kerogen, leading to the presence of gas-prone type.

5.2. Kapur IX

Organic petrographic, vitrinite reflectance, and mineral matter analyses were carried out on 16 shale, claystone, and mudstone samples and

Oil Shale Potential as an Alternative Energy Source, in Selected Sites of Sumatra Island

Table 5.1.1. Rock-Eval Pyrolysis Data of the Butar Shale

No	Location	Sample No. (02)	Lithology	TOC (%)	S1	S2	PY	PI	Tmax (°C)	HI
						kg/t				
1	Penampen	RH.03A	Sh,dkgy/blk,calc	0.71	0.37	0.32	0.69	0.54	461	45
2		RH.03B	Sh,dkgy,sl,weathered	0.18	0.08	0.10	0.18	0.44	TDD	56
3	Juhar	RH.04A	Clst,ltgn-gy,weathered	0.07	0.00	0.08	0.08	0.00	TDD	114
4	Sarinembah	RH.06A	Clst,dkgy,calc	1.71	0.75	2.00	2.75	0.27	450	117
5	Laubuluh	HR.13A	Clst,dkbrn/dkgy,sl,oxd	0.12	0.13	0.15	0.28	0.46	TDD	125
6		HR.14A	Clst,brn/dkgy, sl,oxd	0.09	0.01	0.08	0.09	0.11	TDD	89
7		HR.14B2	Clst, dkkgy/blk, calc	0.17	0.04	0.20	0.24	0.17	TDD	118
8		HR.14C	Clst, dkgy/blk	1.74	0.63	1.02	1.65	0.38	380	59
9	Kutabangun	NS.11	Clst,gngy,yell/red,oxd/weath	0.07	0.03	0.02	0.05	0.60	TDD	29
10	Kutambarupunti	NS.14	Clst, dkbrn/dkgy, slty	0.08	0.02	0.04	0.06	0.33	TDD	50
11	Butar	NS.15B	Clst,gy/dkgy,lam, sl,oxd	0.08	0.05	0.04	0.09	0.56	TDD	50
12		NS.15C	Clst,gy/dkgy/lam w/sltst	0.06	0.02	0.02	0.04	0.50	TDD	33
13		NS.16A	Clst,dkgy,oxidised	0.07	0.02	0.03	0.05	0.40	TDD	43
14		NS.16B	Clst, dkgy, sl,oxidised	0.09	0.05	0.02	0.07	0.71	TDD	22
15		NS.17A	Clst, dkgy	0.08	0.04	0.02	0.06	0.67	TDD	25
16.		NS.19A	Sh, dkgy/blk	0.09	0.07	0.02	0.09	0.78	TDD	22
17.		NS.19B	Sh, dkgy/blk	0.07	0.08	0.08	0.16	0.50	TDD	114

Notes : TDD = Undetected
TOC : total organic carbon   PY : pyrolysis yield (S1+S2)   HI : hydrogen index
S1 : free HC   PI : production index
S2 :   Tmax : maximum temperature

Table 5.1.2. Retort-Oven Analysis Data of Butar Shale

No.	Location	Sample No. (02)	Oil Content (l/t)	Water Content (l/t)
1.	Penampen	RH.03A	NIL	45
2.		RH.03B	NIL	81
3.	Juhar	RH.04A	NIL	50
4.	Sarinembah	RH.06A	NIL	55
5.	Kemkem	RH.08	1	20
6.	Laubuluh	HR.13A	NIL	24
7.		HR.14A	NIL	68
8.		HR.14B2	NIL	58
9.		HR.14C	Trace	32
10.	Kutabangun	NS.11	NIL	28
11.	Kutambarupunti	NS.14	NIL	28
12.	Butar	NS.15B	NIL	14
13.		NS.15C	NIL	30
14.		NS.16A	NIL	10
15.		NS.16B	NIL	44
16.		NS.17A	NIL	32
17.		NS.19A2	NIL	18
18.		NS.19B	NIL	50

88

Table 5.1.3. Result of Petrographic Analysis of DOM (Dispersed Organic Matter) in the Fine Clastics and Coal of the Butar Formation

N o	Sample No. (02)	Litho-logy	Maceral (%)								MM (%)						Rv (%)
											Px						
			Tel	Det.	Gel	V	Sf	Fs	Intr	I	Non	Fr	Cly	Carb	Si	Tot.	
1	NS 14A	Clst	-	1.8	-	1.8	-	-	-	-	11.8	-	76.6	9.8	-	98.2	0.74
2	NS 15B	Clst	-	0.8	-	0.8	-	-	-	-	6.0	-	65.8	27.0	0.4	99.2	0.28
3	NS 15D2	Coal	13.0	37.2	1.0	51.2	0.6	0.2	-	0.8	1.0	1.0	42.8	2.6	-	48.0	1.98
4	NS 15E	Coal	2.6	2.8	-	5.4	-	-	0.2	0.2	8.2	0.2	84.0	2.0	-	94.4	0.57
5	NS 17A	Clst	-	1.4	-	1.4	-	-	-	-	6.0	-	80.6	12.0	-	98.6	1.93
6	NS 17 B	Shale	1.4	2.4	-	3.8	-	-	-	-	7.0	1.2	82.2	-	5.8	96.2	1.71
7	NS 19 A1	Shale	2.0	2.6	-	4.6	0.7	-	0.2	0.9	4.0	-	88.0	0.2	2.4	94.6	1.43
8	NS 19 A2	Coaly shale.	0.6	1.0	-	1.6	-	-	-	-	8.4	0.4	78.0	0.6	11.0	98.4	1.47
9	NS 19 B	Coaly shale	2.0	3.2	-	5.2	-	-	-	-	11.8	0.6	74.8	-	7.6	94.8	1.73
10	NS 19C	Coaly shale	12.6	29.8	1.6	44.0	0.2	-	-	0.2	4.8	-	34.2	16.8	10.0	55.8	2.06
11	NS 20	Coaly shale	14.8	27.2	2.0	44.0	-	-	-	-	2.8	-	36.4	16.8	17.0	56.0	1.89
12	HR 13 A	Clst	-	1.8	-	1.8	-	-	-	-	3.8	-	85.6	7.6	1.2	98.2	0.54
13	HR 14 B2	Clst	-	1.2	-	1.2	-	-	-	-	4.4	-	93.4	1.0	-	98.8	0.56
14	HR 14C	Clst	-	-	-	-	-	-	-	-	11.0	2.6	78.2	8.2	-	100	-
15	RH 03A	Shale	-	1.8	-	1.8	-	-	-	-	5.8	1.2	90.2	-	1.0	98.2	0.20
16	RH 03B	Shale	-	1.2	-	1.2	-	-	0.4	0.4	0.4	8.8	84.6	4.6	-	98.4	0.25
17	RH 06 A	Clst	-	0.4	-	0.4	-	-	-	-	5.2	6.0	76.6	11.8	-	99.6	0.38

Remarks

Tel	: telinite	Sf	: semifusinite	MM	: mineral matter	Cly	: clay	Rv	: vitrinite reflectance
Det	: detrovitrine	Fs	: fusinite	Px	: pyrite	Carb	: carbonates		
Ge	: gelovitrinite	Intr	: inertodetrinite	Non	: non-framboidal	Si	: silica		
V	: vitrinite	I	: inertinite	Fr	: framboidal	Tot	: MM total		

the results were shown on Table 5.2.1. Vitrinite maceral content varies from 5.0 – 10 %, then followed by exinite maceral group significantly ranges between 2.0 – 16.9 %. Besides clay minerals, the amount of framboidal and non-framboidal pyrite is in quite balanced, varies between 0.3 – 10.0 %. The silica content is quite significant.

Based on the content of lamalginite which is more dominant than telalginite, the oil shale in the study area can be classified as lamosite type, deposited in a lacustrine depositional environment (Hutton, 1987; Dyni, 2006).

Moreover, results of TOC and Rock-Eval Pyrolysis analyses are presented in Table.5.2.2 as follows.

Crossplot TOC vs. HI (Figure 5.2.1) indicates that oil shale samples studied, predominantly, tend to be situated in oil area, showing by good to excellent TOC content. Sample WR 1 is possible to produce oil, although its TOC content is fair. Sample WR 7 falls in gas area, due to its low TOC.

Diagram of HI vs. T_{max} (Figure 5.2.2), indicates that kerogen type of all samples can be categorized into Type II and III. Fortunately, Type II is predominant represented by samples WR 1, 2, 9, 14B, and 17B. Whilst, type III kerogen shown in sample WR 7, was derived from humic maceral.

Thermal maturity level of organic materials shown on crossplot HI vs. T_{max} ranges from immature to early mature (Figure 5.2.2), where sample WR 1, 2, 9, 14B, and 17B include into late immature – early mature, whilst WR 7 is situated in the immature category.

Table 5.2.1. Maceral Analysis of Dispersed Organic Matter (DOM) of Koto IX

No.	Sample No.	M a c e r a l (%)							MM Py	(%)			Location
	(18)	Cu	Re	Lam	Tel	Exs	E	V	Fr	Non-Fr	Cly	Si	
1.	WR 1	0.3	0.3	0.7	0.5	0.2	2.0	7.0	9.6	1.3	78.1	2.0	Kototuo
2.	WR 2	1.0	1.6	6.3	7.0	1.0	16.9	5.9	9.6	3.3	63.3	1.0	
3.	WR 3	0.2	0.2	1.8	10	0.1	3.3	6.0	10.0	2.0	76.7	2.0	
4.	WR 6	-	0.6	5.8	7.0	1.6	15.0	9.1	1.3	2.3	70.3	2.0	
5.	WR 7B	0.3	0.4	0.5	0.5	0.3	2.0	10.0	-	1.0	85.0	2.0	Kotobangun
6.	WR 7C	0.2	0.2	0.7	0.6	0.3	2.4	9.3	0.3	1.1	85.7	1.6	
7.	WR 8B	0.6	0.3	7.1	6.8	-	14.8	8.0	0.3	1.3	73.6	2.0	
8.	WR 9	0.3	0.3	7.6	5.6	0.6	14.4	7.3	0.3	1.6	75.1	1.3	
9.	WR 10A	0.3	0.1	7.3	6.7	0.1	14.5	7.3	-	0.6	75.6	2.0	
10.	WR 13B	-	0.2	7.6	6.0	0.1	13.9	5.0	3.0	2.3	75.5	0.3	Galugur
11.	WR 13C	0.3	0.3	7.4	5.0	1.0	14.0	5.3	4.6	3.3	71.5	1.3	
12.	WR 14B	0.2	0.2	2.7	1.3	-	5.0	6.3	3.3	4.0	81.0	1.0	
13.	WR 15A	0.2	0.2	2.6	1.8	-	4.8	5.0	4.6	5.0	78.5	2.1	
14.	WR 16A	0.2	0.1	2.2	1.7	0.1	4.3	6.9	4.3	6.0	77.5	1.0	
15.	WR 16B	0.2	0.1	2.4	1.2	0.1	4.2	7.0	6.2	7.0	73.8	2.0	
16.	WR 17B	-	0.3	2.0	1.5	0.2	4.0	6.3	5.6	4.3	78.8	1.0	

Remarks: Cu : cutinite   Exs : exsudatinite   Fr : framboidal   MM : mineral matter
Re : resinite   **E : exinite**   Non-Fr : non-framboids
La : lamalginite   **V : vitrinite**   Cly : clay
Tel : telalginite   Py : pyrite   Si : silica

Table 5.2.2. Data of TOC and Rock-Eval Pyrolysis of Shales in Koto IX Area

No.	Sample No. (18)	Lithology	TOC % w	S1	S2	S3	PY	S_2/S_3	PI	T_{max} °C	HI HC/TOC	OI CO_2/TOC
					mg/g							
1.	WR1	Shale, med.dkgy	0.84	0.33	2.05	0.46	2.38	4.46	0.14	435	244	55
2.	WR2	Shale, blk.gy	7.10	0.24	32.68	0.41	32.92	79.71	0.01	439	460	6
3.	WR7	Clst. brn.gy	0.30	0.07	0.06	0.33	0.13	0.18	0.54	426	20	110
4.	WR9	Clst. blk.gy	6.95	0.74	30.17	1.32	30.91	22.86	0.02	431	434	19
5.	WR14B	Shale, blk.dk.gy	2.20	0.27	7.34	0.62	7.61	11.84	0.04	440	334	28
6.	WR17	Clst. blk.dk.gy	2.55	0.68	6.03	0.97	6.71	6.22	0.10	439	236	38

According to Rad (1984) supported by Tissot and Welte (1984) classification (Figure 5.2.3.) HC quality varies. Samples WR2 dan WR 9 fall into excellent category, WR 14B is good, WR 1 is fair, whereas WR 7 in poor level. Oil and gas prones are represented by WR 1, 2, 9, 14B, and 17B, whereas WR 7 only as gas prone.

By plotting on the diagram of TOC vs. S_2 contents (Peter and Cassa, 1994) (Figure 5.2.4), several samples show good to excellent level.

They are in oil prone potential, except WR 1 which falls into a fair level leading to gas prone only.

Moreover, on crossplot PI vs. T_{max} (Senguler et al., 2008), the samples are dominated by immature level conditions, except sample WR 7 which is contaminated (Figure 5.2.5) due to the high mineral matter content.

Kerogen type of each sample can be indicated by using diagram HI vs. OI (Peters, 1986) as
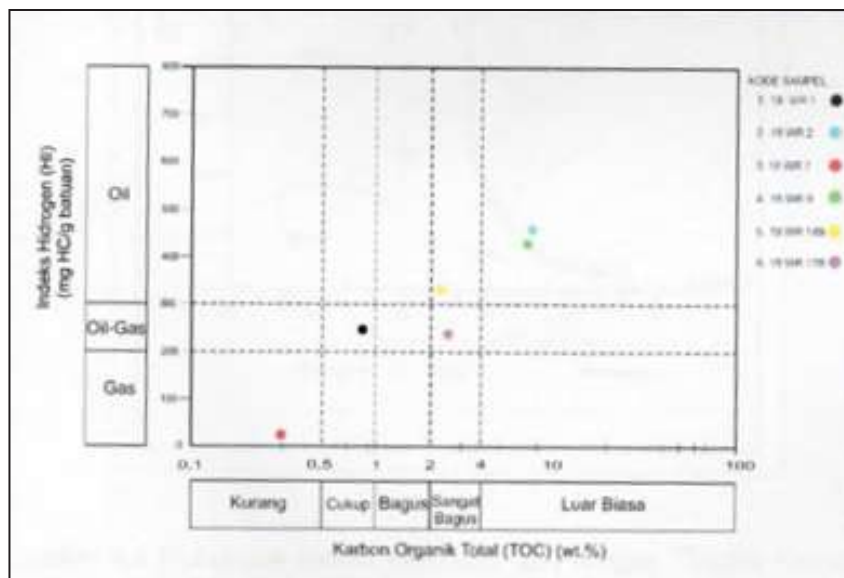
Figure 5.2.1. Cross-plot of hydrogen index (HI) vs. TOC (Peters and Cassa, 1994), showing the category of the Kapur IX source rock samples.
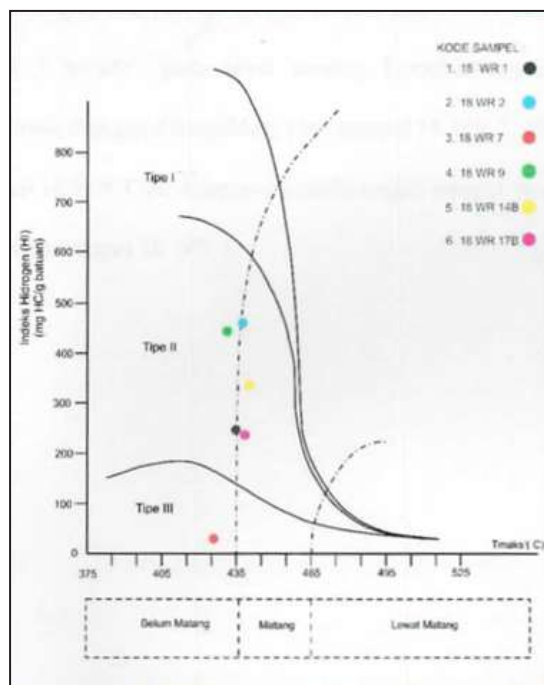
Figure 5.2.2. Cross plot diagram of hydrogen index (HI) vs. T_{max} of the shale unit in Kapur IX area, indicating thermal maturity and kerogen types of the source rocks.
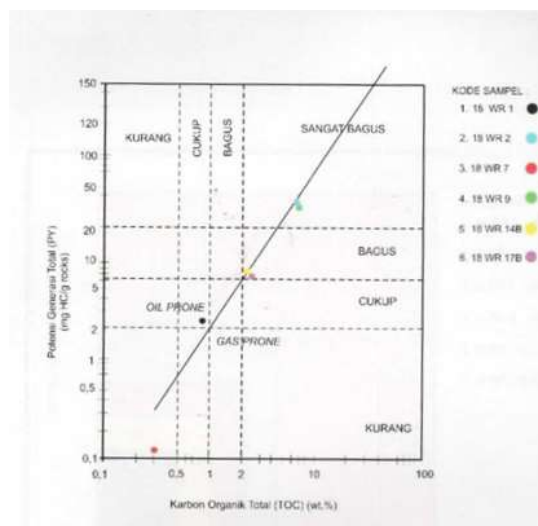
Figure 5.2.3. Diagram showing TOC vs. PY (General Total Potential) of the shale unit in Kapur IX area, indicating oil-gas prone of the source rocks.

displayed in Figure 5.2.6. All samples contain kerogen Type II (oil prone), whilst sample WR 7 belongs to kerogen Type III (gas prone).

91
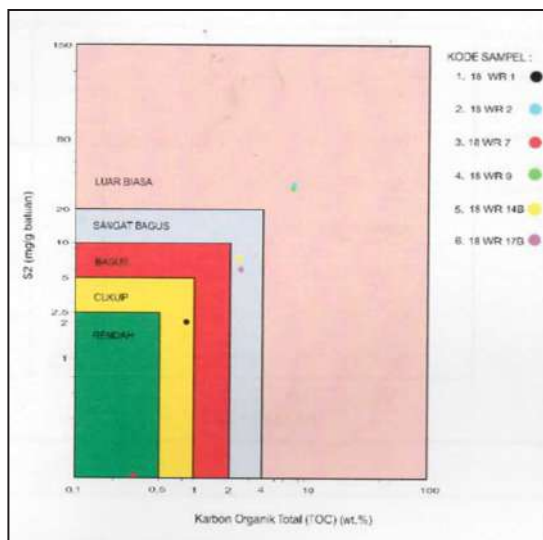
Figure 5.2.4. Cross plot diagram of S_2 vs. TOC of the shale unit in Kapur IX area, showing the source rock potential (modified after Peters, 1986; Langford and Blanc-Valero, 1990).
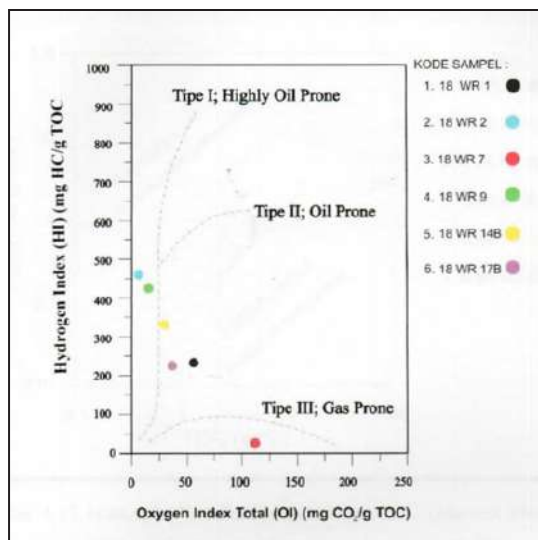
Figure 5.2.6. Diagram of hydrogen index (HI) vs. oxygen index (OI) of Kapur IX source rocks, indicating kerogen types and oil-gas prone level (Espitalie et al., 1977; Tissot and Welte, 1978; Katz, 1983; Peters, 1986).
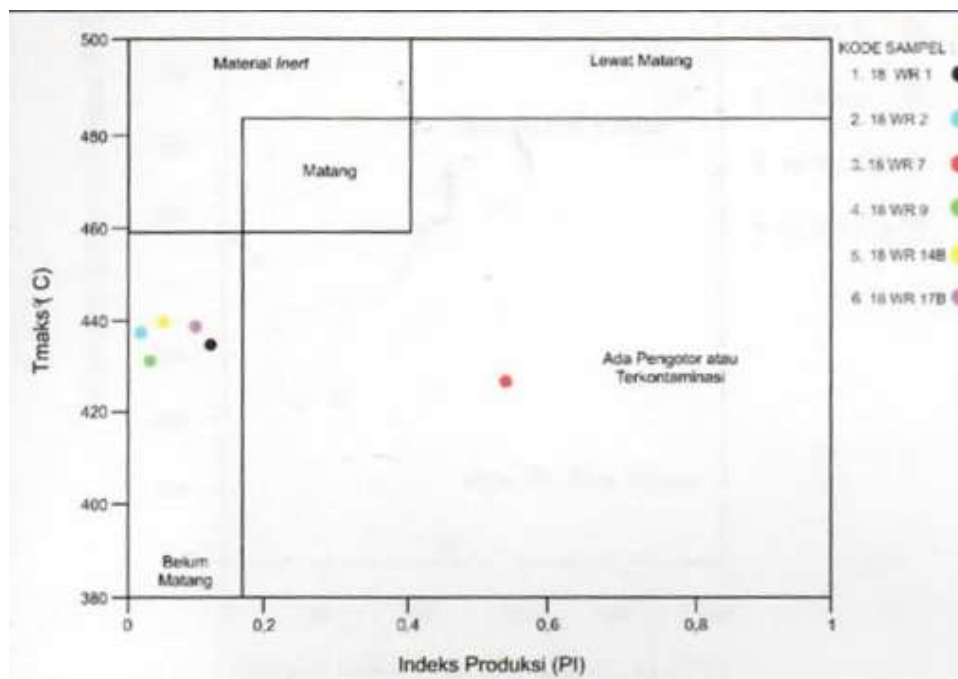
Figure 5.2.5. Diagram showing relationship between T_{max} and Production Index (PI) and thermal maturity of the source rock in Kapur IX shales (Senguler *et al*., 2008).

By using diagram of S_1 vs. TOC (Figure 5.2.7), the contamination on samples can be detected. All of the samples belonging to autochthonous type (indigenous HC) tends to indicate that the samples were deposited in the same site.

Furthermore, by plotting the T_{max} and Rv on the Smith and Cook diagram (1984; modified after Demaison, 1984) the oil shales studied are potential to produce oil and gas. This condition coincides the result shown in Figure 5.2.3.

On the basis of Figures 5.2.1 – 5.2.7, it can be summarized that predominantly the oil shales will be functioned as an effective HC source rock, tending to be an oil-gas prone.

5.3. Kebuntinggi

Rock-Eval Pyrolysis data indicate that 7 oil shale samples collected from Pakboi, and Diano Rivers, contain high TOC varying from 10,06 - 25,42%, with pyrolysis yield between 78,98 -148,09 kg/ton rock (Table 5.3.1). This value is fairly high, and it suggested that the oil shale has an excellent category to produce oil (>40 kg/ ton rock).

Two oil shale samples collected from Diano River and its tributary show TOC content of
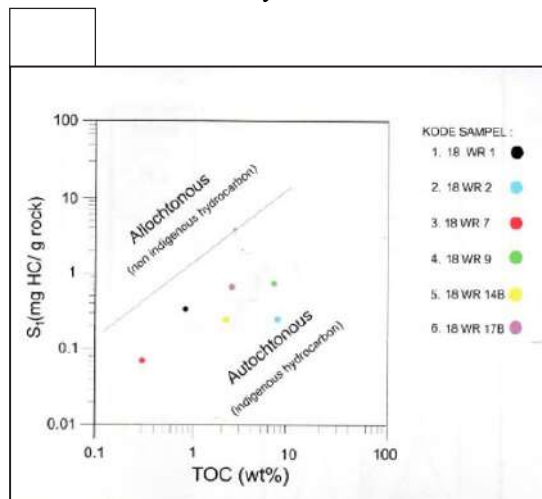
Figure 5.2.7. Cross plot diagram of S_1 vs. TOC content, showing type of hydrocarbon produced in six samples of Kapur IX source rock (Hunt, 1995; Rabbani and Kamali, 2005; Ghori and Haines, 2007).

6,59% dan 6,34%, respectively, which produce oil of sebanyak 36,13 kg/ton rock and 39,5 kg/ ton rock. This value is situated around "*threshold*" of commercial value of oil shale to be exploited.

Six samples gained from area around Jao, Petai Kecil, and Siabu Rivers, and Kampung Dalam having TOC value between 1.73 – 5.45% produced a small amount of oil varying from 3.0 –

31.0 kg HC/ton rock. Therefore, this amount is not commercial, because it is less than "*threshold*" value of 40 kg HC/ton rock.

However, S_1 value, which commonly less than mean value of S_2 tend to indicate that the shale in the research area is an immature organic shale.

By plotting the values of TOC and PY onto Rad's diagram (1984), the majority of shale samples is situated in "*oil to gas prone*" zone within good to excellent level. On the other hand, four samples fall under the excellent gas zone, whilst one sample indicate a moderate oil-gas probability.

Based on the ploting HI *vs*.T_{max} on the diagram, kerogen contained comprises type I and II, mainly derived from alginite sub macerals (Figures 5.3.1 – 5.3.3) with minor sporinite/ resinite (Figure 5.3.4).

Based on petrographic maceral analysis, focused on exinite, it suggested that the dominant organic matter in the shale is alginite and resinite. Alginite is presumed to be the main source matter of oil, whilst resinite and sporinite will produce oil-gas.

Vitrinite reflectance value ranging from 0,14 to 0,4% with mean value around 0.3 % tend to indicate the level of thermal maturity is around immature zone, where the oil contained in the shale must be produced by retorting process.

5.4. Kuansing Area

Rock-Eval pyrolysis carried out on eight samples (03ES16L, 03ES 13A, 03ES13H, 03NS13A, 03NS13C, 03NS16C, 03NS16E, 03RH13C) yielded excellent hydrocarbon source-rocks (PY of 43.09 – 186.75 kg/ton rock), one sample (03NS16A) has yielded a good hydrocarbon

Table 5.3.1. TOC and Rock-Eval Pyrolysis Data of the Kebuntinggi Oil Shales

No.	Sample No. (03)	Lithology	TOC %	S_1	S_2	PY	PI	T_{max} (°C)	HI	Location
						g HC/kg rock				
1	YK34A	Sh. dkgy. dkgy/blk. carb.	4.33	0.39	23.00	23.39	0.02	435	531	Kapas River
2	YK35B	Sh. dkgy	1.73	2.44	8.79	11.23	0.22	453	508	Jao River
3	YK36A	Sh. dkgy. lam w/ whtgy. argill.	1.83	0.69	2.31	3.00	0.23	456	126	
4	NS70	Sh. dkgy	3.47	2.29	16.92	19.21	0.12	442	488	Pakboi River
5	NS71B	Sh. dkgy	19.78	7.40	139.28	146.68	0.05	471	704	
6	NS75A	Sh. gy-dkgy. lam., fissile	4.78	0.64	25.42	26.06	0.02	436	532	Siabu River tributary
7	NS79A	Sh. brn. gy. lam., fissile	5.45	0.54	31.02	31.56	0.02	436	569	Dalam Village
8	ES62A	Sh. dkgy. dkgy/blk	25.42	1.73	146.36	148.09	0.01	438	576	Petai Kecil River
9	ES68A	Sh. dkgy	6.34	1.33	34.80	36.13	0.04	442	549	
10	ES68B	Sh. brndkgy	20.87	2.40	133.92	136.32	0.02	467	642	Diano River tributary
11	ES68D	Sh. dkbrn/dkgy. shally	12.40	4.25	88.48	92.73	0.05	466	714	
12	UM01A	Sh. dkgy. locc. carb.mat.	23.46	3.33	143.36	146.69	0.02	452	611	
13	UM01B	Sh. brngy	6.59	1.29	37.76	39.05	0.03	445	573	Diano River
14	UM06A	Sh. dkgy. lam., fissile	10.06	1.98	77.00	78.98	0.03	444	765	
15	UM06B	Sh. dkgy. papery	11.32	1.70	84.72	86.42	0.02	468	748	No Name

Remarks:

TOC : total organic carbon
S_1 : free hydrocarbon
S_2 : hydrocarbon from kerogene
PY : total hydrocarbon (S1+S2) (Pyrolysis Yield)

T_{max} : maximum temperature (°C) of HC derived from kerogen
HI : hydrogen index
PI : production index

source-rocks (PY of 19.10 kg/ton rock), three samples (03ES16NA, 03RH15G, and 03RH15J) yielded a fair level (PY of 2.02 - 2.57 kg/ton rock) (Table 5.4.1). Whilst six samples (03ES16M, 03NS19A, 03NS19D, 03RH12A, 03RH15E, and 03RH17F) show a poor source rock potential (PY of 0.31 - 1.51 kg/ton rock).

Samples yielding good to excellent hydro-carbon source-rocks have TOC values between 2.99 % and 27.33%, where they are included into the oil – gas prone source rocks (Figure 5.4.1). They have T_{max} ranging from 425° to 451° C, and Hydrogen Index of 488 – 946. The kerogen content is included into type I and II (Figure 5.4.2).

Samples which yield a fair to poor hydrocarbon source rock potential have TOC values less than 2 %, T_{max} from 435 to 471° C, and Hydrogen Index of 55 to 757. They are included into the oil – gas prone source rock (Figure 5.4.1), and their kerogen content is included into type II and III (Figure 5.4.2). This type of kerogen, in the mature stage, will produce 20% oil and 80 % gas (Waples, 1985).

Maceral analysis, carried out by organic petrography from sixteen shale and mudstones samples (Table 5.4.2), shows that the DOM of the Keruh Formation is predominated by exinite (liptinite) group (0.2 – 7.4%). The exinite group comprises alginite (0.4-4.6%) such as lamalginite and telalginite-*Botryococcus* (Figures 5.4.3 and 5.4.4). Other macerals are resinite (0.2-2.8%), bitumen (Figure 5.4.5 and 5.4.6) and bituminite
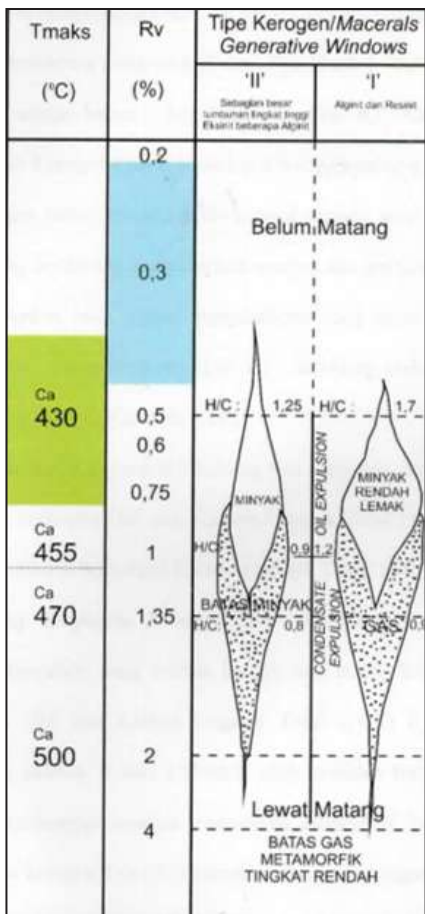
Figure 5.2.8. Diagram indicating immature thermal maturity level of the six samples of Kapur IX source rocks (Smith and Cook, 1984, modified after Demaison, 1984).

Figure 5.3.2. Photomicrograph of *Botryococcus* (telalginite) in Keruh oil shale. Sample 03ES68D. (15 micron). Location: Diano River, Kebuntinggi.

Figure 5.3.3. Photomicrograph of oxidized organic matter (bitumen/?alginite) in Keruh oil shale (sample 03NS79A), Kebuntinggi.. Size of 25 micron.

Figure 5.3.1. Photomicrograph of bitumen in the Keruh oil shale derived from algae. Size of bitumen around 20 micron. Location: Diano River.

Figure 5.3.4. Photomicrograph of oxidized organic matter present as lamellar bitumen originated from sporinite (?). Sample 03UM01, Kebuntinggi. Size 15 micron.

Table 5.4.1. TOC and Rock-Eval Pyrolysis Data of Keruh Samples, Logas, Kuansing Area

No	No. Sample	LITOLOGY	TOC (%)	S₁ Kg/Ton	S₂ Kg/Ton	PY Kg/Ton	PI	Tmax (°C)	HI	AREA
1.	03RH12A	Clyst, gywht, slty	0,20	0,06	0,25	0,31	0,19	TDD	124	Prk TBS
2.	03RH13C	Coaly Shale, blk	23,80	2,67	116,04	118,61	0,02	425	488	Prk TBS
3.	03RH15E	Sh, gy-bmgy,lam slst-sst	0,59	0,06	0,42	0,48	0,13	440	72	Manunggal
4.	03RH15G	Sh, gy	1,35	0,17	1,85	2,02	0,08	440	137	Manunggal
5.	03RH15J	Sh, gy-dkgy	1,86	0,15	2,24	2,57	0,06	440	130	Manunggal
6.	03RH17F	Sh, gy-dkgy	0,68	0,06	0,37	0,43	0,14	441	55	Manunggal
7.	03ES13A	Sh, bmgy-bm, calc, fissile	6,20	0,21	42,88	43,09	0,00	438	692	Prk. TBS
8.	03ES13H	Clyst, dkgy, carb	8,48	4,31	55,36	59,67	0,07	426	653	Prk. TBS
9.	03ES16L	Sh, blk	10,91	1,93	82,60	84,53	0,02	430	757	Makarya
10.	03ES16M	Sh, gy-dkgy, lam, slst	1,02	0,04	1,47	1,51	0,03	471	144	Makarya
11.	03ES16N	Sh, dkgy, lam, slst	1,60	0,13	2,06	2,19	0,06	435	129	Makarya
12	03NS13A	Clst, gy-dkgy, carb/coaly	27,33	12,75	174,00	186,75	0,07	417	637	Sitiung
13.	03NS13C	Sh, bmgy-bm, calc, papery	7,89	0,21	49,10	49,31	0,00	437	623	Sitiung
14.	03NS16A	Sh, blk	2,99	0,66	18,44	19,10	0,03	446	616	Nusa Riau
15.	03NS16C	Sh, blk	12,24	0,98	115,86	116,84	0,01	449	946	Nusa Riau
16	03NS16E	Sh, blk	9,91	0,42	62,94	63,36	0,01	451	635	Nusa Riau
17.	03NS19A	Sh, gy-dkgy	0,88	0,06	1,00	1,06	0,06	TTD	114	Nusa Riau
18.	03NS19D	Sh, gy	1,55	0,06	1,45	1,51	0,04	440	93	Nusa Riau

NOTES :

|				
TOC	:	Total organic carbon	T max	: Temperature maximum (°C) for hydrocarbon formation from kerogen
S₁	:	Quantity of free hydrocarbon		
S₂	:	Quantity of hydrocarbon from kerogen	HI	: Hydrogen Index
PY	:	Total hydrocarbon (S₁ + S₂)	TDD	: Un definite
PI	:	Production Index = S₁ / (S₁ + S₂)	Sh	: Shale
Clst	:	Claystone	slst	: siltstone
ss	:	sandstone	carb.	: carbonaceous
Calc.	:	calcareous	brngy	: brown grey
Gy	:	grey	dkgy	: darkgrey
blk	:	black	Gywht	: grey white
lam.	:	laminated Prk. TBS :	TBS Plantation.	
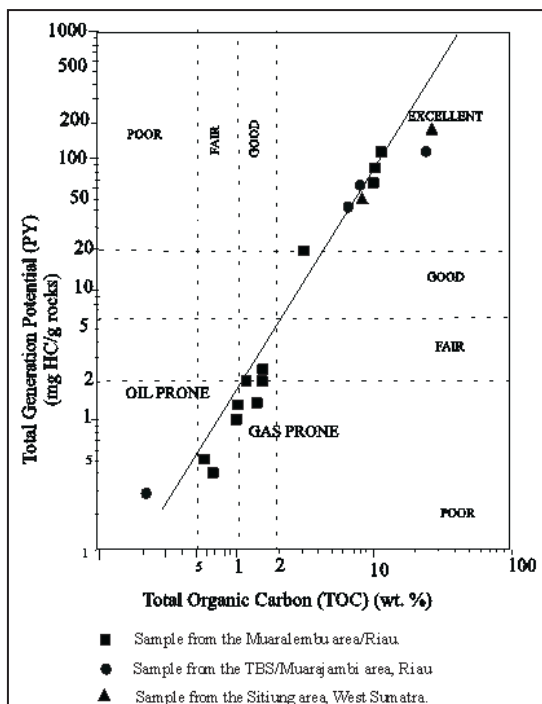
Figure 5.4.1. Diagram of TOC vs Pyrolysis Yields (PY), showing the hydrocarbon potential in the research area, Kuansing.
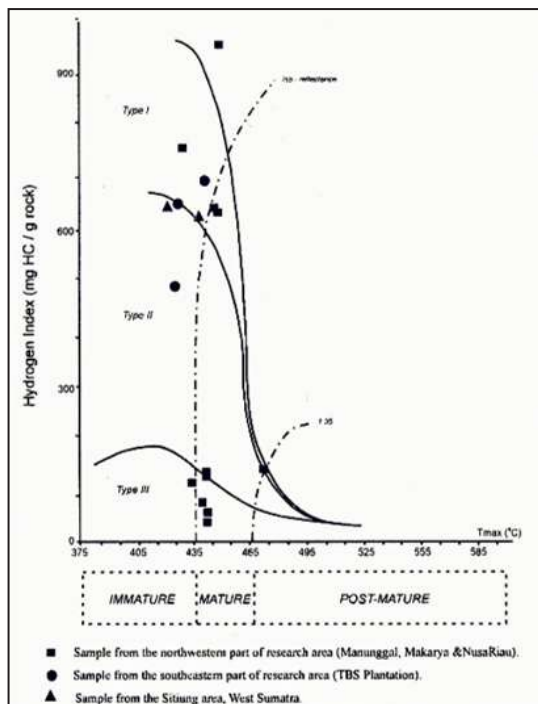

Figure 5.4.2. Diagram of Hydrogen Index (HI) vs. Tmax showing the kerogen type and source rock maturity in the studied area, Kuansing.

Table 5.4.2. Result of Maceral Analysis of Rock Samples, Keruh Formation, Kuantan - Singingi

No	Sample No. (03)	(%) Maceral									Area
		Rs	Cu	Lpt	Alg	Bit	E	Rv min	Rv max	Rv mean	
1.	ES 16 L	2,4	-	1,6	1,2	-	5,2	0,19	0,40	0,25	Makarya
2.	ES 16 M	0,8	-	-	0,4	0,4	1,6	0,36	0,53	0,45	
3.	ES 16 N	0,2	-	-	-	-	0,2	0,22	0,37	0.27	
4.	NS 16 A	0,6	-	-	-	0,4	1,0	0,41	0,43	0,42	NusaRiau
5.	NS 16 C	0,8	-	0,4	0,4	-	1,6	-	-	-	
6	NS 16 E	0,6	-	-	-	-	0,6	0,40	0,53	0,46	
7.	NS 19 A	-	-	-	-	-	-	0,41	0,56	0,49	
8.	NS 19 D	0,2	0,4	-	-	0,2	0,8	0,23	0,29	0,26	
9.	RH 15 E	0,2	-	-	-	-	0,2	0,28	0,49	0,38	Manunggal
10.	RH 15 G	-	-	-	-	-	-	0,34	0,48	0,42	
11.	RH 15 J	0,4	-	0,6	-	0,4	1,4	0,48	0,61	0,57	
12.	RH 17 F	-	-	-	-	-	-	0,60	0,70	0,66	
13.	ES 13 A	2,8	-	-	4,6	-	7,4	0,31	0,58	0,47	Prk.TBS
14.	ES 13 H	1,2	-	-	1,2	2,4	4,8	0,33	0,37	0,35	
15.	RH 12 A	-	-	-	-	-	-	0,12	0,26	0,19	
16.	RH 13 C	1,6	0,4	0,8	0,4	0,6	3,8	0,26	0,38	0,35	
17.	NS 13 A	0,6	-	-	0,4	0,8	1,8	0,24	0,37	0,30	
18.	RH 13 C	1,6	0,4	0,8	0,4	0,6	3,8	0,26	0,38	0,35	Sitiung

Notes:

Rs : resinite   Bit   : bitumen   Rv :   mean vitrinite reflectance
Cu : cutinite   E   : exinite
Lpt : liptodetrinite   Rv min : minimum vitrinite reflectance
Alg : alginite   Rv max : maximum vitrinite reflectance
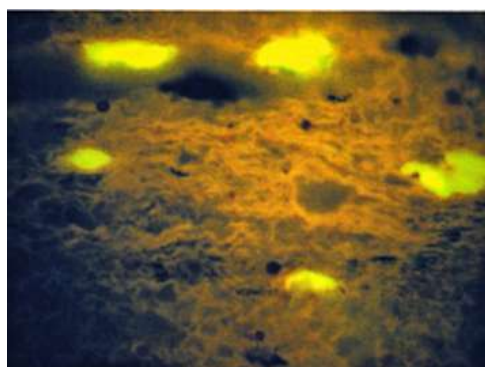
Figure 5.4.3. Photomicrograph of telalginite-*Botryo-coccus* (Tl) and clusters of lamalginite (La). Sample 03NS16E. Fluorescence mode.
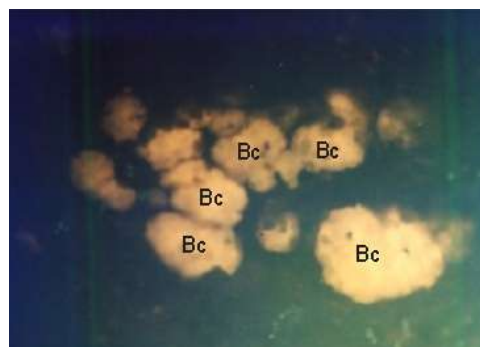
Figure 5.4.4. Photomicrograph of alginite - *Botryocccus* (Bc). (Fluorescence mode). X350.Sample 03ES16L.

(0.2-2.4%) (Figure 5.4.7), with some cutinite and sporinite (Figure 5.4.8) (0.4%), suberinite (Figure 5.4.9), liptodetrinite (0.4-1.6%), and oil droplets and sporinite (Figure 5.4.10). Vitrinite reflectance (Rv_{max}), measured in the DOM within the forma-tion, ranges between 0.29 and 0.70 %, whereas vitrinite reflectance average ranges from 0.23 to 0.66%. This range shows that the sediments are located within the oil window zone,

Some oil drop and bituminite occurrences are also observed in some samples. They can be
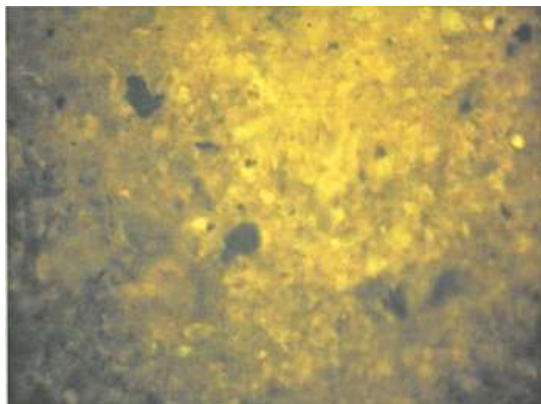
Figure 5.4.5. Photomicrograph of irregular lamination-like of bitumen (B). Sample 03NS16E. Fluorescence mode.

Figure 5.4.8. Photomicrograph of cutinite (Ct), resinite (Rs), and sporinite (Sp). Sample 03ES16L. Fluorescence mode.
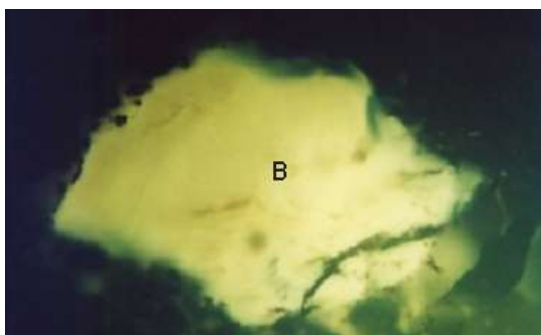
Figure 5.4.6. Photomicrograph of bitumen (B). (Fluorescence mode). X140. Sample 03RH13C.
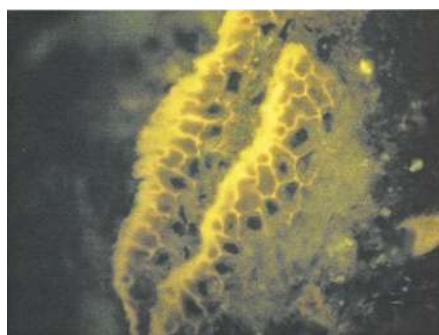
Figure 5.4.9. Photomicrograph of suberinite, in the form of fish fins net. Sample 03NS13A. Flurescence mode.
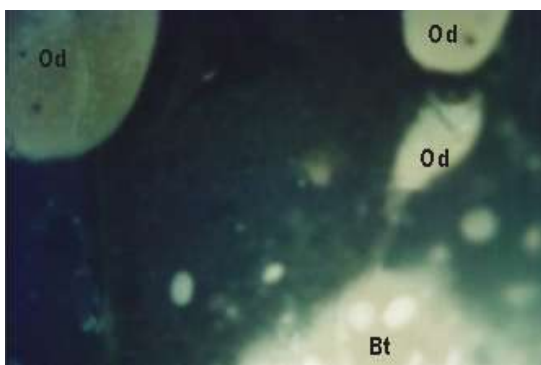
Figure 5.4.7. Photomicrograph of bituminite (Bt) and oil drops (Od) in sample 03ES13H. Fluorescence mode. X140.

Figure 5.4.10. SEM photomicrograph of sporinite (D-H, 1-8) and oil droplet (K,1-2), surrounded by kaolinite and smectite (montmorillonite). X1000. Sample 03NS13A.

identified not only by organic petrology such as in 03ES06H, but also by SEM recorded from the sample 03NS13A.

Organic petrographic analysis on ten coal samples within the Keruh Formation shown in Table 5.4.2 shows that the maceral group is composed of vitrinite (54 – 94%), inertinite (< 1.8 %), and exinite (< 8.8 %). The vitrinite reflectance is ranging from 0.37 % to 0.56 %. The exinite maceral group supporting the genesis of the oil in the source rock is found within the coal samples in the form of resinite (< 2 %), sporinite (< 0.4 %), cutinite (< 7 %), exsudatinite, and alginite (< 0.2%: Figures 5.4.11).

5.5. Ombilin Basin
5.5.1. Sangkarewang Formation

The samples analysed are gained from freshest outcrop and subcrop of shales and mudstones. Rock-Eval pyrolysis was performed on thirteen rock samples from relatively selected representative layers of oil shales.

The TOC content of the investigated samples ranges from 1.10 to 8.12 % (Table 5.5.1) with averages 3.03 %. The highest TOC content occurs in spongy mudstone of 01NS12B (8.12 %) located in Porogadang/Lubuktaruk Hill, followed by
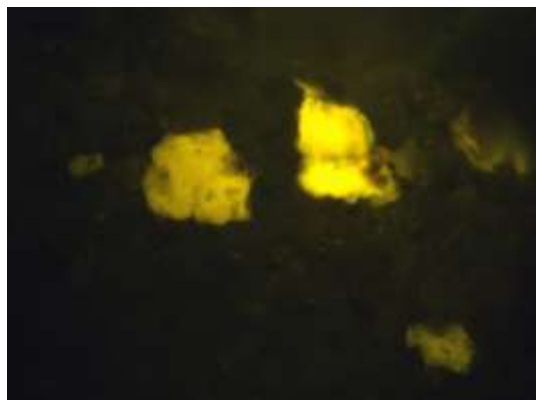
Figure 5.4.11. Photomicrograph of telalginite-?*Botryococcus* in the form of a cauliflower colony. Sample 03ES16L. Location: Muaralembu area, Kuansing. Fluorescence mode.

flaky mudstone of 01NS11C (4.73 %) occurring in Sipang River. On the other hand, the lowest TOC content (1.10 %) occurs on shaly mudstone of 01HR0i situated in Setangkai area.

The recent analyses indicate that, based on Rad classification (1984), the Sangkarewang shales and mudstones from the Sipang River (01NS08A, 10A, and 11C), Porogadang-Lubuktaruk Hill (01NS12B), and Sangka-

Table 5.5.1. Rock-Eval Pyrolysis Data of the Sangkarewang and Sawahlunto Formations, Ombilin Basin

No	Location	Sample Code	Lithology	TOC (%)	S1	S2	PY	PI	T_{max} (°C)	HI
						kg/t				
1		HR. 01 E	Mdst., shaly	1.10	0.13	2.18	2.31	0.06	453	198
2		NS. 01 B	Mdst., dk.gy-blk.	1.63	0.22	3.29	3.51	0.06	446	202
3		NS. 07 A	Mdst., brn.-dk.gy.	1.61	0.07	7.84	7.91	0.01	438	487
4		NS. 08 A	Mdst., dk.gy.	4.41	0.38	26.24	26.62	0.01	440	595
5		NS. 10 A	Mdst., dk.gy.	4.05	0.68	26.44	27.12	0.03	447	653
6	Ombilin Area	NS. 11 C	Siltstone, shaly	4.73	0.82	35.15	35.97	0.03	440	743
7		NS 19 A	Mdst., calc., gy.	2.23	0.21	15.76	15.97	0.01	441	707
8		ES. 07 A	Mudstone	4.51	0.42	34.42	34.84	0.01	446	763
9		SB. 08 B	Siltstone, dk.gy.	2.45	0.11	16.68	16.79	0.01	441	681
10		DS. 07 A	Mdst, dk.gy.	2.03	0.04	6.81	6.85	0.01	439	335
11		ES. 01 A	Mdst., dk.gy.	1.03	0.06	2.12	2.18	0.01	438	206
12		DS. 34 A	Siltstone, dk.gy.	0.18	0.01	0.02	0.03	0.50	ND	11
13		NS. 12 A	Shale, lt.gy.	1.22	0.15	2.52	2.67	0.06	439	207
14	Lubuktaruk Area	NS. 12 B	Mdst., spongy	8.12	0.44	67.28	67.72	0.01	441	829
15		NS 12 E 10	Mdst., spongy	1.34	0.23	3.33	3.56	0.06	443	249

Explanation:
TOC : Total Organic Carbon   S3 : Organic carbon dioxides T_{max} : maximum temperature (oC) at top of S2 peak
S1   : Amount of free HC   PY : Amount of total HC = S1+S2   HI   : hydrogen index (S2/TOC) X 100
S2 : Amount of HC released from kerogen   PI   : production index = S1/S1+S2

rewang River (01ES07A) have excellent hydrocarbon potential (Figure 5.5.1) with TOC values varies from 4.05 to 8.12 % (mainly > 4.0 %), pyrolysis yields (PY) between 26.62 and 67.72 mg HC/g rock (mainly > 20.0 mg HC/g rock), T_{max} of 440 - 447° C, and hydrogen indices (HI) in 595 - 829 range. The kerogen is mainly included into Type I (Figure 5.5.1). The oil shales can be categorised as oil-prone source-rock (Figure 5.5.2).

The good potential category is character-ised by TOC value between 1.0 - 2.0 %, and py-rolysis yields (PY) varying from 6 - 20 mg HC/g rock. This category is represented by the sample 01SR0813 (TOC of 2.45 %, PY of 16.69 mg HC/g rock) occurs in Talawi, mudstone of 01NS19A located in Sangkarewang River (TOC values 2.23 %, PY of 15.97 mg HC/g rock), 01DS28A
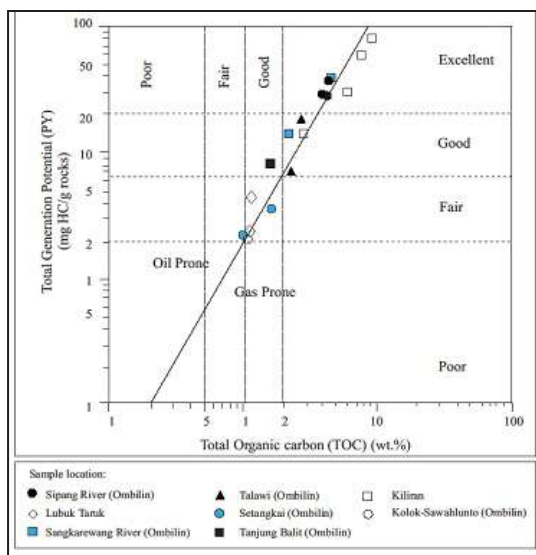
Figure 5.5.2. Diagram of TOC *versus* Pyrolysis Yields (PY) showing the richness and hydrocarbon potential (oil-prone) of the Sangkarewang source rock.

in Talawi (TOC of 2.03 % and PY 6.85 mg HC/g rock), and mudstone of 01NS.07A in Tanjungbalit (TOC value 1.61 %, PY of 7.91 mg HC/g rock). Those samples having T_{max} from 438 to 441°C, and HI (hydrogen indices) between 335 - 707 range. Therefore, the oil shales are in oil-prone level (Figure 5.5.2), and their kerogen is included into Types I and II (Figure 5.5.1).

The rest comprising 4 samples is included into fair potential level (Figure 5.5.2). The samples showing TOC content 1.10 %, and PY 2.31 mg HC/g rock (01HR01E), TOC of 1.63 %, and PY 3.51 mg HC/g rock (01 NS 01 B) both in Setang-kai area; with 01NS12A (TOC of 1.22 %, and PY 2.67 mg HC/g rock), and 01NS12E10 (TOC 1.34 %; PY 3.56 mg HC/g rock) collected from Porogadang/Lubuktaruk Hill. T_{max} of the four-samples ranges from 443 to 453°C. Moreover, their hydrogen indices (HI) are 198 - 249 range. The samples mainly belong to an oil-prone area (Figure 5.5.2), and their kerogen belong to Type II (Figure 5.5.1).

Retort-Oven analysis indicates that the oil content of the analyzed samples predominately

Figure 5.5.1. Hydrogen Index (HI) *versus* T_{max} diagram, showing kerogen type and maturity of oil shale of the Sangkarewang and Sawahlunto Formations.

varies from 3.0 to 97.0 l/t with averages 25.8 l/t (Table 5.5.2). The highest oil content occurs in sample 01NS11A (97.0 1t/t), whereas the lowest oil content (3.0 1/t); both occur in Sipang River. Sixteen of 24 samples representing the Sangkarewang Formation exhibit good to excellent level of hydrocarbon potential (oil content > 18.00 1t/t). This condition is dominated by the Sipang River area, which is represented by 13 samples, that has average oil content of 37.35 1/t.

Petrographically, the maceral composition determined from reflected white light and blue-light (fluorescence) examination on selected-24 samples (Table 5.5.3) is dominated by exinite group (2.0 - 40.0 %) comprising lamalginite of 0.4 - >55 % (Figures 5.5.3 and 5.5.4); with minor bituminite (Figure 5.5.5), resinite (Figure 5.5.6), cutinite (Figure 5.5.7), (?)phytoplankton, liptodetrinite, and sporinite (Figure 5.5.8) that varies from < 0.1 - 2.9 %, and rare telalginite-*Botryococcus* (Figure 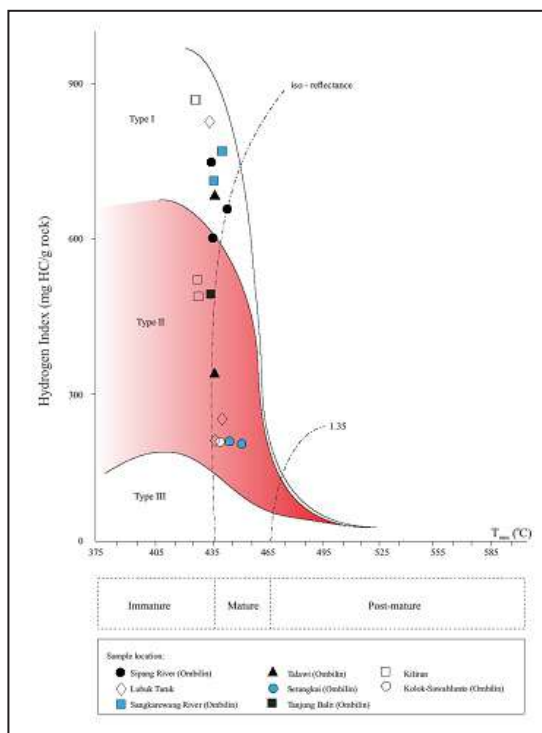5.5.9). Minor amounts of vitrinite macerals of <0.1 - 10.0 % and very rare inertinite are also recognised. Mineral matter present are pyrite (0.1 - 40.0%) and clay minerals, and iron-oxides of 0.5 - 40.0 %. The maximum

Figure 5.5.3. Photomicrograph of lamalginite set in oil shale sample of the Sangkarewang Formation, Ombilin Basin (Fluorescence mode). (Fatimah, 2009).

Figure 5.5.4. SEM photomicrograph of "smectite-illite" (A-E, 1-9 and F-L, 13) with alga of typically *Pediastrum*-lamalginite (F-L, 4-4) in oil shale of the Sangkarewang Formation. Sample 01NS08A. Location: Sipang River.

vitrinite reflectance varies from 0.15 - 0.46%, whereas the mean reflectance between 0.17 - 0.40 %. However, the mean vitrinite reflectance is dominated by 0.19 - 0.25 %-range. Weakly fluorescent matrix (groundmass) is evident in most fine-grained samples, indicating the presence of hydrogen-rich organic matter (Robert, 1981; Bustin *et al.,* 1985). Vitrinite recognised has a granular appearance with micropores and fissures, which are characteristic of oxidation

Table 5.5.2. Retort-Oven Analysis Data of the Sangkarewang and Sawahlunto Formations

No.	Sample Code	Location	Oil Content (l/t)	Water Content (l/t)
1	NS. 01 B		8.0	104.0
2	NS. 02 B		5.0	62.0
3	NS. 04 D		5.0	50.0
4	HR. 01 E		10.0	70.0
5	HR. 03 A		10.0	78.0
6	NS. 06 A		0.0	78.0
7	NS. 07 A		18.0	172.0
8	NS. 08 A		41.0	96.0
9	NS. 08 D		36.0	132.0
10	NS. 08 G		61.0	92.0
11	NS. 08 J		28.0	72.0
12	NS. 08 L		42.0	42.0
13	NS. 10 A	Ombilin Area	18.0	20.0
14	NS. 10 D		41.0	60.0
15	NS. 10 G		3.0	68.0
16	NS. 11 A		97.0	44.0
17	NS. 11 E		36.0	92.0
18	NS. 11 -I		44.0	62.0
19	ES. 06 C		18.0	72.0
20	ES. 06 D		22.0	44.0
21	ES. 07 A		36.0	100.0
22	NS. 18 A		13.0	118.0
23	NS. 19 A		20.0	98.0
24	NS. 05 A		18.0	200.0
25	DS. 34 A		6.4	44.0
26	NS. 12 A	Lubuktaruk	10.0	96.0
27	NS12E		5.0	70.0

Figure 5.5.5. SEM photomicrograph showing lamalginite mixed with smectite-illite (A, 2, 1-5) and bitumen (D-F, 7-8) in oil shale of Sangkarewang Formation. X1000. Sample 01RH02A.

(Bustin *et al.,* 1985).

Furthermore, alginite present in the oil shale samples of the formation is predominantly "lamalginite", because of its parallel lamellar form and an orange fluorescence. However, a very rare of probably *Botryococcus* telalginite also occurs. Therefore, the oil shale deposits can be termed as "lamosites".

The Sangkarewang Formation, predominantly, an organically rich succession, was deposited in a restricted to anoxic condition in a deep-water to marginal lacustrine. The formation is mainly composed of laminated to well-bedded dark grey to brownish organic-rich mud shales (TOC > 3%) with laminated to well-bedded dark to light grey organically poor mud shales (TOC < 2%). Their high organic content reflects changes in organic productivity versus the rate of sedimentary supply, and nor fluctuating oxygen levels in the bottom waters or changes in water depth. Based on the thermal maturity, the oil shales of the Sangkarewang Formation are situated beyond the oil "birth" line, falling in the non-onset oil zone.

5.5.2. Sawahlunto Formation

Thermal maturity evaluated from Rock-Eval pyrolysis (T_{max}) data (Table 5.5.1), shows that oil shales of the Sawahlunto Formation are thermally immature (Figure 5.5.1). T_{max} value of one sample analysed is 438°, and it indicates that the oil shale is in-between the late immature to beginning of the oil window. The PI values of the two samples analysed tend to show that the oil shales are in an immature level, due to their values that are less than 0.1. Those two data displays that the stage of the oil shale is immature.

The formation is represented by two analyzed samples. One sample (01ES0lA) with TOC value of 1.03 % and PY of 2.13 mg HC/g rock is included into oil-prone potential. Its T_{max} value is 438°C, with HI (hydrogen indx) of 206 range. This sample falls under Type II kerogen. However, another sample (01DS34A) is included into lean hydrogen potential.

5.6. Kiliranjao Sub-basin

TOC and Rock-Eval pyrolysis carried out on the shale samples of the Kiliran Formation (Table 5.6.1) show that the TOC values range between 3.00 - 9.03 %, pyrolysis yields (PY) between 14.66 - 79.72 mg HC/gm rock, T_{max} varying from 431 - 432° C, and hydrogen index (HI) of 484 - 864 range. Based on this data, thereby, the Kiliran Formation is classified as an excellent potential level, that is included into Type I and II kerogen (Figure 5.6.1) dominated by oil-prone potential level (Figure 5.6.2).

Thermal maturity of the rock samples is random, but it is consistent, that the rocks are included into an immature level. This condition is supported by the $T_{max} < 440$°C, and the hydrocarbon potential index (PI) = □ 0.02. The maximum vitrinite reflectance (Rv_{max}) varying from 0.26 - 0.38%, is situated within the diagenesis level, also tends to indicate an immature stage.

Rock-Eval pyrolysis, and Retort-Oven analysis, reveal that the samples of the rock formation, show characteristics as described follows. Rock-Eval analyses were performed on 22 rock samples) from relatively selected representative layers of oil shales. Among the 18 pyrolised samples gained from the Kiliranjao area, and
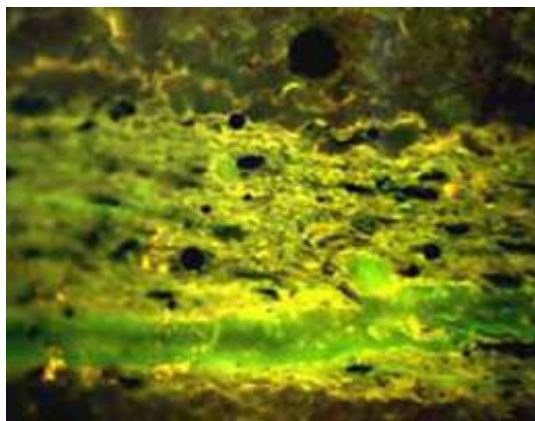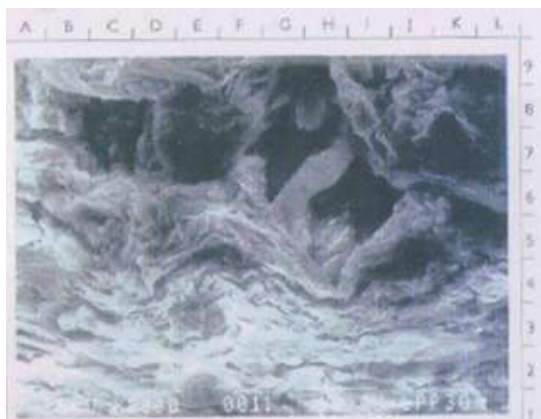
Figure 5.5.6. Photomicrograph of resinite within oil shale sample of the Sangkarewang Formation, Ombilin Basin (Fluorescence mode).
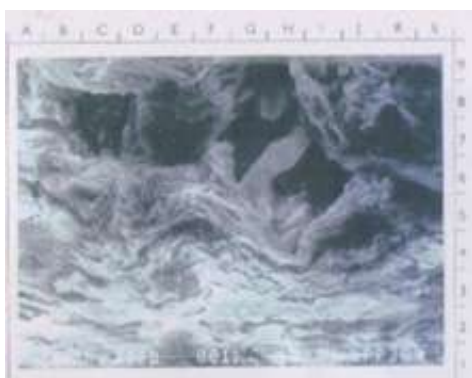
Figure 5.5.7. Photomicrograph of cutinite within oil shale sample of the Sangkarewang Formation, Ombilin Basin (Fluorescence mode).

Figure 5.5.8. Photomicrograph of sporinite within oil shale sample of the Sangkarewang Formation, Ombilin Basin (Fluorescence mode).

4 samples from the Kunangan area, rocks have yields consistent with good or excellent hydrocarbon source rocks (PY of 8.42 - 67.73 mg HC/g rock), except 1 sample (00/SU6B) having hydrocarbon yield of 4.64 mg HC/g rock and tends to indicate fair potential (Figure 5.6.3). Moreover, TOC values vary from 1.52% to 13.49% (mainly more than 6.0%), T_{max} of less than 440º C, and hydrogen indices (HI) in 285 - 689 range.

Based on this pyrolysis yield showing >10 mg HC/g rock (Espitalie *et al*., 1977; Peters, 1986), the shales are classified as a very good or excellent source-rock potential, which also can be classified as an 'effective source-rock'. It is also supported by Peters' observation (1986 and 1989), that rocks with HI>300 mg HC/g TOC (range) will produce oil. The kerogen contained is mainly included into Type II, with very minor Type I (Figure 5.6.4). The oil shales contain both autochthonous and allochthonous organic material. The auchthonous materials consist of Type I kerogen, alginite and exsudatinite, whilst, the allochthonous type comprises Type II and III kerogen, sporinite, vitrinite, and inertinite of floral/humic origin.

Additionally, the Retort-Oven analysis (Table 5.6.2) shows that 1 sample (00/NS-14) has oil content of 40.15 lt/t, whereas sample 00/NS08L of 1.58 lt/t.

Oil content of the seven samples gained from Kunangan, shows values between 22.0 -78.0 1t/t, with average of 35.43 lt/t. This value is classified as good to excellent hydrocarbon potential.

Organic petrographic analysis (Table 5.6.3) on the selected-8 samples shows that the maceral group mainly comprises lamalginite of exinite maceral group (<0.1 - 7.0 %) with sparse-common liptodetrinite (0.1- 0.7 %), sparse cutinite (0.1 %), and rare *Botryococcus* telalginite (< 0.1 %). Sparse to abundant vitrinite maceral group is also recognised, whilst inertinite occurs in rare amount (commonly < 0.1 %). The range of maximum vitrinite reflectance (Rv_{max}) is situated between 0.13 and 0.46 %. Meanwhile, the mean vitrinite reflectance varies from 0.20 - 0.42 %.
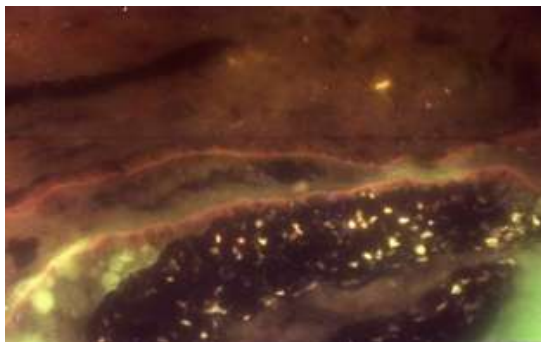
Figure 5.6.5. Photomicrograph of cutinite (Cu) and resinite (Rs) of Kiliran shale. (Fluorescence mode). Location: Kunangan Coalfield.

Figure 5.6.8. SEM photomicrograph of shale showing typical lamalginite (A-E, 1-2) and kaolinite (E-I, 3-9). Sample 00NS08G. Location: Karbindo Coalfield

Figure 5.6.6. Clusters of sporinite
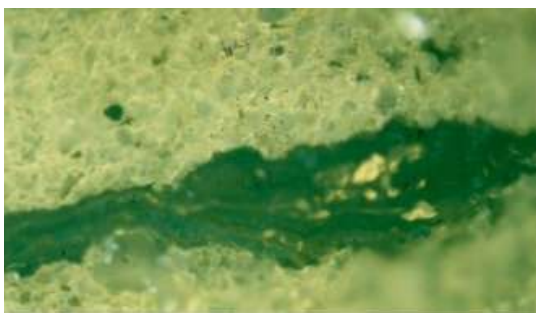
Figure 5.6.9. Photomicrograph of lamalginite (Lam), vitrinite (V), and resinite (Rs) in silty claystone (Cl) of the Kiliran Formation. (Fluorescence mode). Sample 00NS08N2. Location: Karbindo Coal Mines, Kiliranjao.

Figure 5.6.7. SEM photomicrograph of shale containing typical (? mega)sporinite (A-B, 1-32) and in the centre is framboidal pyrite (A-B, 7-8; and F-G, 3-4). Kaolinite is predominant clays. Sample 00NS13. Location: Karbindo Coal Mines.

Figure 5.6.10. Photomicrograph of vitrinite (V) contains framboidal pyrite (Py), embedded in silty claystone (Cl) of the Kiliran Formation. (Reflected white light). Sample 00NS08N2. Location: Karbindo Coal Mines, Kiliranjao.
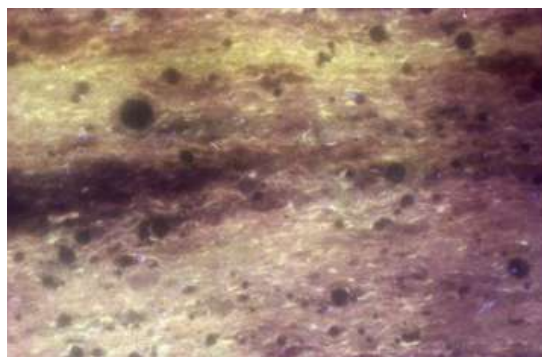
Figure 5.6.11. Photomicrograph of lamalginite contained within shale of the Kiliran Formation. Flurescence mode.

Figure 5.6.12. Photomicrograph of sporinite (?sporangium)contained within mudstone of the Kiliran Formation. Fluorescence mode.

Figure 5.6.13. Photomicrograph of telalginite-*Botryococcus* embedded within clay matrix.

Weakly fluorescent matrix (groundmass) is evident in most fine-grained samples, indicating the presence of hydrogen-rich organic matter (Robert, 1981; Bustin *et al.,* 1985). Some framboidal pyrites (0.5 - 2.0 %) commonly occur.

Thermal maturity evaluation is gained from Rock-Eval pyrolysis (T_{max}) and vitrinite reflectance (% Rv) data. The T_{max} values, varying from 43 - 432° C (Table 6.9), show that the formation is thermally immature. Throughout the sub-basin, the formation samples, indicating by vitrinite reflectance values, are in an immature stage, with an exception. Most vitrinite reflectance values range from 0.20 to 0.26 %, and these values fall beyond the "oil birth" line occupying the non-onset oil zone. The sample 01NS14i has a slightly higher reflectance indicating that it is close to the oil "birth" line, although still within the non-onset oil area. The PI values of the samples that are less than 0.1 (Table 5.6.1), indicate that the Kiliran oil shales are situated within an immature stage. Overall, the vitrinite reflectance agree with the T_{max} and PI values. Due to their Rv_{max} values (<0.4 %), according to the Foscolos *et al.'s* chart (1976), the oil shales had undergone an Eodiagenetic process.

On the basis of Cook *et al.* (1981) and Hutton (1987) terminology, petrographically, alginite observed in the shale and mudstone sample is "lamalginite" type, because of its presence as lamellar forms. Moreover, a very minor amount of probably *Botryococcus* telalginite is also recognized in a very minor amount. Thereby, the shale and mudstone can be classified as "lamosites".

5.7. Bukit Susah Sub-basin

Oil shale, as an alternative energy resource, is recognized in the Eocene – Oligocene Kelesa Formation, located in the Bukit Susah area. The area occupies the Central Sumatera and Jambi Basins, where both are back-arc basins. An almost complete rock sequence of the 86.8 m thick oil shale-bearing formation found in the Punti Kayu River comprises an association of shale with carbonaceous siltstone, sandstone, conglomeratic sandstone, and conglomerate.

Rock-Eval Pyrolysis data (Table 5.7.1) plotted on diagram TOC vs. PY indicate that six samples fall under good potential level, and 12 samples belong to the excellent class. This good excellent hydrocarbon potential level is recognized in the upper part of the unit and within shale bed in the middle of the oil shale succession at Putikayu River. The oil show potential to be *oil-gas prone source rock*. On the other hand, *oil* shale having very good oil potential, with TOC value between 4.06 – 9.63% and PY from 21.70 – 70.72 mg HC/g rock is also potential to be, *oil-gas prone source rock*.

Eleven shale samples having HI value < 600 (268 – 547) contain kerogen type II, whilst sevem samples with HI value >600 (606 – 791) their kerogen content is included into type I. Oil shale in the study area is potential as an oil-gas prone source rock, within good to excellent category.

T_{max} value varies from 430 - 444°C and hydrogen index (HI) ranges from 268 – 791. Kerogen of Types I and II are present.

The dominant maceral group is exinite, composed of alginite (0.4 – 0.6 %), resinite (0.4 – 2.0 %), sporinite (0.4 – 0.8 %), suberinite (0.4 – 2 %), cutinite (0.6 – 1.4 %), and exsudatinite (0.2 – 0.6 %); whilst the minor one is vitrinite ranging from 0.6 – 7.6 %. The maximum vitrinite reflectance varies from 0.29 to 0.56%, whilst the average value from 0.27 to 0.43 %.

Thermal maturity level of the oil shale, in general, is situated in the immature category, although it tends to be close to the immature – mature boundary line, beyond oil birth line. Clay minerals consist of smectite-illite, with illite and kaolinite. The shale has undergone a diagenetic process within an early diagenetic level.

Table 5.7.1. TOC and Rock-Eval Pyrolysis Data of Kelesa Oil Shale, Bukit Susah, Riau

No.	Sample No. (04)	Lithology	TOC (wt.%)	S_1	S_2	PY	PI	T_{max} (°C)	HI
					mg/grock				
1.	ES.13C	Shale, gy-dkgy, fissile	4.06	0.64	21.06	21.70	0.03	443	519
2.	ES.14A	Shale, gy-dkgy, papery	5.66	0.17	22.40	22.57	0.01	433	577
3.	ES.15C	Shale, dkgy, fissile	9.63	0.20	70.72	70.92	0.00	431	734
4.	ES.16B	Shale, gy-brngy, papery	5.20	0.03	25.68	25.71	0.00	430	494
5.	ES.18A	Shale, gy, fissile	5.96	0.30	47.16	47.46	0.01	442	791
6.	NS.29A	Shale, gy-brngy, silty	3.05	0.07	12.02	12.09	0.01	439	394
7.	NS.29B	Shale, brn-dkgy	3.37	0.11	18.42	18.53	0.01	438	547
8.	NS.29C	Shale, gy. fissile	310	0.07	14.68	14.75	0.00	433	474
9.	NS.29G	Shale, brngy, papery	7.93	0.24	61.28	61.52	0.00	444	773
10	NS.29 I	Shale, gy-brngy, silty	4.06	0.16	26.22	26.38	0.01	436	646
11.	NS.29K	Shale, gy-brngy, papery	5.43	0.17	40.48	40.65	0.00	441	745
12.	NS.29M	Shale, brn.dkgy, fissile	4.98	0.18	33.64	33.82	0.01	438	676
13.	NS.29N	Shale, gy, papery	3.40	0.05	11.80	11.85	0.00	437	347
14.	NS.29O	Shale, brngy, papery	7.17	0.20	46.44	46.64	0.00	439	648
15.	NS.29P	Shale, gy, silty, papery	3.74	0.04	14.92	14.96	0.00	435	399
16.	NS.29Q1	Shale, brngy, papery	5.49	0.10	33.28	33.38	0.00	435	606
17.	NS.29Q2	Shale, gy-dkgy, papery	2.31	0.04	6.19	6.23	0.01	438	268
18.	NS.30A	Shale, gy-brngy, papery	4.76	0.20	24.10	24.30	0.01	432	506

Remarks :

TOC : total organic carbon
S1 : free HC (oil quantity)
S2 : HC released from kerogen
S3 : oxygen containing compound

PI : production index (S1/S1+S2)
HI : hydrogen index (S2/TOC)
OI : oxygen index (S3/TOC)
T_{max} : maximum temperature (OC) for HC released from kerogen

Table 5.8.1. TOC and Rock-Eval Pyrolysis Data of the Lakat Formation, East Tigapuluh Mountains

No	Sample Number (00)	Form	Lithology	TOC (%)	S1	S2	PY	PI (%)	T_{Max} (%)	HI
					mg HC/g rock					
1	NS.04A		Mdst,,it.brn-gy. Sl. carb	2.03	0.14	2.94	3.08	0.05	430	145
2	NS.04B		Mdst,brngy	1.75	0.09	2.41	2.50	0.04	430	138
3	NS.04C	L	Mdst, brngy- dkgy	1.79	0.19	3.66	3.85	0.05	428	204
4	NS.06C	A	Mdst,-gy-it. brngy	0.67	0.15	1.06	1.21	0.12	429	159
5	NS.06D	K A	Mdst, dkbrn/dkgy	5.28	0.70	36.68	37.38	0.02	438	695
6	NS.06F	T	Mdst,dkgy	3.46	0.50	11.31	11.81	0.04	424	327
7	NS.06G		Sh, gy-dkgy	1.48	0.11	2.98	3.90	0.04	424	201
8	NS.06I		Sh, dkgy,sl.carb	3.24	0.65	12.12	12.77	0.05	425	374

Remark:

TOC	Total organic Carbon
S_1	Quantity of free HC
S_2	Quantity of HC released from kerogen
Py	Quantity of HC (Pyrolysis yield)

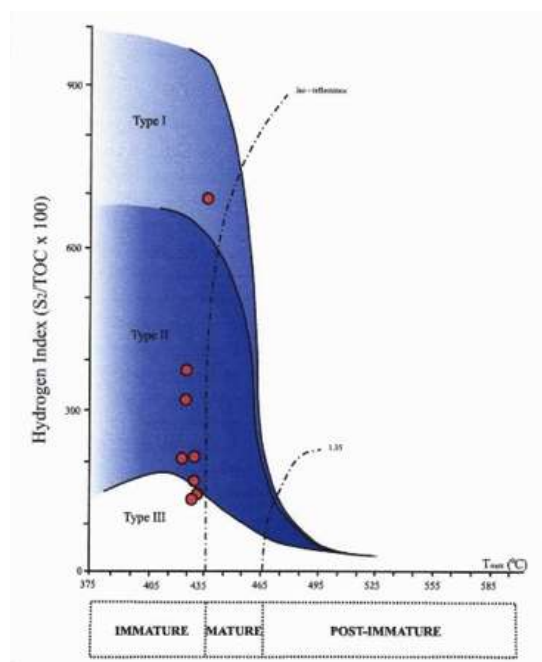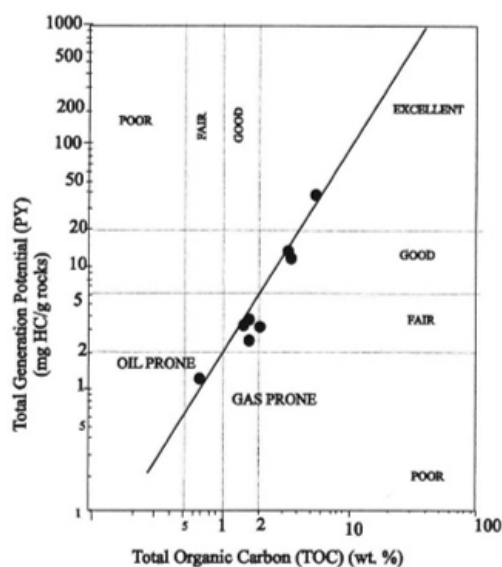|	
T_{max}	Maximum / Peak temperature (oC) for HC generation from kerogen
HI	Hidrogen Index

Figure 5.8.1. Diagram of Hydrogen Index (HI) vs. T_{max} showing the kerogen type and thermal maturity of the Lakat Formation, East 30-Mts.

Figure 5.8.2. Diagram of TOC vs Generation Potential (PY) indicating the hydrocarbon potential and organic matter richness of the Lakat Formation.

5.8. East 30-Mountains

5.9. Bukit Bakar

5.10. Sinamar

5.11. Asai-Rawas

Based on TOC and Rock-Eval Pyrolysis, the potency of source rock is determined. Rock-Eval Pyrolysis data of the Kasiro Formation in the Asai-Rawas region is presented in Table 5.11.1.

5.11.1. Sungai Keruh

Twelve samples were analyzed by screen-ing test (Table 5.11.1). The result shows that total organic carbon (TOC) content value > 2%, except two samples are 0.72% (05ES21) dan 0.06% (05ES28). The highest TOC content vary-ing from 2.11% - 6.82%, were detected within sample 05ES36B, whereas the lowest on sample 05ES33B.

Total hydrocarbon content (PY/*pyrolysis yields*) is represented by three clusters, from the highest to the lowest are 10.31 – 43.38 mg HC/g rock (6 samples), 5.85 – 8.97 mg HC/g rock 4 samples, and the value of < 1.0 mg HC/g rocks

Table 5.10.1. T OC and Rock-Eval Pyrolysis data of Sinamar Formation, Jambi

No.	Sample No. (08)	Lithology	TOC (%)	S1	S2 mg	S3 /g	PY	S2/S3	PI	T_{max} (^0C)	HI	OI
1.	NS 07 C	Sh. gngy	0.49	0.06	0.21	0.15	0.27	1.40	0.22	397	43	31
2.	NS 07 E	Sh. lt.yell/ltgy-gy. calc	0.54	0.05	0.26	0.24	0.31	1.08	0.16	405	48	44
3.	NS 07 G	Sltst. yell-ltgy/gy. loc.purplle	0.30	0.04	0.11	0.25	0.15	0.44	0.27	408	37	84
4.	NS 08 A	Sh. ltgy/gy	0.60	0.08	0.41	0.12	0.49	3.42	0.16	402	69	20
5.	MH 03 B	Sh. ltgy/gy. calc	0.64	0.09	0.42	0.27	0.51	1.56	0.18	402	66	42
6.	MH 11 A	Sh. brndkgy	7.23	34.03	52.58	2.82	86.61	18.65	0.39	365	727	39
7.	MH 11 J	Sh. gy/dkgy	1.60	1.16	4.10	0.48	5.26	8.54	0.22	362	257	30
8.	MH 12 M	Sh. dkgy	0.69	0.02	0.13	0.58	0.15	0.22	0.13	383	19	85
9.	MH 12 P	Sh. gy/dkgy	2.08	0.21	2.83	0.37	3.04	7.65	0.07	420	136	18
10.	MH 12 R	Sh. brn.dkgy	10.52	2.42	63.48	0.00	65.90	∞	0.04	436	603	0
11.	MH 13 A	Sh. brn.gy	9.02	3.00	66.66	0.00	69.66	∞	0.04	436	739	0
12.	MH 13 B	Sh. dkbrngy	9.53	2.34	78.02	0.00	80.36	∞	0.03	439	819	0
13.	MH 13 C	Sh. brngy	7.45	0.97	51.95	0.22	52.92	236.14	0.02	439	697	3
14.	MH 13 D	Sh. brn dkgy, sl hd. oxid	9.12	2.38	64.76	0.00	67.14	∞	0.04	436	710	0
15.	MH 13 E	Sh. dkbrngy. sl hd	10.84	2.11	60.57	1.73	62.68	35.01	0.03	431	559	16
16.	MH 13E2	Sh. dkbrngy. sl hd	8.36	0.80	53.30	0.71	54.10	75.07	0.01	439	638	8
17.	LS 01 A	Clyst. dkgy	4.23	0.97	4.83	0.91	5.80	5.31	0.17	400	114	22
18.	LS 01 G	Clyst. Wht lt.gy	0.77	0.16	0.48	0.20	0.64	2.40	0.25	402	62	26
19.	RL 04 B	Clyst. gy/dkgy	3.28	0.55	6.22	0.39	6.77	15.95	0.08	425	189	12
20.	RL 04 C	Sltst. yell-red wht	0.07	0.00	0.00	0.14	0.00	0.00	∞	312	0	197
21.	RL 05	Sst. yell-gywht. c-m.g. carb.mat.fragments	0.15	0.00	0.07	0.37	0.07	0.19	0.00	335	48	255
22.	RL 06 A	Sst. rdsh creamy wht. m-f.g. qtz. friable	0.03	0.00	0.00	0.06	0.00	0.00	∞	431	0	230
23.	RL 08 B	Sst. yell-brngywht. m-f.g. carb.mat.	0.27	0.02	0.06	0.67	0.08	0.09	0.25	285	22	251
24.	RL 25 A	Clyst. dkgy/blk. hd	3.29	0.22	0.59	0.27	0.81	2.19	0.27	543	18	8

Remarks:

TOC : Total Organic carbon
S1 : free hydrocarbon
S2 : hydrocarbon released from kerogen
S3 : organic carbon dioxide
PY : total hydrocarbon = (S1+S2)

PI : production index = (S1/S1+S2)
T_{max} : Maximum Temperature (^0C) at the top of S2 peak
HI : hydrogen index = (S2/TOC) x 100
OI : oxygen index = (S3/TOC) x 100

Table 5.10.2. Results of Organic Petrographic Analysis of Sinamar Formation

No.	Sample No. (08)	Maceral (%)												Mineral (%)				Rv (%)		
		Tc	Dc	Cr	Vd	V	Re	Alg	E	Sf	Fu	Idt	I	Cly	Py	Carb	MM	Min	Max	Mean
1.	NS 08 A	-	6,4	-	-	6,4	-	-	-	-	-	-	-	-	-	93,6	93,6	0,36	0,40	0,38
2.	MH 03 B	-	-	-	4,0	4,0	-	-	-	-	-	-	-	92,0	4,0	-	96,0	0,36	0,42	0,36
3.	MH 12 P	1,4	1,0	0,4	13,6	16,4	1,6	-	1,6	-	0,4	-	0,4	79,2	2,4	-	81,6	0,36	0,40	0,38
4.	MH 12 R	-	-	-	14,4	14,4	-	-	-	-	-	-	-	83,6	2,0	-	85,6	0,44	0,46	0,44
5.	MH 13 A	0,4	-	-	16,4	17,0	5,6	3,4	9,0	-	-	-	-	67,0	3,0	4,0	74,0	0,42	0,46	0,44
6.	MH 13 C	-	0,4	-	16,4	16,8	2,6	18,0	20,6	-	-	-	-	58,4	1,6	2,6	62,6	0,40	0,44	0,42
7.	MH 13 D	0,4	0,4	-	14,6	15,4	2,0	7,0	9,0	-	-	-	-	68,0	5,0	2,6	75,6	0,40	0,44	0,42
8.	MH 13 E	0,4	0,6	-	8,4	9,4	2,0	10,6	12,6	-	-	0,4	0,4	77,0	0,6	-	77,6	0,42	0,44	0,43
9.	MH 13 E2	0,4	0,8	-	9,6	0,8	1,6	9,6	11,2	-	-	-	-	76,0	0,6	1,4	78,0	0,36	0,42	0,34
10.	LS 01 A	-	28,4	1,0	-	29,4	0,8	-	0,8	-	-	-	-	64,8	4,6	0,4	69,8	0,36	0,40	0,38
11.	RL 04 B	1,6	19,4	7,6	-	28,6	0,8	-	0,8	0,4	-	-	0,4	69,0	0,6	0,8	70,4	0,4	0,42	0,41
12.	RL 25 A	-	15,0	0,6	4,6	19,2	0,6	-	0,6	-	0,6	-	0,6	80,2	1,4	0,6	82,2	0,48	0,52	0,50

Remarks :

Tc : telocollinite	E : exinite	Carb : carbonate
Dc : desmocollinite	Sf : semifusinite	MM : mineral matter
Cr : corpocollinite	Fu : funginite	Rv : vitrinite reflectance
Vd : vitrodetrinite	Idt : inertodetrinite	Min : Minimun
V : vitrinite	I : inertinite	Max : Maximum
Re : resinite	Cly : clay	
Alg : alginite	Py : pyrite	

Figure 5.10.1. Photomicrograph of telalginite-*Botryococcus* embedded within Sinamar sediments. Sample 08MH13. Fluorescence mode.

Figure 5.10.2. Photomicrograph of telalginite-*Botryococcus* recognized within Sinamar sediments. Sample 08MH13E. Fluorescence mode.

within 2 samples, respectively.

Furthermore, 8 samples show T_{max} varying between 434 – 442°C; 2 of them are 449°C and 458°C, 1 sample is 514°C, and the rest is unable to be detected. Then, hydrogen index (HI) from 83 – 665, whilst PI (*production index*) generally <0.10 (0.00 – 0.06) except samples 05ES25 (0.19) and 05ES28 (0.50).

5.11.2. Sekeladi

Analysis result of 4 oil shale samples exhibits TOC content > 2.0%, those vary between 3.69 -

Figure 5.10.3. Photomicrograph of lamalginite recognized within Sinamar sediments. Sample 08MH13E.
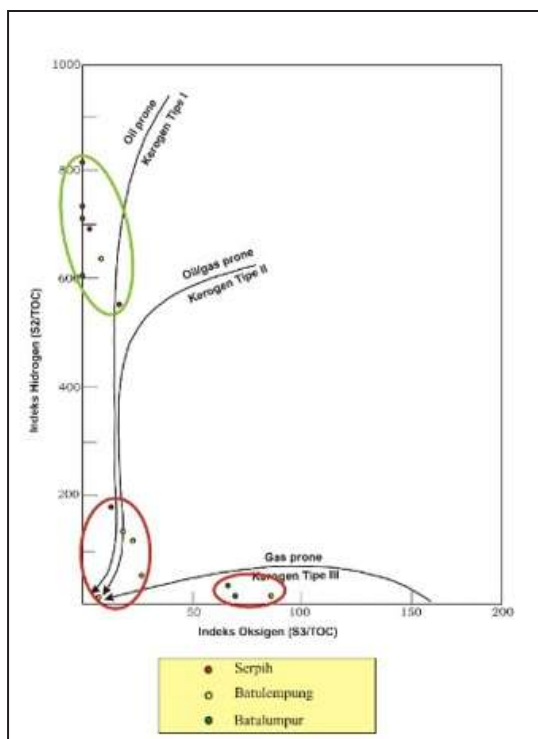

Figure 5.10.5. Cross plot of Hydrogen Index (HI) vs. Oxygen Index (OI) of Sinamar shales, on van Krevelen (19..) diagram, showing kerogen type of the sample.

Figure 5.10.4. Photomicrograph of (?) bitumen contained within Sinamar sediments. Sample 08MH13E. Fluorescence mode.

14.76%. The highest TOC value is recognized within sample 05MH04C (1.76%), whereas the lowest one in sample 05MH05E (Table 5.11.1).

The sediments are occupied by 2 clusters of total hydrocarbon content (PY/*pyrolysis yields*), those, the highest is between 132.21-138.50 mg HC/g rock, represented by samples 05MH04B and 05MH04C; and another cluster ranges from 17.24-63.46 mg HC/g rock (samples 05MH05E dan 05MH05A).

Moreover, two levels of T_{max} are recognized, those varying from 444 – 447ºC and 507ºC. Hy-

drogen Index (HI) varies from 461 – 906; and PI (*production index*) value averaged < 0.10, ranging between 0.01 – 0.03.

5.11.3. Asai River Upstream Region

From this area, 6 shale samples were analyzed. TOC content varies from 2.16 – 4.71%, except sample 05NS46A showing value of 0.72% (Table 5.11.1).

Total hydrocarbon (PY/*pyrolysis yields*) produced can be divided into three clusters, those having value of < 1.0 mg HC/g rock (05NS46A of 0.60 mg HC/g rock), values between 2.98 – 7.34 mg HC/g rock (4 samples), and PY of 36.19 mg HC/g rock (05NS40).

In general, T_{max} value ranges between 448 – 451ºC, except one sample having Tmax value of 575ºC. Then, hydrogen index (HI) value varies

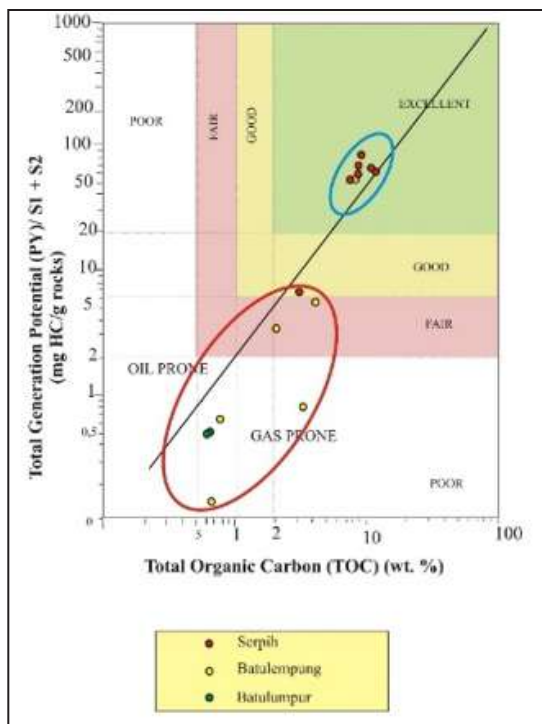Figure 5.10.6. Crossplot diagram of TOC vs. Pyrolysis Yields (PY) indicating hydrocarbon potential in Sinamar sub-basin.
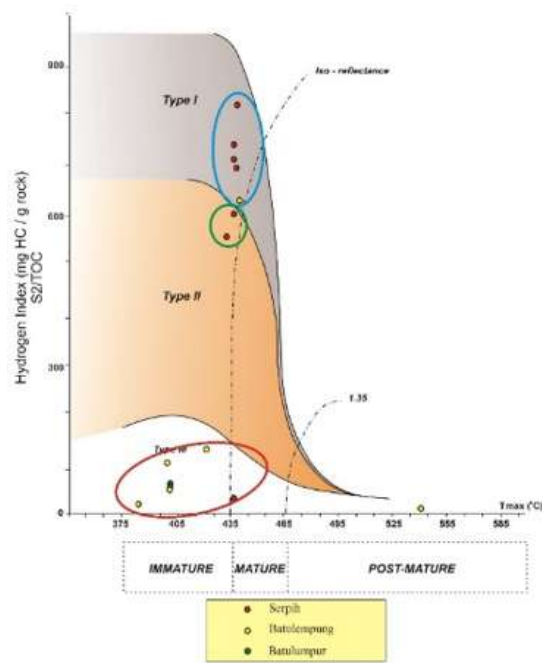
Figure 5.10.7. Diagram of Hydrogen Index (HI) vs. Tmax showing kerogen type and thermal maturity of source rocks in Sinamar Sub-basin.
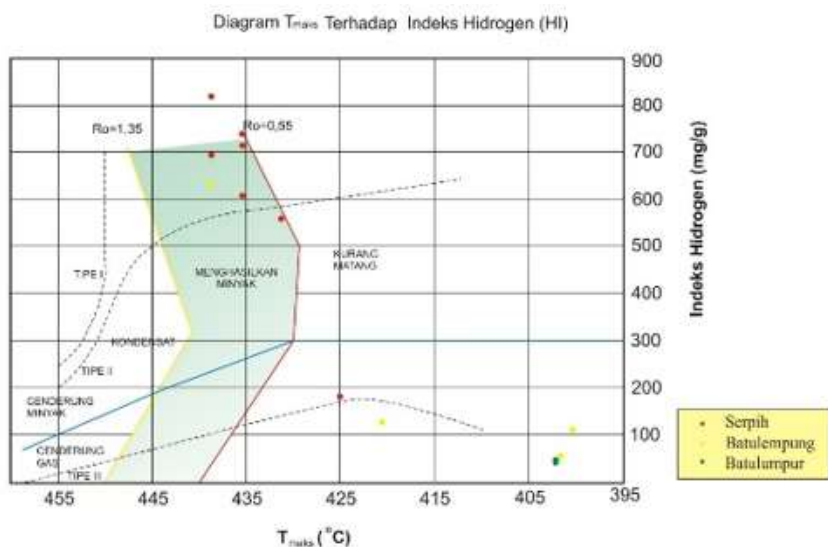

Figure 5.10.8. Diagram of crossplot T_{max} vs. Hydrogen Index (HI) indicating thermal maturity level and oil-gas potential of Sinamar source rocks.
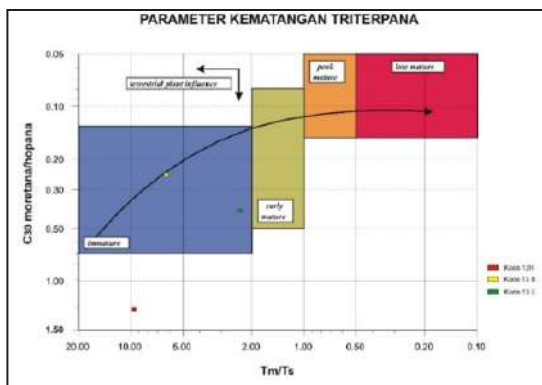
Figure 5.10.9. Crossplot of Sinamar source rock maturity based on triterpene parameter indicating the three rock samples included immature to early mature.

from 78 – 760, and PI (*production index*) between 0.01 and 0.14.

5.11.4. Sungai Lepat

TOC value of 18 oil shale samples analyzed, in general, varies from 2.49 - 10.1%. However, one exception showing a high value (16.11%) is represented by sample 05NS21.

Total hydrocarbon content (PY/*pyrolysis yields*) obtained comprises 2 clusters, those having value 10.75 – 60.75 mg HC/g rock and 9.15 mg HC/g rock recognized on sample 05ES49C.

In general, T_{max} ranges between 431 – 443°C, except on samples 05ES47D and 05ES49B the T_{max} value is 512°C. Moreover, a value range of hydrogen index (HI) is 275 – 828; whilst PI (*production index*) < 0.10, varying 0.01 – 0.04 (Table 5.11.1).

On the basis of Rad classification (1984), the Kasiro shale and mudstone from Keruh, Sekeladi, Lepat, as well as Hulu Asai River area contain significant organic matter. This indication is shown by the the presence of TOC content >> 1.0% and Pyrolysis Yield (PY) > 5 mg HC/g rock, except 3 samples falling under category of lean, due to their TOC content of 0.06 and 0.72%, as well their PY < 0.7 mg HC/g rock.

Furthermore, Figure 5.11.1 showing the richness and kerogene type of source rock in those four study localities, can be categorized into oil-prone potential. This assumption is indicated by hydrogen index value of > 300 (HI=mg
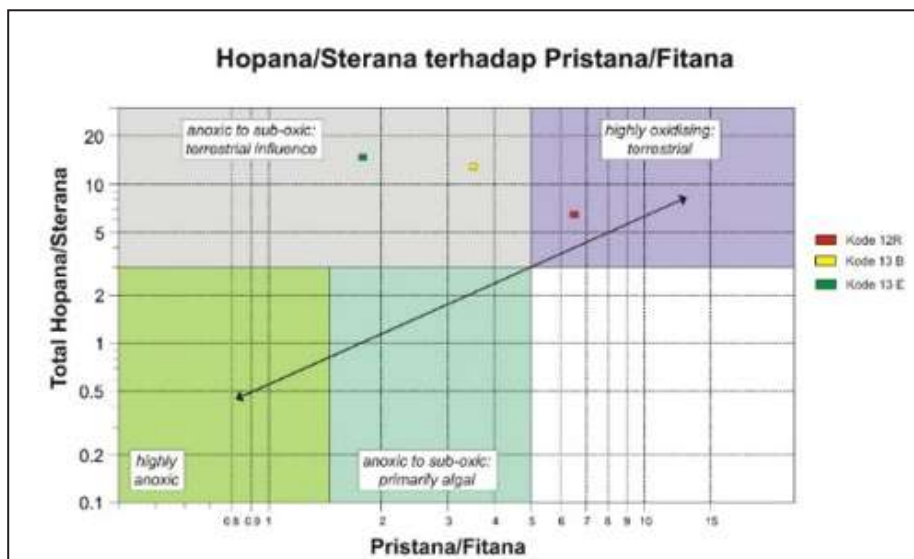

Figure 5.10.11. Triangular diagram showing depositional environment of Sinamar Formation rocks (Huang and Meinschein, 1979; in Waples and Machihara,1991).
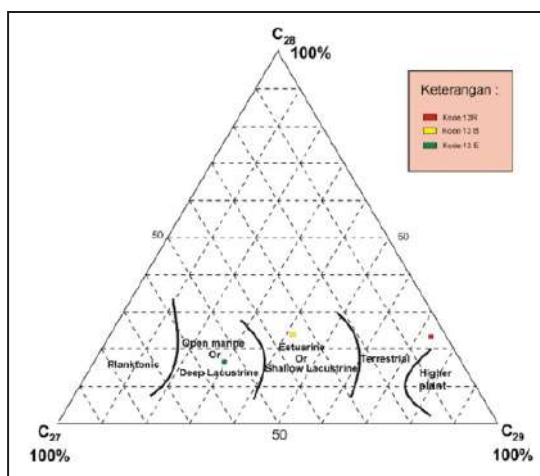
Figure 5.10.10. Crossplot of hopane/sterane vs. Pristane/Phitane in Sinamar source rocks.

HC/g TOC). In the study area, an indication of gas-oil prone to gas prone condition occurs, as recognized within samples 05ES25, 05ES33B, 05ES39B, 05ES40A, 05ES41K (Keruh River), 05NS21C (Lepat River), 05MH05E (Sekeladi), and also samples 05NS41B, 05NS41D, 05NS47A, and 05NS47C (Asai Upstream areas) (Figure 5.11.2). Therefore, from this characteristics, it can be concluded, oil shale from the Lepat River and Sekeladi tend to indicate oil-prone potential, whilst the Keruh River and Hulu Asai are occupied by oil-prone and gas-prone levels.

Moreover, the potency and quality, thermal maturity, and kerogen type of each source rock of the Kasiro oil shale is dominated by hydrocarbon potency of good to excellent levels, with rare fair degree (Figure 5.11.2).

Those three levels shows that TOC content varies from > 5% to around 10%, whilst total bydrocarbon produced (PY) generally > 4.91 mg HC/g rock. The fair level tend to indicate gas-prone potential, whilst good to excellent degree tends to produce a similar probability in gas prone and oil prone levels. The Sekeladi oil shale is suggested to be occupied by an oil prone condition, Lepat River by potential oil- and gas-prones, whereas

Keruh River and Hulu Asai only as gas-prone potential. Those characteristics is concommittant with the prediction based on Rad classification (1984), as discussed above. Additionally, kerogen of the Kasiro oil shale is dominated by type-II, with some of types-I and III.

Due to the presence of abundant lamalginite (3.0 – 30.0%) (Figure 5.11.3), the Kasiro oil shale deposit, in general, can be classified as lamosites (Hutton, 1987 and Cook *et al*., 1981). An appearance of groundmass, showing a weak fluorescence colour, is indicative of the presence of organic matter rich-in hydrogen (Robert, 1981; Bustin *et al*., 1985) within the oil shales. The exinite group, being one of the important oil-generating constituents, appears in two distinct forms, dispersed in the clay matrix leading to visible background fluorescence of the clay dominated sections (Figures 5.11.4 – 5.11.6) and bigger nodule-like structures, derived from algae (Figure 5.11.7).

Bituminite which is also the common predominant maceral of oil shales and other source rocks (Stach *et al*., 1982) and is considered to have formed from organisms rich in fats and proteins (Teichmuller, 1974; Teichmuller and Ottenjann, 1977) is a characteristic constituent of subaquatic organic matter types. The hydrocarbon-generating capacity of the organic matter contained in bituminite (Figure 5.11.8) and "mineral-bituminous groundmass" is significantly higher than other macerals in liptinite/exinite group (Teichmuller, 1974; Stach *et al*., 1982; Hutton, 1994). However, the bituminite of oil source rocks is undoubtedly the main precursor of petroleum (Hutton *et al*., 1980).

Telalginite-*Botryococcus* colonies appeared well-formed, with an intense yellow colouration under fluorescence (Figure 5.11.9). Some samples contain these algae in different amorphization stages, with greenish to orangish yellow colour under fluorescence mode. The macerals remaining from palynomorph group exhibit a low occurrence, represented by the sporomorph (sporinite; Figure 5.11.10), in a spore-tetrad

Table 5.11.1. Analysis Results of TOC and Rock-Eval Pyrolysis, Kasiro Oil Shales

No.	Sample No. (05)	Location	TOC	S₁	S₂	PY	PI	T_{max}	HI	Error T_{max}
			(%)		mg/g			(°C)		
1.	ES 21		0.72	00.4	0.60	0.64	0.06	434	83	
2.	ES 25		2.61	1.15	4.80	5.95	0.19	458	184	
3.	ES 28		0.06	0.04	0.04	0.08	0.50	NDP	67	570
4.	ES 33B		2.11	0.15	5.70	5.85	0.03	437	270	
5.	ES 36A		3.69	0.24	13.48	13.72	0.02	442	365	
6.	ES 36B		6.50	0.18	43.20	43.38	0.00	514	665	
7.	ES 36D	Keruh	4.86	0.15	31.12	31.27	0.00	449	640	
8.	ES 39B	River	6.82	0.17	10.14	10.31	0.02	436	149	
9.	ES 40A		4.52	0.18	7.56	7.74	0.02	436	167	
10.	ES 41E		3.14	0.13	11.49	11.62	0.01	441	366	
11.	ES 41E1		2.54	0.09	11.19	11.28	0.01	440	440	
12.	ES 41K		5.79	0.27	8.70	8.97	0.03	435	150	
13.	NS 21A		6.72	0.75	25.00	25.75	0.03	436	371	
14.	NS 21C		16.11	1.60	44.40	46.00	0.03	434	275	
15.	NS 22B		8.07	0.91	33.32	34.23	0.03	439	413	
16.	ES 47A		7.29	0.95	45.00	45.95	0.02	443	617	
17.	ES 47B		7.18	1.32	44.14	45.46	0.03	440	615	
18.	ES 47C		3.79	0.66	19.86	20.52	0.03	440	523	
19.	ES 47D	Lepat	10.1	0.97	59.78	60.75	0.02	512	592	
20.	ES 45A	River	3.25	0.38	12.45	12.83	0.03	437	383	
21.	ES 45B		3.68	0.54	12.78	13.32	0.04	436	347	
22.	ES 49A		3.68	0.34	14.12	14.46	0.02	439	384	
23.	ES 49B		8.30	1.86	53.20	55.06	0.03	512	641	
24.	ES 49C		2.49	0.25	8.90	9.15	0.03	438	358	
25.	MH 08A		14.45	4.05	128.16	132.21	0.03	507	887	
26.	MH 10A		14.76	4.78	133.72	138.50	0.03	507	906	
27.	MH 04B		7.55	1.14	62.32	63.46	0.02	447	826	
28.	MH 04C	Sekeladi	3.69	0.23	17.01	17.24	0.01	444	461	
29.	MH 05A		5.81	0.56	48.08	48.64	0.01	442	828	
30.	MH 05E		3.56	0.19	10.56	10.75	0.02	431	297	
31.	NS 40		4.71	0.43	35.76	36.19	0.01	449	760	
32.	NS 41B		2.59	0.73	6.61	7.34	0.10	451	255	
33.	NS 41D	Asai	2.40	0.47	4.44	4.91	0.10	449	185	
34.	NS 46A	Upstream	0.72	0.04	0.56	0.60	0.07	575	78	575
35.	NS 47A		2.16	0.41	2.57	2.98	0.14	449	119	
36.	NS 47C		2.35	0.28	5.86	6.14	0.05	448	249	

Remarks:

TOC : total organic carbon   PI : production index
S1   : T_{max} :
S2   :   HI : hydrogen index
PY   :

form, that are always associated with proximal environments and low-energy conditions with fast sedimentation (Tyson, 1993).

Vitrinite occurring as subangular fragments of telocollinite (Figures 5.11.11 and 5.11.12) are present as small fragments with their minor amount is displayed in Table 5.11.1. Inertinite (Figures 5.11.13 and 5.11.14) which is counted together with vitrinite also appear in a very low amount. The observed inertinite macerals are semifusinite (Figure 5.11.15), funginite (Figure 5.11.16), and probably inertodetrinite most derived from semifusinite. Due to their subangular shape, the inertinite macerals in
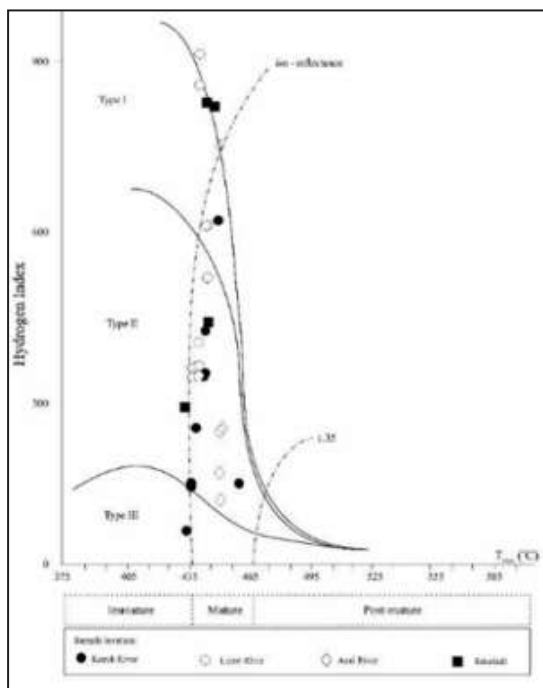
Figure 5.11.1. Diagram of Hydrogen Index vs. T$_{max}$ of Kasiro Oil Shale (Keruh River, Lepat River, Asai River, and Sekeladi areas).
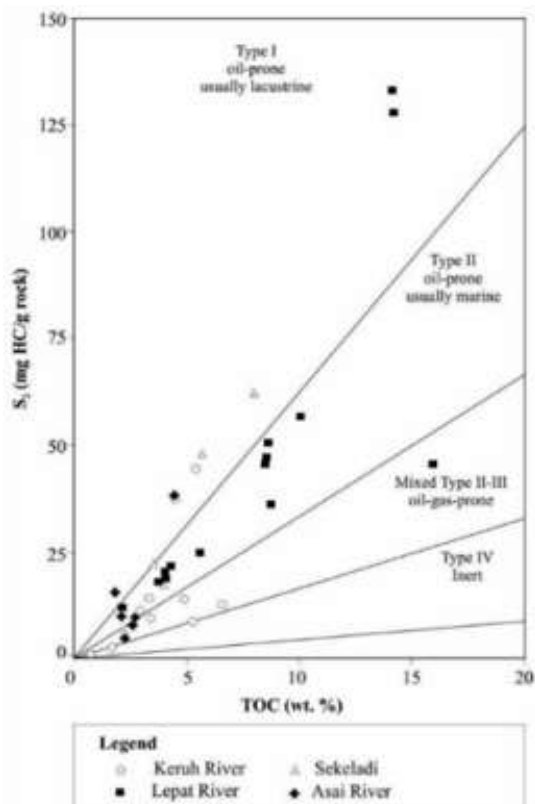

Figure 5.11.3. Graphic of the S$_2$ vs. TOC showing the organic matter richness, kerogene types, and oil possibilities of the Kasiro oil shales, in Keruh River, Sekeladi, Asai Upstream, and Lepat River Regions.
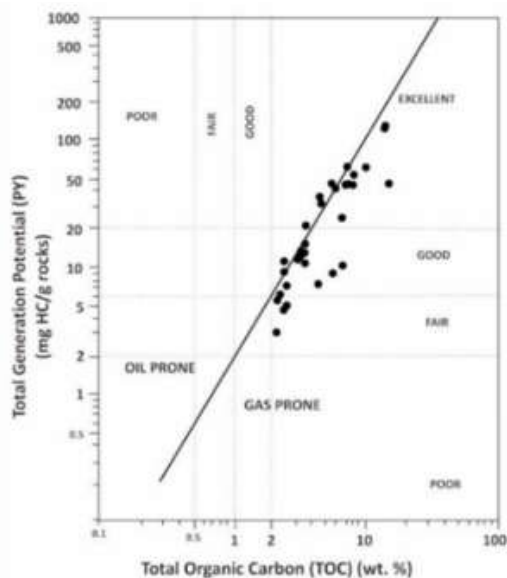
Figure 5.11.2. Plotting TOC vs. PY showing organic matter richness of the Kasiro oil shales.

the study areas only have experienced a short distance transportation.

The presence of vitrinite and inertinite, tends to indicate that the sedimentary environment of the oil shales in the study area has little relation to swamp, but rather, the deepwater environment of lake within relatively anoxic condition.

Additionally, the content and type of exinite maceral, especially alginite contained in the oil shale, and rock characteristic based on SEM analysis, can support the prediction of source rock potential.

Organic material content (TOC) of less than 0.5% is classified as poor, 0.5 – 1.0% fair, 1 – 2% good, 2-4% very good, and > 4% included into
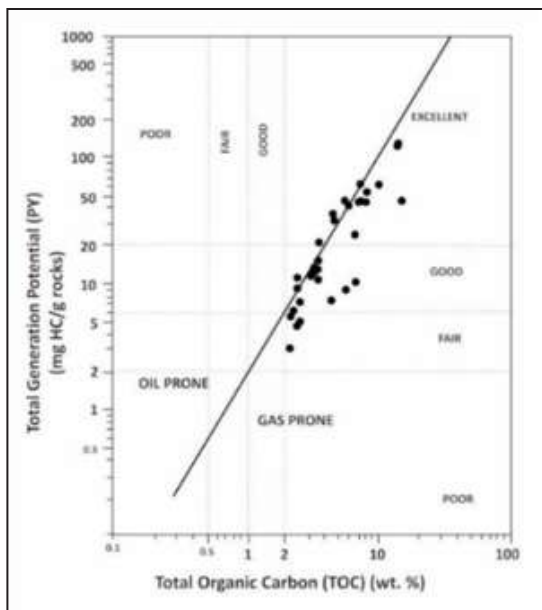
Figure 5.11.4. Plotting TOC *vs.* PY showing organic matter richness of the Kasiro oil shales, in Keruh River, Sekeladi, Asai Upstream, and Lepat River Regions.

Figure 5.11.17. Correlation of some maturation indicators of organic matter (in coal and kerogen) and phases of hydrocarbon generation. (CPI: carbon preference index, PI: production index). These maturation indicators can be also correlated with those shown in Figures 13 and 18. Modified from Hunt (1996).

Figure 5.11.16. SEM photomicrograph of smectite (Sm) containing sporinite (Sp). Magnification X2500. Sample 05UM11A.

Figure 5.11.18. SEM photomicrograph of organic matter of sporinite (Sp) within smectite (Sm). Magnification X4000. Sample 05ES39B.

excellent level. Oil prone category if HI ranges between 200 – 300 will produce hydrocarbon of oil-gas prone, the lower HI (< 200) will produce gas.

6. THERMAL MATURITY

The thermal maturity of an oil shale refers to the degree to which the organic matter has been altered by geothermal heating. If the oil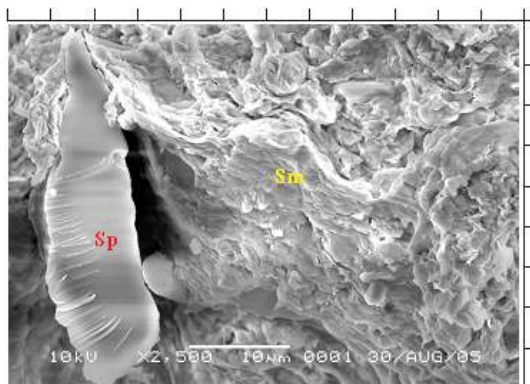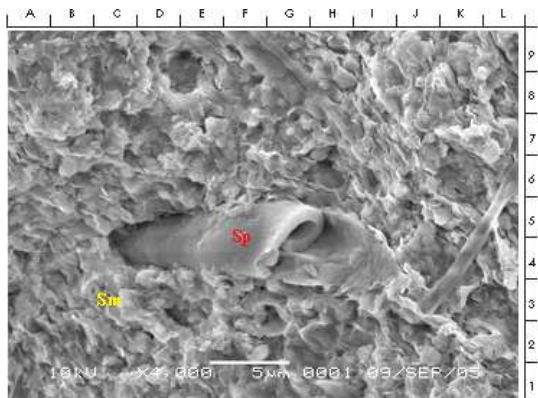 shale is heated to a high enough temperature, as may be the case if the oil shale were deeply buried, the organic matter may thermally decompose to form oil and gas. Under such circumstances, oil shales can be source rocks for petroleum and natural gas. On the other hand, oil-shale deposits that have economic potential for their shale-oil and gas yields are geothermally immature and have not been subjected to excessive heating. Such deposits are generally close enough to the surface to be mined by open-pit, underground mining, or by in-situ methods.

The degree of thermal maturity of an oil shale can be determined in the laboratory by several methods. One technique is to observe the changes in colour of the organic matter in samples collected from varied depths in a borehole. Assuming that the organic matter is subjected to geothermal heating as a function of depth, the colours of certain types of organic matter change from lighter to darker colours. These colour differences can be noted by a petrographer and measured using photometric techniques.

To gain thermal maturity, TOC, Rock-Eval pyrolysis, organic petrography, and GC-MS processes are conducted. Additionally, the SEM analysis is also important to be performed, to obtain the thermal maturity.

Vitrinite reflectance is commonly used by petroleum explorationists to determine the degree of geothermal alteration of petroleum source rocks in a sedimentary basin. A scale of vitrinite reflectances has been developed that indicates when the organic matter in a sedimentary rock has reached temperatures high enough to generate oil and gas. However, this method can pose a problem with respect to oil shale, because the reflectance of vitrinite may be suppressed by the presence of lipid-rich organic matter.

6.1. Kabanjahe Sub-basin

Tmax obtained from Rock-Eval Pyrolysis (Table 6.1.1) shows value between $380 - 461o$ C, which tend to indicate mature to late mature stage. Then, PI value varies from $0.11 - 0.78$. This condition showing thermal maturity level of kerogen contained in the sediments also belongs to late mature stage, support the Tmax characteristic. However, the dominant Tmax values range from $436 - 4450C$ indicate that they are in the early part of the effective oil window that corresponds to the beginning of the generation of hydrocarbons which can escape and migrate.

On the basis of vitrinite reflectance mainly varying from 0.74 % to 1.98 %, essentially, almost all the organic matter contained in the Upper Member of the Butar Formation has a high thermal maturity (Table 6.1.2). However, Penampen and Sarinembah areas are characterised by low vitrinite reflectances (0.20 - 0.38 %) tending to show a thermally immature or low thermal maturity condition. Moreover, medium vitrinite reflectance values ranging between 0.54 to 0.56 %, that are observed in Laubuluh area, tend to exhibit a transition from thermally immature to early mature or medium thermal maturity condition. The organic matter might be included into type III kerogen (gas-prone type).

Additionally, SEM analysis result indicates that authigenic clay minerals, with smectite-illite matrix, and micritic calcite cement are present. Clay minerals (< 10%) forming sediments are dominated by quartz with the combination of smectite-illite, with illite and kaolinite. Foraminifera fossil is detected. The presence of smectite-illite, illite, kaolinite, and compaction tends to indicate that the sediments have undergone a diagenetic process within Late Eodigenesis to Late Mesodiagenesis.

The presence of authigenic mineral, based on Burley et al. (1987) falls under Mudrock Diagenesis Stage that is equivalent to Early Mesogenetic stage of Schmidt and Mc Donald (1979). This diagenesis process occurred within paleotemperature up to 65o C which was buried around 1000 m deep.

Table 6.1.1. Rock-Eval Pyrolysis Data of the Butar Sediments

No	Location	Sample No. (02)	Lithology	TOC (%)	S1	S2	PY	PI	Tmax (°C)	HI
						kg/t				
1	Penampen	RH.03A	Sh,dkgy/blk,calc	0.71	0.37	0.32	0.69	0.54	461	45
2		RH.03B	Sh,dkgy,sl,weathered	0.18	0.08	0.10	0.18	0.44	TDD	56
3	Juhar	RH.04A	Clst,ltgn-gy,weathered	0.07	0.00	0.08	0.08	0.00	TDD	114
4	Sarinembah	RH.06A	Clst,dkgy,calc	1.71	0.75	2.00	2.75	0.27	450	117
5		HR.13A	Clst,dkbrn/dkgy,sl,oxd	0.12	0.13	0.15	0.28	0.46	TDD	125
6	Laubuluh	HR.14A	Clst,brn/dkgy, sl,oxd	0.09	0.01	0.08	0.09	0.11	TDD	89
7		HR.14B2	Clst, dkkgy/blk, calc	0.17	0.04	0.20	0.24	0.17	TDD	118
8		HR.14C	Clst, dkgy/blk	1.74	0.63	1.02	1.65	0.38	380	59
9	Kutabangun	NS.11	Clst,gngy,yell/red,oxd/weath	0.07	0.03	0.02	0.05	0.60	TDD	29
10	Kutambarupunti	NS.14	Clst, dkbrn/dkgy, slty.	0.08	0.02	0.04	0.06	0.33	TDD	50
11		NS.15B	Clst,gy/dkgy,lam, sl,oxd	0.08	0.05	0.04	0.09	0.56	TDD	50
12		NS.15C	Clst,gy/dkgy/lam w/sltst	0.06	0.02	0.02	0.04	0.50	TDD	33
13		NS.16A	Clst,dkgy,oxidised	0.07	0.02	0.03	0.05	0.40	TDD	43
14	Butar	NS.16B	Clst, dkgy, sl,oxidised	0.09	0.05	0.02	0.07	0.71	TDD	22
15		NS.17A	Clst, dkgy	0.08	0.04	0.02	0.06	0.67	TDD	25
16.		NS.19A	Sh, dkgy/blk	0.09	0.07	0.02	0.09	0.78	TDD	22
17.		NS.19B	Sh, dkgy/blk	0.07	0.08	0.08	0.16	0.50	TDD	114

Notes : TDD = Undetected
TOC : total organic carbon   PY : pyrolysis yield (S1+S2)   HI : hydrogen index
S1   : free HC   PI : production index
S2   :   Tmax : maximum temperature

6.2. Kapur IX

Peter and Cassa (1994) stated that vitrinite reflectance (Rv) is used to be one of thermal maturity parameter. The Rv value obtained from organic petrographic analysis is highly recommended to be supported by the Tmax value got from Rock-Eval Pyrolysis. According to the results of organic petrographic analysis on six samples of Kapur IX, their vitrinite reflectance values vary from 0.22 – 0.40 %, whilst on the basis of rock-eval pyrolysis, the Tmax values range between 435 – 440O C. Those both thermal maturity measurements are concomitant each other, showing a strong positive correlation that the thermal maturity of oil source rock of Kapur IX falls in an immature to early mature category.

6.3. Kebuntinggi Sub-basin

Evaluation on Rock-Eval Pyrolysis (Tmax) data, shows that oil shale of the Kebuntinggi area is thermally immature to marginally (early) mature. Tmax values are commonly present between 436 - 471oC (Table 5.3.1). However, the dominant Tmax values range from 436 - 4450C indicate that they are in the early part of the effective oil window that corresponds to the beginning of the generation of hydrocarbons which can escape and migrate.

Furthermore, vitrinite reflectance values indicate that the whole analysed samples are immature throughout the basin. Most mean vitrinite reflectance values ranging from 0.14 to 0.41 % averaged- 0.30 %, (Table 5.3.2) are situated beyond the oil "birth" line. However, some samples having a slightly higher reflectance (0.37 - 0.41 %) tend to indicate that they are located close to the oil "birth" line. Moreover, PI (hydrocarbon potential index) values varying from 0.01 – 0.12 are situated within an immature – early mature level. Thereby, overall, vitrinite reflectance agreeing with Tmax values, are also in concomitant with the PI values. Based on the Foscolos et al.'s

chart (1976), the oil shales are situated within the eodiagenetic stage.

6.4. Kuansing Sub-basin

A diagram of Hydrogen Index (HI) versus Tmax as shown in Figure 4.4.1 indicates that six samples are included into the immature category, whereas eight samples are in a mature category. Samples included to both immature and mature categories are mostly located in the area close to the boundary between immature and mature level, whereas only one sample located in the area which close to the boundary between mature and post mature. This diagram indicates that source rock samples of the Keruh Formation are present as a late immature to early mature condition.

Based on the Maturation Range Chart from Demaison and Moore (1980), the oil window or the maturation of hydrocarbon starts at the mean value of the vitrinite reflectance (Rv) at 0.50%.

The vitrinite reflectance value from Keruh shale/mudstone source rock samples shows that the mean value ranges from 0.19 to 0.66% (Table 6.4.1), whereas the vitrinite reflectance from the coal seams indicates the mean value between 0.39 and 0.56% (Table 5.4.2). Based on the vitrinite reflectance of shale/mudstone samples, two samples (03RH15J and 03RH17F) show the vitrinite reflectance value more than 0.50%, but they have the Pyrolysis Yield (PY) of 0.43 kg/ton rock and 2.57 kg/ton rock (Table 5.4.3). These conditions indicate that hydrocarbon derived from these samples have already changed into gas, which is also indicated by their Potential Index (PI) less than 0.1 (Table 5.4.4).

6.5. Ombilin Basin
6.5.1. Sangkarewang Formation

Thermal maturity evaluated from Rock-Eval Pyrolysis (Tmax) and vitrinite reflectance

Table 6.4.1. Result of Maceral Analysis of Shale Samples of the Keruh Formation, Kuansing, showing Vitrinite Reflectance Values

| No | Sample No. (03) | Maceral (%) | | | | | | | | | Area |
		Res	Cu	Lipt	Alg	Bit	E	Rv min	Rv max	Rv	
1.	ES 16 L	2,4	-	1,6	1,2	-	5,2	0,19	0,40	0,25	Makarya
2.	ES 16 M	0,8	-	-	0,4	0,4	1,6	0,36	0,53	0,45	Makarya
3.	ES 16 N	0,2	-	-	-	-	0,2	0,22	0,37	0.27	Makarya
4.	NS 16 A	0,6	-	-	-	0,4	1,0	0,41	0,43	0,42	NusaRiau
5.	NS 16 C	0,8	-	0,4	0,4	-	1,6	-	-	-	NusaRiau
6	NS 16 E	0,6	-	-	-	-	0,6	0,40	0,53	0,46	NusaRiau
7.	NS 19 A	-	-	-	-	-	-	0,41	0,56	0,49	NusaRiau
8.	NS 19 D	0,2	0,4	-	-	0,2	0,8	0,23	0,29	0,26	NusaRiau
9.	RH 15 E	0,2	-	-	-	-	0,2	0,28	0,49	0,38	Manunggal
10.	RH 15 G	-	-	-	-	-	-	0,34	0,48	0,42	Manunggal
11.	RH 15 J	0,4	-	0,6	-	0,4	1,4	0,48	0,61	0,57	Manunggal
12.	RH 17 F	-	-	-	-	-	-	0,60	0,70	0,66	Manunggal
13.	ES 13 A	2,8	-	-	4,6	-	7,4	0,31	0,58	0,47	Prk.TBS
14.	ES 13 H	1,2	-	-	1,2	2,4	4,8	0,33	0,37	0,35	Prk.TBS
15.	RH 12 A	-	-	-	-	-	-	0,12	0,26	0,19	Prk.TBS
16.	RH 13 C	1,6	0,4	0,8	0,4	0,6	3,8	0,26	0,38	0,35	Prk.TBS
17.	NS 13 A	0,6	-	-	0,4	0,8	1,8	0,24	0,37	0,30	Sitiung
18.	RH 13 C	1,6	0,4	0,8	0,4	0,6	3,8	0,26	0,38	0,35	Sitiung

Remarks:

Res : resinite   Alg : alginate   Rv max. : Maximum vitrinite reflectance
Cu : cutinite   Bit : bitumen   Rv   : Mean vitrinite reflectance.
Lipt : liptodetrinite   E   : exinite
Rv min : Minimum vitrinite reflectance

(%Rvmax) data, show that oil shale of the Sangkarewang Formation is thermally immature to marginally (early) mature. Tmax values are usually less than 445oC (Table 6.5.1). However, the Tmax values of some samples, which range between 446 - 4530C indicate that they are in the early part of the effective oil window that corresponds to the beginning of the generation of hydrocarbons which can escape and migrate (Figure 6.5.1).

Vitrinite reflectance indicates that the whole analysed samples are immature throughout the basin. Most mean vitrinite reflectance values ranging from 0.17 to 0.32 % (Table 6.5.2) are situated beyond the oil "birth" line. However, some samples have a slightly higher reflectance (0.36 - 0.40 %) indicating that they are located close to the oil "birth" line (Figure 6.5.2). Moreover, PI (hydrocarbon potential index) values present of <0.1 indicate an immaturity level. Thereby, overall, vitrinite reflectance agreeing with Tmax values, are also in concomitant with the PI values. Based on the Foscolos et al.'s chart (1976), the oil shales are situated within the Eodiagenetic stage.

Additionally, from SEM analysis data, the diagenesis level of Sangkarewang oil shale falls under the Late Eodiagenesis - Early Mesodiegenesis level, where the oil shale deposit has been burried around 1000 m in depth (Table 6.5.3).

6.5.2. Sawahlunto Formation

Thermal maturity evaluated from Rock-Eval pyrolysis (Tmax) data, shows that oil shales of the Sawahlunto Formation are thermally immature. Tmax value analysed is 438o (Table 4.5.1), and it indicates that the oil shale is in-between the late immature to beginning of the oil window. The PI values analysed (Table 6.5.1) tend to show that the oil shales are in an immature level, due to their values that are less than 0.1. Those two data display that the stage of the oil shale are immature.

6.6. Kiliranjao Sub-basin

Thermal maturity evaluation is gained from Rock-Eval pyrolysis (Tmax) and vitrinite reflec-

tance (% Rvmax) data. The Tmax values of Kiliran oil shale samples, varying from 431 - 432o C (Tables 6.6.1 and 6.6.2), show that the formation is thermally immature. Throughout the sub-basin, the oil shale samples, indicating by vitrinite reflectance values, are in an immature stage, with an exception (Figure 6.6.1). Most vitrinite reflectance values range from 0.20 to 0.26 %, and these values fall beyond the oil "birth" line occupying the non-onset oil zone (Figure 6.6.2). The sample 01NS.14i has a slightly higher reflectance indicating that it is close to the oil "birth" line, although still within the non-onset oil area. The PI values of the samples that are less than 0.1 (Tables 6.6.1 and 6.6.2), indicate that the Kiliran oil shales are situated within an immature stage. Overall, the vitrinite reflectance agrees with the Tmax, and PI values. Due to their Romax values (<0.4 %), according to the Foscolos et al.'s chart (1976), the oil shales had undergone an eodiagenetic process.

Moreover, SEM analysis indicates that the diagenesis level of the Kiliran oil shale is situated on Late Eodiagenesis - Early Mesodiegenesis level, where the oil shale deposit has been burried around 1000 m in depth (Table 6.6.3). This condition is concommittant with pyrolysis and organic petrographic data, showing the Late Eodiagenesis – Early Mesodiagenesis level.

6.7. Bukit Susah Sub-basin

Petrographic analysis indicates that organic matter content of 18 oil shale samples (Table 6.7.1) is dominated by exinite maceral group (0.4 – 3.0 %). comprising alginite (0.4 – 0,6 %), resinite (0.4 – 2.0 %), sporinite (0.4 – 0.8 %), suberinite (0.4 – 2 %), cutinite (0.6 – 1.4 %), and exsudatinite (0.2 – 0.6 %). Vitrinite amount detected is 0.6 – 7.6 %. Carbonate 0.8 – 24.2 %, and pyrite (0.8 – 16.0%). Maximum vitrinite reflectance value varies between 0.31 and 0.52 %, with mean average from 0.27 to 0.43 %; mainly occupy area of Rvmax 0.50%. This reflectance value suggests that the thermal maturity of oil shale is situated in an immature level.

Generally, SEM and XRD analyses indicate

that quartz is present as the main (11 - >70 %) (Table 6.7.2; Figures 6.7.1 and 6.7.2)) Clay minerals (< 10%) forming shale is dominated by the combination of smectite-illite, with illite and kaolinite. The others are biotite, feldspar, crystobalite, hematite, siderite, and framboidal pyrite (< 10%). Laumantite as zeolite-mineral also occurs; oil trace or bitumen is detected. The presence of smectite-illite, illite, kaolinite, laumontite, and chlorite tends to indicate that the oil shale has undergone diagenetic process within early mesodiagenesis level (Susanto et al., 2004).

Rock-Eval analysis data of seven oil shale samples, as plotted on Figure 6.7.3, are located close to immature - mature level line equivalent to oil-birth line. On the other hand, other eleven shale samples occur within the immature area. However, those samples tend to occur nearby the boundary line between immature – mature level. It can be concluded that Bukit Susah oil shale samples tend to be situated within an immature level.

Leythaeuser et al. (198) stated that, in general, oil originated from type-I kerogen occupies the area of Rvmax 0.50%, whilst type II kerogen on Rvmax 0.55%. This condition is supported by the value in Maturation Range Chart of Demaison and Moore (1980), showing that the oil maturity is started on mean vitrinite reflectance (Rv) of 0.50 %. Therefore, reflectance analysis of 18 Bukit Susah oil shale samples exhibiting the Rvmax values of 0.29 to 0.56 %, which only two shale samples having Rvmax >0.56 %, tends to indicate the position of thermal maturity of oil shale is still beyond oil birth line that is equivalent to an immature degree. This characteristic is also supported by value of PI of < 0.1.

6.8. East Tigapuluh Mountains

Vitrinite reflectance of the Lakat clastics, in this area, varies from 0.29 – 0.38 %. Based on Kantsler et al. (1978), organic maturity of the sediments is categorized as immature level, with maximum paleotemperature of less than 60o C, buried at depth of < 1500 m. (Tables 6.8.1 and

6.8.2).

Tmax value of the sediments being < 435o C, tend to indicate maturity of kerogen contained is included into an immature degree; whilst the others having value of 435o to 465o C, their kerogen falls under mature to post-mature level (Figure 6.8.1).

Scanning Electron Microscopy analysis show that the sediments analyzed consist of rare smectite-illite and smectite (Table 6.8.2). The other substances are vitrinite and alginite. The appearance of authigenic mineral (Figure 6.8.2), based on Burley et al. (1987) falls under Mudrock Diagenesis Stage-1 that is equivalent to Early Mesogenetic stage of Schmidt and Mc Donald (1979). This diagenesis process occurred within paleotemperature up to 65o C which was buried at 1500 m deep.

6.9. Bukit Bakar

6.10. Sinamar

6.11. Asai-Rawas

Rock-Eval data on eight samples show Tmax varying between 434 – 442o C; 2 of them are 449o C and 458o C, 1 sample is 514o C, and the rest is not able to be detected (Table 6.11.1). Then, hydrogen index (HI) from 83 – 665, whilst PI (production index) generally <0.10 (0.00 – 0.06) except samples 05ES25 (0.19) and 05ES28(0.50). These characteristics tend to indicate that the thermal maturity of Kasiro oil shales falls under late immature to early mature level (Figure 6.11.2).

Two levels of Tmax are recognized in the Sekeladi oil shale samples, those varying from 444 – 447oC and 507oC. Those values are situated within mature degree. However, PI (production index) value averaged < 0.10, ranging between 0.01 – 0.03 shows the immature level.

From Asai Upstream area, Renahpisangkemali region, six shale samples were analyzed (Table 6.11.1). In general, Tmax value ranges between 448 – 451oC, except 1 sample having Tmax value of 575oC. Then, PI (production index) value var-
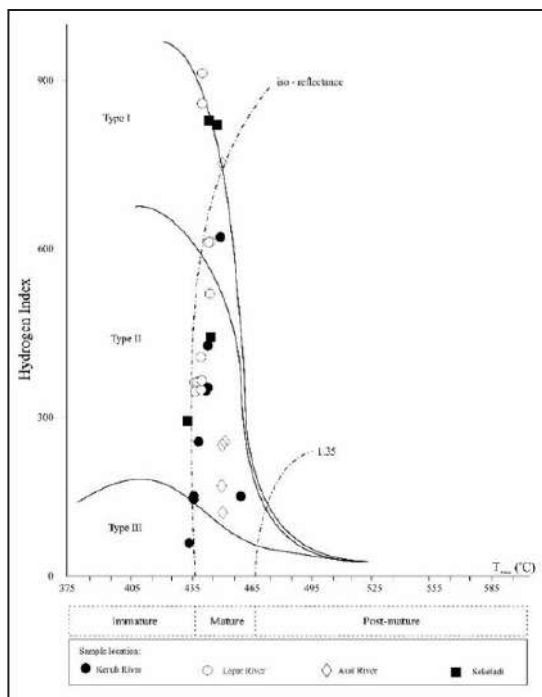
Figure 6.11.1. Diagram of Hydrogen Index (HI) vs. Tmax of Kasiro Oil Shale (Keruh River, Lepat River, Asai River, and Sekeladi areas) showing kerogen type and thermal maturity level of the source rocks.

ies from 0.01 – 0.14. This characteristic coincides with the Sekeladi shales, which falls under an immature degree.

Of 18 Sungai Lepat oil shale samples analyzed, in general, Tmax ranges between 431 – 443oC, except on samples 05ES47D and 05ES49B the value of their Tmax is 512oC. Moreover, a value PI (production index) is < 0.10, varying from 0.01 – 0.04.

Based on Tmax value, in general, varying from 435 to 449oC, supported by %Rv (0.60 – 0.70%) (Suwarna, 2004b), and PI values, the thermal maturity of oil shale of the Kasiro Formation is situated within late immature to early-middle

mature or oil window category. However, some samples are included into mature to post mature category. Furthermore, SEM analysis reveals that diagenesis level of the Kasiro oil shale is situated on the Early Mesodiegenesis level, where the oil shale deposit has been burried around 2000 m in depth (Table 6.11.2). This condition is concommittant with pyrolysis and organic petrographic data, showing late immature to early mature level similar to Late Eodiagenesis – Early Mesodiagenesis level.

Additionally, the PI (production index) value generally < 0.10, tends to show an immature thermal maturity. However, some Tmax values are not concomitant with PI condition. According to Foscolos et al. (1976), diagenesis level of oil shale studied is situated within Late Eodiagenesis position.

Furthermore, SEM data (Table 6.11.1) also indicates that oil shale diagenetic level falls in Late Eodiagenesis to Early Mesodiagenesis category; and oil shale deposits have been buried within 2000 m deep. This diagenetic level coincides with organic petrographic and pyrolysis results showing Late Eodiagenesis - Early Mesodiagenesis category.

Coal intercalations of 0.5 – 1.0 m thick is recognized in the Kasiiro Formation, which lithotipically includes into banded to bright banded type. The coal is rich in vitrinite-A content of 14.7 – 77.6%) and vitrinite-B ranging from 18.0 – 56.6%. The range of vitrinite reflectance is 0.75-0.95% dan 0,54-0,80% (Suwarna, 2004). According to their high vitrinite reflectance values, the source rock is fall into oil window level (Figure 6.11.2).

The thermal maturity of Kasiro Formation has reached oil window level (Figure 6.113), proven by their Rv rank and fluorescence colour range of exinite maceral, varying from amber to light brown colour.

7. POTENTIAL AND DISCUSSIONS

The quality and type of organic matter which provide the source rock potential of Eo-Oligocene oil shales of the Sangkarewang (Ombilin, Kebuntinggi, and Kapur IX areas), Keruh (Kuansing), Kiliran (Kiliranjao), Lakat and Kelesa (Tigapuluh Mts.and Bukit Susah), Sinamar, Bukit Bakar,and Kasiro (Asai – Rawas) Formations were evaluated by geochemical techniques including Rock-Eval Pyrolysis, GC-MS, and also by organic petrography, supported by SEM-XRD analyses. The summary result of analyses is presented later.

Hydrocarbon utilization is one of highlight of Indonesia's energy diversification policy to projected decline in crude oil production. Therefore, to anticipate the increasing demand, additional data and information on unconventional fossil fuels must increase in finding alternative energy sources to crude oil as well as promote innovative utilization of hydrocarbon. Thus, information on oil shale (shale oil) is one of the probable efforts in intensifying the national energy resources.

The result of TOC on many samples of shales from ten areas in Sumatra (Kapur IX, Kuansing, Kebuntinggi, Ombilin, Kiliranjao, Bukitsusah, East Tigapuluh Mts., Bukit Bakar, and Asai-Rawas) illustrates that it has a range from 0.20% to 25.42 % corresponding to a fair up to excellent category of source rock characterization (Tissot and Welte, 1984; Bordenave et al.,1992). The T_{max} value varies from 424 to 451° C. The hydrogen index (HI) for all samples shows a variety of values of 126-946, and pyrolysis yield (PY) ranges from 8.42 to 148.09 mg HC/g rock, with production index (PI) commonly less than 0.10. On the basis of HI versus T_{max} plotting, the kerogen present is suggested to be situated in Type II and Type I with minor Type III (Figure 7.1). The diagram also illustrates that there are two main groups of kerogen types. One is the group of Type II and I that are samples of oil shale rocks derived from Kuansing, Kiliranjao, Ombilin and Asai Rawas areas. The second one is the group of Type II and

III that are largely found in the East Tigapuluh Mountains, Bukit Ssusah, and Kebuntinggi.

Thermal maturity of the oil shales is positioned in the immature to marginally mature stage (Figure 7.1), although the samples of oil shales collected from Ombilin, East Tigapuluh Mountains, Kebuntinggi, Kuansing and Asai-Rawas regions appear to be situated in the early mature zone. On the other hand, the immature stage is found in samples from the Kiliranjao and Bukitsusah regions. Nevertheless, there is a concomitance in a thermal maturity level analysis by using both T_{max} and vitrinite reflectance value. Due to their Romax values (<0.4 %), according to the Foscolos et al.'s chart (1976), the oil shales had undergone an eodiagenetic process. On the basis of SEM analysis mode, diagenetic level of the oil shale occupies a late eodiagenetic position. Thereby, overall, vitrinite reflectance agreeing with T_{max} rates, are also in concomitant with the PI $(production$ $index)$ values.
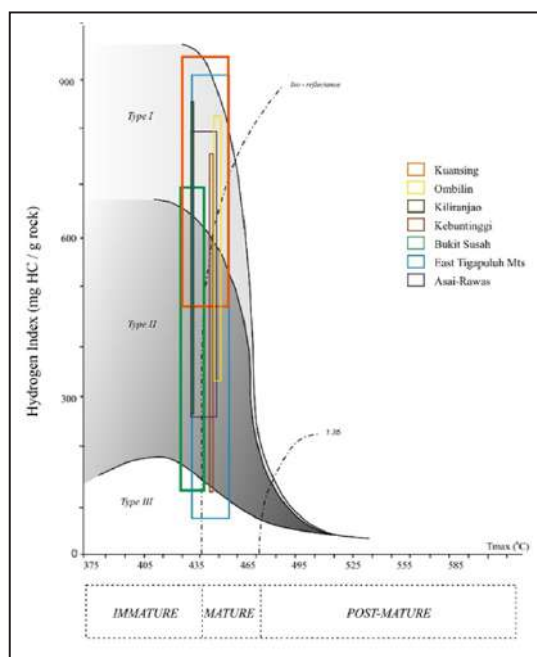

Figure 7.1. Hydrogen Index (HI) vs. Tmax diagram, indicating thermal maturity and kerogen type of oil shale sequence in the selected study areas of Sumatra.
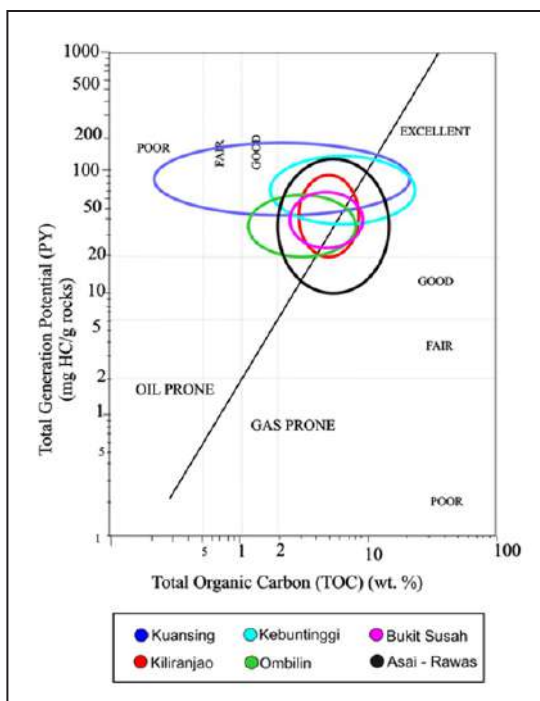
Figure 7.2. Crossplot of TOC vs. Pyrolysis Field (PY), showing hydrocarbon potential of oil shale sequences in the selected sites of Sumatra.

By plotting the TOC and PY values on the Rad diagram (1984), the majority of oil shales are situated within "oil to gas prone" areas on the fair to excellent level (Figure 7.2). Samples of oil shales collected from Kuansing, Ombilin, Kiliranjao and Bukitsusah regions appear to be positioned to more oil prone rather than gas prone, whilst other samples are in gas prone area. This condition is also presumed to have a high *shale gas* potential, also tending to show potential of *oil-gas prone*. The kerogen is mainly included into Type II of autochthonous materials those are alginite, exsudatinite, and suberinite; with minor Type I of allochthonous substances those associated with sporinite, vitrinite, and inertinite of floral/humic origin.

By evaluating all the results of geochemical and organic petrological analyses conducted on shaly rocks (shale and mudstone), it can be concluded that the oil shales in those areas are favorable potential for shale oil or gas to include the alternating energy resources in the future. Additionally, all oil shale measures in Sumatera are strongly assumed to be good potential for source rock of petroleum.

In terms of their maceral compositions and kerogen types, the Sangkarewang oil shale exposed in the areas of Ombilin and Kebuntinggi (the intra-montane Ombilin Basin and Kebuntinggi Sub-Basin) is comparable to the Kiliran sample found in the Kiliranjao area (inter-montane Kiliranjao Sub-Basin; Suwarna *et al*., 2001) as well as to the Keruh Formation in the Kuansing area. Most of the oil shale sequence is typically of an organically rich-succession and consists of predominantly well-bedded, laminated and fissile, brownish to dark grey organic-rich shale and mudstone rocks.

Some shale found in Kiliranjao appears to have a spongy character. In these areas, the oil shale consists of exinite group (2.0 - 40.0%), comprising lamalginite of 0.4 - >40%, with minor cutinite, resinite, (?) phytoplankton, liptodetrinite, sporinite, and bituminite that varies from ≤ 0.1 - 2.9 %, and rare *Botryococcus*-telalginite (Kusumahbrata & Suwarna, 2003; Rudistyan, 2005). Therefore, the oil shale deposits can be described as "lamosites". Weakly fluorescent matrix is evident in most fine-grained samples, indicating the presence of hydrogen-rich organic matter (Robert, 1981; Bustin *et al*., 1985). Minor amounts of vitrinite macerals, < 0.1 % - 10.0 % and very rare inertinite are also recognized. The vitrinite recognized has a granular appearance with micropores and fissures that are characteristics of oxidation (Bustin *et al*., 1985). Mineral matter present comprises pyrite, clay minerals, and iron-oxides. Some framboidal pyrites are commonly occurrs. The majority of oil shale beds in these areas are present in typical siliciclastic sedimentary sequences that are dominated by organically rich-successions accumulated in an anoxic to restricted freshwater conditions in a deep-water to marginal lacustrine basin.

The oil shale beds observed in the Bukit Susah area, East Tigapuluh Mountains and Asai-Rawas area are presentin namely the Eo-Oligocene aged Kelesa , Lakat, and Kasiro formations, respectively. The oil shale beds comprise shale and mudstone rocks that are commonly well-bedded and laminated with some massive, light brown to brownish grey and grey in colored.

Quantitatively, the organic matter contained in the shale and mudstones in the Bukit Susah area comprises typically vitrinite and exinite macerals in similar amounts, ranging between 0.6 – 5.0% and between 0.4 – 3.0%, respectively. However, minor samples contain a higher vitrinite proportion (7.5 %) compared to the exinite content. The exinite group comprises sporinite (0.4 – 0.8%), suberinite (0.4 – 2.0%), cutinite (0.6 – 1.4%), alginite (0.4 – 0.6%), and exsudatinite (0.2 – 0.6%), occurrinng in a similar amount in the East Tigapuluh Mountains, where the shale and mudstone beds contain organic matters predominantly of algae of typical lamalginite, with minor vitrinite. A very minor amount of probable *Botryococcus* telalginite is also recognized. The organic matter of oil shale beds found in the Asai-Rawas area comprises the alginite sub-maceral of a lamalginite type varying from 2.4 – 30%. However, the occurrences of a significant amount of telalginite (0.6 – 4.0%), with liptodetrinite (0.8 – 4.0%), bituminite (0.2 – 2.0%), and resinite (0.3 – 1.0%) are also recognized.

Moreover, due to the abundances of lamalginite content within the shale and mudstone beds in these areas, accordingly they can be classified as lamosite type that is suggested to have been deposited in an an-aerobic (anoxic) lacustrine environment. However, the occurrence of a marine incursion may also be suggested by the presence of significant amounts of framboidal pyrites (0.6 – 4.0%). The occurrence of bitumen or bituminite within the rock is indicated by the appearance of a matrix (*groundmass*) showing a weak fluorescence.

The result of TOC analyses on many samples of shale lithologies from seven areas in Sumatera (Kuansing, Kiliranjao, Kebontinggi, Ombilin, Bukitsusah, East Tigapuluh Mts. and Asai-Rawas) illustrate that the shale have a range from 0.20% to 25.42 % corresponding to a fair up to excellent category of source rock characterization (Tissot & Welte, 1984; Bordenave *et al*.,1992). The T_{max} value varies from 424°C to 451 C. The hydrogen index (HI) for all samples shows a range of values from 78-946, and pyrolysis yield (PY) ranges from 8.42 mg HC/g rock to 186.75 mg HC/g rock with a production index (PI) commonly less than 0.10. On the basis of the HI versus T_{max} plot the kerogen present is suggested to be of mixed Type II and Type I category with minor Type III (Figure 7.1). The diagram also illustrates that there are two main groups of kerogen types. One is the group of Type II and I that are samples of oil shale rocks derived from Kuansing, Kiliranjao, Kebuntinggi, Ombilin and Bukit Susah. The second one is the group of Type II and III kerogens that are largely found in the Tigapuluh Mountains and Asai - Rawas.

Thermal maturity of the oil shales is indicated to be in the immature to marginally mature stage, although the samples of oil shales collected from the Ombilin, East Tigapuluh Mountains, Kebuntinggi, Kuansing and Asai-Rawas regions appear to be situated in the early mature zone. On the other hand, the immature stage is found in samples from the Kiliranjao and Bukitsusah regions. Nevertheless, there is a consistenvy in the thermal maturity level results by using both T_{max} and vitrinite reflectance value. Due to their Ro*max* values (<0.4 %), according to the Foscolos *et al*.'s chart (1976), the oil shales have undergone an eodiagenetic process. On the basis of SEM analysis, the diagenetic level of the oil shale occupies a late eodiagenetic position. Thereby, overall, vitrinite reflectance agreeing with T_{max} rates, are also consisten with the PI (*production index*) values.

By plotting the TOC and PY values on the Rad diagram (1984), the majority of oil shales are situated within "oil to gas prone" areas at the fair to excellent level (Figure 7.2). Samples

of oil shales collected from Kuansing, Ombilin, Kiliranjao and Bukitsusah regions appear to be positioned to being more oil prone rather than gas prone, whilst other samples are in the gas prone area. This condition is also presumed to have a high *shale gas* potential, also tending to show potential of being *oil and gas prone*. The kerogen type is represented mainly by Type II & I autochthonous materials such as alginite, exsudatinite, and suberinite; with minor Type III of allochthonous substances represented by sporinite, vitrinite, and inertinite of floral/humic origin.

By evaluating all the results of geochemical and organic petrological analyses conducted on shale lithologies (shale and mudstone), it can be concluded that the oil shales in those areas have favorable potential for generation of shale oil or gas to be included as alternative energy resources in the future. Additionally, all oil shale measures in Sumatera can be strongly assumed to have good potential for source rocks of petroleum.

Alternative hydrocarbon utilization is one of the highlights of Indonesia's energy diversification policy to adress the projected decline in crude oil production. Therefore, to anticipate the increasing energy demand, additional data and information covering unconventional fossil fuels must be acquied to promote the usage of alternative energy sources to crude oil as well as promoting innovative utilization of hydrocarbons. Thus, information on oil shale (shale oil) is one of the probable efforts needed in intensifying the national energy resources.

Related to the presence of organic materials, SEM data show the occurence of telalginite and lamalginite, oil droplets, and bitumen, as the source materials of oil source rock. This condition support the evaluation result of TOC, Rock-Eval Pyrolysis, and organic petrology, that the oil shale studied is a potential source rock.

SELECTED BIBLIOGRAPHY

Adiwidjaja, P. and De Coster, G. L. (1973). Pre-Tertiary paleotopography and related sedimentation in South Sumatra. *Indonesian Petroleum Association, Proceedings of the 2nd Annual Convention*, 2, p. 89–104.

Andersson, Astrid and others, 1985. The Scandinavian alum shales: *Sveriges Geologiska Undersökning, Avhandlingar Och Uppsatser* I A4, Ser. Ca, nr. 56, 50 pp.

Bai, Y., Liu, Z., George, S.C., and Meng, J., 2022. **A** Comparative Study of Different Quality Oil Shales Developed in the Middle Jurassic Shimengou Formation, Yuqia Area, Northern Qaidam Basin, China. *Energies*, 15 (3), 1231. DOI: 10.3390/en15031231

Barber, A. J., 2000. The origin of the Woyla Terranes in Sumatra and the Late Mesozoic evolution of the Sundaland margin. *Journal of Asian Earth Sciences*, 18, p.713–738.

Barber, A. J. and Crow, M. J., 2003. Evaluation of Plate Tectonic model for the development of Sumatra. *Gondwana Research*, 20, p.1–28.

Barber, A.J. and Crow, M.J., 2005. Structure and structural history. In: Sumatra, Geology, Resources and Tectonic Evolution. *Geological Society Memoir*, 31, p.175–233.

Barber, A. J., Crow, M. J. and Milsom, J. S., 2005. Sumatra: Geology, Resources and Tectonic Evolution. *Geological Society Memoirs*, 31.

Bauert, Heikki, 1994. The Baltic oil shale basin: an overview. *Proceedings, 1993 Eastern Oil Shale Symposium*, University of Kentucky Institute for Mining and Minerals Research, p. 411-421.

Bertrand, R., 1993. Standardization of solid bitumen reflectance to vitrinite in some Paleozoic sequences of Canada. *Energy Sources*, 15, p.269-287.

Bertrand, Ph., Bordenave, M.L., Brosse, E., Espitalié, J., Houzay, J.P., Pradier, B., Vandenbroucke, M., Walgenwitz, F., 1993. Other methods and tools for source rock appraisal. *In*: Bordenave, M.L., (Ed.). Applied Petroleum Geochemistry. Ed. Technip. Paris. Chapter II. 3, 279-371.

Bissada, K.K., 1979. *Definitions of organic geochemical terms*. Prepared by Texaco Inc., Bellaire Research Laboratories.pp.

Bishop, M. G., 1988. Clastic depositional processes in response to rift tectonics in the Malawi Rift, Malawi, Africa: *Master's Thesis*, Duke University. 122pp.

Bishop, M. G., 2001. South Sumatra Basin Province, Indonesia: The Lahat/Talang Akar Cenozoic Total Petroleum System. United States Geological Survey. *Open-file report* 99–50S.

Bordenave, M.L., Espitalie, J., Leplat, P, Oudin, J.L., and Vandenbroucke, M., 1992. Screening Techniques for Source Rock Evaluation. Applied Petroleum Geochemistry. *In*: Bordenave, M.L. (ed.), *Editios Technip*, 27 Rue Ginoux 75015 Paris. p. 220-278.

Burley, S.D., Kantorowicz, J.D. and Waugh, B., 1987. Clastic Diagenesis. *In*: Beaumont E.A. and Foster, N.H. (ed.); Reservoirs II, sandstone, *Treatise of Petroleum Geology Reprint Series No 4, American Association of Petroleum Geologists*, p. 408-445.

Bustin, R.M., Cameron, A.R., Grieve, D.A., and Kalkreuth, W.D., 1985. Coal Petrology: Its Principles, Methods and Applications. *Geological Association of Canada, Short Course Notes*, 3, 2nd ed., 273 pp.

Cameron, N.R., Aspden, J.A., Suwarna, N., and Suharsono, 1981. *The Geology of Ombilin Basin, Singkarak Block, West Sumatra*. Unpublished Rept., P.T. Caltex Pacific Indonesia, Nov. 1981, Rumbai, Sumatra.

Carr, A.D., 1999. Avitrinite reflectance kinetic model incorporating overpressure retardation. *Marine and Petroleum Geology*, 16, p.355–377.

Carvalho, D. da Silva, Purwoko, Siswoyo, Thamrin, N., and Vacquier, V., 1980. Terrestrial heat flow in the Tertiary basin of central Sumatra. *Tectonophysics*, 69, p.163-188

Clarke, M.C.G., Kartawa, W., Djunuddin, A., Suganda, E., and Bagdja, M., 1982. *Geol-*

ogy of the Pakanbaru Quadrangle, Sumatra. GRDC, 30 pp.

Clure, J., 1991. Spreading centers and their effect on oil generation in the Sunda region. *Indonesian Petroleum Association, Proceedings of the 20th Annual Convention*, 1, p.37–48.

Clure, J., 2005. Fuel resources: oil and gas. *In*: Sumatra, Geology, Resources and Tectonic Evolution. *Geological Society Memoir*, 31, p.131–141

Cole, J. M. and Crittenden, S., 1997. Early Tertiary basin formation and the development of lacustrine and quasi-lacustrine /marine source rocks on the Sunda Shelf of SE Asia. *In*: Fraser, A. J., Matthews, S. J., and Murphy, R. W. (Eds.), *Petroleum Geology of Southeast Asia: Geological Society Special Publication*, 126, p.147–183.

Cook, A.C., Hutton, A.C., and Sherwood, N.R., 1981. Classification of oil shales. *Bulletin of Cent. Rech. Exploration-Production Elf-Aquitaine,* 5, p.353-381.

Coster, G.L. de, 1974. The geology of the central and south Sumatra basins. *Indonesian Petroleum Association*, p. 77-110.

Crisp, P.T., and others, 1987, Australian oil shale: a compendium of geological and chemical data. *CSIRO Inst. Energy and Earth Sciences*, Division of Fossil Fuels, North Ryde, NSW, Australia, 109 pp.

Curtis, J.B., 2002. Fractured shale-gas systems. *American Association Petroleum Geologist, Bulletin*, 86 (11), p. 1921-1938.

Daly, M.C., Hooper, B.G.D., and Smith, D.G., 1987. Tertiary plate tectonics and basin evolution in Indonesia. *Indonesian Petroleum Association*, p. 399-428.

Daly, M.C., Cooper, M.A., Wilson, I., and Hooper, B.G.D., 1991. Cenozoic plate tectonics and basin evolution in Indonesia. *Marine and Petroleum Geology*, 8, p.2-21.

De Coster, G.G., 1974. The geology of the Central and South Sumatra Basins. *Indonesian Petroleum Association, Proceedings of the 3th Annual Convention*, 3, p.77–110.

De Haan, W., 1942. Over de stratigrafie en de tektoniek van het Mangani gebied. *Geologie and Mijnbouw*, IV, p.21-25.

De Smet, M.E.M., 1992. A guide to the stratigraphy of Sumatra, Part 2: Tertiary. The geology of the Central and South Sumatra Basins. University of London Consortium for Geological Research in Southeast Asia, *Internal Report*. 108.

Demaison, G.J., and Moore, G.T, 1980. Anoxic environment and source oil genesis. *Organic Geochemistry,* 2, p. 9-31.

Doust, H. and Noble, R.A., 2008. Petroleum systems of Indonesia. *Marine and Petroleum Geology*, 25, p.103–129.

Duncan, D.C. and Swanson, V.E., 19 .. Organic-rich shale of the United States and world land areas. *U.S. Geological Survey Circular,* 523, 30 pp.

Dyni, J.R. and others, 1989. Comparison of hydroretorting, Fischer assay, and Rock-Eval analyses of some world oil shales. *Proceedings Eastern Oil Shale Symposium*: University of Kentucky Institute for Mining and Minerals Research, p. 270-286.

Dyni, J.R., 2004. Oil Shale. *Energy Minerals Division*. EMD Home > Technical Areas: Oil Shale, 10 p.

Espitalie, J., Laporte, J.L., Madec, M., Marquis, F., Leplat, P., Paulet, J., and Boutefeu, A., 1977. Methode rapide de caracterisation des roches meres, de leur potentiel petrolier et de leur degre d'evolution. *Rev. Inst. Franc. Petrole*, 32, 1, p.23-40.

Espitalié, J. and Bordenave, M.L., 1993. Source rock parameters. *In*: Bordenave, M.L., (Ed.), *Applied Petroleum Geochemistry,* 2, p.237-272.

Eubank, R. T. and Makki, A. C., 1981. Structural geology of the Central Sumatra back-arc basin. *Indonesian Petroleum Association, Proceedings of the 10th Annual Convention*, 10, p.153–196.

Falcon, R.M.S. and Snyman, C.P., 1986. An introduction to coal petrography: Atlas of petrographic constituents in the bituminous coals

of Southern Africa. The Geological Society of South Africa. Review Paper, 2. Kelvin House, 2 Hollard Street. (Johannesburg).

Fitch, F.J., 1972. Plate convergence, transcurrent faults and internal deformation adjacent to southeast Asia and western Pacific. *Journal of Geophysical Research*, 77, p. 4432-4460.

Foscolos, A.E., Powell, T.G., and Gunther, P.R., 1976. The use of clay minerals and inorganic and organic geochemical indicators for evaluating the degree of diagenesis and oil generating potential of shales. *Geochimica et Cosmochimica, Acta, 40,* p.953-966.

Gafoer, S., Cobrie, T., and Purnomo, J., 1986. *Geological Map of the Lahat Quadrangle, South Sumatra, scale 1:250.000.* Geological Research and Development Centre, Bandung, Indonesia

Gluyas, J. and Swarbrick, R. E., 2004. *Petroleum Geoscience.* Blackwell Science Limited.

Goodarzi, F., Davies, G.R., Nassichuk, W.W., and Snowdon, L.R., 1987. Exsudatinite in Carboniferous oil shales from Arctic Canada. *Fuel*, 66, p.771-773.

Hamilton, W., 1979. *Tectonics of the Indonesian Region*. United States Geological Survey Professional Paper. 1078pp.

Hartanto, K., Widianto, E. and Safrizal, 1991. Hydrocarbon prospect related to the local unconformities of the Kuang Area, South Sumatra Basin. Indonesian Petroleum Association, Proceedings of the 20th Annual Convention, 1, p.17–36.

Hennings, P., Allwardt, P., Paul, P., Zahm, C., Reid R., Alley, H., Kirschner, R., and Hough, E., 2012. Relationship between fractures, fault zones, stress, and reservoir productivity in the Suban gas field, Sumatra, Indonesia. *American Association of Petroleum Geologists Bulletin*.

Heryanto, R., Suwarna, N., and Panggabean, H., 2001, The Lakat Formation in the Northeastern Flank of the Tigapuluh Mountains and Its Possibilities as a Source Rock: *Proceedings of 30th Annual Convention Indonesian Associa-tion of Geologist and 10th Geosea Regional Congress on Geology, Mineral, and Energy Resources*.

Heryanto, R., Suwarna, N., and Panggabean, H., 2004, Hydrocarbon Source Rock Potential of the Eocene-Oligocene Keruh Formation in the Southwestern Margin of the Central Sumatera Basin. *Journal of Geological Resources*, XIV (3), p. 293-306.

Heryanto, R. and Hermiyanto, H., 2006, Potensi Batuan Sumber (*Source Rock*) Hidrokarbon di Pegunungan Tigapuluh, Sumatera Tengah. *Indonesian Journal of Geology*, 1 (1), p.37-48.

Hunt, J.M. and Jameison, C.W., 1958. Oil and organic matter in source rocks of petroleum. *In*: Weeks, L.G. (Ed.) *American Habitat of oil.*

Hutapea, O.M., 1981. The prolific Talang Akar Formation in Raja Field, South Sumatra. *Indonesian Petroleum Association, Proceedings of the 10th Annual Convention*, p.251–268.

Hutton, A.C., 1980. Organic petrology of some Australian and overseas oil shales. *In*: Cook, A.C. and Kantsler, A.J. (eds.), *Oil Shale Petrology Workshop,* Wollongong, 1980. Keiraville Kopiers, Wollongong, p. 42-49.

Hutton, A.C., 1987. Petrographic classification of oil shales. *International Journal of Coal Geology*, 8, p. 203-231.

International Committee for Coal Petrology (ICCP). 1963. International Handbook of Coal Petrography. 2nd Ed. Centre National de la Recherche Scientifique. Academy of Sciences of the USSR. Paris, Moscow.

International Committee for Coal Petrology, (ICCP), 1971. International Handbook of Coal Petrography, 1st Supplement to 2nd Edition. CNRS (Paris).

International Committee for Coal Petrology, (ICCP), 1975. International Handbook of Coal Petrography, 2nd Supplement to 2nd Edition. CNRS (Paris).

International Committee for Coal Petrology, (ICCP), 1993. International Handbook of Coal Petrography, 3rd Supplement to 2nd Edition. University of Newcastle on Tyne (England).

International Committee for Coal and Organic Petrology, (ICCP), 1998. The new vitrinite classification (ICCP System 1994). Fuel 77, 349–358.

International Committee for Coal and Organic Petrology (ICCP), 2001. The new inertinite classification (ICCP System 1994). Fuel 80, 459–471.

Jacob, H., 1989. Classification, structure, genesis and practical importance of natural solid oil bitumen ("migrabitumen"). International Journal of Coal Geology 11, 65-79.

Jacob, H., 1993. Nomenclature, Classification, Characterization, and Genesis of Natural Solid Bitumen (Migrabitumen). *In*: Parnell, J., Kucha, H., Landais, P., (Eds.), Bitumens in ore deposits. *Special Publication of the Society for Geology Applied to Mineral Deposits*, 9. Springer-Verlag, p.11-27.

Kruge, M., Suárez –Ruiz, I., 1991. Organic geochemistry and petrography of Spanish oil shales. *Fue*l, 70, p.1298-1302.

Landis, Ch., Castaño, J., 1995. Maturation and bulk chemical properties of a suite of solid hydrocarbons. *Organic Geochemistry*, 271, p.137-149.

Karig, D.E., Suparka, S., Moore, G.F., and Hehunassa, P.E., 1979. Structure and Cenozoic evolution of the Sunda Arc in the central Sumatra region. *In*: Watkins, J.S., Montadert, L., and Dickerson, P.W. (Eds.) Geological and Geophysical Investigations of the Continental Margins. *American Association of Petroleum Geologists Memoirs*, 29, p.223–237.

Karig, D.E., Lawrence, M. B., Moore, G.F., and Curray, J.R., 1980. Structural framework of the fore-arc basin, NW Sumatra. *Journal of the Geological Society*, 137, p.77–91.

Katz, B.J., 1983. Limitations of 'Rock-Eval' pyrolysis for typing organic matter. *Organic Geochemistry*, 4, p.195-199.

Khumongkol, D. and Suwannathong, A. 2007. Aspect of Oil Shales in Thailand. *GEOTHAI'07, International Conference on Geology of Thailand: Towards Sustainable Development*, p. 399-403.

Koesoemadinata, R.P. and Matasak, Th., 1981. Stratigraphy and Sedimentation in Ombilin Basin, Central Sumatra (West Sumatra Province). *Proceedings of 10th Annual Convention of Indonesian Petroleum Association*, Jakarta, p. 217-249.

Koning, T., 1985. Petroleum geology of the Ombilin Intermontane Basin, West Sumatra. *Proceedings 14th Annual Convention of Indonesian Petroleum Association.*, Jakarta, October, p.117-137.

Kusumahbrata, Y., Gunawan, W., Satria, D., and Rachmansyah, 2002. Penelitian Sedimentologi dan Stratigrafi Daerah Dairi-Tanahkaro, Sumatera Utara. *Laporan Internal Proyek Kajian dan Informasi Geologi Tematik, Tahun Anggaran 2002*. Puslitbang Geologi, Bandung.

Kusumahbrata, Y. and Suwarna, N., 2003. Characteristic of the Keruh Formation Oil Shale: It implication to oil shale resource assessment. *Prosiding Kolokium Energi and Sumber Daya Mineral,* p.362-370.

Liu, Z., Ron, H., Yang, H., Yao, S., and Ma, Ch., 2023. Characteristics of Oil Shale Quality and Prospects for Comprehensive Development and Utilization in the Dalianhe Coal Mining Area, Northeastern China. *Energies*, 16 (13), p.5069.

Longley, I. M., Barraclough, R., Bridden, M. A., and Brown, S., 1990. Pemantang lacustrine petroleum source rocks from the Malacca Strait PSC, Central Sumatra, Indonesia. *Indonesian Petroleum Association, Proceedings of the 19th Annual Convention,* 1, p.279–298.

Macauley, G., 1981. Geology of the oil shale deposits of Canada. *Geological Survey of Canada Open File Report* OF 754, 155 pp.

Matthews, R.D., 1983. The Devonian-Mississippian oil shale resource of the United States. *In*: Gary, J.H. (ed.), *Sixteenth Oil Shale Symposium Proceedings: Colorado School of Mines Press*, p. 14-25.

Matson, R.G. and Moore, G., 1992. Structural influences on Neogene subsidence in the central Sumatra forearc basin. *In*: Watkins, J.S., Zhiquiang, F. et al. (Eds.), Geology and Geophysics of Continental Margins. *American Association of Petroleum Geologists Memoirs*, 53, p.157–181.

McCaffrey, R., 2009. The Tectonic Framework of the Sumatran Subduction zone. *Annual Review Earth Planetary Science*, 37, p.345–366.

McCarthy, A. J., 1997. *The evolution of the trans-current Sumatran Fault System*. PhD Thesis, University of London.

Mertosono, S. and Nayoan, G.A.S., 1974. The Tertiary basinal area of Central Sumatra. *Indonesian Petroleum Association*, *Proceedings of the 3rd Annual Convention*, p. 63-127.

Moore, G. F., Curray, J.R., and Emmel, F. J., 1982. Sedimentation in the Sunda Trench and the forearc region. *In*: Leggett, J. K. (ed.), Trench – Forearc Geology. *Geological Society, London, Special Publication*s. 10, p.245–257.

Moulds, P. J., 1989. Development of the Beng-kalis depression, Central Sumatra and its subsequent deformation – a model for other Sumatran grabens?. *Proceedings of Indonesian Petroleum Association 18th Annual Convention*, p.217–246.

Padula, V.T., 1969. Oil shale of Permian Iratí Formation. *Bulletin American Association of Petroleum Geologists*, 53, p. 591-602.

Peters, K.E., 1986. Guidelines for evaluating petroleum source rock using programmed pyrolysis. *American Association of Petroleum Geologists. Bull*etin, 70, p.1-36.

Pittman, E.D., 1979. Porosity, diagenesis and productive capability of sandstone reservoir. *SEPM Special Publ*ication, 26, p.159-173.

Pitman, J.K. and others, 1989. Thickness, oil-yield, and kriged resource estimates for the Eocene Green River Formation, Piceance Creek Basin, Colorado. *U.S. Geological Survey Oil and Gas Investigations Chart* OC-132.

Pulunggono, A., 1986. Tertiary structural features related to extensional and compressive tectonics in the Palembang Basin, South Sumatra. Indonesian Petroleum Association, Proceedings of the 15th Annual Convention, I, p.187–214.

Peters, K.E., 1986. Guidelines for evaluating petroleum source rock using programmed pyrolysis. *American Association of Petroleum Geologists, Bulletin*, 70, p.318-329

Powell, T.G., Foscolos, A.E., Gunther, P.R., and Snowdon, L.R., 1978. Diagenesis of organic matter and fine clay minerals. *Geochimica et Cosmochimica Acta*, 42, p.1181-1197.

Rad F.K., 1984. Quick Look Source Rock Evaluation by Pyrolysis Technique. *Proceedings of 13th Annual Convention of Indonesian Petroleum Association*, p.113-124.

Samuel, M. A., Harbury, N.A. Jones, M.E., and Matthews, S.J., 1995. Inversion-controlled uplift of an outer-arc ridge: Nias island, offshore Sumatra. In: Buchanan, J.G and Buchanan, P.G. (Eds.), Basin Inversion. *Geological Society of London Special Publication*, 88, p.473–492.

Samuel, M. A., Harbury, N. A., Barkri, A., Banner, F. T., and Hartono, L., 1997. A new stratigraphy for the islands of the Sumatran Forearc, Indonesia. *Journal of Southeast Asian Earth Sciences,* 15, p.330–380.

Sarjono, S. and Sardjito, 1989. Hydrocarbon source rock identification in the South Palembang Sub-basin. *Indonesian Petroleum Association, Proceedings of the 18th Annual Convention*, 1, p.419–468.

Sardjito, Fadianto, Eddy, Djumlati, and Hansen, S. (1991). Hydrocarbon prospect of the PreTertiary basement in Kuang Area, South Sumatra. *Proceedings of Indonesian Petroleum Association 12th Annual Convention*, p.101–113.

Rahmola, W.R., 2019. *Potensi Batuan Induk dan Lingkungan Pengendapan Serpih Minyak, Berdasarkan Karakteristik Petrografi dan Geokimia Organik, di Daerah Kapur IX,*

Sumatra Barat. Skripsi S1 (In Indonesian), *Unpublished*, Fakultas Teknik Geologi, Universitas Padjadjaran.

Robert, P., 1981, Classification of Organic Matter by Means of Fluorescence: Application to Hydrocarbon Source Rocks. *International Journal of Coal Geology*, 1, p.101-137.

Rudistyan, I., 2005, *Karakteristik Oil Shale di Daerah Kuantan-Singingi, Riau, Berdasarkan Analisis Petrografi Organik. Skripsi S-1* (in Indonesia), Jurusan Geologi, MIPPA, Universitas Padjadjaran.

Russell, P.L., 1990. *Oil shales of the world, their origin, occurrence, and exploitation*. Pergamon Press, New York, 753 pp.

Schmidt, V. and McDonald, D.A., 1979. The rocks of secondary in the course of sandstone diagenesis. *Soc. Econ. Pal. Min.., Spec. Publ.* 26, p. 175-207.

Scholle, P.A., 1979. A colour illustrated guides to constituents, textures, cements, and porosity of sandstone and associated rocks. *American Association of Petroleum Geologists, Mem*oir, 28., 201pp.

Silitonga, P.H. and Kastowo, 1995. *Geological Map of the Solok Quadrangle, scale 1: 250 000*. Geological Research and Development Centre, Bandung (2nd Edition).

Sladen, C., 1997. Exploring the lake basins of east and Southeast Asia. *In*: Frazer, A.J., (Ed.). Petroleum Geology of Southeast Asia. *Geological Society Special Publication*, 126, p.49–76.

Spruyt, 1956. Subdivisions and nomenclature of the Tertiary sediments of the Djambi, Palembang area. *Pertamina Internal Report*.

Stach, E., Mackowsky, M-Th., Teichmuller, M., Taylor, G.H., Chandra, D., Teichmuller, R., (Eds.)., 1982. Coal Petrology. Gebruder Borntraeger (Berlin - Stuttgart), 535 pp.

Suárez-Ruiz, I., Iglesias, M.J., Jiménez Bautista, A., Laggoun-Defarge, F., Prado, J.G., 1994. Petrographic and geochemical anomalies detected in the Spanish Jurassic jet. *In*: Mukhopadhyay, P.K. and Dow, W.G., (Eds.), Vitrinite reflectance as a maturity parameter. Applications and limitations. *American Chemical Society Symposium Series*. ACS Books 570, p.76-92.

Smith, J.W., 1980. Oil shale resources of the United States. *Colorado School of Mines Mineral and Energy Resources*, 23 (6), 30 pp.

Suhendan, A.R., 1984. Middle Neogene depositional environments in Rambutan area, South Sumatra. *Proceedings of Indonesian Petroleum Association 13th Annual Convention*, p. 63–73.

Susanto, E., Suwarna, N., and Hermiyanto, H., 2004. Penelitian Fosil Fuel dan Paleontologi, Kajian Oil Shale, di Sumatera Bagian Tengah. *Laporan Internal*, Pusat Penelitian dan Pengembangan Geologi, Bandung.

Suwarna, N. dan Suharsono, 1984. *Laporan Geologi Lembar Bangko (Sarolangun), Sumatra. Open-file Report*, Pusat Penelitian dan Pengembangan Geologi, Bandung.

Suwarna, N., Suharsono, Gafoer, S., Amin, T.C., Kusnama, and Hermanto, B., 1992. *Geology of the Sarolangun Quadrangle, Sumatera, scale 1:250.000*. Geological Research and Development Centre, Bandung.

Suwarna, N., Budhitrisna, T., Santosa, S., and Andi Mangga, S., 1994. *Geological Map of The Rengat Quadrangle, scale 1: 250.000*. Geological Research and Development Centre, Bandung.

Suwarna, N., 1997. *Peta Geologi Lembar Gununghijau, Sumatera, sekala 1:100.000*. Pusat Penelitian dan Pengembangan Geologi, Bandung.

Suwarna, N., Suharsono, Hermanto, B., and Amiruddin, 1998. *Peta Geologi Lembar Bangko, Sumatera, sekala 1:100.000*. Pusat Penelitian dan Pengembangan Geologi, Bandung.

Suwarna, N., Panggabean, H., and Heryanto, R., 2001. Oil Shale Study in the Kiliranjao Sub-basin, Central Sumatera. *Proceedings, IAGI and GEOSEA*, Yogyakarta, Indonesia.

Suwarna, N., 2004a. Relation of Organic Facies to Palaeoenvironmental Deposition: Case

Study in the "Papanbetupang-Kasiro Coal Measures", South Sumatera. *Jurnal Sumber Daya Geologi*, XIV (2), p. …….

Suwarna, N., 2004b. Maceral Composition and Rank of Kasiro Coals: Implications for Hydrocarbon Generation. *Jurnal Sumber Daya Geologi*, XIV (2), p. …..

Taylor, G.H., Teichmuller, M., Davis, A., Diessel, C.F.K., Littke, R., and Robert, P., 1998. *Organic petrology*. Gebrüder Borntraeger. Berlin. 704 pp

Teichmüller, M., Durand, B., 1983. Fluorecence microscopical rank studies on liptinite and vitrinite in peat and coals and comparison with results of the Rock-Eval pyrolysis. *International Journal of Coal Geology*, 2, p.197-230.

Tissot, B.P. and Welte, D.H., 1984. *Petroleum Formation and Occurrence, a New Approach to Oil and Gas Exploration*. 2nd Edition. Berlin, Springer-Verlag, 699 pp.

Tyson, R.V., 1993. Palynofacies analysis. *In*: Jenkings, D.G., (Ed.), *Applied micropaleontology*. Kluwer Academic Publishers, Dordrecht. The Netherlands, p.153- 191.

Tyson, R.V., 1995. *Sedimentary organic matter: Organic facies and palynofacies*. Chapman and Hall, London. 615 pp.

Vandenbroucke, M., Largeau, C., 2007. Kerogen origin, evolution and structure. *Organic Geochemistry*, 38, p.719-833.

Wain, A.N. and Jackson, B.A., 1995. New Pematang depocentres on the Kampar uplift, Central Sumatra. *Indonesian Petroleum Association*, p. 215-223.

Waples, D.W., 1985. Geochemistry in petroleum exploration. *Reidel,* Dortrecht, p. 223.

Welton, J.E., 1984. SEM Petrology Atlas. *AAPG methods in exploration series*, 4. 437pp.

Widianto, E. and Muskin, N., 1989. Seismic stratigraphic record study on the Talangakar Formation in the Selat Area, Jambi. *Indonesian Petroleum Association, Proceedings of the 18th Annual Convention*, I, p.323–338.

Williams, H. H., Fowler, M., and Eubank, R. T., 1995. Characteristics of selected Palaeogene and Cretaceous lacustrine source basins of Southeast Asia. *In*: Lambiase, J. J. (Ed.) Hydrocarbon Habitat in Rift Basins. *Geological Society of London, Special Publication*, 80.

William, H.H., Kelley, P.A., Janks, J.S., and Christensen, R.M., 1985. The Paleogene rift basin source rocks of central Sumatra. *Indonesian Petroleum Association*, p. 57-89.

Wilson, M.D. and Pittman, E.D., 1979. Authigenic clays in sandstone: Recognised and influence on reservoir properties and palaeoenvironmental analysis. *Journal of Sedimentary Petrology*, 47, p. 3-31.

Woodside, P.R., 1984. A look at the petroleum geology of Indonesia. *Oil and Gas Journal*, p. 78-82.